Chrysanthi Papadimitriou

Thermodynamic performance indicators in offshore oil and gas processes

Master's thesis in Energy and Process Engineering
Supervisor: Even Solbraa
Co-supervisor: Marlene Louise Lund / Efstathios Skouras-Iliopoulos
July 2021

Master's thesis

NTNU
Norwegian University of Science and Technology
Faculty of Engineering
Department of Energy and Process Engineering

NTNU
Norwegian University of
Science and Technology

Chrysanthi Papadimitriou

Thermodynamic performance indicators in offshore oil and gas processes

Master's thesis in Energy and Process Engineering
Supervisor: Even Solbraa
Co-supervisor: Marlene Louise Lund / Efstathios Skouras-Iliopoulos
July 2021

Norwegian University of Science and Technology
Faculty of Engineering
Department of Energy and Process Engineering

NTNU
Norwegian University of
Science and Technology

Abstract

With the environmental awareness increasing in recent decades and the imminent prospect of carbon neutrality more attention has been paid to the ways in which the greenhouse gas emissions and the energy demand of industrial activities can be reduced, especially in the oil and gas field which occupies a prominent place in the global energy consumption.

Energy- and exergy-based thermodynamic performance indicators constitute a useful tool for the evaluation of oil and gas processes that can motivate optimal operation of offshore platforms. The objective of this thesis is to perform an energy and exergy analysis of a typical North Sea offshore processing plant, consider the power and heat demands of different process design configurations and frame conditions, as well as calculate and evaluate different thermodynamic performance indicators introduced in literature. The energy and exergy efficiencies are then assessed in order to identify improvement potentials and a new idea is proposed for more efficient performance of the oil and gas processes. Finally, a simplified method for the evaluation of the indicators examined in this thesis is presented.

In this work the simulation of a typical offshore platform (Base Case scenario) is considered based on realistic data provided from the oil and gas company Equinor, Norway and it is simulated in ASPEN HYSYS ®. An energy and exergy analysis is carried out and the thermodynamic performance indicators are calculated. The indicators presented are the following: Specific CO2 emissions, Specific energy and exergy use, Specific power consumption, Specific exergy destruction, Total, Task and Component-by-Component exergy efficiency, Exergy destruction ratio, Exergy loss ratio and Efficiency defect.

The results of the conducted calculations indicate a power consumption of the platform around 23.1 MW mainly detected in the gas compression train (20.5 MW). Heat demands are approximately 11.2 MW, while energy of cooling reaches the number of 42.8 MW. The total exergy destruction rate is around 19.1 MW and it is mostly due to throttling in the production manifold. Exergy losses which range around 5.2 MW result mainly from cooling, which accounts for 65.2% of the total exergy lost.

In order to get a more complete view of the performance of the indicators examined in this work different case studies are set that consider changes in various frame conditions and process configurations for the case at issue, while the effect of the component chemical exergy and the oil production lifetime of the field are also investigated. The parameters under discussion are the following: reservoir fluid composition, Cricondenbar pressure (CDB) and True vapor pressure (TVP) specifications, pressure of export gas, efficiency of the rotating equipment, temperature of cooling and temperature and pressure levels of the separation train.

These case studies show that overall energy-based indicators are easier and quicker to use. They change according to the variations in heat and power demands when a specific platform with small deviations in the products is examined. However, some of them (Specific power consumption, CO2 intensity) may not reflect important changes in heating duties giving incomplete information regarding the performance of the process. When different platforms are considered they focus on the reservoir fluid treated in the process without promoting the most efficient utilization of the resources. ExU and ExD indicators seem to perform similarly, but when they are expressed per product exergy (ExUexergy, ExDexergy) they show not only the effect of heat and power demands, but also the effect of the different export conditions.

Total exergy efficiency is insensitive to any type of changes in the process, due to the high exergy of the hydrocarbons passing through the system producing misleading results and conclusions over the performance of the platform. On the other hand, Task and Component-by-Component exergy efficiency focus on the optimal utilization of the exergy resources of a processing plant and not the type of field examined. Task exergy efficiency ε_{II-3} is heavily influenced by variations in the conditions of the inlet well stream and the export products even leading to negative results that make the evaluation process more difficult. Task exergy efficiency ε_{II-4} responds to changes in both heat and power demands and outlet conditions of the platform or the distribution of the components in the two product streams. Task exergy efficiency ε_{II-5} and Component-by-Component exergy efficiency ε_{III} take into account the allocation of the components in the two product streams, but the latter shows a higher sensitivity to the inlet and outlet conditions, as well as the chemical exergy increases of the inlet and outlet fluid streams.

The Exergy destruction ratio and the Efficiency defect give inspection of the distribution of exergy in the subsystems of the process, with the former giving more accurate results even without the calculation of the component chemical exergy term. Exergy loss ratio can pinpoint where in the process exergy is mainly lost to the environment indicating and it is more useful when the utilities are also included in the system being studied.

The exergy analysis performed for the Base Case highlights that inefficiencies are mainly detected in the production manifold due to the exergy destruction associated with choking. In this work a new idea is proposed that aims in saving a part of exergy lost due to throttling and transform it to useful energy, work. This approach is based on a combined separation-multiphase flow expansion system for the substitution of choke valves in the production manifold and it is applied and simulated for the Base Case scenario of this work. The energy and exergy analysis conducted underlines that the implementation of such a combined system could results in a rise in efficiency of up to 34% and a 27% reduction in work demands and CO2 emissions.

The analyses conducted in this thesis show that choosing between the different indicators at issue for the description of the performance of a platform is a complicated process that depends on multiple parameters. On that account an evaluation procedure is proposed based on the Multicriteria analysis that aims to reveal the most appropriate indicator or combination of indicators according to the desired use through a scoring process. For that reason, a set of six criteria is established that aim to cover all the characteristics an indicator is desired to attain and scores are assigned to each indicator against each criterion. The weighting factors defined from the user derive from the expected application and determine the priority of the criteria when calculating the overall score of the indicators. According to an example presented in this work the combination of the Task exergy efficiency ε_{II-4} and the Exergy destruction ratio are considered to be the best for the investigation of an oil and gas processing plant, like the one investigated in this work.

KEY WORDS: exergy analysis, thermodynamic performance indicators, exergy destruction, exergy losses, oil and gas field, design parameters, frame conditions, specifications, multiphase expander, scoring process

Acknowledgements

This diploma thesis entitled "Thermodynamic performance indicators in offshore oil and gas processes" concludes the 5-year Master's degree program in Chemical Engineering at the National Technical University of Athens (NTUA). It was written in the spring of 2021 within the framework of the exchange program "Erasmus Plus".

I wish to express my sincerest gratitude to my supervisor at NTNU Professor Even Solbraa for the advice and encouragement he provided during this project. Moreover, I would like to thank my supervisor at NTUA Professor Epaminondas Voutsas for his proper guidance, exceptional direction and expertise. This work could not have been completed without their unconditional support and motivation. I would, also like to use this opportunity to express my appreciation to my co-supervisors at Equinor ASA, Marlene Louise Lund for always willingly providing assistance and guidance for the technical parts of my work, as well as Dr. Efstathios Skouras-Iliopoulos for his advice and support.

Finally, I would like to thank my dear friends at NTUA for the five wonderful years we have spent together as students. Last but not least, I wish to express my profound gratitude to my family and closest friends, for all the support and love I have received throughout my education and my life. This accomplishment would not have been possible without them.

Contents

List of Tables

List of Figures

Nomenclature

List of symbols

Latin letters

Symbol	Description	Units
e	Specific exergy	kJ/kg
$\dot{E}$	Exergy rate	kW
E	Exergy	kJ
$\dot{Q_b}, \dot{Q_{in}}$	Energy transfer by heat	kW
$\dot{W_{cv}}, \dot{W_{in}}$, Consumed power	Energy transfer by work	kW
$E_{\dot{W},in}$, $\mathrm{E}^{\dot{\mathrm{W}}}$	Exergy transfer by work	kW
$E_{\dot{Q},in}, E_{heat}^{\dot{Q}}$	Exergy transfer by heat	kW
$\dot{Ed}$, $E_{d,PP}$	Exergy destruction rate (or exergy destruction)	kW
$\dot{El}$	Exergy loss rate (or lost exergy or exergy losses)	kW
h	Specific enthalpy	kJ/kg
s	Specific entropy	kJ/kgK
T	Temperature	K
P	Pressure	bar
t	Time	s
LHV	Lower heating value	kJ/kg
$\dot{V}$	Volume flow rate	Sm^3 o.e., boe
ExU_{volume}	*Specific exergy use* per standard volume of oil equivalent exported	kJ/Sm^3 o.e.
ExU_{exergy}	*Specific exergy use* per exported exergy	-
ExD_{volume}	*Specific exergy destruction* per standard volume of oil equivalent exported	kJ/Sm^3 o.e.
ExD_{exergy}	*Specific exergy destruction* per exported exergy	-
y_d^*	*Exergy destruction ratio*	-
y_l^*	*Exergy loss ratio*	kW
$\dot{I}$	Rate of irreversibilities of the investigated system	kW
$\dot{E}_i$	Total exergy flowing into the control volume	kW
$\dot{m}$	Mass rate	kg/s
$\dot{n}$	Molar rate	moles/s
n	Number of criteria	-
w	Weighting factor	-
v	Indicator v	-

Greek letters

Symbol	Description	Units
ρ	Density	kg/m^3
Δ	Difference	-
ε	*Exergetic efficiency*	-
δ_i	*Efficiency defect*	-
λ	*Irreversibility ratio*	-
ε_{I-1}	*Total exergy efficiency*	-
ε_{I-2}	*Total exergy efficiency*	-
ε_{II-1}	*Task exergy efficiency*	-
ε_{II-2}	*Task exergy efficiency*	-
ε_{II-3}	*Task exergy efficiency*	-
ε_{II-4}	*Task exergy efficiency*	-
ε_{II-5}	*Task exergy efficiency*	-
ε_{III}	*Component-by-Component exergy efficiency*	-
η_k	*Exergetic efficiency of a k component*	-

Subscripts

Symbol	Description
D, d	Destroyed
L, l	Lost
W, w	Waste or work
P	Product
U, u	Useful
F, f	Fuel
$feed$	Feed
k	Product k (*Total-Task-Component-by-Component* exergy efficiency definition) / Process component k
$export$	Of the export product
b	Heat exchange surface b
o	Of the environment
CV	In the control volume
in	Entering the system
out	Leaving the system
$Q, heat$	Heat
$cool$	Cooling
i	Subsystem i / Component i (chemical and physical exergy & *Component-by-Component* definition)/ Criterion i (Evaluation method)
BAT	Best available technology
mix	Of mixing
P, P	Processing plant
$k-$	Stream k with a lower physical exergy than the feed
$k+$	Stream k with a higher physical exergy than the feed
j	Feed j

Superscripts

Symbol	Description
ch	Chemical
ph	Physical
W, w	Waste or work
$Q, heat$	Heat
$cool$	Cooling
^	Mixture
+	Increases
-	Decreases

List of abbreviations

Symbol	Description
API	American Petroleum Institute gravity
SG	Specific gravity / Relative density
BOE	Barrel of Oil Equivalent
Sm^3	Standard cubic meters
$Sm^3 o.e.$	Standard cubic meters of oil equivalent
BAT	Best Available Technology
PI	Performance indicators
HP	High pressure
LP	Low pressure
C	Carbon
H_2	Hydrogen
O_2	Oxygen
S	Sulfur
H_2O	Water
N_2	Nitrogen
SRK	Soave-Redlich-Kwong
ASPEN	Advanced System for Process Engineering
CDB	Cricondenbar
CDT	Cricondentherm
TVP	True vapour pressure
GLR	Gas-to-Liquid ratio
C-b-C exergy efficiency	*Component-by-Component exergy efficiency*
UV	User Variables
VBA	Visual Basic for Applications
GOR	Gas-to-Oil ratio

1. Introduction

1.1 Motivation

Energy production – mainly associated with fossil fuels – constitutes the largest driver of climate change accounting for around three quarters of the global greenhouse gas emissions.

Oil and gas industry occupies a prominent place in the global primary energy consumption serving around 57% of the world's energy demands (2019) (Figure 1). Especially, in Europe over 59% of the energy needs in 2019 were covered by oil and gas exploitation (Figure 2), while around half of the European production of oil and gas in 2018 was located in Norway. (Ritchie & Roser, 2020), (BP, 2019)

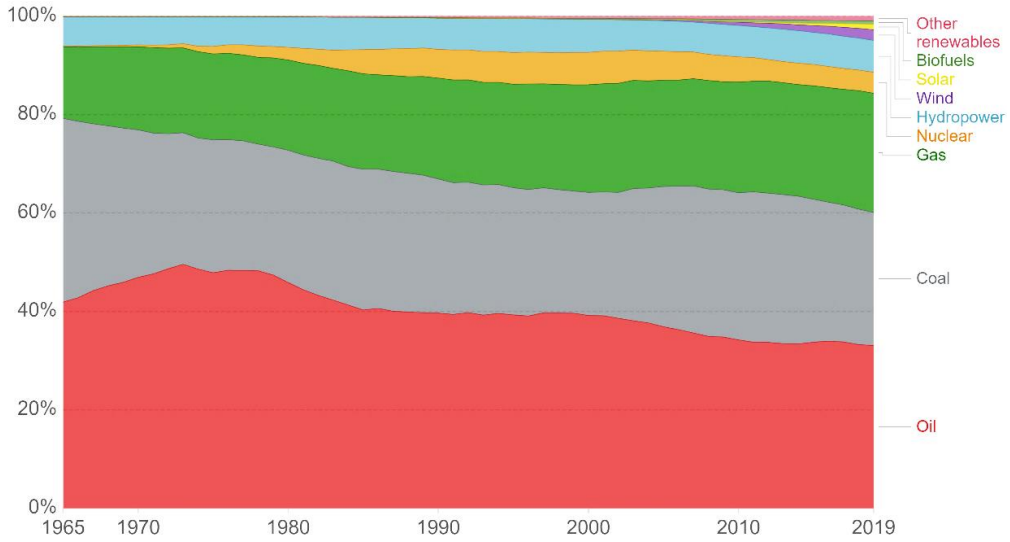

Figure 1 Global energy consumption by source (1965-2019) (Ritchie & Roser, 2020)

The extended use of oil and gas on a global level, in combination with the natural gas or diesel oil combustion for power generation on offshore installations sets the oil and gas extraction and processing sector as one of the main fields responsible for the world's greenhouse gas emission. (Voldsund M. , 2014).

According to the *International Energy Agency* (*IEA*), in 2017 the oil and gas industry was responsible for around 7% of the worldwide energy related greenhouse gas emissions (Figure 3) (IEA, 2019), while in Norway greenhouse gas emissions from petroleum activities corresponded to about 13.2 million tonnes CO_2 eq (carbon dioxide equivalent) in 2019, accounting for about 25% of Norway's aggregate greenhouse gas emissions (Norwegian Petroleum, 2020).

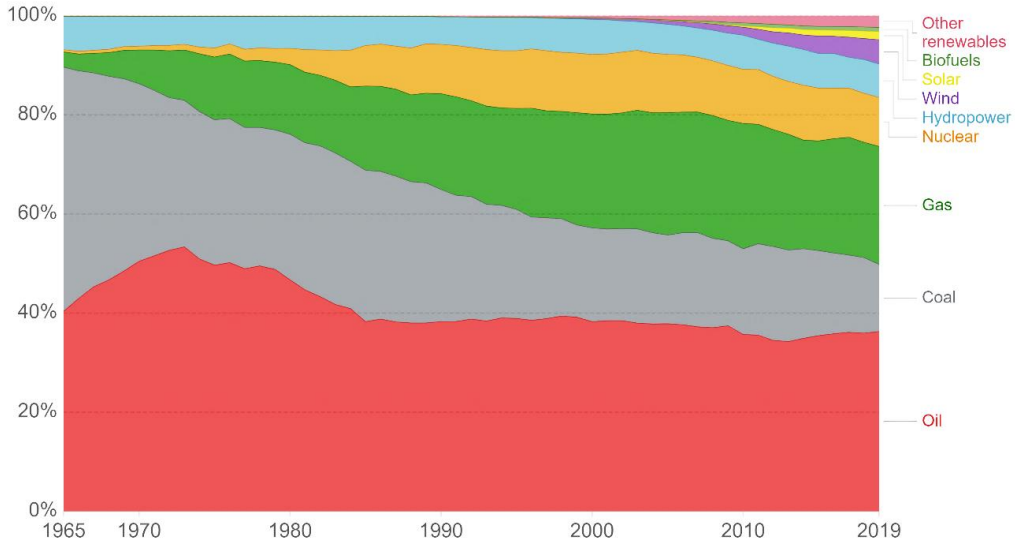

Figure 2 Energy consumption by source in Europe (1965-2019) (Ritchie & Roser, 2020)

Since, environmental awareness has increased in recent decades, with various energy companies launching ambitious climate roadmaps giving reduction goals for the carbon footprint of their operations and the EU setting a target of carbon neutrality by 2050 (European Comission) and a minimum reduction of emissions by 2030 at 55% compared to 1990 (Update of the *NDC*) (European Comission), more attention has been paid to the ways in which the greenhouse gas emissions and the energy demand of industrial activities can be reduced.

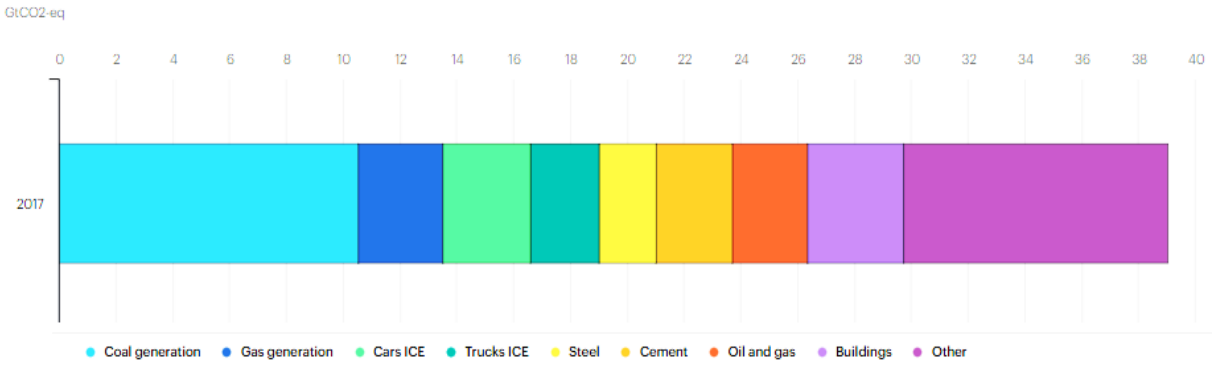

Figure 3 Energy-related greenhouse gas emissions from selected sectors in 2017 (adapted from (IEA, 2019))

The *Paris Agreement* (December 2015) sets out a global framework to avoid dangerous climate change by limiting global warming to well below 2°C (efforts to limit it to 1.5°C). This 2°C goal is thoroughly presented in the *Energy Technology Perspectives 2012* (together with two other scenarios for 2012 to 2050). In all cases, oil and natural gas will remain crucial for the global energy system for decades. Even in the 2 °C scenario (*2DS*) the share of natural gas will initially rise, displacing coal and some growth in nuclear power. Gas-powered generation will increasingly serve as peak-load power after 2030, while oil use will fall by more than 50% by 2050, still playing an important role in transport and as a feedstock in industry. Except for the growing use of renewables, the 2

°C scenario involves the improvement in energy efficiency in the energy production processes. This is driving the need for improved energy efficiency in offshore oil and gas processes. (European Comission), (Voldsund M. , 2014), (Internantional Energy Agency, 2012)

An important tool both in field development projects and installations in production is suitable performance indicators reflecting energy efficiency of the processing plant. Energy efficiency, which is the most commonly use measure for calculating the efficiency of a process is directly associated with energy demands and thus fuel consumption and greenhouse gas emissions. The term is used in numerous contexts and thus its interpretation may vary accordingly. In terms of thermodynamics, the energy efficiency derives from the 1st law of thermodynamics and it is linked to the energy analysis. In that case all kinds of energy are treated as equal, no matter the temperature, pressure etc. of the stream carrying it.

Another approach for the evaluating the efficiency of a process in exergy analysis. Exergy analysis is a result of the combination of the 1st and the 2nd law of thermodynamics and thus it takes into account the entropy production in a real process associated with the decreasing potential to perform work. Exergy analysis provides a better evaluation of the utilization of resources than energy analysis, as it gives the possibility to identify where in a process inefficiencies occur (losses to the environment and internal irreversibilities). (Voldsund M. , 2014)

1.2 Scope of work

The objective of this thesis is to perform an energy and exergy analysis of a typical North Sea offshore processing plant, as well as to calculate and evaluate different thermodynamic performance indicators introduced in literature for a set of different process design parameters and frame conditions. In addition, energy and exergy efficiencies are evaluated in order to identify improvement potentials, suggestions are made and indicators are calculated and assessed. Finally, a simplified method for the evaluation of the indicators is presented, the cases examined are compared and general conclusions are drawn where possible.

1.3 Outline

In the beginning of this diploma thesis (Chapter 2) an overview of the offshore oil and gas processes is presented together with an introduction of the exergy concept and the set of thermodynamic performance indicators investigated in this work. Chapter 3 represents the Base Case study investigated representing a typical North Sea oil and gas processing plant, as well as the results of the energy and exergy analysis and the calculations of the PIs examined. In Chapter 4 the effect of the component chemical exergy on the calculations is investigated, while Chapter 5 and 6 include case studies regarding changes in the frame conditions and the process design parameters, respectively together with the corresponding results. Next, the effect of the oil production lifetime on the indicators is examined in Chapter 7. In Chapter 8 a new idea about enhancing the performance of an oil and gas process is investigated and results are provided. Chapter 9 presents a method for the evaluation of the PIs calculated in

previous analyses and an example of the application of this approach is given. The discussion of the results and the conclusions are offered in Chapters 10 and 11, respectively.

2. Theoretical background

2.1 Offshore oil and gas platforms

In this work the oil and gas processing systems to be studied include a typical offshore oil and gas platform in which the reservoir fluid is processed so that stabilized oil and rich gas are received. The function of the process is described below.

The aim of an offshore oil and gas process is to separate the oil, aqueous and gas phase of the reservoir fluid and produce oil and gas. The oil should be stabilized reaching specifications, such as the TVP (true vapor pressure), while the gas, which is further processed onshore, should meet specifications, such as the CDB (Cricondenbar) and the CDT (Cricondentherm).

Reservoir fluids are complex multiphase mixtures that contain a wide variety of chemical components, which are grouped in three categories:

1. Petroleum or Crude oil: consists mainly of heavy hydrocarbons
2. Natural Gas: consists of lighter hydrocarbons and mostly of methane
3. Water

The aim of an efficient offshore separation of the oil, gas and water phases is to maximize the oil production (oil is the product with the highest energy content) and to minimize its contents of water and gas.

The stabilized oil that is produced offshore is transported to the shore, via pipelines or shuffle tanks. Gas can be exported to the coast via a pipeline network or injected either into the reservoir to enhance oil production or into the oil wells to boost the reservoir fluid lift. The water that is produced is purified and either discharged overboard or injected into the reservoir for pressure maintenance.

It should be pointed out that oil and gas platforms across the world may operate under completely different conditions producing various products. These variations are related to reservoir characteristics (e.g. temperature and pressure, gas-to-oil ratio (GOR)) and reservoir fluid properties (e.g. chemical composition, thermophysical properties), as well as technical requirements (e.g. export temperature and pressure) and technological choices (e.g. number of trains, gas lift).

Overall, in offshore oil and gas process, reservoir fluid streams are separated to gas, oil and water streams. Gas is compressed and either exported to the shore, meeting the specifications required (mainly the CDB specification regarding safe transportation), or reinjected into the reservoir. In some cases, gas is submitted to extra purification from water before being exported to the shore. The oil produced is stabilized, pumped and finally exported to the shore, while water is discharged to the sea, or injected into the reservoir to enhance oil production. (Voldsund M. , 2014)

A typical North Sea offshore platform consists of a processing section, a utility system, drilling modules, and a living quarter as presented in the process diagram of Figure 4. Most of oil and gas platforms follow the same process structure.

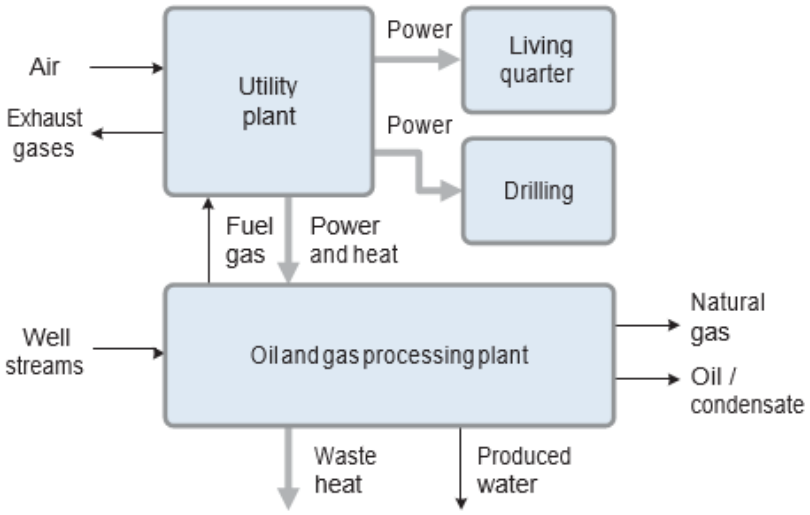

Figure 4 Schematic overview of a typical North Sea oil and gas platform. Black arrows represent material streams, while grey arrows represent energy streams. *(Voldsund M. , 2014)*

The processing section includes the separation of the reservoir fluid into produced water, oil/condensate and gas. As mentioned before, the water produced is purified and discharged or reinjected in the reservoir. The petroleum is processed and delivered at the required quality. Seawater may be, also compressed and injected to enhance oil recovery. Power and heat necessary for compression, pumping as well as separation and gas dehydration, respectively are delivered by the utility system, normally by combusting gas produced at the platform. The utility system also delivers power to the living quarter and to the drilling modules. Gas reinjection is not illustrated in Figure 4. (Voldsund M. , 2014)

A more detailed description of a typical oil and gas platform of the North Sea region is given in the following Figure 5 and Table 1.

Table 1 Description of the subsystems of a typical North Sea oil and gas platform

Sub-system	Description
Production manifold	It consists of valves and chokes, through which the reservoir fluid streams (1) are transferred to the platform, mixed and depressurized to ease further gas and liquid separation in the separation train (2).
Crude oil separation	Oil, gas and water are separated by gravity usually in three stages. The pressure of the well-fluid is decreased by throttling valves and its temperature is increased by preheating with a heat medium at the inlet of each stage, in order to ease the separation of the three phases. The two first stages consist of three-phase separators, the third one consists of a two-phase separator and an electrostatic coalescer (3).
Oil pumping and export	The oil from the separation train mixed with oil and condensate removed in other parts of the processing plant enters the export pumping system where the last traces of gas and water are removed by flashing, the oil is pumped and finally exported onshore (4).
Gas recompression	The gas leaving the separation and oil pumping steps is cooled in heat exchangers and then sent to a scrubber where condensate and water droplets are partly removed. Then the gas is recompressed to the pressure of the previous separation stage (5).
Gas purification (Water removal)	Wet gas enters at the bottom of a packed contactor, in which water is captured by physical absorption with liquid triethylene glycol (TEG). The wet glycol is depressurized to nearly atmospheric pressure and cleaned of water vapour in a desorption column. A small fraction of dry natural gas is sent for stripping in this unit in order to increase the glycol purity to at least 98.5 mol% (6). Regenerated glycol is pumped to its initial pressure and preheated before re-entering the absorber. This step may be skipped.
Gas compression and exportation	Most of the dry gas is sent to the compression train (7) where it is cooled and scrubbed to further remove heavy hydrocarbons, and compressed for storage and export to the shore. A certain fraction of the dry gas is usually recycled to control the volume of gas entering the compressors and to prevent surge issues (anti-surge recycle).
Wastewater treatment	The water from the separation and purification trains enters hydrocyclones in which suspended particulates and dissolved hydrocarbons are removed. It then passes through valves and flows through degassers where the last oil and gas traces are recovered before disposal to the sea (9).
Seawater injection	Seawater is treated on the platform for further injection into the reservoir, in order to sustain high pressure conditions and to enhance oil production. Seawater treatment aims to prevent corrosion and reservoir degradation. Water is thus cleaned before being pumped into the reservoir (10). The seawater injection train includes a succession of filters to remove solid impurities such as sand particles and algae, deoxygenation towers to reduce the oxygen content, booster and high-pressure pumps.
Power generation and heat recovery – Utility system	The utility system is responsible for providing the other processes of the platform with the heat and power required. There the part of the dry gas that is not recompressed is used for power generation directly onsite (8). It is expanded through a succession of valves and combusted with air (11) in gas turbine engines. The waste heat from the exhaust gases is partly used to increase the temperature of the heating medium (glycol-water or hot oils) used in the heat exchangers of the process and the remaining is released to the atmosphere via the stack (12).
Heating, ventilation and air conditioning (HVAC)	
Miscellaneous utilities (e.g. sewage)	

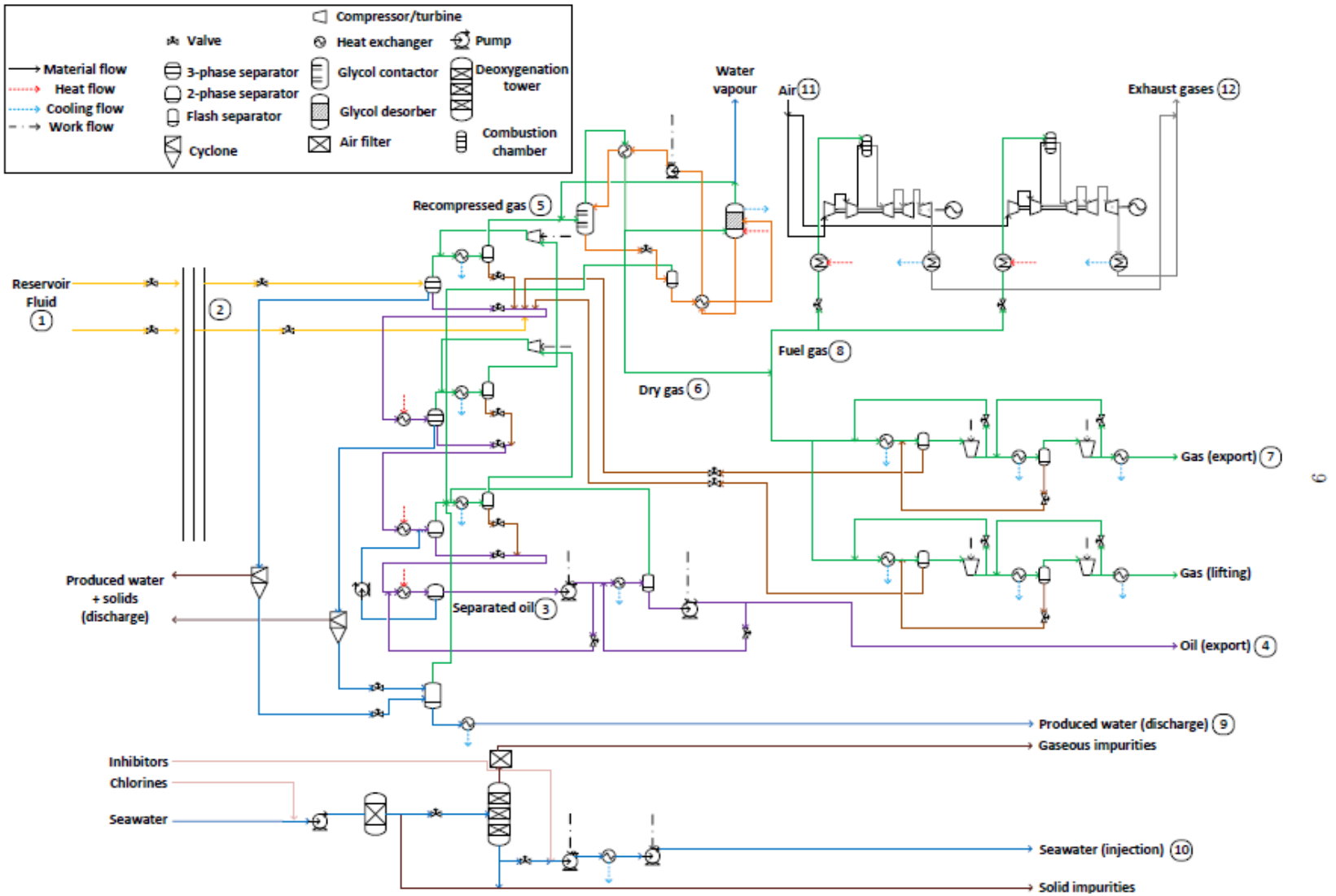

Figure 5 Simplified flow diagram of the offshore platform model *(Nguyen, et al., 2013)*

A North Sea offshore platform like the one presented in Figure 4 exhibits a typical power consumption varying from 10 to some hundreds of MW. It is evident that the work and heat duties of a platform depend on the subprocesses included in the system (e.g. seawater or gas injection used), as well as the integration of the utility plant in the system under investigation. According to similar cases studied in literature the power consumption of a processing plant is around 5 to 30 MW, while the heat required is around 10 MW *(Riboldi & O. Nord, 2017)*. The destroyed exergy may range from 70-80 MW when utilities are not disregarded and 10-30 MW when only the processing plant is taken to be the system at issue. The exergy that is lost to the environment when the utilities are included in the system vary from 30 to 40 MW *(Voldsund M. , 2014)*. The concept of exergy, as well as the terms of exergy losses and exergy destruction are presented in Pragraph 2.2 .

In this work an energy and exergy analysis is conducted for a system that includes the oil and gas processing plant , in which there is no gas purification. The subprocesses included may differ according to the technological choices and configurations of each case under consideration. In the Base case examined in this work water and gas injection, gas lifting, antisurge recycle and wastewater treatment are not taken into consideration.

2.2 Exergy analysis

Exergy analysis constitutes a useful tool for evaluating the utilization of resources giving the possibility to pinpoint where in a process inefficiencies occur: both losses to the surroundings and internal irreversibilities (Voldsund M. , 2014). This is why many performance indicators presented below are based on exergy analysis.

2.2.1 Exergy

The exergy of a system is defined as *the maximum theoretical work obtainable when the system interacts with the environment to reach equilibrium. This maximum theoretical work is obtained when all processes involved are reversible*. Since real processes are not reversible, unlike energy, exergy is not conserved, but some is destroyed due to internal irreversibilities. (Nguayen, Voldsund, Elmegaard, Ertesvåg, & Kjelstrup, 2014)

2.2.2 Exergy rate balance

On a time rate form and for a control volume with in- and outgoing flows, the exergy rate balance is expressed as:

$$\frac{dE_{CV}}{dt} = \sum_k \left(1 - \frac{To}{Tk}\right) \dot{Q}_k - (\dot{W_{cv}} - p_0 \frac{dV_{CV}}{dt}) + \sum \dot{m_{in}} e_{in} - \sum \dot{m_{out}} e_{out} - \dot{Ed} \qquad (1)$$

where $\frac{dE_{CV}}{dt}$ is the rate of change of exergy in the control volume, $\left(1 - \frac{To}{Tk}\right) \dot{Q}_k$ denotes the exergy transfer accompanying heat transfer of the time rate of energy transfer by heat $\dot{Q}_k$ through a surface of temperature Tk. The $\dot{W_{cv}} - p_0 \frac{dV_{CV}}{dt}$ term indicates the exergy transfer accompanying work, with the term $\dot{W_{cv}}$ denoting the time rate of energy transfer by work and the term $p_0 \frac{dV_{CV}}{dt}$ indicating the physical energy flow of the system. $\dot{Ed}$ is the exergy destruction rate (or simply the exergy destruction) inside the control volume and $\sum \dot{m_{in}} e_{in}$, $\sum \dot{m_{out}} e_{out}$ indicate the exergy entering and leaving the system, respectively. The symbol $\dot{m}$ denotes the mass flow rate of a stream of matter and e is

the specific flow exergy of a stream of matter. The subscripts *in* and *out* denote the inlet and outlet of the system and k the boundary of the component.

The symbols To and Tk stand for the environmental and the local temperature where heat transfer takes place, respectively and the symbol p_0 denotes the environmental pressure.

Under steady state conditions $\frac{dE_{CV}}{dt} = 0$ and $\frac{dV_{CV}}{dt} = 0$. (Moran, Shapiro, Boettner, & Bailey, 2019)

In this case, the **steady state exergy rate balance** is received:

$$\dot{Ed} = \sum \dot{E_{in}} - \sum \dot{E_{out}} = \sum_k \left(1 - \frac{To}{Tk}\right) \dot{Q}_k - \dot{W_{cv}} + \sum \dot{m_{in}} e_{in} - \sum \dot{m_{out}} e_{out} \qquad (2)$$

The exergy destruction rate can also be calculated from the Gouy-Stodola theorem, which is expressed as:

$$\dot{Ed} = To\dot{S_{gen}} \qquad (3)$$

where $\dot{S_{gen}}$ is the entropy generation rate inside the control volume.

Exergy destruction is also called *internal exergy losses*, since this is exergy that is lost because of the irreversibilities taking place inside the control volume under consideration. The exergy discharged to the environment without any practical use (e.g. exergy content of exhaust gases from a gas turbine – exergy transferred to the cooling water) is referred to as *external exergy losses* or just *exergy losses* [21,51]. The exergy losses, unlike the exergy destruction, do not result from internal irreversibilities of a system, but rather from the rejection of exergy to the environment without any practical use[13, 86]. The lost exergy is destroyed when the waste streams reach equilibrium while being mixed into the environment. The exergy loss rate $\dot{El}$ is defined (Nguayen, Voldsund, Elmegaard, Ertesvåg, & Kjelstrup, 2014), (Voldsund M. , 2014), (Moran, Shapiro, Boettner, & Bailey, 2019)as:

$$\dot{El} = \sum \dot{E_{rejected}} \qquad (4)$$

where $\dot{E_{rejected}}$ is the exergy rate of each stream discharged to the environment.

Some important quantities in exergy analysis are the following:

- The *product exergy*, E_P, that represents the desired result (expressed in terms of exergy) generated by the system at issue.

- The *utilized exergy*, E_U, or *fuel exergy* (or *exergetic fuel*), E_F that represents the resources (in terms of exergy) used to drive the process being considered.

- The *exergy destruction*, E_D, that represents the thermodynamic inefficiencies of a system associated with the irreversibilities (entropy generation) within the system boundaries.

- The *exergy losses*, E_L, that represent the thermodynamic inefficiencies of a system associated with the transfer of exergy (through material and energy streams) to the surroundings. (Tsatsaronis G. , 2007)

2.2.3 Environment - Equilibrium

Before considering the different forms of exergy it is important to describe two basic concepts used in defining the exergy terms.

2.2.3.1 Environment

The environment is a very large body or medium in the state of perfect thermodynamic equilibrium. This means that no gradients or differences involving pressure, temperature, chemical potential, kinetic or potential energy exist in the environment. Thus, there is no possibility of work production from any form of interaction between parts of the environment.

Any system outside the environment which has one or more parameters different from the corresponding environmental parameter (such as pressure) has a work potential in relation to the environment. The environment, therefore, is a natural reference medium for assessing the work potential of different kinds of systems.

For practical reasons, in cases of terrestrial applications, the environment is considered to consist of the atmosphere, the seas, the oceans, and the earth's crust. The environment can interact with a system through thermal, mechanical or chemical interaction. Through these types of interactions, the environment determines the zero reference levels for pressure, temperature and chemical potential, so exergy can be evaluated. (Kotas T. , 1985)

2.2.3.2 Equilibrium

Two types of equilibrium between the system and the environment are examined: the restricted equilibrium (the environment state) and the unrestricted equilibrium (the dead state).

2.2.3.2.1 Restricted equilibrium – Environmental state

Restricted equilibrium is achieved when the conditions of mechanical and thermal equilibrium between the system and the environment are satisfied. This requires the pressure and the temperature of the system and environment to be equal. This type of equilibrium is called "restricted" as it is achieved when the substances of the system are restrained by a physical barrier that prevents the exchange of matter between system and environment. In this case there is no chemical equilibrium between the system and the environment. The state of restricted equilibrium is called ***environmental state***. (Kotas T. , 1985)

2.2.3.2.2 Unrestricted equilibrium – Dead state

Unrestricted equilibrium is achieved when the conditions of mechanical, thermal and chemical equilibrium between the system and the environment are satisfied. This means that not only the pressures and the temperatures, but also the chemical potentials of the substances of the system and the environment are equal. Under these conditions of full thermodynamic equilibrium, the system cannot undergo any changes of state through any form of interaction with the environment. In this state of unrestricted equilibrium, the exergy of the system is of zero value. This state is called the ***dead state***. (Kotas T. , 1985)

2.2.4 Flow exergy

In the absence of nuclear, magnetic and electrical interactions, the exergy associated with a stream of matter is a function of its physical e^{ph}, chemical e^{ch}, kinetic e^{kin} and potential e^{pot} components (Bejan, Tsatsaronis, & Moran, 1996). The molar exergy of a material stream is expressed as:

$$e = e^{ph} + e^{ch} + e^{kin} + e^{pot} \quad (5)$$

Kinetic and potential contributions on the flow exergies are assumed to be negligible compared to physical and chemical exergies in the case of offshore oil and gas processes. (Nguayen, Voldsund, Elmegaard, Ertesvåg, & Kjelstrup, 2014)

2.2.4.1 Physical exergy

Physical exergy is *equal to the maximum amount of work obtainable when the stream of substance is brought from its initial state to the environmental state defined by P_0 and T_0, by physical processes involving only thermal interaction with the environment*. (Kotas T. , 1985)

Thus, it accounts for temperature and pressure differences from the environmental state and is defined as:

$$e^{ph} = (h - h_0) - T_0(s - s_0) = \underbrace{h - h(T_0, p) - T_0\big(s - s(T_0, p)\big)}_{I} + \underbrace{h(T_0, p) - h_0 - T_0(s(T_0, p) - s_0)}_{II} \quad (6)$$

where *h* and *s* are the specific enthalpy and entropy of a stream of matter, respectively at the temperature and pressure conditions (*T, P*) of the stream. h_0 and s_0 are the specific enthalpy and entropy of the stream at environmental conditions (T_0, P_0).

Terms I and II refer to the *temperature-based* and *pressure-based* components of the physical exergy (Kotas T. , 1995), respectively, and they are also named ***thermal*** and ***mechanical exergies*** (Tsatsaronis G. , 1993). (Nguayen, Voldsund, Elmegaard, Ertesvåg, & Kjelstrup, 2014)

In order to calculate the physical exergy of a stream enthalpy and entropy at the stream (*T, P*) and reference (T_0, P_0) conditions should be evaluated for the same chemical composition (x) of the stream of matter and considering all mixing effects if the stream contains several components. It should be highlighted that this evaluation has to be conducted using the most suitable method for predicting thermodynamic properties for the streams at issue (Rivero, Rendon, & Monroy, 1999).

2.2.4.2 Chemical exergy

Chemical exergy is equal *to the maximum amount of work obtainable when the substance under consideration is brought from the environmental state (T_0, P_0) to the dead state by processes involving heat transfer and exchange of substances only with the environment.* (Kotas T. , 1985)

It results from the deviation of chemical composition of the material under consideration from the composition of the commonly appearing components of the natural environment (reference substances present in the environment). (Nguayen, Voldsund, Elmegaard, Ertesvåg, & Kjelstrup, 2014) Chemical exergy represents the

component of the total available exergy, determined at environmental temperature and pressure and should be taken into account not only in chemical processes, but also in all processes involving changes in compositions of the participating materials (such as mixing and separation). (Szargut J. , 1989)

According to the reference environment defined in works of Szargut (Szargut, Morris, & Steward, 1988), (Szargut J. , 1989), (Morris & Szargut, 1986), the specific chemical exergy of a given mixture is calculated as (Sato, 2004):

$$e^{ch} = \underbrace{\sum_i x_i e_{i,mix}^{ch}}_{I} = \underbrace{\sum_i x_i e_{i,0}^{ch}}_{II} + \underbrace{(\sum_i x_i (h_{i,mix} - h_{i,0})) - T_0 (\sum_i x_i (s_{i,mix} - s_{i,0}))}_{III} \quad (7)$$

where the mass fraction, the chemical component and the mixture are noted by *x*, *i* and *mix*, respectively.

The specific exergy of a given chemical component is expressed as $e_{i,mix}^{ch}$ when it is in the mixture and $e_{i,0}^{ch}$ when it is in a pure component state.

Another expression of the equation (7) is (Voldsund M. , 2014):

$$e^{ch} = \underbrace{\sum_i x_i e_{i,mix}^{ch}}_{I} = \underbrace{\sum_i x_i e_{i,0}^{ch}}_{II} + \underbrace{\left(h_0 - \sum_i x_i h_{i,0} - T_0 \left(s_0 - \sum_i x_i s_{i,0} \right) \right)}_{III} \quad (8)$$

where $h_{i,0}$ is the specific enthalpy of pure *i* at T_0, P_0 and $s_{i,0}$ is the molar entropy of pure *i* at T_0, P_0. Term I illustrates the chemical exergy of each individual chemical component in the mixture, term II the chemical exergy of these components in an unmixed form and term III the reduction in chemical exergy due to mixing effects. If no chemical transformation is taking place within a separation system, the terms related to the chemical exergy of pure components are constant and the change in chemical exergy is equal to the exergy used to perform the separation work (Kotas T. , 1995).

Term II of equation (8) can be calculated using the ***standard chemical exergies*** of the components of the system. Standard chemical exergies for a variety of substances have been calculated and are available in the form of tables. The standard state for which the values of chemical exergy have been computed is defined by the ambient pressure P_0=1.01325 bar and temperature T_0=298.15 K. The reference substances selected for the calculations represent different parts of the environment (atmosphere, earth's crust, seas) assuming that these parts of the environments are in mutual equilibrium. (Kotas T. , 1985)

At this point it is important to highlight the fact that not every component characterizing the reservoir fluid of an oil and gas processing plant corresponds to one chemical compound, but it can represent a group of components with similar characteristics or properties. This kind of component is called **pseudo-component** and this categorization is used in order to limit computational time. It is obvious that this process may lead to losses in accuracy and flexibility in the equation of state calculations. Therefore, considerable effort has been put into the task of formulating

methods that describe the fluids as accurately as possible. (Mahmudi & Sadeghi, 2014)

As far as pseudocomponents are concerned the standard chemical exergy can be determined using empirical expression as a function of the elementary composition and the heating value of each pseudo-component. (Szargut, Morris, & Steward, 1988)

The standard specific chemical exergy (e.g. in kJ/kg) of each pseudo-component is calculated using the following expression:

$$e_{i,0}^{ch} = LHV_i * \beta_i + \sum z_j * e_{j,0}^{ch} \quad (9)$$

where e_i^{ch} is the specific chemical exergy of a pseudo-component i, LHV_i is the lower heating value of the *i* component, β_i is the chemical exergy correction factor of the *i* component, z_j is the mass fraction of the metal *j* or water in the pseudo-component *i* and e_j^{ch} is the corresponding specific standard chemical exergy value found in literature (Szargut, Morris, & Steward, 1988). (Rivero, Rendon, & Monroy, 1999)

The chemical exergy correction factor β_i is a function of the mass fraction of the C, H_2, O_2, S, N_2 in the pseudo-component *i* and is calculated as:

$$\beta_i = 1.0401 + 0.1728\frac{z_{H_2}}{z_C} + 0.0432\frac{z_{O_2}}{z_C} + 0.2169\frac{z_S}{z_C}\left(1 - 2.0628\frac{z_{H_2}}{z_C}\right) + 0.0428\frac{z_{N_2}}{z_C} \quad (10)$$

The lower heating value of the *i* pseudo-component can be calculated using the following equation.

$$LHV = \frac{1}{0.429923}(16840 + 76.60API - 1.230API^2 + 0.008974API^3)\ [kJ/kg] \quad (11)$$

where API is the American Petroleum Institute gravity. The API can be calculated using the specific gravity/relative density SG of the component according to the following equations.

$$API = \frac{141.5}{SG} - 131.5 \quad (12)$$

$$SG = \frac{\rho}{\rho_{H_2O}} \quad (13)$$

where ρ is the density of the component and ρ_{H_2O} is the density of water at 4°C. (Maxwell, 1950), (Munson, Young, & Okiishi, 2002)

In case of an offshore oil and gas process, reactions do not take place, while separation and mixing are used widely throughout the process. In this case the component chemical exergy (term II in equation (8)) can be ignored when calculating the exergy of the streams of such a process, since this type of exergy only passes through the system. The chemical exergy calculated corresponds to the term III of equation (8). However, this approach may give misleading results when absolute numbers of the

exergetic content of each stream are used. This may affect calculations regarding several performance indicators as described later in this work. This is why in the case under discussion the component chemical exergy is taken into account when calculating the chemical exergy of the streams of the process, while an investigation regarding the effect of term II of equation (8) on the results is conducted.

2.3 Thermodynamic performance Indicators

As mentioned above performance indicators constitute a means to evaluate the performance of a process detecting any possible room for improvement and motivating optimal operation of offshore oil and gas platforms. Working in that direction several thermodynamic performance indicators presented in the literature are tested on the Case study presented below and the results are discussed and evaluated.

Thermodynamic performance indicators can be divided into two categories regarding the type of analysis used (energetic or exergetic analysis) giving the *energy-based indicators* and the *exergy-based indicators*. They can be, also further grouped in *efficiencies of the process* and *efficiencies of the subprocesses*, which are based on energy/exergy accounting.

2.3.1 Energy-based Indicators

2.3.1.1 Specific volumes of CO_2 emitted or of Gas consumed onsite

Specific volumes of CO_2 emitted or of *Gas consumed onsite of the fuel*, venting and flaring have been proposed by Svalheim and King (2003) as a measure of the performance of an offshore platform. This indicator expressed in terms of volumetric flow of oil equivalents per oil and gas exported (*Energy Metric %)* is defined as:

$$Energy\ Metric\ \% = \frac{Energy\ consumed\ (barrels\ of\ oil\ equivalent)}{Oil\ and\ gas\ exported\ (barrels\ of\ oil\ equivalent)}$$

These metrics simple enough to be calculated could be misrepresentative and favor facilities that process oil and gas with higher energy contents or platforms with certain operating conditions that achieve their tasks with low power consumption. (Svalheim & King, 2-5 September 2003), (Voldsund, Nguyen, Elmegaard, Ertesvåg, & Kjelstrup, 2014)

These indicators are equivalent to the environmental indicator *Specific CO_2 emissions per unit of produced petroleum* which is widely used in oil and gas industry.

2.3.1.2 Specific energy use

S*pecific energy use* can be given per standard volume of oil equivalent export rate $\dot{V}_{export}$: (Voldsund, Nguyen, Elmegaard, Ertesvåg, & Kjelstrup, 2014)

$$EnU_{volume} = \frac{\dot{W}_{in} + \dot{Q}_{in}}{\dot{V}_{export}} \qquad (14)$$

The standard volume of oil equivalent is used as a measure of energy for the products of an oil and gas company. More specifically, the measure commonly used is the ***Barrel of Oil Equivalent (BOE)*.**

One Barrel of Oil Equivalent is defined as the amount of energy released by burning 1bbl (42gal or 160L) of crude oil. The energy equivalent of a barrel of oil depends on

atmospheric conditions, which results in a range of heating values. Thus, 1 BOE averages 5.8 million Btu, which is roughly equal to 6.1 GJ. The value is necessarily approximate as various grades of oil and gas have slightly different heating values. If one considers the lower heating value instead of the higher heating value, the value for one BOE would be approximately 5.4 GJ. Typically, 5,800 cubic feet of natural gas or 58 CCF (164.2 m^3) are equivalent to one BOE.

In Table *2* Energy Contents of Common Fuels are given. (Martínez, Ebenhack, & Wagner, 2019)

Table 2 Energy Contents of Common Fuels

Fuel Type	Heat Value (Btu/lb)	Heat Value (Btu/vol)	Joule/Volume Equivalent
Dry wood	6621	6621 Btu/ft^3	247 MJ/m^3
Natural gas	20262	983 Btu/ft^3	36 MJ/m^3
Liquid petroleum gas	1961	87664 Btu/gal	24.4 MJ/L
Ethanol	11479	75583 Btu/gal	21.0 MJ/L
Gasoline	18659	114761 Btu/gal	32.0 MJ/L

Usually, as indicated in the indicator EnU_{volume} the term $\dot{V_{export}}$ is expressed in standard cubic meters of oil equivalent (abbreviated as $Sm^3\ o.e.$). This means that the volume flow of both gas and oil (the products of the offshore oil and gas process) is expressed in standard cubic meters of oil equivalent, so that the volume flows correspond to equal amounts of energy content. $\dot{V_{export}}$ stands for the sum of the volume flows of oil and gas expressed in $Sm^3\ o.e.$. Table *3* shows the factors used for the conversions of the oil and gas volume flowrates from Sm^3 to $Sm^3\ o.e.$. (Norwegian Petroleum)

Table 3 Factors for conversions to standard cubic meters of oil equivalent $(Sm^3 o.e.)$

1 Sm^3 oil	=	1 Sm^3 o.e.
1 Sm^3 condensate	=	1 Sm^3 o.e.
1000 Sm^3 gas	=	1 Sm^3 o.e.
1 Sm^3 NGL	=	1 Sm^3 o.e.
1 tonne NGL	=	1 Sm^3 o.e.

Another expression of the *specific energy use* is that given per energy exported.

Since the calorific value of the oil and gas produced on-site differs with the characteristics of the oil field it is relevant to also calculate the *specific energy use* per energy exported, with $\dot{LHV_{export}}$ being the lower heating value export rate.

$$EnU_{energy} = \frac{\dot{W_{in}} + \dot{Q_{in}}}{\dot{LHV_{export}}} \tag{15}$$

EnU_{energy} indicator is the norm in the Norwegian oil and gas industry.

Even if the specific energy indicators are widely used in the oil and gas industry, they usually provide limited information on the performance of the offshore oil and gas processes, as discussed by Svalheim and King (2003) as well as by Margarone et al. (2011). At the same time, these indicators do not take into account the different qualities of power and heat energy. This could lead to unfair comparisons between the different facilities, as important parameters that describe the process are not taken into consideration. These could be specific conditions of the platform such as:

- The field conditions (e.g., initial pressure, temperature, and well-fluid composition)

- The specifications of the oil- and gas-processing system (e.g., the export pressures of the oil-pumping, gas-recompression, and treatment sections)

- The possible additional processes (e.g., condensate treatment, seawater injection, produced-water treatment, crude-oil heating, gas dehydration, and purification) (Voldsund, Nguyen, Elmegaard, Ertesvåg, & Kjelstrup, 2014)

EnU_{energy} indicator (expressed as percentage) can be compared to *the Energy metric %*, which is the percentage of the energy consumed expressed in volume flow compared to the quantity of oil and gas exported expressed in volume flow. (Svalheim & King, 2003)

$$Energy\ Metric\ \% = \frac{Energy\ consumed\ (boe)}{Oil\ and\ gas\ export\ (boe)} \tag{16}$$

The Energy Metric is equivalent to the EnU_{energy} indicator when the *Energy consumed* is calculated in BOE considering the lower heating value for one BOE (5.4 GJ).

In general, a life of field energy metric below 2% is considered as good performance and corresponds to lower CO_2 emissions.

It is pointed out that if the power and heat demands of the process are produced on on-site utilities systems then the *EnU* indicators are representative of the specific CO_2 emissions per unit of oil produced unless CO_2 capture is integrated on the platform.

2.3.1.3 Specific power consumption

Specific power consumption is defined as the power consumed per unit of oil produced. As long as all power comes from the same fossil fuel source, this is proportional to specific CO_2 emissions. This is because power production on an offshore oil and gas platform can also cover the heat duties required. (Nguayen, Voldsund, Elmegaard, Ertesvåg, & Kjelstrup, 2014)

$$Specific\ power\ consumption = \frac{\text{Consumed power}}{\dot{V}_{oil\ produced}} \tag{17}$$

2.3.1.4 BAT efficiency

BAT efficiency proposed by Margarone et al. (2011) is defined as the ratio of the energy content of the fuel required on-site using the Best Available Technology (*BAT*) for compression and pumping, to the energy content of the fuel consumed on-site in the reference case.

$$\eta_{BAT} = \frac{\dot{W}_{BAT,in} + \dot{Q}_{BAT,in}}{\dot{W}_{in} + \dot{Q}_{in}} \quad (18)$$

where the subscript *BAT* denotes that the variable is for a process using *BAT*.

The state-of-the-art components are assumed to be:

- Intercooled compressors suitable for the relevant flow rates (i.e., without gas recirculation to prevent surge) with an isentropic efficiency of 85% and intercoolers with a maximum discharge temperature of 100°C (if intercooling does not cause formation of liquid droplets) and equal pressure ratios in the compression trains with the minimum number of intercoolers
- Pumps suitable for the relevant flow rates with efficiencies of 85%
- Fuel-to-electricity conversion efficiency equal to 52% (referring to Combined cycle gas turbine)

BAT may also include a better process integration.

The BAT efficiency motivates optimal energy management, and thus triggers CO_2 emission reductions. (Voldsund, Nguyen, Elmegaard, Ertesvåg, & Kjelstrup, 2014), (Margarone, et al., March 2011)

It should be emphasized that this indicator could also be used taking into account a state-of-the-art technology different than that presented above based on the various components of the process under examination, as well as the most efficient methods and equipment applicable in that case.

2.3.2 Exergy-based Indicators

2.3.2.1 Specific exergy use

Specific exergy use is the indicator corresponding to the specific energy use in terms of exergy analysis.

The indicator can be given per standard volume of oil equivalent exported as:

$$ExU_{volume} = \frac{\dot{E}_{W,in} + \dot{E}_{Q,in}}{\dot{V}_{export}} \quad (19)$$

Or per exported exergy as:

$$ExU_{exergy} = \frac{\dot{E}_{W,in} + \dot{E}_{Q,in}}{\dot{E}_{export}} \quad (20)$$

where the subscript *W*, *Q* denotes that exergy is transferred to the system with work or heat, respectively.

The term exported exergy refers to the exergy content of oil and gas transported to the shore.

ExU, as well as *EnU* indicators, as mentioned above, are directly related to the specific CO_2 emissions per unit of oil equivalent, as long as the heat and power are produced on on-site utility systems and unless CO_2 capture is integrated on the platform. (Voldsund, Nguyen, Elmegaard, Ertesvåg, & Kjelstrup, 2014)

2.3.2.2 Specific exergy destruction

Specific exergy destruction can be defined per standard volume of oil equivalent exported as:

$$ExD_{volume} = \frac{\dot{E}_d}{\dot{V}_{export}} \tag{21}$$

Or per exported exergy as:

$$ExD_{exergy} = \frac{\dot{E}_d}{\dot{E}_{export}} \tag{22}$$

Exported exergy refers to the exergy content of oil and gas transported to the shore and should not be confused with the term product exergy.

The CO_2 emissions are indirectly related to the ExD indicator, as the amount of destroyed exergy gives rise to fuel use that could have been avoided. (Voldsund, Nguyen, Elmegaard, Ertesvåg, & Kjelstrup, 2014)

2.3.2.3 Exergetic efficiency

Exergetic efficiency ε is:

$$\varepsilon = \frac{E_P}{E_U} \tag{23}$$

This parameter takes into account the minimum theoretical work that has to be done for a given process. The interpretation of E_P and E_U vary. E_P can be defined as the exergy difference between process streams leaving and entering the system and E_U as the power delivered to the process units. This definition is equivalent to the exergetic efficiency presented in the work of de Oliveira Junior and van Hombeeck (1997), except for the fact that they included the utility system in the system and thus they used as utilised exergy the exergy of the fuel gas and not the power consumption. (Voldsund M. , 2014)

As highlighted by Voldsund (2014) the exergetic efficiency defined this way corresponds to the theoretical minimum exergy input required to drive the process with the current boundary conditions for the material streams, divided by the actual exergy input.

The Exergetic efficiency constitutes the basic concept for the development of the Total and Task exergy efficiency presented below for deferent interpretations of the E_P and E_U .

2.3.2.4 Exergy destruction ratio

The *exergy destruction ratio* y_d^* is defined as the part of the exergy destruction rate within the whole system $\dot{E}_d$ that takes place within a specific process component *k* $\dot{E_{d,k}}$ as given in the following equation (Nguyen, et al., 2013):

$$y_d^* = \frac{\dot{E_{d,k}}}{\dot{E}_d} \tag{24}$$

The process component k corresponds to the process k taking place in the system under consideration. Thus, the exergy destruction ratio gives information on the breakdown of the total exergy lost in an offshore oil and gas system.

2.3.2.5 Exergy loss ratio

The *exergy loss ratio* y_l^* is defined as the part of the exergy loss rate of the whole system $\dot{E}_l$ that takes place within a specific process component *k* $\dot{E_{l,k}}$ and it is calculated as (Nguyen, et al., 2013):

$$y_l^* = \frac{\dot{E_{l,k}}}{\dot{E}_l} \tag{25}$$

2.3.2.6 Efficiency defect

Efficiency defect δ_i of substream *i* is the fraction of the input exergy to the whole system E_U which is lost through irreversibilities in the subsystem $E_{D,i}$ (Kotas T. , 1995):

$$\delta_i = \frac{E_{D,i}}{E_U} \tag{26}$$

Efficiency defect δ_i is an indication of the way the different subsystems of the process contribute to the reduction of the exergetic efficiency. (Voldsund M. , 2014)

2.3.2.7 Irreversibility ratio

According to Kotas (1980), (1995) in case of systems that include separators or dissipative devices the relationship between the irreversibilities of a system and its total exergy input can be expressed with the exergy loss ratio *λ*. The exergy loss ratio *λ* represents the proportion of the total exergy flowing into the control volume that is lost through irreversibilities and it is based on the exergetic efficiency definition proposed by Grassmann (Fratzscher, Brodjanskij, & Michalek, 1986). This indicator is also known under the name of *irreversibility ratio* and is calculated as:

$$\lambda = \frac{\dot{I}}{\dot{E}_\iota} \tag{27}$$

where $\dot{I}$ is the rate of irreversibilities of the investigated system and $\dot{E}_\iota$ represents the

total exergy flowing into the control volume. (Nguyen, et al., 2013)

The *irreversibility ratio* λ is representative of the total control volume and not of the subsystems of it.

2.3.2.8 Total exergy efficiency

The exergy balance of a system at steady state presented in Equation 2 can be also expressed as:

$$\sum \dot{E_{in}} = \sum \dot{E_{out}} + \dot{E_d} = \sum \dot{E_{out,u}} + \sum \dot{E_{out,l}} + \dot{E_d} \tag{28}$$

describing an open thermodynamic system where $\dot{E_{in}}$ and $\dot{E_{out}}$ are the exergy inputs and outputs of the system, respectively that are associated with streams of matter and of energy, and $\dot{E_d}$ is the exergy destruction. The exergy output can be divided into useful $\dot{E_{out,u}}$ and lost $\dot{E_{out,l}}$ exergy output. The former represents the amount of exergy found in the products of the process, while the latter represents the exergy of the waste products that is not used, but discharged to the environment.

Two are the main expressions of the *Total exergy efficiency* that derive from the exergy balance of Equation 28:

1. The *total exergy efficiency* ε_{I-1} (known also as overall, input-output, universal exergy efficiency) that is defined as the ratio of all exergy outflows to inflows.

$$\varepsilon_{I-1} = \frac{\sum_{out} \dot{E_{out}}}{\sum_{in} \dot{E_{in}}} = 1 - \frac{\dot{E_d}}{\sum_{in} \dot{E_{in}}} \tag{29}$$

2. The *total exergy efficiency* ε_{I-2} that takes into account only the useful exergy outputs of the system.

$$\varepsilon_{I-2} = \frac{\sum_{out,u} \dot{E_{out,u}}}{\sum_{in} \dot{E_{in}}} = 1 - \frac{\sum_{out,l} \dot{E_{out,l}} + \dot{E_d}}{\sum_{in} \dot{E_{in}}} \tag{30}$$

Voldsund (2014) highlights that according to previous works *Total exergy efficiency* is considered to be adequate when (i) the ingoing and outgoing exergy flows are converted to other forms of exergy (Cornelissen R. , 1997) or (ii) a major part of the out-flowing exergy can be considered as useful, as it is the case of power plants (Lior & Zhang, 2007) or (iii) for dissipative processes and devices (BP, 2013), (Manning & Thompson, 1991).

The two equations of the *Total exergy efficiency* presented above can be applied to an oil and gas processing plant according to the following reasoning. Figure 6 shows schematically the exergy streams entering and leaving the processing plant, as well as the utility plant and clarifies the notation used in the analysis below. (Nguayen, Voldsund, Elmegaard, Ertesvåg, & Kjelstrup, 2014), (Voldsund M. , 2014), (Voldsund, Nguyen, Elmegaard, Ertesvåg, & Kjelstrup, 2014)

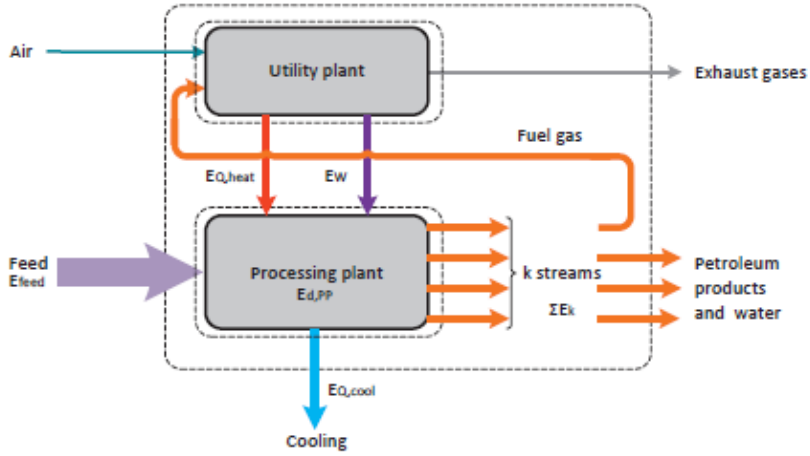

Figure 6 Schematic overview of exergy streams entering and exiting the processing and utility plants. *(Voldsund M. , 2014)*

A feed stream (i.e. reservoir fluid) enters the processing plant with an exergy content of $\dot{E}_{feed}$. Heat and work delivered by the utility plant are added to the system in the form of heat $\dot{E}^{\dot{Q}}_{heat}$ and power $\dot{\mathrm{E}}^{\mathrm{W}}$ exergy, respectively in order to receive the useful products of the process (i.e. oil, gas condensate, fuel gas) which carry an exergy of $\sum_{k,u} \dot{E}_{k,u}$ (or $\sum_{out,u} \dot{E}_{out,u}$). Together with the useful material streams a number of wasted outlet streams is produced, too (i.e. flared gas, produced water) with an exergy content of $\sum_{k,w} \dot{E}_{k,w}$. Exergy is, also lost in the process due to cooling ($\dot{E}^{\dot{Q}}_{cool}$), because of the thermal energy leaving the plant through the cooling system. An amount of exergy is additionally destroyed due to internal irreversibilities ($\dot{E}_{d,PP}$) taking part in the process: the destroyed exergy. The sum of the exergy added in the stream through the feed, heating and compression or pumping work is considered to be the input exergy $\sum_{in} \dot{E}_{in}$ of the stream, while the useful outlet material streams are counted as useful output exergy $\sum_{out,u} \dot{E}_{out,u}$. The exergy lost due to the waste stream or cooling comprises the lost exergy of the system $\sum_{out,l} \dot{E}_{out,l}$.

So the exergy balance that describes the processing plant of an oil and gas facility can be expressed as:

$$\underbrace{\dot{E}_{feed} + \dot{E}^{\dot{Q}}_{heat} + \dot{\mathrm{E}}^{\mathrm{W}}}_{\sum_{in} \dot{E}_{in}} = \underbrace{\sum_{k,u} \dot{E}_{k,u}}_{\sum_{out,u} \dot{E}_{out,u}} + \underbrace{\sum_{k,w} \dot{E}_{k,w} + \dot{E}^{\dot{Q}}_{cool}}_{\sum_{out,l} \dot{E}_{out,l}} + \underbrace{\dot{E}_{d,PP}}_{\dot{E}_d} \qquad (31)$$

It should be noted that the produced water which is extracted along with oil and gas is normally considered as waste, since it is discharged to the surroundings without being used. The exception to this rule is if the produced water is injected back for enhanced oil recovery. (Voldsund M. , 2014)

The above-mentioned exergy balance of the oil and gas processing plant results in the following total exergy efficiencies. (Voldsund, Nguyen, Elmegaard, Ertesvåg, & Kjelstrup, 2014), (Voldsund M. , 2014)

1. The *total exergy efficiency* of an oil and gas process system without differentiating the useful from the waste streams is expressed as (Nesselmann, 1952):

$$\varepsilon_{I-1} = \frac{\sum_{k,u} \dot{E_{k,u}} + \sum_{k,w} \dot{E_{k,w}} + \dot{E_{cool}^{Q}}}{\dot{E_{feed}} + \dot{E_{heat}^{Q}} + \dot{\mathrm{E}^{\mathrm{W}}}} \tag{32}$$

2. And the *total exergy efficiency* considering only the useful streams:

$$\varepsilon_{I-2} = \frac{\sum_{k,u} \dot{E_{k,u}}}{\dot{E_{feed}} + \dot{E_{heat}^{Q}} + \dot{\mathrm{E}^{\mathrm{W}}}} \tag{33}$$

A complete overview of the definition and the different expressions of the *Total exergy efficiency* is given by Voldsund (2014) .

2.3.2.9 Task exergy efficiency

Task exergy efficiency has been proposed in order to address the deficiencies of the *Total exergy efficiency* which has been criticised for considering all the inlet and outlet exergy flows of a system, including, also the part of the exergy that does not undergo any thermodynamical conversion just flowing in and out the system. The *task exergy efficiency*, on the other hand, distinguishes the exergy flows that are submitted to transformations from these that do not undergo any changes, such as the exergy streams of a system that are neither used or produced.

Grassmann (1950) first suggested a general definition of the *Task exergy efficiency* as *the ratio of the intended increase to the used decrease in ability to do work* or in other words *the ratio of the production of exergy that is desired to the reduction of exergy that is utilised*. This definition is directly associated with the *exergetic product* and the *exergetic fuel* presented in paragraph 2.2 .

A variant of this formulation was given by Baehr (1950) who considered *the ratio of all the exergy increases to all the exergy decreases* without taking into account whether the exergy flows are produced or utilised.

Next Szargut (1980), (1988), (1998) and Kotas (1980), (1995) based on the reasoning of Grassmann (1950) argued that the exergy efficiency should be defined as *the ratio of the desired output or useful exergetic effect and the necessary input or driving exergy expense*. As also, mentioned above these terms correspond to the *exergetic product* $\dot{E_P}$ and the *exergetic fuel* $\dot{E_F}$, respectively. In this case the *Task exergy efficiency* is defined as:

$$\varepsilon_{II-1} = \frac{\dot{E_P}}{\dot{E_F}} = 1 - \frac{\dot{E_l} + \dot{E_d}}{\dot{E_F}} \tag{34}$$

where $\dot{E_l}$ is the exergy lost to the environment, $\dot{E_d}$ is the destroyed exergy and the *exergetic product* $\dot{E_P}$ is defined as:

$$\dot{E_P} = \dot{E_F} - \dot{E_l} - \dot{E_d} \quad (35)$$

It should be emphasized that (i) exergy efficiencies based on exergy differences exhibit a higher sensitivity to changes in the system compared to the total exergy efficiency and (ii) different numerical values could be obtained with the formulation of exergy efficiency proposed by Grassmann (1950), depending on whether an exergy difference is considered as *useful*, *used* or none of those.

Brodyansky (1994) and Sorin (1994) (Brodyansky, Sorin, & Le Goff, 1994), (Sorin, Paris, & Brodjanskij, 1994) proposed a different definition of the exergy efficiency based on the concept of *transit exergy* which was introduced by Kostenko (Brodyansky, Sorin, & Le Goff, 1994)), and further developed by Brodyansky (Brodyansky, Sorin, & Le Goff, 1994). In this case the exergy efficiency is defined as *the ratio of the total exergy output to the total exergy input*, *minus the transit* exergy $\dot{E}_{tr}$ in both numerator and denominator:

$$\varepsilon_{II-2} = \frac{\sum_{out} \dot{E_{out}} - \sum_{tr} \dot{E_{tr}}}{\sum_{in} \dot{E_{in}} - \sum_{tr} \dot{E_{tr}}} \quad (36)$$

The transit exergy is the part of the exergy supplied to a system that flows through the system without undergoing any physical or chemical transformation.

This concept was also mentioned by Cornelissen (1997), who applied this method to an air separation unit and a crude oil distillation plant. The lack of ambiguity and the complexity of the calculations were underlined, as this method requires a precise decoupling of the exergy flows into their components. This efficiency can also be regarded as a variant of the *total exergy efficiency*. (Voldsund M. , 2014)

Based on the definition of the *Task exergy efficiency* given by Szargut (1980), (1988), (1998) and Kotas (1980) various concepts that describe the efficiency of a petroleum system through considering different fuel and product exergies have been developed in literature. Some of these have been summarized in the work of Voldsund (2014) and they are presented in Table *4*.

Table 4 The concepts of task exergy efficiencies for petroleum systems found in literature *(Voldsund M. , 2014)*

System	Fuel	Product
General separation **(1995)** Offshore platform **(2002)**, **(2013)**	Added heat and work	Physical and chemical exergy changes
LNG plant **(2012)** Crude oil distillation **(1997)**	Added heat and work +input physical exergy	Chemical exergy increase +output physical exergy
Distillation **(2002)**	Added heat and work +physical exergy decrease	Chemical exergy increase +output physical exergy

The *Task exergy efficiency* can be applied to an oil and gas processing plant based on the analysis conducted by Kotas (1995) (Equation 34)and used by Oliveira and Van Hombeeck (1997) for petroleum separation processes on a Brazilian offshore platform. The same method has been used for the processing plant of a North Sea oil platform by Voldsund et al. (Voldsund, He, Røsjorde, Ertesv°ag, & Kjelstrup, 2012), (Voldsund I. , Ertesv°ag, He, & Kjelstrup, 2013), (Voldsund M. , Ertesv°ag, Røsjorde, He, & Kjelstrup, 2010) representing the first case presented in Table 4.

For this analysis the same reasoning as that of the *Total exergy efficiency* is applied, based on the schematic overview of the exergy streams given in Figure 6.

The exergy balance for the processing plant of Equation 37 can be rewritten as:

$$\underbrace{\dot{E^Q_{heat}} + \dot{\mathrm{E}^{\mathrm{W}}}}_{\dot{E_f}} = \underbrace{\sum_{k,u} \dot{E_{k,u}} - \dot{E_{feed}}}_{\dot{E_p}} + \underbrace{\dot{E^Q_{cool}}}_{\dot{E_l}} + \underbrace{\dot{E_{d,PP}}}_{\dot{E_d}} \tag{37}$$

The left-hand side terms represent the resources required to drive the processing plant (the exergetic fuel $\dot{E_f}$), while the exergetic product $\dot{E_p}$ is defined as the difference of exergy between the inlet and outlet material streams.

This expression of the exergy balance highlights that the desired effect of the offshore platforms is the exergy increase between the inlet and outlet streams (i.e. due to separation or physical processes such as compression), while the resources required to drive the processing plant and separate the three phases correspond to the exergy of heat and power required on-site. The exergy destruction $\dot{E_d}$ represents the exergy destroyed due to internal irreversibilities. The exergy that is lost to the environment corresponds to the exergy of cooling ($\dot{E^Q_{cool}}$) leaving the plant through the cooling system.

The formulation of the exergy efficiency received from the exergy balance of Equation 37 is:

$$\varepsilon_{II-3} = \frac{\sum_{k,u} \dot{E_{k,u}} - \dot{E_{feed}}}{\dot{E^Q_{heat}} + \dot{\mathrm{E}^{\mathrm{W}}}} = 1 - \frac{\dot{E^Q_{cool}} + \dot{E_{d,PP}}}{\dot{E^Q_{heat}} + \dot{\mathrm{E}^{\mathrm{W}}}} \tag{38}$$

However, calculations of this efficiency can lead to negative results if the exergy of the feed streams is higher than the exergy of the output streams. This can be a result of higher input pressures and temperatures of the input streams in comparison to the pressures and temperatures of the oil and gas streams. In this case, there is no need for gas compression for exportation and the reductions of physical exergy greatly outweigh the increases of chemical exergy, leading to negative task exergy efficiencies.

Taking that into account it has been suggested that the differences of physical and chemical exergy between the input and the output streams are considered apart. This is how the next expression for the task exergy efficiency was developed.

An alternative expression of the exergy balance for an air distillation plant was suggested by Kotas (1995), where the physical and chemical exergy in the material streams are treated separately, as presented in Equation 39.

$$\underbrace{E_{feed}^{\dot{ph}} + E_{heat}^{\dot{Q}} + \mathrm{E}^{\dot{\mathrm{W}}}}_{\dot{E_f}} = \sum_{k} E_{k}^{\dot{ch}} - E_{feed}^{\dot{ch}} + \sum_{k,u} E_{k,u}^{\dot{ph}} + \sum_{k,\mathrm{w}} E_{k,\mathrm{w}}^{\dot{ph}} + E_{cool}^{\dot{Q}} + \dot{E_{d,PP}}$$

$$= \underbrace{\Delta \mathrm{E}^{ch} + \sum_{k,u} E_{k,u}^{\dot{ph}}}_{\dot{E_p}} + \underbrace{\sum_{k,\mathrm{w}} E_{k,\mathrm{w}}^{\dot{ph}} + E_{cool}^{\dot{Q}}}_{\dot{E_l}} + \underbrace{\dot{E_{d,PP}}}_{\dot{E_d}} \tag{39}$$

According to this formulation the exergetic fuel is taken to be the sum of the exergy transferred in the form of heat, $E_{heat}^{\dot{Q}}$, power, $\mathrm{E}^{\dot{\mathrm{W}}}$ and the physical exergy of the feed $E_{feed}^{\dot{ph}}$. The difference of chemical exergies between the inlet and outlet streams of the processing plant, $\Delta \mathrm{E}^{ch}$, as well as the physical exergy of the useful output streams $\sum_{k,u} E_{k,u}^{\dot{ph}}$ represent the exergetic product of the process. In this case exergy is lost due to cooling $E_{cool}^{\dot{Q}}$ and the wasted outlet material streams $\sum_{k,w} E_{k,w}^{\dot{ph}}$, while $\dot{E_{d,PP}}$ is the exergy that is destroyed in the system.

The expression of the *task exergy efficiency* that corresponds to the exergy analysis previously described is given by:

$$\varepsilon_{II-4} = \frac{\Delta \mathrm{E}^{ch} + \sum_{k,u} E_{k,u}^{\dot{ph}}}{E_{feed}^{\dot{ph}} + E_{heat}^{\dot{Q}} + \mathrm{E}^{\dot{\mathrm{W}}}} = 1 - \frac{\sum_{k,\mathrm{w}} E_{k,\mathrm{w}}^{\dot{ph}} + E_{cool}^{\dot{Q}} + \dot{E_{d,PP}}}{E_{feed}^{\dot{ph}} + E_{heat}^{\dot{Q}} + \mathrm{E}^{\dot{\mathrm{W}}}} \tag{40}$$

It should be noted that the formulation presented above is similar to the one applied by Cornelissen (1997) for a crude oil distillation plant and by Rian and Ertesvåg (2012) for an LNG plant. In these cases, the physical exergy of the feed streams is consumed along with exergy associated with heat and power. The desired result is the physical exergy of the outlet streams together with the chemical exergy increase due to separation. This approach represents the second case of Table 4.

Another approach for the *task exergy efficiency* was proposed by Tsatsaronis and Cziesla (2002) that considers the physical exergy decreases together with the heat and power consumed on-site as the exergetic fuel, while the exergetic product consists of the physical exergy increases and the chemical exergy increase between the inlet and the outlet streams of the process. This method based on previous works of Baehr (1950) and Grassmann (1950) can be found in compliance with the SPECO analysis proposed by Lazzaretto and Tsatsaronis (1999), (2006) and Cornelissen & Hirs (2002). (Voldsund M. , 2014)

The distinctive feature of this method presented here is the form in which exergy increases and decreases are used. The physical exergy decreases and increases are defined in terms of specific physical exergies of the outlet and inlet streams on a mass basis (Voldsund M. , 2014).

More specifically, this formulation implies that the fuel exergy is the sum of the physical exergy decreases between the inflowing feed and all the separated streams with a lower specific physical exergy (e^{ph}) (k-) and the exergy associated with heating and power. The product exergy is defined as the sum of the physical exergy increases between the inflowing feed (feed) and the separated useful products with a higher specific physical exergy (k+,u) and the chemical exergy increases between the feed and products. The

lost exergy is considered to be the physical exergy difference between the inflowing feed and the wasted products with a higher physical exergy (k+,w) (if any) along with the exergy lost due to cooling. (Voldsund M. , 2014)

So the exergy balance of the Equation can be rewritten as:

$$\underbrace{\sum_{k-} \dot{m}_{k-} * (e^{ph}_{feed} - e^{ph}_{k-}) + \dot{E}^{Q}_{heat} + \dot{\mathrm{E}}^{\mathrm{W}}}_{\dot{E}_f} = \sum_{k} \dot{E}^{ch}_{k} - \dot{E}^{ch}_{feed} + \sum_{k,u} \dot{E}^{ph}_{k,u} + \sum_{k,\mathrm{w}} \dot{E}^{ph}_{k,\mathrm{w}} + \dot{E}^{Q}_{cool} + \dot{E}_{d,PP}$$
$$= \underbrace{\Delta \mathrm{E}^{ch} + \sum_{k+,u} \dot{m}_{k+,u} * (e^{ph}_{k+,u} - e^{ph}_{feed})}_{\dot{E}_p} + \underbrace{\sum_{k+,\mathrm{w}} \dot{m}_{k+,w} * (e^{ph}_{k+,w} - e^{ph}_{feed}) + \dot{E}^{Q}_{cool}}_{\dot{E}_l} + \underbrace{\dot{E}_{d,PP}}_{\dot{E}_d} \quad (41)$$

And the following expression for the *task exergy efficiency* is given:

$$\varepsilon_{II-5} = \frac{\Delta \mathrm{E}^{ch} + \sum_{k+,u} \dot{m}_{k+,u} * (e^{ph}_{k+,u} - e^{ph}_{feed})}{\sum_{k-} \dot{m}_{k-} * (e^{ph}_{feed} - e^{ph}_{k-}) + \dot{E}^{Q}_{heat} + \dot{\mathrm{E}}^{\mathrm{W}}}$$
$$= 1 - \frac{\sum_{k+,\mathrm{w}} \dot{m}_{k+,w} * (e^{ph}_{k+,w} - e^{ph}_{feed}) + \dot{E}^{Q}_{cool} + \dot{E}_{d,PP}}{\sum_{k-} \dot{m}_{k-} * (e^{ph}_{feed} - e^{ph}_{k-}) + \dot{E}^{Q}_{heat} + \dot{\mathrm{E}}^{\mathrm{W}}} \quad (42)$$

This approach corresponds to the third case of Table 4, which is the application of the afore-mentioned method for a generalized distillation column presented by Tsatsaronis and Cziesla (Cornelissen & Hirs, 2002).

Voldsund (2014) has applied this expression of the *task exergy efficiency* also on a molar basis highlighting that if a molar basis is selected the indicators return different values and conclusions, due to the different compositions of the inlet and outlet streams of the process. In the case of distillation columns that separate similar components, the two expressions are expected to give similar results. However, inconsistencies can be much higher for the oil and gas processes at issue because of the highly different chemical components treated. (Voldsund M. , 2014)

2.3.2.10 Component-by-component exergy efficiency

Voldsund (2014) emphasizes in her work that there is no straightforward definition of the exergy efficiency of an oil and gas processing plant. This is because in such processes there is (i) a high amount of transit chemical exergy (and sometimes also physical exergy) of the hydrocarbon components passing through the system without undergoing any change. There is, also (ii) a great variety of chemical components, as well as (iii) various differences in the process conditions and the product specifications of the platforms.

To this effect a different formulation of the exergy efficiency was proposed (Voldsund M. , 2014) which builds on the same reasoning as presented in the work of Tsatsaronis and Cziesla (Tsatsaronis & Park, 2002) considering the concept of the *transit exergy* (developed by Brodyansky (1994)) and carried out on a chemical component level. This new indicator is known under the name of *Component-by-Component exergy efficiency*.

In order to better understand the way the physical exergies are defined based on a chemical component level, a schematic overview of the component flows for a system with two components, two feeds and two products is given in Figure 7. This approach is thoroughly presented by Voldsund (2014).

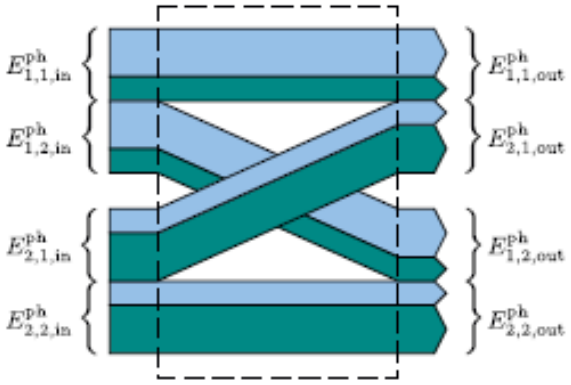

Figure 7 Schematic overview of component flows in and out of a control volume for a system with two components marked with different colors, two feeds at the left and two product streams at the right. *(Voldsund M. , 2014)*

$E^{\dot{ph}}_{J,k,in}$ is the physical exergy of a stream coming from feed j and ending up in product k at the inlet of the process, while $E^{\dot{ph}}_{J,k,out}$ is the exergy of the same stream at the outlet of the process. It should be pointed out for clarification that these two exergy streams consist of the same components.

In order to calculate the physical exergies $E^{\dot{ph}}_{J,k,in}$ and $E^{\dot{ph}}_{J,k,out}$ the following equations are used:

$$E^{\dot{ph}}_{J,k,in} = \sum_i \dot{n_{i,J,k}}\, \widehat{e^{ph}_{i,J}} \tag{43}$$

$$E^{\dot{ph}}_{J,k,out} = \sum_i \dot{n_{i,J,k}}\, \widehat{e^{ph}_{i,k}} \tag{44}$$

where $\widehat{e^{ph}_{i,J}}$ is the partial molar physical exergy of the component i in the feed stream j and $\widehat{e^{ph}_{i,k}}$ is the partial molar physical exergy of the component i in product stream k. $\dot{n_{i,J,k}}$ denotes the molar flow of the component i from feed j to product k. The partial molar physical exergy of component i is defined as:

$$\widehat{e^{ph}_{i,J}} = \left(\frac{\partial E^{ph}}{\partial n_i}\right)_{T,P,n_{l\neq 1}} \tag{45}$$

And it should not be confused with the molar physical exergy.

The calculations of the physical exergies are conducted under the assumption that the fraction of the component ending up in each product stream is the same as the fraction

of the total amount of this component entering as feeds ending up in each product stream for each component in each feed stream. (Voldsund M. , 2014)

An example of how exergy flows are defined is given in Appendix B for a simplified flash separator.

Moving on to defining the physical exergy increases and decreases, physical exergy increases of parts of streams can be expressed mathematically as:

$$\left(\Delta \dot{E}^{ph}_{J,k}\right)^{+} = \begin{cases} E^{p\dot{h}}_{J,k,out} - \dot{E}^{ph}_{J,k,in} & if\ E^{p\dot{h}}_{J,k,out} > \dot{E}^{ph}_{J,k,in} \\ 0 & if\ E^{p\dot{h}}_{J,k,out} < \dot{E}^{ph}_{J,k,in} \end{cases} \tag{46}$$

Oppositely, physical exergy decreases of parts of streams can be expressed as:

$$\left(\Delta \dot{E}^{ph}_{J,k}\right)^{-} = \begin{cases} 0 & if\ E^{p\dot{h}}_{J,k,out} > \dot{E}^{ph}_{J,k,in} \\ E^{p\dot{h}}_{J,k,in} - \dot{E}^{ph}_{J,k,out} & if\ E^{p\dot{h}}_{J,k,out} < \dot{E}^{ph}_{J,k,in} \end{cases} \tag{47}$$

The exergy balance equation can, thus be rewritten as:

$$\underbrace{\sum_{j}\sum_{k}\left(\Delta \dot{E}^{ph}_{J,k}\right)^{-} + \dot{E}^{Q}_{heat} + \dot{\mathrm{E}}^{\mathrm{W}}}_{\dot{E}_f} = \underbrace{\Delta \dot{E}^{ch} + \sum_{j}\sum_{k,u}\left(\Delta \dot{E}^{ph}_{J,k}\right)_{u}^{+}}_{\dot{E}_p} + \underbrace{\sum_{j}\sum_{k,w}\left(\Delta \dot{E}^{ph}_{J,k}\right)_{w}^{+} + \dot{E}^{Q}_{cool}}_{\dot{E}_l} + \underbrace{\dot{E}_{d,PP}}_{\dot{E}_d} \tag{48}$$

In this case the exergetic product consists of the chemical exergy increase between the inlet and outlet streams of the process, as well as the increases in physical exergy of the useful product streams $\sum_j \sum_{k,u}\left(\Delta \dot{E}^{ph}_{J,k}\right)_u^{+}$. The fuel exergy of the system is considered to be the exergy of heat and work along with the decrease of physical exergy of all the fractions that lose physical exergy on the way from feed to product $\sum_j \sum_k \left(\Delta \dot{E}^{ph}_{J,k}\right)^{-}$. The lost exergy is taken as the sum of the decrease in physical exergy of the fractions that gain exergy going from the feed to a waste product $\sum_j \sum_{k,w}\left(\Delta \dot{E}^{ph}_{J,k}\right)_w^{+}$ and the exergy of cooling. The first term of the lost exergy is usually of zero value as no waste product shows an increase in exergy compared to the feed. The destroyed exergy $\dot{E}_{d,PP}$ represents the exergy lost because of internal irreversibilities.

It should be noted that for each feed stream, different parts may end up in different products. This is why, the physical exergy of each such part in the feeds are compared with the physical exergy of the corresponding parts in the products.

The exergy balance of Equation 48 results in the following expression for the exergy efficiency:

$$\varepsilon_{III} = \frac{\Delta \dot{E}^{ch} + \sum_j \sum_{k,u} \left(\Delta \dot{E}_{j,k}^{ph}\right)_u^+}{\sum_j \sum_k \left(\Delta \dot{E}_{j,k}^{ph}\right)^- + \dot{E}_{heat}^{Q} + \dot{\mathrm{E}}^{\mathrm{W}}} = 1 - \frac{\sum_j \sum_{k,w} \left(\Delta \dot{E}_{j,k}^{ph}\right)_w^+ + \dot{E}_{cool}^{Q} + \dot{E}_{d,PP}}{\sum_j \sum_k \left(\Delta \dot{E}_{j,k}^{ph}\right)^- + \dot{E}_{heat}^{Q} + \dot{\mathrm{E}}^{\mathrm{W}}} \quad (49)$$

This approach is based on the fact that in separation processes there is no change in the chemical components of the inlet and outlet streams, but the only parameter changing is the quantities of the components and the conditions of the streams. The main point of this formula is that different types of chemical components carry different quantities of physical exergy, because of their different enthalpies and the entropies at the same environmental conditions. For that reason, more accurate conclusions can be drawn through decomposing the physical exergy of a stream into the physical exergy per chemical component. As it is highlighted by Nguyen and Voldsund (Nguayen, Voldsund, Elmegaard, Ertesvåg, & Kjelstrup, 2014), (Voldsund M. , 2014) in this way the allocation of an exergy flow as an exergy product or fuel will depend solely on the partial physical exergy, which is a function of the temperature and pressure conditions, and not on whether the specific or molar exergy of the stream of interest is smaller or higher than of the feed stream.

It is important to highlight that calculations based on this method do not depend on whether a mas or molar basis is chosen, while at the same time the formulation does not concern only oil and gas platform, but can be generalised to various separation processes. (Voldsund M. , 2014), (Nguayen, Voldsund, Elmegaard, Ertesvåg, & Kjelstrup, 2014)

2.3.2.11 Exergetic efficiency of a component k

Another expression of the exergy efficiency is that of the *Exergetic efficiency of a k component* η_k that investigates separately each k component taking part in the process through identifying the fuel and product of interest, as described above. $\dot{E}_{f,k}$ is the fuel exergy of the k component and $\dot{E}_{P,k}$ stands for the product exergy of the k component. It is marked that the fuel and product exergies are not necessarily equal to the input $\dot{E}_{i,k}$ and output $\dot{E}_{o,k}$ exergies of the k component. (Nguyen, et al., 2013)

$$\eta_k = \frac{\dot{E}_{P,k}}{\dot{E}_{f,k}} = 1 - \frac{\dot{E}_{d,k} + \dot{E}_{l,k}}{\dot{E}_{f,k}} \quad (50)$$

Other analysis presented in literature that define new performance indicators for the evaluation of an oil and gas process based on exergy analysis are the following:

- Exergoeconomic analysis
- Exergoenvironmental analysis
- Advanced exergy-based analysis

However, since these analyses require a wide range of data, as well as complex calculating operations they are outside the scope of this work.

The indicators calculated in this work above can be found in Table 5.

Table 5 The thermodynamic indicators under investigation

	Energy-exergy efficiency		**Energy-Exergy accounting**	
Energy-based	Specific CO_2 emissions per unit of produced petroleum			
	Specific energy use	$EnU_{volume} = \frac{\dot{W}_{in} + \dot{Q}_{in}}{\dot{V}_{export}}$		
		$EnU_{energy} = \frac{\dot{W}_{in} + \dot{Q}_{in}}{\dot{LHV}_{export}}$		
	Specific power consumption	$Specific\ power\ consumption = \frac{\text{Consumed power}}{\dot{V}_{oil\ produced}}$		
Exergy-based	Specific exergy use	$ExU_{volume} = \frac{\dot{E}_{W,in} + \dot{E}_{Q,in}}{\dot{V}_{export}}$	Exergy loss ratio	$y_l^* = \frac{\dot{E}_{l,k}}{\dot{E}_l}$
		$ExU_{exergy} = \frac{\dot{E}_{W,in} + \dot{E}_{Q,in}}{\dot{E}_{export}}$		
	Specific exergy destruction	$ExD_{volume} = \frac{\dot{E}_d}{\dot{V}_{export}}$	Efficiency defect	$\delta_i = \frac{E_{D,i}}{E_U}$
		$ExD_{exergy} = \frac{\dot{E}_d}{\dot{E}_{export}}$	Exergy destruction ratio	$y_d^* = \frac{\dot{E}_{d,k}}{\dot{E}_d}$
	Total exergy efficiency	$\varepsilon_{I-1} = \frac{\sum_{k,u} \dot{E}_{k,u} + \sum_{k,w} \dot{E}_{k,w} + \dot{E}^{\dot{Q}}_{cool}}{\dot{E}_{feed} + \dot{E}^{\dot{Q}}_{heat} + \dot{\mathrm{E}}^{\mathrm{W}}}$		
		$\varepsilon_{I-2} = \frac{\sum_{k,u} \dot{E}_{k,u}}{\dot{E}_{feed} + \dot{E}^{\dot{Q}}_{heat} + \dot{\mathrm{E}}^{\mathrm{W}}}$		
	Task exergy efficiency	$\varepsilon_{II-3} = \frac{\sum_{k,u} \dot{E}_{k,u} - \dot{E}_{feed}}{\dot{E}^{\dot{Q}}_{heat} + \dot{\mathrm{E}}^{\mathrm{W}}}$		
		$\varepsilon_{II-4} = \frac{\Delta \dot{\mathrm{E}}^{ch} + \sum_{k,u} \dot{E}^{ph}_{k,u}}{\dot{E}^{ph}_{feed} + \dot{E}^{\dot{Q}}_{heat} + \dot{\mathrm{E}}^{\mathrm{W}}}$		
		$\varepsilon_{II-5} = \frac{\dot{\Delta E}^{ch} + \sum_{k+,u} \dot{m}_{k+,u} * (e^{ph}_{k+,u} - e^{ph}_{feed})}{\sum_{k-} \dot{m}_{k-} * (e^{ph}_{feed} - e^{ph}_{k-}) + \dot{E}^{\dot{Q}}_{heat} + \dot{E}^{\dot{W}}}$		
	Component-by-component exergy efficiency	$\varepsilon_{III} = \frac{\dot{\Delta E}^{ch} + \sum_j \sum_{k,u} \left(\dot{\Delta E}^{ph}_{j,k}\right)^+_u}{\sum_j \sum_k \left(\dot{\Delta E}^{ph}_{j,k}\right)^- + \dot{E}^{\dot{Q}}_{heat} + \dot{E}^{\dot{W}}}$		

2.4 Criteria for the evaluation of Thermodynamic Performance Indicators

In order to evaluate the indicators calculated for the different Cases presented below a set of criteria has been set in order to determine the functions which an indicator is desired to fulfill. So, six criteria for the assessment of the calculated indicators are presented in order to compare and evaluate the different indicators in terms of their ability to describe the efficiency of an oil and gas process. The six criteria presented are the following:

1. Sensitivity
   The indicator should be sensitive to design choices and measures. For instance, the indicator that refers to a certain process that treats a specific fluid under given frame conditions needs to respond to changes regarding the process configurations (e.g. pressure, temperature changes). It should, also show the improvements made in the process that may include the use of more efficient equipment (e.g. compressors, pumps), or a better process integration.

2. Clear approach
   The indicator should be based on a solid theoretical basis without being open to various interpretations. The method and the data used for the calculation of the indicator should be clear, well-defined and consistent.

3. Workload
   The computation of the indicator should not require complex calculations, difficult programming or puzzling and time-consuming preparation. The workload in terms of effort and time devoted in order to obtain the indicator value should be kept low.

4. Motivation
   The indicator should provide the distance to an achievable target. This target could represent the highest possible efficiency in terms of thermodynamics (e.g. all processes reversible, zero exergy destruction rate), or the highest possible efficiency according to the available process design parameters (e.g. use of the most efficient available equipment). The second interpretation may give a most realistic approach of the achievable target, however in most cases this is not possible, since the majority indicators are based on an exergy/exergy balance and thus show the distance from the thermodynamically accessible target. At the same time, the indicator should give information regarding the part of the process where the highest potential to enhance the efficiency of the process exists.

5. Comparability
   The indicator should not be sensitive to frame conditions (e.g. TVP, CDB, CDT). It needs to show low sensitivity to changes regarding the reservoir fluid processed (e.g. fluid composition, pressure and temperature of the inlet stream). For example, the indicator that refers to a certain process working under specific process configurations should remain practically unchanged when different frame conditions are used. All in all, the comparison between different field types, power sources etc. should be possible using this indicator.

6. Simplicity
   The indicator should be simple and easy to understand and to communicate to all public types.

The evaluation of the six criteria presented are examined in an attempt to assess the indicators at issue on equal terms.

2.5 Method for the evaluation of Thermodynamic Performance Indicators

The performance of the thermodynamic indicators is examined in this work for several changes of the process design parameters. This investigation may give various and sometimes controversial results for the indicators at issue.

The complexity of the indicators, in terms of both definition and variations may preclude the selection of one indicator most appropriate for the evaluation of an oil and gas processing plant unless the terms of this evaluation are set. In this way, the mainly qualitative assessment conducted for the case studies presented in this work can lead to numerical results that - according to the intended application - can show which indicator is most appropriate to use.
Consequently, a set of criteria for the evaluation of the indicators has been formulated (Paragraph 2.4) which try to include all the different parameters someone might need to consider while choosing the most suitable indicator. These criteria aim to address both the need of a purely scientifical use and the application of the indicators to the oil and gas industry.

The method that has been chosen for the assessment of the indicators derives from the multi-attribute utility (MAU) analysis, which is a technique of the multi-criteria analysis (MCA) of the wider field of decision analysis. In general, the aim of MCA is to provide a systematic approach for complex decisions based on multiple and sometimes conflicting predetermined criteria and objectives. The scope of this analysis is to determine the most appropriate alternative (here indicator) or to rank or short-list possible alternatives. (Department for Communities and Local Government UK), (Geneletti, 2014)

In the case under consideration the MAU technique is used in order to produce a clear evaluation of the indicators providing a rationale that can be used in order to select one alternative (in this case an indicator) from a set of alternatives. This process involves four different stages:
1. Establishing a set of criteria useful for the evaluation
2. Setting a scheme for scoring products against the criteria
3. Defining the relative importance of the criteria using weighting factors
4. Computing the total score for each criterion in order to make the final decision

These four different stages of the MAU technique applied are more thoroughly presented below for the case of the evaluation of a set of indicators based on a group of criteria describing the advantages and disadvantages of the application of each indicator. (Brown, May 2007)

Stage One: Establishing Evaluation Criteria

One of the most important steps of the evaluation process is setting a set of criteria that describe the optimal performance of an indicator, as described above. These criteria should cover all aspects and objectives of the problem and reply to the question of who is supposed to use the criteria and for what reason. In the case under discussion the criteria have been presented and analyzed in Paragraph 2.4 . (Brown, May 2007)

Stage Two: Scoring the Products

In order to assign a score to each indicator for every criterion separately first the scale of scoring should be determined. By convention, in MAU analysis normalized scores are used that fall in the range from 0 to 1, where an indicator that fully meets the criterion receives a score of 1 and an indicator that does not respond to the criterion receives a

score of 0. The set of values to be assigned may be either discrete or continues. (Brown, May 2007)
A method useful for the scoring of the indicators against the criteria examined is the *relative scaling*. According to this method, the most preferred option (behavior of the indicator towards one of the criteria) is assigned the highest preference score (1 as presented above) and the least preferred option the lowest score (0 as presented above). Scores are assigned to the remaining options so that differences in the numbers represent differences in strength of preference. (Department for Communities and Local Government UK)

Stage Three: Setting weighting factors for the criteria examined

Next, weighting factors are assigned to each criterion. These weights are scaling factors that specify the relative importance of each criterion. Since they aim to specify the relative importance in the overall set of criteria, they are nonnegative numbers that sum to 1.
Various methods have been proposed for calculating weighting factors including the Weighted Ranking, the Paired Comparison and the Referenced Comparison etc. (Edwards, 1994), (Modelling and Decision Support Tools, 2007), (Ulvila & et al., 2001). According to Brown (May 2007) the Paired Comparison and the Referenced Comparison are mostly recommended, as they are widely accepted and easier to implement. (Brown, May 2007)

Stage Four: Computing the overall score for each indicator

If n is the number of criteria examined for a certain indicator k, $u_{i,k}$ is the score of the indicator k for the i criterion and w_i is the weighting factor of the i criterion, then the overall score u_k of the k indicator is calculated as:

$$u_k = \sum_{i=1}^{n} w_i * u_{i,k} \tag{51}$$

Equation 51 is used for the calculation of the overall score of all indicators. The indicator with the highest overall score is considered to be the most appropriate indicator to use according the criteria presented. (Brown, May 2007)

This simple weighted average in order to be used implies that the criteria examined are preferentially independent of each other. This means that the judged strength of preference for an option on one criterion will be independent of its judged strength of preference on another. The method is, also based on the lack of uncertainty about the future. (Department for Communities and Local Government UK)

At this point it should be noted that the criteria given in Paragraph 2.4 can be prioritized in *Mandatory* and *Desirable Criteria* before calculating the weighting factors of the criteria and the overall score of the indicators. The *Mandatory Criteria* represent requirements that should be definitely satisfied for an indicator to be considered feasible and they are not further prioritized. Only in case the indicator meets all the *Mandatory Criteria* the indicator takes part in the process described above for the *Desirable Criteria* this time. (https://www.ucalgary.ca/)

The method presented above may be further applied for a combination of two (or more) options (indicators). In this way, indicators that complement each other in terms of the performance towards the criteria examined may exhibit a better overall score than the options originally considered. In case relative scaling is used and the new option is least

preferred on some criteria or most preferred on others, then it is easier to assign scores less than 0 or more than 1, respectively, in order to use the same weights.

3. Thermodynamic performance indicators: Application to a typical North Sea offshore oil and gas processing plant – the Base Case Scenario

In this Chapter the case study that corresponds to the Base Case Scenario of a typical offshore oil and gas processing plant investigated for the calculation and evaluation of the thermodynamic performance indicators is presented.

3.1 Process description and simulation

The process under consideration includes the oil and gas processing plant of o typical North Sea oil and gas platform without taking the utility plant into consideration. In the process at issue no seawater injection, gas treatment or purification of the produced water take place. The flow diagram of the process is illustrated in Figure 8.

The process simulation is carried out using the ASPEN HYSYS® version 8.8 simulator and SRK Equation of State for the calculation of the thermodynamic properties. This case is based on a typical North Sea offshore platform and the data are provided by the oil and gas company Equinor, Norway. The complete flowsheet of the HYSYS simulation can be found in Appendix F .

The well stream treated in this process (1.well stream) - reservoir fluid stream leaving the pipelines and coming in the manifold - enters an Inlet manifold where it is first heated in order to ease the separation taking place in the next steps and then depressurized so as to reach the conditions of the first stage separation (51.21bar, 65.74°C) (5.ws2). The pressure of 51.21 bar is considered to be the high pressure of the separation train (HP). Next, the reservoir fluid is submitted to a three-stage separation (separation train). The first stage consists of a three-phase separator where the well stream fluid is separated into gas (35.vapour1), oil (10.oil) and water (6.aqueous). The aqueous solution is further separated in gas (8.gas from water treatment) and wastewater (9.water to further treatment) after being depressurized to atmospheric pressure. In this case, the last two streams are considered to be discharged to the environment and not used for further processing. They are, thus considered to be waste products.

The oil produced in the first stage separation is heated to 85°C and depressurized to 15bar to reach the conditions of the second 2-phase separation. The pressure of 15bar is considered to be the medium pressure of the separation train (MP). The oil leaving the second stage separator (15.oil 4) is depressurized to 1.5bar and further separated in the third 2-phase separator to gas (18.gas 4) and stabilized oil (17.stabilized oil). The pressure of 1.5bar is set to be the low pressure of the separation train (LP). The gas leaving the third-stage separator is compressed to the MP and cooled to 33°C before entering the second stage scrubber. SET-1 and SET-2 (Figure F61) have been applied to set the outlet pressure of the compressors, so that all mixing streams are at the same pressure level.

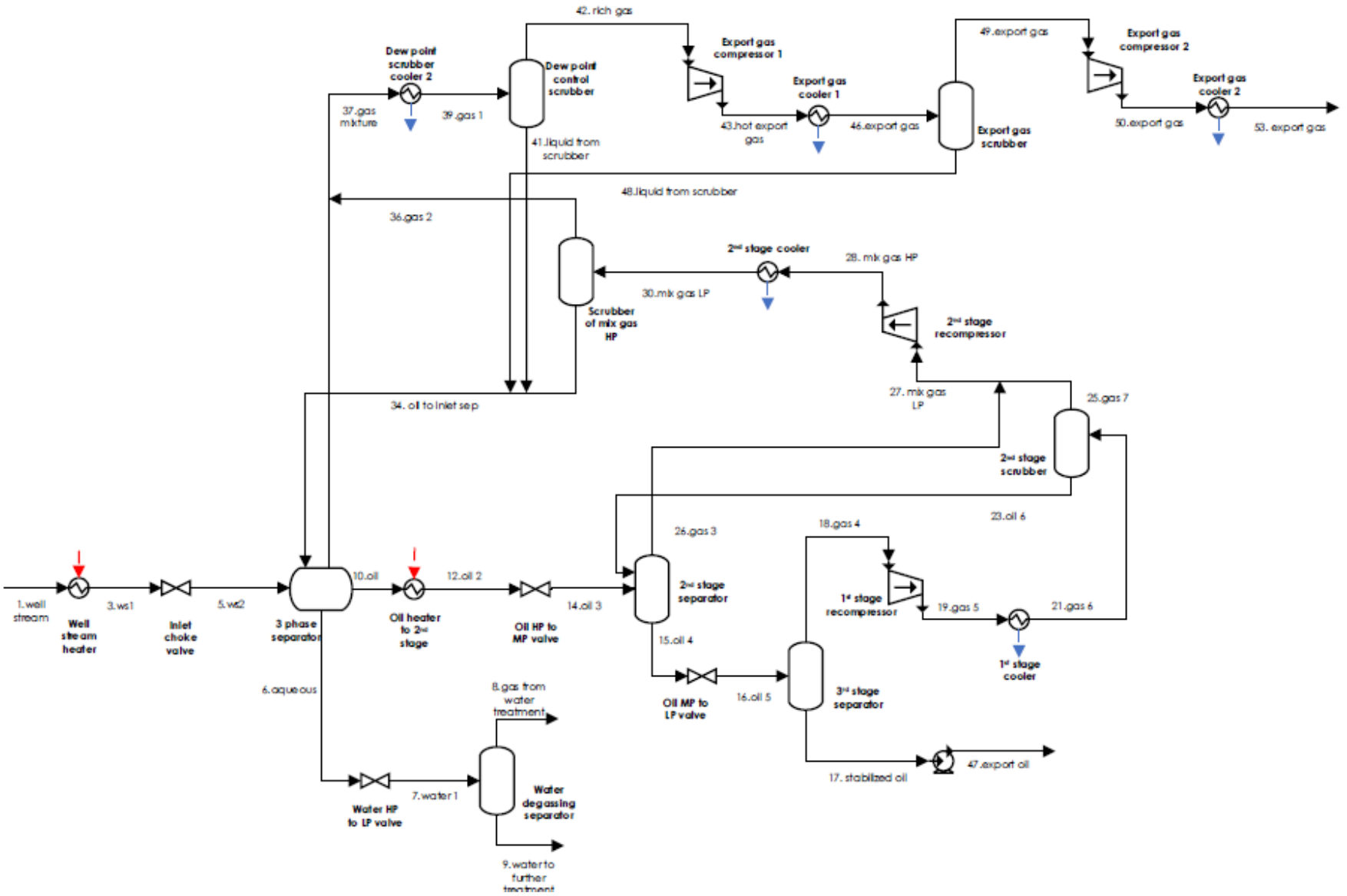

Figure 8 Process flow diagram of Case Study 1

The oil produced in the second stage scrubber (23.oil 6) is added to the feed of the second stage separator to be further processed. The gas leaving the second stage scrubber (25.gas7) is mixed with the gas leaving the second stage separator, compressed to the HP of the system, cooled to 33°C and then separated in the scrubber of mix gas at HP. The produced gas (36.gas 2) is mixed along with the gas leaving the three-stage separator, cooled to 25°C and separated in the dew point control scrubber to rich gas (42.rich gas) and liquid (41.liquid from scrubber). The liquid stream from the dew point control scrubber is mixed with the oil from the scrubber of mix gas at HP (32.oil 7) and the liquid stream from the export gas scrubber (48.liquid from scrubber) and sent back to the three-phase separator.

The produced oil (17.stabilized oil) is pumped to 10 bars to reach the oil export pressure specification (47.export oil). The rich gas leaving the dew point control scrubber (42.rich gas) is further compressed to meet the export pressure specification of 200bar (53.export gas). The gas compression train includes a two-stage compression, intercooling and a scrubber. The rich gas (42.rich gas) is first compressed at 101.2bar (43.hot export gas) and then cooled so as the rich gas (46.export gas) is saturated vapour. The rich gas leaving the heat exchanger is first submitted to separation in case any liquid exists in the gas stream and then further compressed reaching the pressure of 200bar (50.export gas). The gas is, then cooled at 60° C, which is the highest acceptable export gas temperature (53.export gas). The two material streams 53.export gas and 47.export oil represent the product streams of the process.

SET-3 to SET-9 (Figure F61) are used to set the outlet temperature of the cooling and heating mediums used in the heat exchangers using the minimum temperature difference of 5°C.

It should, also be noted that the cold water pumping network is not included in the system under consideration. This means that cooling is only associated with energy losses and not work production so that increases in cooling demands do not lead to extra duties for pumping.

For the platform at issue, the selection of the pressure ratio and the number of compression stages regarding the gas compression train is discussed in more detail in Appendix D.

Table 6 gives some of the process design parameters. The product specifications are presented in Table 7.

Table 6 Process design parameters

Reservoir fluid	120 bar and 65°C
Production or inlet manifold	One pressure level: 51.21 bar
Separation train	Pressure levels: LP=1.5bar. MP=15bar. HP=51.21bar Temperature levels: ≈65-80°C Pressure drops: 0 Ideal separation (zero entrainment)
Shell and Tube Heat exchangers	Minimum temperature difference in heat exchangers: ΔTmin=5°C Heating medium: Steam 5 bar. 200°C Cooling medium: Water 1.013 bar. 15°C Pressure drops: 0, except in well stream heater (67.79 bar)
Centrifugal compressors	Adiabatic efficiency of compressors: 75%

Table 7 Product specifications

Export gas	Cricondenbar < 105 bar
	Cricondentherm < 40°C
	Gas export pressure: 200 bar
	Gas export temperature < 60°C
Export oil	TVP (37.8°C) < 1 atm
	Oil export pressure: 10 bar

3.2 Reservoir fluid properties

The reservoir fluid processed in this case corresponds to a gas-condensate field, which means that the oil produced is condensate. Condensate oils are characterized by high light hydrocarbons content. This type of fluids is generally located at greater depths, resulting in higher reservoir pressures. (Mokhatab, Poe, & Mak, 2015)

The molar composition of the reservoir fluid examined in this case is presented together with the molar composition of the products of the platform in Table 9.

Components C7*-C20* are hypothetical components or pseudocomponents, whose properties derive from the true boiling point curve. The properties of pseudocomponents in this case are presented in

Table E50 (Appendix E).

3.3 Simulation results

Table 8 shows the flowrates of the input well stream, as well as the output products: rich gas and stabilized oil, along with the flowrates of the wastewater produced.

Table 8 The flowrates of the inlet and outlet streams of the system of Case 1

Stream	Molar flow (kmol/h)	Volume flow (Sm^3/h)
1.well streams	21550	
8.gas from water treatment	4E-1	9
9.water to treatment	1945	35
53.export gas	17797	420808
47.export oil	1808	313

The compositions of the products of export gas and export oil (mol fractions) are presented in the following table (Table 9).

The values of the thermodynamic properties regarding the product specifications reached in the simulated process are presented in Table 10. It should be emphasized that all the product specifications of Table 7are satisfied.

Table 9 Molar composition of well stream 1.well stream and the product streams 53.export gas and 47.export oil

	1.well stream	53.export gas	47.export oil
Nitrogen	0.0048	0.0058	3.6700E-07
CO2	0.0300	0.0363	0.0003
H2O	0.0909	0.0008	0.0001
C7*	0.0121	0.0011	0.1330
C8*	0.0121	0.0003	0.1409
C9*	0.0071	4.6300E-05	0.0841
C10*	0.0055	6.0100E-06	0.0660
C11*	0.0038	1.1300E-06	0.0455
C12*	0.0030	2.8900E-07	0.0358
C13*	0.0038	1.2400E-07	0.0455
C14*	0.0022	2.9100E-08	0.0260
C15*	0.0027	7.6700E-09	0.0325
C16*	0.0015	1.2800E-09	0.0184
C17*	0.0019	0.0000	0.0228
C18*	0.0014	0.0000	0.0163
C19*	0.0014	0.0000	0.0163
C20*	0.0073	0.0000	0.0867
Methane	0.6634	0.8032	0.0007
Ethane	0.0698	0.0842	0.0030
Propane	0.0373	0.0431	0.0204
i-Butane	0.0064	0.0063	0.0139
n-Butane	0.0129	0.0114	0.0415
i-Pentane	0.0049	0.0028	0.0310
n-Pentane	0.0061	0.0030	0.0429
n-Hexane	0.0077	0.0016	0.0766

Table 10 Product specifications results

Export gas	Cricondenbar = 103.1 bar
	Cricondentherm = 25.07°C
	Gas export pressure = 200 bar
	Gas export temperature = 60°C
Export oil	TVP (37.8°C) = 0.9862
	Oil export pressure = 10 bar

The exergy content of the material streams taking part in the process are calculated as the sum of their physical and chemical molar exergy multiplied by the molar flow of the stream (similarly on a mass basis).

$$\dot{E}_{stream\,i} = \dot{m}_{stream\,i} * (e^{phys}_{stream\,i} + e^{chem}_{stream\,i}) \quad (52)$$

The physical exergy of each stream is calculated using Equation 6, where h (molar) and s (molar) can be retrieved from the *Properties* of the stream given in the simulation stream *Worksheet* and h_0 and s_0 are calculated for each stream at the environmental temperature and pressure. On this account for each stream of the process a new stream is creating of the composition and the molar flow of the existing stream setting the temperature of the stream at 25°C (T_0) and the pressure of the stream at 101.3 kPa (P_0).

Chemical exergy of each stream is calculated using Equation 8. Both the component chemical exergy and the chemical exergy of mixing are taken into consideration.

The molar enthalpy $h_{i,0}$ and the molar entropy $s_{i,0}$ of pure component i at T_0, P_0 are calculated using again a new stream for each component i (stream of pure i) at T_0, P_0.

The molar fraction x_i of each component i in the stream under consideration can be found in the *Composition* of the stream *Worksheet*.

As mentioned before, term II of Equation (8) can be calculated using the *standard chemical exergies* of the components taking part in the process as:

$$\sum_i x_i e_{i,0}^{ch} = \sum_i \dot{n}_i (kmoles/h) * e_{i,0}^{ch} (kJ/kgmoles) \quad (53)$$

If mass flows are used for the calculation of the total exergy flow of a stream (in kW) then Equation 53 can be used on a mass basis.

The standard chemical exergies of the identified components of the process have been retrieved from standard chemical exergy tables found in literature (Kotas T. , 1985), while the standard chemical exergy of the pseudocomponents C7*-C20* have been calculated using Equations 9, 10 and 11 and the *API* values calculated in *Hysys*.

The standard chemical exergies used are found in Table 11.

Table 11 Standard chemical exergy of the components of the process

	Standard chemical exergy (kJ/kg)
Nitrogen	25.7
CO2	457.6
H2O	173.2
C7*	47178.5
C8*	46842.7
C9*	46553.0
C10*	46568.7
C11*	46486.9
C12*	46352.6
C13*	46199.7
C14*	46051.5
C15*	45988.6
C16*	45893.9
C17*	45954.5
C18*	45915.9
C19*	45797.9
C20*	45470.4
Methane	52151.5
Ethane	50028.6
Propane	49051.9
i-Butane	48501.9
n-Butane	48501.9
i-Pentane	48171.7
n-Pentane	48171.7
n-Hexane	47929.6

The physical exergy, the chemical exergy of mixing and the component chemical exergy have been calculated using *User Variables* (UV) defined for each stream of the process. The VBA codes used for this process (Appendix A) are based on similar cases found in literature (Jøssang, 2013), (Abdollahi-Demneh, Moosavian, Omidkhah, & Bahmanyar, 2011). User variables that set the ambient temperature (at 25°C) and pressure (at 1.013 bar) for all material streams have also been made in order to define the environmental conditions used in exergy calculations. For the calculation of the Component-by-Component exergy efficiency additional UV have been created for the calculation of the physical exergies of the parts of a stream coming from feed j and ending up in product k. These calculations demand the use of two extra UV that define the temperature and the pressure of the inlet reservoir fluid. These VBA codes (Appendix A) have been applied to the feed and the product streams only.

3.4 Thermodynamic performance indicators - Results

In this paragraph the thermodynamic indicators calculated for the case at issue are presented.

Calculation of the indicators is carried out under certain assumptions. First of all, (i) *streams 8* and *9* (produced water and gas from water treatment) are considered to be waste products discharged to the environment. Also, given the fact that heat and work are provided to the processing plant (the system under discussion) by the utility plant of the platform, energy and exergy of heat and work are not of zero value. Especially, as far as energy and exergy of heating and cooling are concerned the following method is followed. (ii) Heaters and coolers are replaced with heat exchangers where the heating and cooling mediums used are:

- Heating medium: steam at 200 °C & 5 bar
- Cooling medium: water at 15 °C & 1.013 bar

Table 12 Energy and Exergy heating and cooling values in each heat exchanger and Power consumption for compression (kW)

Equipment	Energy of cooling	Exergy of cooling
1st stage cooler	4445	835
2nd stage cooler	2495	468
dew point scrubber cooler	11569	402
export gas cooler 1	14969	983
export gas cooler 2	9328	675
Total	42805	3364
Equipment	Energy of heating	Exergy of heating
well stream heater	7516	2172
oil heater to 2nd stage	3709	1070
Total	11225	3242
Equipment	Energy/Exergy of compression/ pumping	
1st stage recompressor	1468	
2nd stage recompressor	982	
export gas compressor 1	10402	
export gas compressor 2	10131	
export oil pump	103	
Total	23087	

Since there is no work consumption/production in heating/cooling, the thermal energy exchanged is equal to the enthalpy change of the stream heated or cooled. The exergy of heating or cooling is equal to the exergy decrease or increase of the heating or cooling medium, respectively as presented in Equation 49 (Appendix C).

The calculated values of the energy and exergy of heating and cooling are given in Table 12. In the same Table the power consumption for compression and pumping is presented.

3.4.1 Specific CO_2 emissions per unit of oil produced

In order to calculate the *Specific CO_2 emissions per unit of oil produced* the way in which the power consumed on-site is produced should be defined.

The electrical power required is generated by gas turbines, fueled with a fraction of the natural gas extracted along with oil, and atmospheric air. The waste heat from the exhaust gases is partly used to increase the temperature of the heating medium used. The excess of heat is released to the environment. In the case under consideration the fuel used in the turbines is considered to be the rich gas exported from the processing plant, while it is given that 100 MW (expressed in lower heating value) of the fuel consumed results in 30 MW of power and 50 MW of steam (heating medium used). If the power and heat demands of the Base Case are considered, it follows that the gas consumption for power production covers the heat demands of the platform. So, no extra fuel consumption is required for heat production.

The annual fuel consumption is given as:

$$Fuel\ consumption = \frac{Power\ duty}{0.30 * LHV} = 55.6\ MSm^3/y$$

The amount of CO_2 produced by 1 Sm3 of fuel consumed is a fraction of the composition of the fuel. In the case at issue the factor of 2.429 kg CO_2 per Sm3 of fueled gas is used, which corresponds to a typical natural gas. So, the daily emissions of the platform are calculated as:

$$C0_2\ emissions\ (kg/d) = Fuel\ consumption\ (Sm^3/d) * 2.129\ (kg\ CO_2/Sm^3) = 370.1\ tn/d$$

The *CO_2 emissions per barrel of export product* (oil and gas) are calculated as:

$$\boldsymbol{C0_2\ emissions}\ (kg/bbl) = \frac{C0_2\ emissions\ (kg/d)}{\dot{V}_{export}(Sm^3o.e./d) * 6.290\ (bbl/Sm^3o.e.)} = \boldsymbol{3.3\ kg/bbl}$$

where $6.290\ (bbl/Sm^3o.e.)$ again is representative of a typical oil.

The volume flowrate of the export product is calculated as:

$$\dot{V}_{export}(Sm^3o.e./h) = \dot{V}_{export_{oil}}(Sm^3o.e./h) + \dot{V}_{export_{gas}}(Sm^3o.e./h)$$
$$= 1\frac{Sm^3o.e.}{Sm^3\ oil}\ \dot{V}_{export_{oil}}(Sm^3oil/h) + 1000\frac{Sm^3o.e.}{Sm^3\ gas} * \dot{V}_{export_{gas}}(Sm^3gas/h) = 733.8\ Sm^3o.e./h$$

using the factors of Table 3 are used. New factors adapted to the composition of the produced oil and gas could otherwise be calculated and used.

The *CO_2 emissions per barrel of export product* is also known as *CO_2 intensity* (Voldsund, Nguyen, Elmegaard, Ertesvåg, & Kjelstrup, 2014).

The *CO_2 intensity* calculated in this case is low compared to the numbers found in literature for offshore operators that vary between 6 and 17 kg CO_2 per boe. This is related to the fact that in the analysis under discussion (i) only the processing plant of the platform is examined, (ii) some subprocesses such as the water or gas injection are disregarded and (iii) heat exchanging and compression/pumping show high efficiencies (Table 6). (Rystad Energy, 2021)

3.4.2 Specific energy use

S*pecific energy use* per standard volume of oil equivalent export rate is calculated using Equation 14.

The value of the calculated indicator is: $\boldsymbol{EnU_{volume} = 168.3\ MJ/Sm^3 o.e.}$

This value can be compared to EnU_{volume} values found in literature. Voldsund et al. (2014) (Voldsund, Nguyen, Elmegaard, Ertesvåg, & Kjelstrup, 2014) have calculated such indicators for different platforms that process different fluids.

Platform C of their work shows an EnU_{volume} value ($\approx 130\ \mathrm{MJ/Sm^3 o.e.}$) similar to that of the Case at issue. This could be explained if the pressure profiles of both cases are taken into consideration. According to Figure 9 and Figure 10 the pressure profiles for both platforms are almost identical with the exception of the pressure range of the well streams entering the production manifold (three different well streams) and the pressure of compression of the export oil.

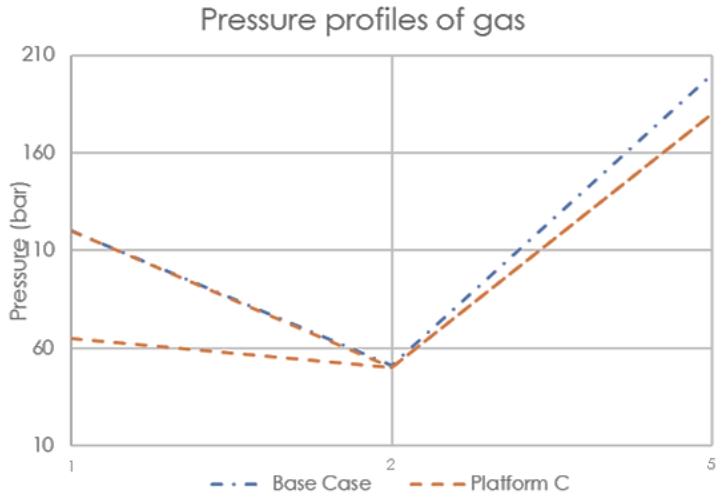

Figure 9 Pressure profiles of gas for the case at issue and Platforms C (2014) from well to outlet of production manifold (1→2) and from outlet of production manifold to outlet of gas treatment (2→5).

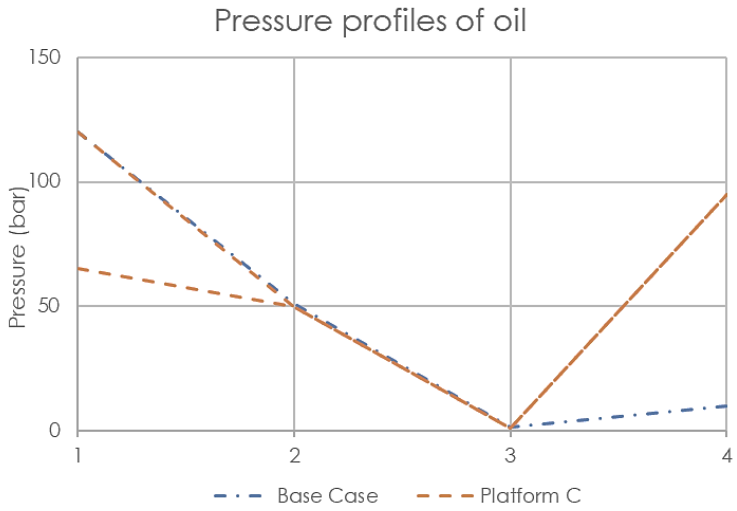

Figure 10 Pressure profiles of oil for the case at issue and Platforms C (2014) from well to outlet of production manifold (1→2), from outlet of production manifold to outlet of separation train (2→3), from outlet of separation train to oil export (3→4).

However, it should be noted that the flow rates and the gas to oil ratios of the two cases are significantly different (gas to oil ratio: 1345 (Base Case) vs 360 (Platform C)), while there can be no comparison between the reservoir fluids treated in both cases. (Voldsund, Nguyen, Elmegaard, Ertesvåg, & Kjelstrup, 2014), (Voldsund M. , 2014)

Indicators calculated by Voldsund et al. (2014) (Voldsund, Nguyen, Elmegaard, Ertesvåg, & Kjelstrup, 2014) are used as frame of reference.

Specific energy use per energy exported is calculated using Equation 15, where:

$$\dot{LHV}_{export} = \dot{V}_{oil}\left(\frac{Sm^3 oil}{h}\right) * \dot{LHV}_{export_{oil}}\left(\frac{MJ}{Sm^3 oil}\right) + \dot{V}_{gas}\left(\frac{Sm^3 gas}{h}\right) * \dot{LHV}_{export_{gas}}\left(\frac{MJ}{Sm^3 gas}\right)$$
$$= 8380.2\ MW$$

The Lower Heating Value of the oil and gas exported are calculated using an algorithm based on Dulong's formula (NTUA, 2019).

So, the value of the indicator is: $\boldsymbol{EnU_{energy} = 0.0041}$

which is again similar to the EnU_{energy} value of Platform C (<30% difference) (Voldsund, Nguyen, Elmegaard, Ertesvåg, & Kjelstrup, 2014). The relation between EnU_{volume} and EnU_{energy} is similar to that found in literature (Voldsund, Nguyen, Elmegaard, Ertesvåg, & Kjelstrup, 2014), which means that the density of the product of the process are within the expected range. EnU_{energy} is considered to be more accurate thermodynamically, as it takes into account the calorific value.

3.4.3 Specific power consumption

Specific power consumption is calculated using Equation 17. The calculated value is:

$$\boldsymbol{Specific\ power\ consumption} = \mathbf{113.3}\ \boldsymbol{MJ/Sm^3o.e.}$$

which is lower than the *Specific power consumption* value found in literature (≈179 $MJ/Sm^3o.e.$ = 644 $MJ/Sm^3o.e.$) (Voldsund M. , 2014). This is expected, as in both cases the total power consumption is similar (23.0 MW in Case 1 vs 23.8 MW in the case found in literature (Voldsund M. , 2014)), but in the case described in literature only the export oil is taken into account when calculating the volume flow rate of the export products, as the produced gas is not exported, but used for gas injection.

It is evident that in the case under examination the *Specific power consumption* is proportional to the Specific CO_2 emissions of the platform (Nguayen, Voldsund, Elmegaard, Ertesvåg, & Kjelstrup, 2014) and should, thus be kept low.

3.4.4 Specific exergy use

S*pecific exergy use* per standard volume of oil equivalent export rate is calculated using Equation 19, getting the value of:

$$\boldsymbol{ExU_{volume}} = \mathbf{129.2}\ \boldsymbol{MJ/Sm^3o.e.}$$

which is once more similar to the ExU_{volume} value of Platform C (around $120\ MJ/Sm^3o.e.$). (Voldsund, Nguyen, Elmegaard, Ertesvåg, & Kjelstrup, 2014).

ExU_{volume} value is lower than EnU_{volume} value, because heat is added to the system. If no heat was added then $ExU_{volume} = EnU_{volume}$. This is typical for North Sea platforms where the heat demand is low. In the Case under examination there is significant difference between the two indicators (around 30%), since a great part of energy added to the system is heat (33%).

It should be noted, though that the difference between $ExU_{volume}$and EnU_{volume} in the case under discussion is high (around 30%) compared to the values found in literature (less than 5-10% difference), which indicates either a higher heating energy input/work ratio in our case or different type of heating or heating mediums that leads to higher exergy of heating.

In order to calculate the S*pecific exergy use* per exported exergy Equation 20 is used, where:

$$\dot{E}_{export} = \dot{E}_{export\ gas} + \dot{E}_{export\ oil} = 8078.0\ MW$$

The calculated value of ExU_{exergy} is:

$$\boldsymbol{ExU_{exergy}} = \mathbf{0.0033}$$

This value is close to that of the same indicator for Platform C (around 0.003) (Voldsund, Nguyen, Elmegaard, Ertesvåg, & Kjelstrup, 2014). The relation between ExU_{volume} and ExU_{exergy} is again similar to that found in literature (Voldsund, Nguyen, Elmegaard, Ertesvåg, & Kjelstrup, 2014). ExU_{exergy} is -similarly to the *Specific energy use*- considered to be more accurate thermodynamically compared to ExU_{volume}, as it takes into account the exergetic content of the product.

3.4.5 Specific exergy destruction

In order to calculate S*pecific exergy destruction* per standard volume of oil equivalent export rate the exergy balance of Equation 21 is used in the following form for the terms of exergy of heating, cooling and work noted in Table 12:

$$\dot{Ed} = E^{\dot{Q}}_{heat} - E^{\dot{Q}}_{cool} + \dot{W}_{cv} + \sum \dot{m_{in}} e_{in} - \sum \dot{m_{out}} e_{out} \quad (54)$$

where

$$\sum \dot{m_{out}} e_{out} = \dot{E_8} + \dot{E_9} + \dot{E_{53}} + \dot{E_{47}} = 8079.8\ MW$$

$$\sum \dot{m_{in}} e_{in} = \dot{E_1} = 8075.9\ MW$$

The amount of exergy destruction rate is: $\boldsymbol{\dot{E_d} = 19.1\ MW}$

Using Equation 21 and the volume export rate of $\dot{V_{export}}(Sm^3 o.e.) = 730.9\ Sm^3 o.e.$, the calculated value of ExD_{volume} is:

$\boldsymbol{ExD_{volume} = 93.6\ MJ/Sm^3 o.e.}$

This value is similar to the ExD_{volume} values of Platform C (around 80 MJ/Sm^3 o.e.) (Voldsund, Nguyen, Elmegaard, Ertesvåg, & Kjelstrup, 2014) and is relatively low when compared to the values of the other platforms. The higher the ExD indicators the worse the performance of the platform, as the exergy density in the exported oil equivalents is lower.

S*pecific exergy destruction* per exported exergy is calculated using Equation 22. The calculated value of ExD_{exergy} is:

$\boldsymbol{ExD_{exergy} = 0.0024}$

That approaches the ExD_{exergy} value of Platform C (around 0.002) (Voldsund, Nguyen, Elmegaard, Ertesvåg, & Kjelstrup, 2014).

These *ExD* values are low when compared to the values of the other platforms, as found, also in ExU_{exergy} calculations, which means that a small amount of exergy is destroyed in the platform in order to produce oil and gas of high exergetic content. This could be a result of the high efficiencies of the compressors and the pumps used (75%), as well as the low minimum temperature difference used in heat exchanging (ΔTmin=5°C).

3.4.6 Total exergy efficiency

In order to calculate the total exergy efficiencies given in Equations 29 and 30 the exergy balance of Equation 31 is used. The efficiencies ε_{l-1} (Equations 29 and 32)and ε_{l-2} (Equations 30 and 33) calculated in both ways give the same results, as the second expression is equivalent to the first one, but expressed for oil and gas processing plants. The calculated terms of Equation 31 are:

$$\sum \dot{E_{in}} = \dot{E_{feed}} + \dot{W} + \dot{E_{heat}^{Q}} = 8102.3\ MW \qquad \sum_{k,w} \dot{E_{k,w}} = \dot{E}_8 + \dot{E}_9 = 1.8\ MW$$

$$\sum_{out,u} \dot{E_{out,u}} = \sum_{k,u} \dot{E_{k,u}} = \dot{E_{53}} + \dot{E_{47}} = 8078.0\ MW \qquad \sum_{out,l} \dot{E_{out,l}} = \sum_{k,w} \dot{E_{k,w}} + \dot{E_{cool}^{Q}} = 5.2\ MkW$$

The exergy destruction rate is:

$$\dot{E_d} = \sum_{in} \dot{E_{in}} - \sum_{out,u} \dot{E_{out,u}} - \sum_{out,l} \dot{E_{out,l}} = 19.1\ MW$$

This value is equal to that calculated using the exergy balance of Equation 54.

The total exergy efficiency values received from the calculations are:

$\boldsymbol{\varepsilon_{I-1}} = \mathbf{99.8}\%$

$\boldsymbol{\varepsilon_{I-2}} = \mathbf{99.7}\%$

The ε_{I-1} and $\boldsymbol{\varepsilon_{I-2}}$ values are again similar to the values of Platform C (Voldsund, Nguyen, Elmegaard, Ertesvåg, & Kjelstrup, 2014), (Voldsund M. , 2014) (99.9% and 99.8%, respectively (Voldsund M. , 2014)), while the values of ε_{I-2} are lower than values of ε_{I-1} as expected. According to Equations 29 and 30 the difference between the two total efficiencies is due to exergy lost because of cooling and waste streams, which accounts to around 0.1% of the useful exergy of the product.

In general, in oil and gas processes high *total exergy efficiencies* (ε_I) are expected, because the exergy content of hydrocarbons passing through the system is very high.

3.4.7 Task exergy efficiency

Task exergy efficiency of Equation 38 is first calculated using the exergy balance of Equation 37. It is pointed out that the exergy of the waste Streams 8 and 9 is included in the lost exergy term $\dot{E}_l$, even if, by the way it is presented in the exergy balance, the term corresponds to the exergy lost due to cooling. The calculated terms of the exergy balance are:

$$\dot{E_{feed}} = \dot{E}_1 = 8075.9\ MW \qquad \sum_{k,u} \dot{E_{k,u}} = \dot{E_{53}} + \dot{E_{47}} = 8078.0\ MW$$

$$\dot{E}_f = \dot{E_{heat}^{Q}} + \dot{E^{W}} = 26.3\ MW \qquad \dot{E}_l = \dot{E_{cool}^{Q}} + \dot{E}_8 + \dot{E}_9 = 5.2\ MW$$

$\dot{E_p} = \sum_{k,u} \dot{E_{k,u}} - \dot{E_{feed}} = 2.1\ MW$, which means that the exergy content of the useful products is higher than the exergy content of the reservoir fluid as expected. The product exergy $\dot{E_p}$ represents the desired exergy increase between the useful and the feed streams.

The value of the task efficiency calculated is: $\boldsymbol{\varepsilon_{II-3}} = \mathbf{7.9}\%$

This value is similar to the ones found in literature (Voldsund, Nguyen, Elmegaard, Ertesvåg, & Kjelstrup, 2014), but it is lower than the $\boldsymbol{\varepsilon_{II-3}}$ value of Platform C (21%) (Voldsund, Nguyen, Elmegaard, Ertesvåg, & Kjelstrup, 2014). This is a result of lower exergy of product (similar exergy of heat and work according to previous indicators). This could be the case of different pressure conditions for the two processes.

Next, the task efficiency of Equation 40 is calculated using the exergy balance of Equation . The terms calculated are:

$$\dot{E}_{feed}^{ph} = \dot{E}_{1}^{ph} = 57.2 \text{ MW}$$

$$\dot{E}_{f} = \dot{E}_{feed}^{ph} + \dot{E}_{heat}^{Q} + \dot{\mathrm{E}}^{\mathrm{W}} = 83.6 \text{ MW}$$

$$\Delta \mathrm{E}^{ch} = \dot{E}_{53}^{ch} + \dot{E}_{47}^{ch} + \dot{E}_{8}^{ch} + \dot{E}_{9}^{ch} - \dot{E}_{1}^{ch} = 0.9 \text{ MW}$$

$$\sum_{k,u} \dot{E}_{k,u}^{ph} = \dot{E}_{53}^{ph} + \dot{E}_{47}^{ph} = 60.1 \text{ MW}$$

$$\dot{E}_{p} = \Delta \mathrm{E}^{ch} + \sum_{k,u} \dot{E}_{k,u}^{ph} = 61.0 \text{ MW}$$

$$\sum_{k,\mathrm{w}} \dot{E}_{k,\mathrm{w}}^{ph} = \dot{E}_{8}^{ph} + \dot{E}_{9}^{ph} = 0.1 \text{ MW}$$

$$\dot{\mathrm{E}}_{\mathrm{l}} = \sum_{\mathrm{k,w}} \dot{\mathrm{E}}_{\mathrm{k,w}}^{\mathrm{ph}} + \dot{\mathrm{E}}_{\mathrm{cool}}^{\mathrm{Q}} = 3.5 \text{ MW}$$

$$\dot{\mathrm{E}}_{\mathrm{d}} = \dot{\mathrm{E}}_{\mathrm{f}} - \dot{\mathrm{E}}_{\mathrm{l}} - \dot{\mathrm{E}}_{\mathrm{p}} = 19.1 \text{ MW}$$

The task exergy efficiency calculated is: $\boldsymbol{\varepsilon_{II-4}} = \mathbf{73.0}\%$

This value is similar to the $\boldsymbol{\varepsilon_{II-4}}$ value of Platform C (71.0%) (Voldsund M. , 2014), and it is high compared to the values found in literature (Voldsund M. , 2014). The higher performance can be explained by the high rate of physical exergy transiting throughout the plant with the produced gas (in this case all the gas produced is considered to be in the useful products) and the low power demands of the process.

In order to calculate the task exergy efficiency given in Equation 42 first the mass physical exergy of all inlet and outlet streams is calculated. The exergy of the feed stream is noted as e_{feed}^{ph}, while for the product streams (export gas and export oil) and the waste streams (water and gas from wastewater treatment) the exergy is noted as $e_{k+,u}^{ph}$ and $e_{k+,w}^{ph}$, respectively, if the mass exergy of the outlet stream is higher than the mass exergy of the feed stream. In case of outlet streams with lower exergetic content than the feed stream, the mass exergy of the outlet streams is noted as $\mathrm{e}_{\mathrm{k-,u}}^{\mathrm{ph}}$. For the process under discussion the mass exergy, as well as the mass flow rate of all inlet and outlet stream are presented in Table 13**.**

Table 13 Mass exergy and flow rate of inlet and outlet stream

Inlet/Outlet streams	Mass exergy (kJ/kg)		Mass flow rate (kg/s)	
1. well stream	$e_{feed}^{ph} =$	315.0		
8. gas from water treatment	$e_{k-,u}^{ph} =$	23.3	$\dot{m}_{k-} =$	0.0
9. water from water treatment	$e_{k-,u}^{ph} =$	10.7	$\dot{m}_{k-} =$	9.7
47. export oil	$e_{k-,u}^{ph} =$	5.1	$\dot{m}_{k-} =$	69.0
53. export gas	$e_{k+,u}^{ph} =$	580.9	$\dot{m}_{k+} =$	102.9

The terms of Equation 41 are, thus calculated similarly to previous calculations and

The *task exergy efficiency* is: $\boldsymbol{\varepsilon_{II-5}} = \mathbf{55.7}\%$

Which s again in agreement with the values found in literature (Voldsund M. , 2014) (39-54%).

It should be noted at this point that a deviation of 0.002% is detected between the exergy destruction calculated in this case and the previous ones. This is because of a

0.0006% error in the mass balance due to the convergence that is satisfied in the algorithm used in HYSYS that is translated in destroyed exergy. Such convergence errors may occur also in the following calculations without however affecting the values of the indicators calculated.

It is underlined that in the case under consideration the indicator is calculated for specific exergy of stream on a mass basis. The same calculations could be performed on a molar basis, but different results would occur, as presented above.

3.4.8 Component-by-Component exergy efficiency

In order to calculate the *component-by-component exergy efficiency* the partial molar physical exergy of each component i $\widehat{e_{i,J}^{ph}}$ in feed stream j should first be calculated. Since for the -mainly- hydrocarbon mixture of the feed and product streams taking part in the process the excess enthalpy and entropy can be considered negligible, the partial molar physical exergy of each component in the stream can be calculated as the molar exergy of the pure i component at the temperature and the pressure of the mixture.

Next, the physical exergies of the part of each stream coming from feed j, $E_{J,k,in}^{\dot{ph}}$, and ending up in product k, $\mathrm{E}_{\mathrm{J,k,out}}^{\dot{\mathrm{ph}}}$ are calculated using equations 43, 44. The results can be found in Table 14.

Table 14 Physical exergy of each stream (MW)

$E_{1,53,in}^{\dot{ph}}$	53.6	$E_{1,8,in}^{\dot{ph}}$	8.6E-4
$E_{1,53,out}^{\dot{ph}}$	58.3	$E_{1,8,out}^{\dot{ph}}$	1.3E-5
$E_{1,47,in}^{\dot{ph}}$	1.7	$E_{1,9,in}^{\dot{ph}}$	2.6E-1
$E_{1,47,out}^{\dot{ph}}$	4.8E-1	$E_{1,9,out}^{\dot{ph}}$	1.0E-1

The value of the physical exergy increases and decreases (Equations 46, 47), as well as the terms of Equation 48 are presented in

Table 15 Component-by-Component exergy balance results (MW)

$\left(\Delta E_{J,k}^{\dot{ph}}\right)_u^+$	4.7	$\Delta E^{\dot{ch}}$	8.1E-1
$\left(\Delta E_{J,k}^{\dot{ph}}\right)_w^+$	0.0	$\dot{E_p}$	5.5
$\left(\Delta E_{J,k}^{\dot{ph}}\right)^-$	1.4	$E_{cool}^{\dot{Q}}$	3.4
$E_{heat}^{\dot{Q}} + \mathrm{E}^{\dot{\mathrm{W}}}$	26.3	$\dot{E_l}$	3.4
$\dot{E_f}$	27.7	$\dot{E_d}$	18.8

It needs to be pointed out that a deviation of 1.8% between the exergy destruction calculated in this case and the cases presented above exists. This difference in the calculated values is a result of the assumption that the partial molar physical exergy of each component is equal to the molar exergy of the same component when it is pure at the conditions (*T,P*) of the mixture.

The *Component-by-Component exergy efficiency* calculated by Equation 49 is:

$\boldsymbol{\varepsilon_{III} = 20.0\%}$

which is again comparable with the value of the same indicator for Platform C found in literature (Voldsund M. , 2014) (26.9%).

3.4.9 Exergy destruction ratio

Exergy destruction ratio corresponds to the different process components of an off-shore oil and gas platform. The typical sub-systems of an offshore platform process are the following: Production manifold, Separation, Recompression, Dehydration, Fuel gas and flaring, Gas compression, Oil pumping, Wastewater treatment and Seawater injection.

In the Case at issue the subsystems used are the Production manifold the Separation train, the oil pumping and export, the waste water treatment, the gas recompression and the gas compression and exportation. The exergy of the inlet and outlet streams for each sub-system is presented in Table 16, where the subscripts of the exergy terms symbolize for which matter of stream or the equipment exergy is calculated and used.

Table 16 The exergy streams of the sub-systems under examination for the calculation of the *exergy destruction ratio*

Sub-system	Inlet streams	Outlet streams	Heating/cooling	Work
Production manifold	$\dot{E}_1$	$\dot{E}_5$	$\dot{E}^Q_{heat_{well\ stream\ heater}}$	-
Separation	$\dot{E}_5$, $\dot{E}_{24}$, $\dot{E}_{32}$, $\dot{E}_{41}$, $\dot{E}_{48}$	$\dot{E}_6$, $\dot{E}_{26}$, $\dot{E}_{17}$, $\dot{E}_{18}$, $\dot{E}_{35}$	$\dot{E}^Q_{heat_{oil\ heater\ to\ 2nd\ stage}}$	-
Oil pumping & export	$\dot{E}_{17}$	$\dot{E}_{47}$	-	$\dot{W}_{in_{export\ oil}}$
Wastewater treatment	$\dot{E}_6$	$\dot{E}_8$, $\dot{E}_9$	-	-
Gas compression & exportation	$\dot{E}_{35}$, $\dot{E}_{36}$	$\dot{E}_{41}$, $\dot{E}_{48}$, $\dot{E}_{53}$	$\dot{E}^Q_{cool_{dew\ point\ scrubber\ cooler}}$ $\dot{E}^Q_{cool_{export\ gas\ cooler\ 1}}$, $\dot{E}^Q_{cool_{export\ gas\ cooler\ 2}}$	$\dot{W}_{in_{export\ gas\ 1}}$, $\dot{W}_{in_{export\ gas\ 2}}$
Gas recompression	$\dot{E}_{26}$, $\dot{E}_{18}$	$\dot{E}_{32}$, $\dot{E}_{36}$, $\dot{E}_{24}$	$\dot{E}^Q_{cool_{1st\ stage\ cooler}}$, $\dot{E}^Q_{cool_{2nd\ stage\ cooler}}$,	$\dot{W}_{in_{1\ stage\ recompre}}$ $\dot{W}_{in_{2nd\ stage\ recomp}}$

In order to calculate the exergy destruction ratio, the exergy balance of Equation 2 is used. The indicator is calculated using Equation 24. The results of the calculations are presented together with the efficiency defect in Table 17.

Table 17 The results of the exergy destruction ratio and the efficiency defect calculations

Sub-system	$\dot{E}_{Q,in}$ (MW)	$\dot{E}_{W,in}$ (MW)	$\sum \dot{m}_{in} e_{in}$ (MW)	$\sum \dot{m}_{out} e_{out}$ (MW)	$\dot{Ed}_k$ (MW)	y_d^*	δ_i
Production manifold	2.2	0.0	8075.9	8067.3	1008	**56.8%**	**0.3E-3**
Separation	1.1	0.0	8712.0	8710.9	2.2	**11.7%**	**2.7E-4**
Gas compression & exportation	-2.1	-20.5	5043.1	5055.8	5.7	**30.1%**	**7.1E-4**
Gas recompression	-1.3	-2.5	639.4	640.4	0.2	**1.1%**	**3.2E-5**
Oil pumping	0	-0.1	3202.9	3203.0	0.0	**0.1%**	**1.5E-6**
Wastewater treatment	0	0	1.9	1.8	0.1	**0.3%**	**7.3E-6**
SUM					19.1	**1.0**	**2.4E-3**

According to the results presented in Table 17, most of the exergy is destroyed in the production manifold than in the separation train, as expected, since there is also exergy increase due to separation. As found in literature, the maximum exergy destruction ratio in most cases is that of the production manifold. Especially, in Case 6 presented by Nguyen et al. 2014 (Nguayen, Voldsund, Elmegaard, Ertesvåg, & Kjelstrup, 2014), where the well stream's composition and the gas to oil ratio are similar to these of the case at issue, most exergy is destroyed in the production manifold, followed by the gas compression, as found, also in the case at issue. It should be noted that the exergy destroyed in each sub-system may differ significantly in case of different pressures in the different sub-systems of the process under discussion.

3.4.10 Efficiency defect

Efficiency defect is calculated for the different process components of an off-shore oil and gas platform. The typical sub-systems of an offshore platform process are these presented above. In this case. the efficiency defect of Equation 26 is calculated using the exergy balance of Equation 54 for the separation train, the oil pumping and export, the waste water treatment, the gas recompression and the gas compression and exportation. The results of the calculation are presented in Table 17.

It is pointed out that the exergy entering the system is considered to be:

$$E_U = \dot{E}_{feed} + \dot{E}^{Q}_{heat} + \mathrm{E}^{\mathrm{W}} = 8102.3\ MW$$

According to the results presented in Table 17 more exergy is destroyed in the production manifold than in the separation train, as it is also denoted by the exergy destruction ratio. The sum of the efficiency defects are equal to the ratio of the total exergy destroyed to the input exergy to the system.

The high exergy destruction in the production manifold could explain the substitution of choke valves by expanders for multiphase flow, in order to recover the exergy destroyed in the valves.

3.4.11 Exergy loss ratio

Exergy loss ratio is calculated using Equation 25. In the case under examination exergy is lost due to cooling, gas exhausted from water treatment and produced water discharged to the environment. The results of lost exergy accounting are presented in Table 18.

Table 18 The results of the exergy loss ratio calculations

Process component k	$\dot{E_{l,k}}$ (MW)	y_l^*
Cooling	3.4	**65.2%**
Gas exhausted from water treatment	2.6E-3	**0.1%**
Produced wastewater	1.8	**34.7%**
SUM	5.2	**1.0**

According to the results of Table 18, exergy is mainly lost due to cooling. This is because the utility system, which usually shows the greatest part of the exergy losses due to the exhaust gases from combustion is out of scope for the system under examination.

4. The effect of the calculation of the *component chemical exergy* on the thermodynamic indicators

In this chapter the effect of the calculation of the *component chemical exergy* on the indicators is examined with the aim to highlight for which indicators the calculations could be simplified excluding the part of the *component chemical exergy.*

4.1 Description of the Case

As mentioned above the term of the *component chemical exergy* when calculating the chemical exergy of a material stream taking part in the process can be ignored, as this part of chemical exergy is passing through the system without changing, in case no chemical reaction takes place. However, this does not mean that the indicators calculated in both cases (using or not the component chemical exergy) are of the same value, as some of them use the absolute exergetic content of some streams.

Calculations are made for the Base Case Scenario (Case 1) disregarding the part of the component chemical exergy for the chemical exergy term and the results are presented below.

4.2 Results & Discussion

The results of the energy and exergy analysis for the case of no calculation of the *component chemical exergy* are given in Table 19, Table 20 and Table 21.

The energy and exergy consumption and the exergy destruction are presented in comparison with the Base Case in Table 19. According to Table 19, excluding the *component chemical exergy* from the calculations does not affect none of these terms, as no chemical reactions take place in cooling, heating or compressing. The exergy destruction remains constant as the *component chemical exergy* entering the system is

equal to the *component chemical exergy* leaving the system, again because of the absence of chemical reactions in the system.

Table 19 Energy and exergy use/destruction in the case of no component chemical exergy compared with the Base Case

Energy/Exergy used/destroyed (MW)		Base Case 1	No component chemical exergy
Energy	cooling	42.8	42.8
	heating	11.2	11.2
	compression/ pumping	23.1	23.1
Exergy	cooling	3.4	3.4
	heating	3.2	3.2
	compression/ pumping	23.1	23.1
	destruction	19.1	19.1

Table 20 The values of performance indicators in the case of no component chemical exergy compared with the Base Case

Indicator			Base Case 1	No component chemical exergy
Energy		$CO2\ intensity\ (kg/bbl)$	3.3	3.3
		$EnU_{volume}\ (MJ/Sm3o.e.)$	168.3	168.3
		$Specific\ power\ con\ sumption\ (MJ/Sm3o.e.)$	113.3	113.3
		EnU_{energy}	0.0041	0.0041
Exergy		$ExU_{volume}\ (MJ/Sm3o.e.)$	**129.2**	**129.2**
		ExU_{exergy}	0.0033	0.5594
		$ExD_{volume}\ (MJ/Sm3o.e.)$	**93.6**	**93.9**
		ExD_{exergy}	0.0024	0.4065
	Total exergy efficiency	ε_{I-1}	99.8%	72.5%
		ε_{I-2}	99.7%	67.6%
		ε_{II-3}	7.9%	14.2%
	Task exergy efficiency	ε_{II-4}	**73.0%**	**72.9%**
		ε_{II-5}	**55.7%**	**55.6%**
	C-by-C exergy efficiency	ε_{III}	**20.0%**	**20.0%**

According to the values of the indicators presented in Table 20, when the *component chemical exergy* is not calculated, the energy-based indicators remain the same as in the Base Case, as expected. Practically no change between the two cases can be, also

found in the ExU_{volume} and the ExD_{volume} indicators, as the exergy destruction, the exergy of work and heat and the volume flow rate of the product in both cases remain the same. This is also the case for the ε_{II-4}, ε_{II-5} and ε_{III} indicators, which take into account the chemical exergy increase of the process and the physical exergy of the inlet and outlet streams separately. In this way the total chemical exergy increase is only a function of the chemical exergy increase of mixing (*component chemical exergy* increase of zero value). The slight differences between the values of ExU_{volume}, ExD_{volume}, ε_{II-4} and ε_{II-5} can be explained if the convergence error of the simulation algorithm in each case is taken into consideration. The rest of the exergy-based indicators do not give the same results in both cases, as for their calculations the absolute exergy of the inlet and outlet streams is used.

Table 21 shows that the *component chemical exergy* has practically no effect on the *exergy destruction ratio*, as in both cases the exergy destruction is the same and the *component chemical exergy* flows through each sub-system. This is not the case for the *exergy loss ratio*, which takes into account the absolute exergy of the streams discharged to the environment and the *efficiency defect* that includes the absolute exergetic content of the feed stream. More specifically, in case the *component chemical exergy* is not included in the calculations the inlet exergetic flow is significantly lower leading to much higher results in case of the *efficiency defect.*

Table 21 Exergy loss ratio and exergy destruction ratio in the case of no component chemical exergy compared with the Base Case

Energy/Exergy used/destroyed		Base Case 1	No component chemical exergy
Exergy loss ratio	cooling	65.2%	97.0%
	gas exhausted	0.1%	0.0%
	wastewater	34.7%	3.0%
Exergy destruction ratio	production manifold	56.8%	56.6%
	separation	11.7%	11.6%
	gas compression and exportation	30.1%	30.0%
	gas recompression	1.1%	1.3%
	oil pumping	0.1%	0.1%
	wastewater treatment	0.3%	0.3%
Efficiency defect	production manifold	1.3E-3	1.6E-1
	separation	2.7E-4	3.2E-2
	gas compression and exportation	7.1E-4	8.2E-2
	gas recompression	3.2E-5	3.7E-3
	oil pumping	1.5E-6	1.7E-4
	wastewater treatment	7.3E-6	8.5E-4

5. Case studies over changes in the product specifications and frame conditions

The performance of the platform presented in Chapter 3 is examined under a set of changes in the product specifications and frame conditions with the aim to get an overview of the function of the thermodynamic indicators for an offshore oil and gas processing plant. These changes correspond to the three new case studies introduced in this Chapter.

5.1 Description of the Case studies

5.1.1 The effect of the reservoir fluid composition on the thermodynamic indicators

In this case study the efficiency of the oil and gas processing plant presented in Chapter 3 is investigated for three different reservoir fluids processed. All the process parameters are the same, while the only variable changing is the composition of the well stream fluid treated in the process. In order to examine the effect of the reservoir fluid composition on the indicators two different Cases that include two different reservoir fluids have been added to the analysis conducted in this thesis.

One of the new cases together with the Base Case describe a lighter reservoir fluid representative of a gas-condensate field (Case 1 and Case 2), while Case 3 corresponds to a well fluid with a higher content of heavy hydrocarbons. All three Cases represent a different GLR (Gas-to-Liquid ratio) of the platform at issue, where GLR represents the ratio of the volume flow rate at standard conditions of the gas product stream to the volume flow rate at standard conditions of the liquid/condensate product.

The compositional data of Cases 2 and 3 have been provided by the oil and gas company Equinor, Norway representing a real case of a gas/condensate and an oil field, respectively. The composition of the reservoir fluids of Cases 1 to 3 are presented in Table E48 (Appendix E). For the pseudocomponents used in Cases 2 and 3 all the properties required have been given and they can be found in Table E51 and Table E49 (Appendix E).

Cases 2 and 3 have been simulated in ASPEN HYSYS® according to the process configurations of the Base Case and for the same molar flow rate of the inlet well stream, as well as the same product specifications. In this way the results of the energy and exergy analysis conducted for the four new Cases can be comparable to those of Case 1.

The results of the calculations are presented in Paragraph 5.2.1 .

5.1.2 The effect of the product specifications (CDB, TVP) on the thermodynamic indicators

A parameter that is important for the function of an oil and gas processing plant is the specifications of the products of the platform, as they not only define the product of the process but also determine the operating conditions (pressure, temperature levels etc.) of the platform. It is thus interesting to investigate the effect of these specifications on the indicators at issue. This is why the two following product specifications are selected to be tested for the processing plant of Chapter 3.

Cricondenbar Specification

The specification that is first tested is the Cricondenbar (CDB) of the export gas produced on the platform. This specification can give important information regarding how performance indicators respond to changes in the product specifications, with the focus on the case examined (Case 1) that represents a gas field (GLR=1345). In order to reach a specific CDB of the export gas the temperature of the dew point control scrubber is set appropriately (stream 39.gas 1 Figure 8) using the ADJUST function in the ASPEN HYSYS ® simulation. It should be noted that the temperature of the intercooling between the two compressors in the compression train is kept equal to 32.8°C, so that the results of the calculations can be comparable.

The temperature of the dew point controller calculated for each CDB selected is presented in Table 22 together with the values of CDB examined, while Cricondentherm specification of the export gas is in the given boundaries for all CDB tested.

Table 22 Data of CDB test for Case 1

CDB (bar)	Temperature of 39.gas 1 (°C)
100.0	19.82
103.1	25.00
105.0	28.09
110.0	35.92

Energy and exergy analysis is performed for the different cases of CDB and the results are presented in Paragraph 5.2.2. It should be noted that the indicators focusing on the performance of each sub-system are out of scope for these calculations that aim to investigate the overall performance of the platform.

True Vapour Pressure Specification

Next the effect of the true vapour pressure (bar) (TVP) at 37.8°C on the performance indicators is investigated. In this perspective the temperature of the oil heater is tested in order to achieve one the TVP of the export oil presented in Table 23 working again on the simulation of Case 1. It should be noted that the TVP of 0.9234 has been selected so that it corresponds to a TVP 6.7% lower than that of the Base Case, as is the relation between the CDB of the Base Case (103.1 bar) and the maximum CDB tested (110 bar).

The outlet temperature of the oil heater (stream 12.oil 2) in order to reach the given TVP specification is given in Table 23.

Table 23 Data of TVP test for Case 1

TVP	Temperature of 12.oil 2 (°C)
0.9234	90.63
0.9550	87.75
0.9650	86.86
0.9750	85.98
0.9896	85.00

The results of the conducted calculations are presented in Paragraph 5.2.2.

5.1.3 The effect of the decrease in the pressure of the gas exported on the thermodynamic indicators

The export pressure (as well as the temperature) of the products of the platform are given as product requirements and they are considered to be parameters externally defined that should be satisfied, as also are the CDB and the TVP specifications examined above. In this case the pressure of the gas leaving the compression train is set from 200 bar to 150bar, while the pressure of the first stage compression changes from 101.2 bar to 87.6 bar, so that equal pressure ratios are used (Appendix D).

Table 24 Pressure decrease of the export gas

Parameter changed	Value of Base Case	New Case
Pressure of the gas exported (stream 53) (bar)	200	150
Pressure of the first stage compression (stream 43) (bar)	101.2	87.6

A simulation is performed based on Case 1 and the results of the conducted calculations are presented in Paragraph 5.2.2.

5.2 Results & Discussion

In this Chapter the results of the energy and exergy analysis, as well as the calculation of the performance indicators for the aforementioned case studies are presented and discussed.

5.2.1 The effect of the reservoir fluid composition on the thermodynamic indicators

The results of the energy and exergy analysis for the cases of different reservoir fluids are given in the following Tables.

Some terms critical for the calculation of the indicators presented regarding Cases 1 to 3 can be found in Table 25.

It is evident that the since the separation design parameters (pressure levels, temperatures, number of stages etc.) are the same for all three Cases treating different reservoir fluids, the Gas-to-Liquid ratio (GLR) of the plant varies according to the fluid type treated. The highest GLR corresponds to Case 2, which is the Case with the lighter reservoir fluid (GLR=4943), while Case 3 shows the lowest GLR (GLR=50), as the fluid treated in that case is the richest in heavy hydrocarbons.

Table 25 Results of Cases 1, 2 & 3

	Case 3	Case 1	Case 2
GLR	**50**	**1345**	**4943**
$\dot{V_{export}}$ $(Sm^3 o.e./\mathrm{h})$	3838.3	733.8	543.5
$\dot{LHV_{export}}$ (MW)	44712.3	8380.2	6349.8
Exergy of well stream (MW)	43160.8	8075.9	6076.7
$\dot{E_{export}}$ (MW)	43153.6	8078.0	6079.5
$\dot{Ed}$ (MW)	36.5	19.1	18.4

All product specifications are satisfied for all three Cases, as presented in Table 26.

Table 26 Product specifications results of Cases 1, 2 & 3

		Case 3	Case 1	Case 2
Export gas	Cricondenbar < 105 bar	98.55 bar	103.1 bar	104.6 bar
	Cricondentherm < 40°C	26.13°C	25.07°C	25.27°C
	Gas export pressure = 200 bar	200 bar	200 bar	200 bar
	Gas export temperature < 60°C	60°C	60°C	60°C
Export oil	TVP (37.8°C) < 1.013 bar	0.9414 bar	0.9862 bar	0.8754 bar
	Oil export pressure = 10 bar	10 bar	10 bar	10 bar

The energy and exergy of heating, cooling and compression/pumping of Cases 1 to 3 can be found in Table 27, as well as in Figure 11.

Table 27 Energy and Exergy of heating, cooling and compressing/pumping of Cases 1 to 4 (MW)

	Energy of cooling	Exergy of cooling	Energy of heating	Exergy of heating	Energy/Exergy of compression/ pumping
Case 3	-93.8	-15.6	45.2	13.0	33.2
Case 1	-42.8	-3.4	11.2	3.2	23.1
Case 2	-39.6	-2.6	8.4	2.4	23.1

It is evident that the greatest amount of energy/exergy of cooling and compression/ pumping can be found in Case 3. This is because this Case represents a heavier reservoir fluid and thus, for the same process configurations a greatest amount of gas is separated in the last stages of the separation train. In this way, the cooling and work demands in the recompression train are higher. The energy/exergy heating duties are also higher in Case 3, due to the greater amount of oil processed in the separation train.

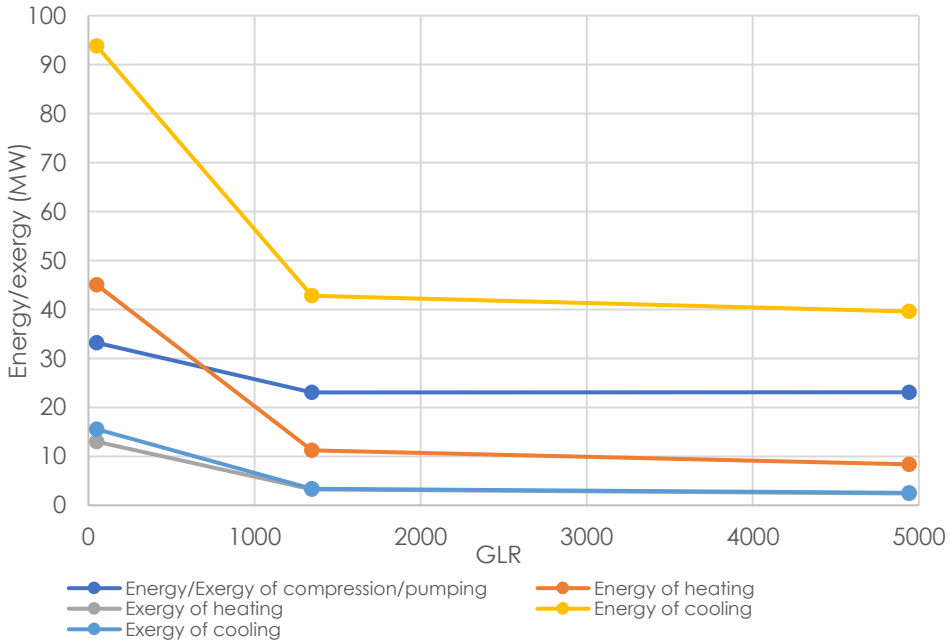

Figure 11 Energy & Exergy demands for heating, cooling and compression/pumping of Cases 1-3 as a function of the GLR

The calculation of the energy-based indicators for Cases 1, 2 and 3 are presented in Table 28, while the exergy-based indicators *ExU* and *ExD* are given in Table 29. The *EnU*, *ExU*, *ExD* and *Specific power consumption* are given in Figure 12 as a function the GLR.

Table 28 Energy-based indicators of Cases 1, 2 & 3

	CO_2 intensity (kg CO_2 / bbl)	EnUvolume (MJ/std m3 o.e.)	Specific power consumption (MJ/std m3 o.e.)	EnUenergy
Case 3	0.8	73.4	31.1	0.0018
Case 1	3.3	168.3	113.3	0.0041
Case 2	4.6	208.4	152.9	0.0050

According to Table 28 and Table 29, the process of Case 3 seems to perform better than Cases 1 and 2, even though Case 3 exhibits the highest heating, cooling and work demands. This is because Case 3 shows the highest volume export rate, LHV and exergetic content of the product of all three Cases. The indicators presented in Table 28 and Table 29 show a better energy/exergy efficiency for the platforms treating heavier reservoir fluids due to the lower energy/exergy consumed per unit of product.

Table 29 Exergy-based indicators ExU & ExD of Cases 1, 2 & 3

	ExUvolume (MJ/std m3 o.e.)	ExUenergy	ExDvolume (MJ/std m3 o.e.)	ExDexergy
Case 3	43.4	0.0011	34.2	0.0008
Case 1	129.2	0.0033	93.6	0.0024
Case 2	169.0	0.0042	121.7	0.0030

Specific Power Consumption and *CO_2 intensity* develop in a similar way, as they both take into account the work demands and the volume flow rate of the export product. They are not, however proportional, since the *CO_2 intensity*, also includes the LHV of the export gas produced.

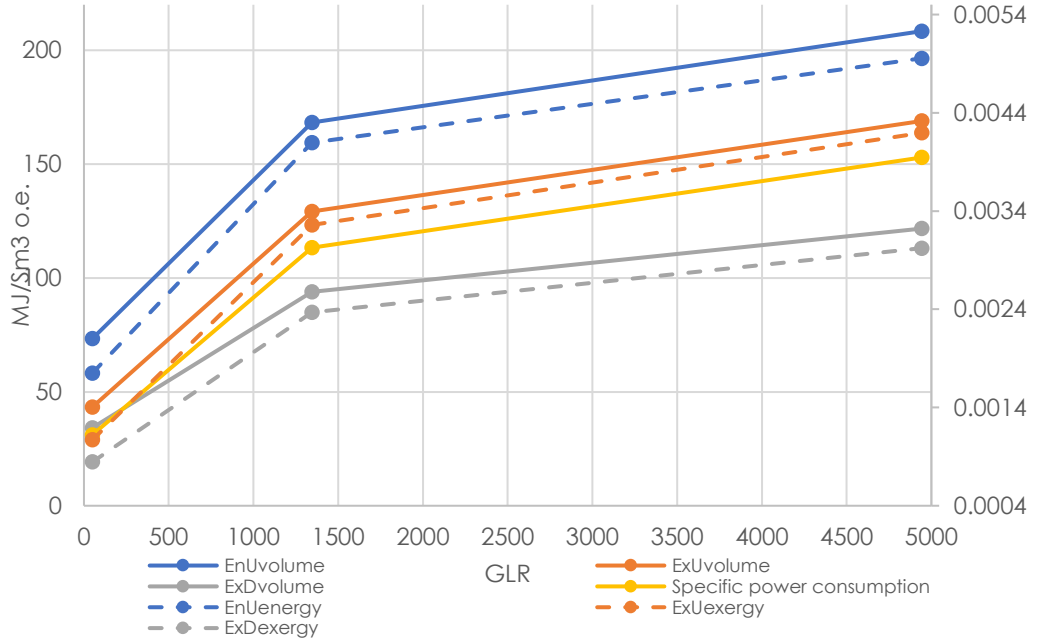

Figure 12 ExU, EnU, ExD of Cases 1-3 as a function of the GLR (solid lines are read on the left axis and shed lines on the right axis)

According to Table 30 the *Total exergy efficiency* shows significantly low sensitivity to the fluid type. The *Total exergy efficiency* seems to be always high, as for the calculation of the exergy terms the chemical exergy of each stream (which is very high as hydrocarbon mixtures are treated) is taken into account. The high values of the indicator lead to the fact that the *total exergy efficiency* would be difficult to use in order to compare the performance of oil and gas facilities, due to the similar values of the indicator for all Cases. (Voldsund M. , 2014).

Table 30 *Total* exergy efficiency of Cases 1, 2 & 3

	Total exergy efficiency	
	$\varepsilon_{I-1} = \frac{\sum_{k,u} \dot{E}_{k,u} + \sum_{k,w} \dot{E}_{k,w} + \dot{E}^{Q}_{cool}}{\dot{E}_{feed} + \dot{E}^{Q}_{heat} + \dot{E}^{W}}$	$\varepsilon_{I-2} = \frac{\sum_{k,u} \dot{E}_{k,u}}{\dot{E}_{feed} + \dot{E}^{Q}_{heat} + \dot{E}^{W}}$
Case 3	99.9%	99.9%
Case 1	99.8%	99.7%
Case 2	99.7%	99.6%

Kotas (1995) and Tsatsaronis (1993) supported this view in their works pointing out that *Total exergy efficiency* does not give any indication regarding the potential of increasing the efficiency of the system. In this way, and giving similar results for different cases *total exergy efficiency* could produce misleading results and conclusions.

They also, pointed out that *Total exergy efficiency* does not highlight the purpose of the process; the separation of oil, gas and water and the exportation of the products. (Voldsund M. , 2014)

Task exergy efficiency denotes that-unlike energy-based indicators and *ExU* and *ExD*- Case 3 corresponds to the least efficient process of all three. This comparison, however cannot be made when *task exergy efficiency* ε_{II-3} is used, as this indicator gives a negative result for Case 3. This is a result of an export pressure of the product lower than the inlet pressure of the feed, as the main product of Case 3 is the produced oil which is exported at 10 bar compared to the 120 bar of the well stream feed.

Table 31 *Task* and *Component-by-Component exergy efficiency* of Cases 1, 2 & 3

	Task exergy efficiency			Component-by-Component exergy efficiency
	$\varepsilon_{II-3}=\frac{\sum_{k,u}\dot{E_{k,u}}-\dot{E_{feed}}}{\dot{E_{heat}^{Q}}+\dot{\mathrm{E}^{\mathrm{W}}}}$	$\varepsilon_{II-4}=\frac{\Delta\dot{\mathrm{E}^{ch}}+\sum_{k,u}\dot{E_{k,u}^{ph}}}{\dot{E_{feed}^{ph}}+\dot{E_{heat}^{Q}}+\dot{\mathrm{E}^{\mathrm{W}}}}$	$\varepsilon_{II-5}=\frac{\Delta\dot{\mathrm{E}^{ch}}+\sum_{k+,u}\dot{m_{k+,u}}*(e_{k+,u}^{ph}-e_{feed}^{ph})}{\sum_{k-}\dot{m_{k-}}*(e_{feed}^{ph}-e_{k-}^{ph})+\dot{E_{heat}^{Q}}+\dot{\mathrm{E}^{\mathrm{W}}}}$	$\varepsilon_{III}=\frac{\Delta\dot{E^{ch}}+\sum_{j}\sum_{k,u}\left(\Delta\dot{E_{j,k}^{ph}}\right)_{u}^{+}}{\sum_{j}\sum_{k}\left(\Delta\dot{E_{j,k}^{ph}}\right)^{-}+\dot{E_{heat}^{Q}}+\dot{\mathrm{E}^{\mathrm{W}}}}$
Case 3	-15.7%	36.5%	31.2%	4.5%
Case 1	7.9%	73.0%	55.7%	20.0%
Case 2	10.9%	75.7%	46.0%	22.0%

Task exergy efficiency ε_{II-4} indicates Case 2 as the most efficient process. This is because this indicator takes into account as product exergy the increase of chemical exergy and the physical exergy of the product streams. The second term -dominant term- is significantly higher in Case 2, as the greatest amount of gas which is the dominant product of Case 2 is produced at a pressure much higher than that of the feed stream and the oil product.

On the other hand, the *task exergy efficiency* ε_{II-5} shows the highest efficiency for Case 1, as this process corresponds to the highest physical exergy gain between the feed and the export oil and gas (mainly due to gas) streams, as presented in Table 32.

Table 32 Specific physical exergy (mass basis) of the inlet and outlet streams of Cases 1, 2 & 3

Inlet/Outlet streams	Mass exergy (kJ/kg)	Case 3	Case 1	Case 2
1. well stream	$e_{feed}^{ph}=$	37.29	315.0	447.6
8. gas from water treatment	$e_{k-,u}^{ph}=$	22.9	23.3	24.6
9. water from water treatment	$e_{k-,u}^{ph}=$	10.6	10.7	11.0
47. export oil	$e_{k-,u}^{ph}=$	4.8	5.1	7.2
53. export gas	$e_{k+,u}^{ph}=$	467.3	580.9	610.9

In case of the *Component-by-Component exergy efficiency* Case 2 is more efficient than the other three processes and this is because of the greatest physical exergy increases and the lowest physical exergy decreases of all cases, as found also in Table 34. The *Component-by-Component exergy efficiency* is based on the same reasoning as *Task exergy efficiency* ε_{II-5}, but carried out on the chemical component level. This could explain the different results provided by the calculation of these two indicators.

Table 33 Physical exergy of each stream (MW)

Physical exergy	Case 3	Case 1	Case 2
$\dot{E}^{ph}_{1,53,in}$	22.0	53.6	58.2
$\dot{E}^{ph}_{1,53,out}$	23.8	58.3	63.4
$\dot{E}^{ph}_{1,47,in}$	17.5	1.7	4.8E-1
$\dot{E}^{ph}_{1,47,out}$	5.3	4.8E-1	1.8E-1
$\dot{E}^{ph}_{1,8,in}$	1.5E-3	8.6E-4	4.0E-4
$\dot{E}^{ph}_{1,8,out}$	2.2E-5	1.3E-5	6.3E-6
$\dot{E}^{ph}_{1,9,in}$	2.1E-4	2.6E-4	2.6E-4
$\dot{E}^{ph}_{1,9,out}$	8.3E-5	1.0E-4	1.1E-4
$\left(\Delta\dot{E}^{ph}_{j,k}\right)^{+}_{u}$	1.9	4.7	5.2
$\left(\Delta\dot{E}^{ph}_{j,k}\right)^{+}_{w}$	0.0	0.0	0.0
$\left(\Delta\dot{E}^{ph}_{j,k}\right)^{-}$	12.3	1.4	4.6E-1

Total, Task and *Component-by-Component* exergy efficiency of Cases 1-3 are given in Figure 13.

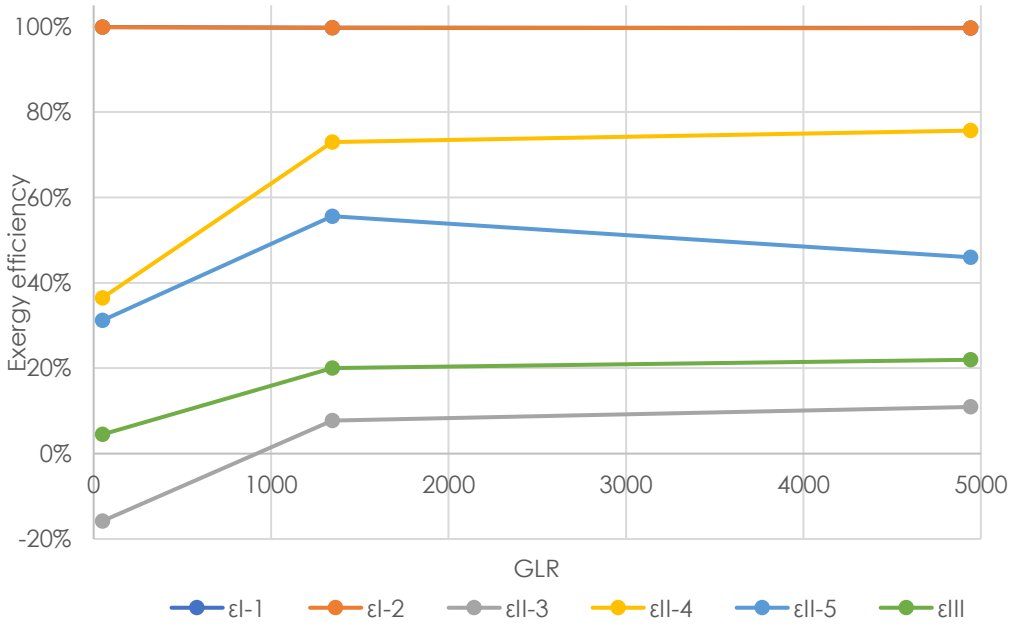

Figure 13 *Total, Task* and *Component-by-Component exergy efficiency* of Cases 1-3 as a function of the GLR

The *exergy loss ratio* (Table 34) and the *exergy destruction ratio* (Table 35) show a similar breakdown of the exergy loss and the exergy destruction rate for Cases 1 and 2. This is probably because both Cases represent a gas/condensate field with similar energy/exergy heating, cooling and work duties (<25% deviation). However, in Case 2 the exergy destruction ratio in the compression train is higher, as higher is the amount of gas exported. The exergy destruction ratio in the separation train in Case 2 is on the other hand lower, as for the design parameters of the Base Case most gas is separated in the first stages of the separation train.

Case 3 shows the highest amount of exergy lost due to cooling since, as mentioned above, a great amount of gas is separated in the last stages of the separation train and, thus cooling demands in the recompression train are higher.

Table 34 *Exergy loss ratio* for Cases 1, 2 & 3

	Exergy loss ratio		
	Cooling	Gas exhausted	Wastewater
Case 3	91.5%	0.0%	8.5%
Case 1	65.2%	0.1%	34.7%
Case 2	58.7%	0.0%	41.3%

According to the *exergy destruction ratio* of Case 3, most exergy is destroyed in the separation train. This is because the process configurations used for the simulation of this case correspond to a gas/condensate field (lighter reservoir fluid), while the well stream fluid corresponds to an oil field. In this case, the heavier the reservoir fluid is, the more oil is treated in the 3-stage separation train and, thus more exergy is destructed for heating, expanding and pumping the oil processed.

Table 35 *Exergy destruction ratio* for Cases 1, 2 & 3

	Exergy destruction ratio					
	Production Manifold	Separation	Gas compression & exportation	Gas recompression	Oil pumping	Wastewater treatment
Case 3	22.4%	66.2%	6.4%	4.1%	0.8%	0.1%
Case 1	56.8%	11.7%	30.1%	1.1%	0.1%	0.3%
Case 2	62.3%	3.2%	33.8%	0.4%	0.0%	0.3%

Again, the *Efficiency defect* shows a similar breakdown for Cases 1 and 2 (Table 36), while Case 2 exhibits the highest value for the production manifold and Case 3 for the Separation train, similarly to the *Exergy destruction ratio.* It should be noted that the values of the *Efficiency defect* are higher for Case 2, followed by Case 1 and finally Case 3. This is because, *Efficiency defect* takes into account the exergetic content of the feed stream in the denominator, which is higher for heavier reservoir fluids (same temperature, pressure and flow rate).

Table 36 *Efficiency defect* for Cases 1, 2 & 3

	Efficiency defect					
	Production Manifold	Separation	Gas compression & exportation	Gas recompression	Oil pumping	Wastewater treatment
Case 3	1.9E-4	5.6E-4	5.4E-5	3.5E-5	6.5E-5	1.1E-6
Case 1	1.3E-3	2.7E-4	7.1E-4	3.2E-5	1.5E-6	7.3E-6
Case 2	1.9E-3	9.8E-5	1.0E-3	1.1E-5	6.9E-7	9.7E-6

5.2.2 The effect of the product specifications (CDB, TVP) on the thermodynamic indicators

The results of the calculations for changes in the CDB and the TVP specification are presented below.

Cricondenbar Specification

The heat, work and cooling demands of the platform are presented in Figure 14 as a function of the CDB specification of the export gas (bar). According to Figure 14 work demands are higher for greater CDB specifications (up to 3% increase). This can be explained by the higher inlet temperature in the 1st export gas compressor that results in greater compression duties, as well as the higher amounts of gas treated in the compression train (increase up to 0.4%). This work increase outweighs the work decreases of 5-6% detected in the recompression train, as the flowrates of the oil processed in the platform is lower for higher CDB. This is explained by the higher GLR gained for higher CDB (up to 2% increase) (Figure 22). Cooling duties show a slight decrease of 1% for higher CDB. The higher the CDB the less the oil that is treated, that means lower amounts of oil recompressed and cooled. At the same time, the temperature of cooling in the dew point control scrubber cooler is higher for higher CDB resulting in lower cooling demands for higher CDB. The only cooler that shows an increase in duty is the 1st export gas cooler that has a higher inlet temperature for higher CDB. The exergy of cooling on the other hand shows an increase for higher CDB (12%) as it considers the temperatures of the cooling medium used in each case. Heating duties decrease for higher CDB (up to 3%) due to the drop in the amount of oil treated (rise in GLR for higher CDB), as well as the temperature increase of the liquid stream leaving the dew point control scrubber that increases the temperature of the 3-phase separation which is followed by the oil heater.

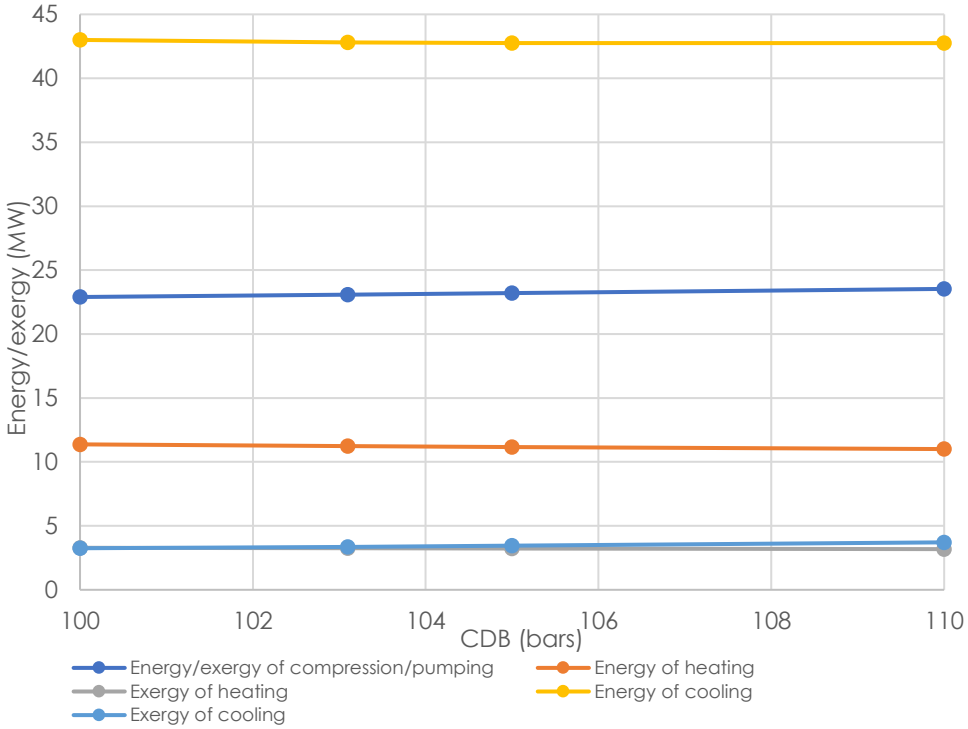

Figure 14 Energy/exergy of heating, compression and pumping of Case 1 for various CDB of the export gas

Specific CO_2 emissions, *EnU*, *ExU*, *ExD* and *Specific power consumption* show an increase for higher CDB specifications that indicates a worse performance of the platform when less strict demands in CDB are used. This is a result of the higher work demands for producing oil and gas of practically the same energy content (deviation of 0.1%) (Figure 16) that shows the high effect of the temperature of scrubbing on the work demands in the compression train.

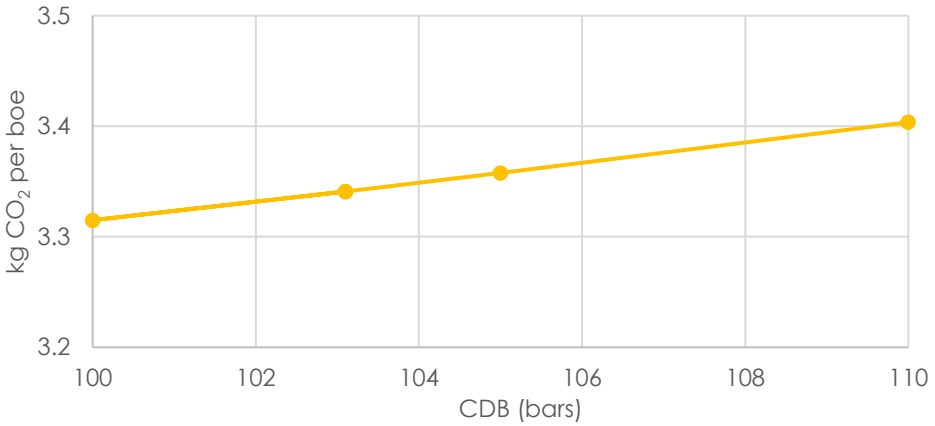

Figure 15 *Specific CO_2 emissions* of Case 1 for various CDB of the export gas

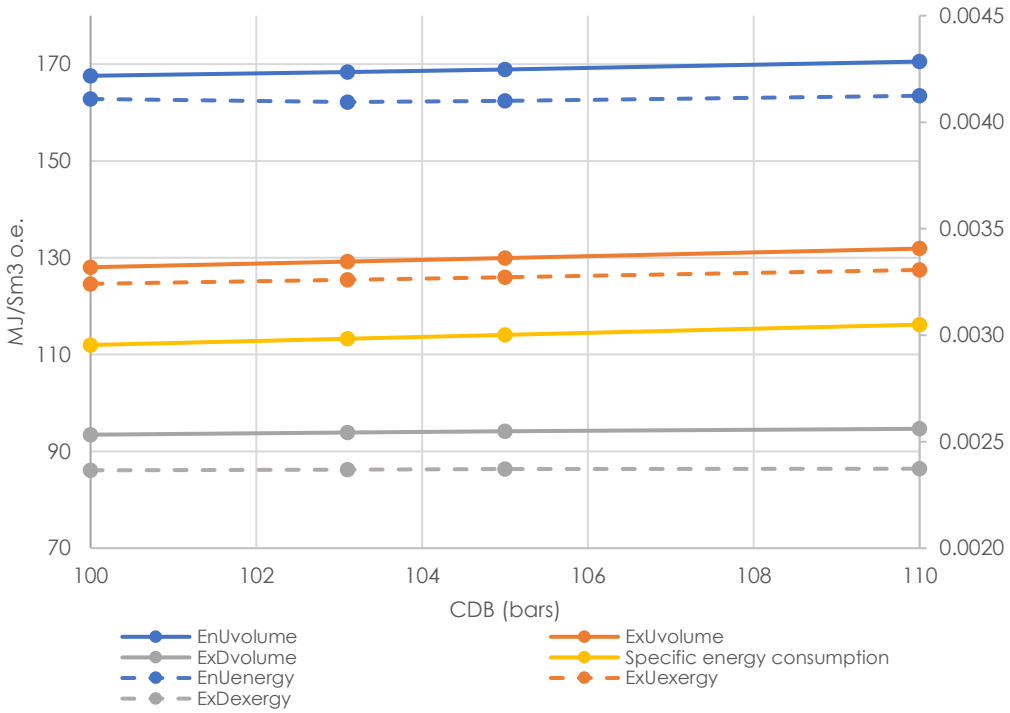

Figure 16 *EnU, ExU, ExD* & *Specific power consumption* of Case 1 for various CDB of the export gas (solid lines are read on the left axis and dashed lines on the right axis)

According to Figure 17, *Total exergy efficiency* remains constant for different CDB specifications, which is explained by the lack of sensitivity of these indicators as mentioned in previous analysis. *Task exergy efficiency* and *Component-by-Component exergy efficiency* indicate a worse performance for higher CDB showing a drop between 1% and 5%. For the *Task exergy efficiencies* ε_{II-3} and ε_{II-4} this decrease is a result of the higher exergy demands for compression and heating (as a sum) for greater CDB specifications (for the same product exergy). This is, also the case for the *Component-by-Component exergy efficiency,* together with the fact that for higher CDBs the product exergy decreases due to the lower chemical exergy gain of separation. Only for the *Task exergy efficiency* ε_{II-5} the fuel exergy drops for higher CDBs, as the exergy decrease between the feed and the export oil is lower, because of the less oil that is produced in this case (GLR increase). The product exergy again drops for higher CDBs due to the lower specific exergy of the export gas stream. As a result, the *Task exergy efficiency* ε_{II-5} is lower for higher CDB specifications. Overall, it could be highlighted that in this case *Task exergy efficiencies* ε_{II-3} and ε_{II-4} focus more on the heat and work increases/decrease, while *Task exergy efficiency* ε_{II-5} and *Component-by-Component exergy efficiency* take also into account the separation performance - the displacement of some component from the oil to the gas product (and vice versa).

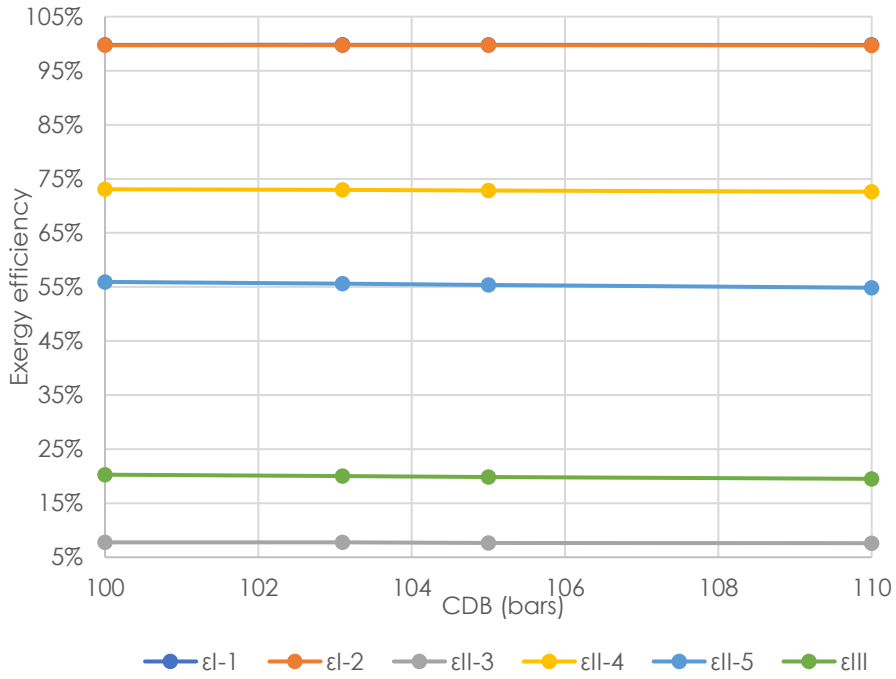

Figure 17 *Total, Task* & *Component-by-Component exergy efficiency* of Case 1 for various CDB of the export gas

True Vapour Pressure Specification

Figure 18 shows the heat, work and cooling duties of the platform for the different TVP specification tested. According to Figure 18 work demands show a decrease of up to 0.6% for greater TVP, as the GLR drops for higher TVP (up to 0.3%) resulting in lower compression duties in the compression train (Figure 22). At the same time the temperature of heating is lower for higher TVP resulting in lower temperatures of the streams entering the compressors in the recompression train and thus lower work demands. Cooling demands decrease for higher TVP (up to 4%) as lower is the temperature of the gas compressed in the recompression train. As it is evident heating drops (up to 9%) for higher TVP as the oil is heated at lower temperatures.

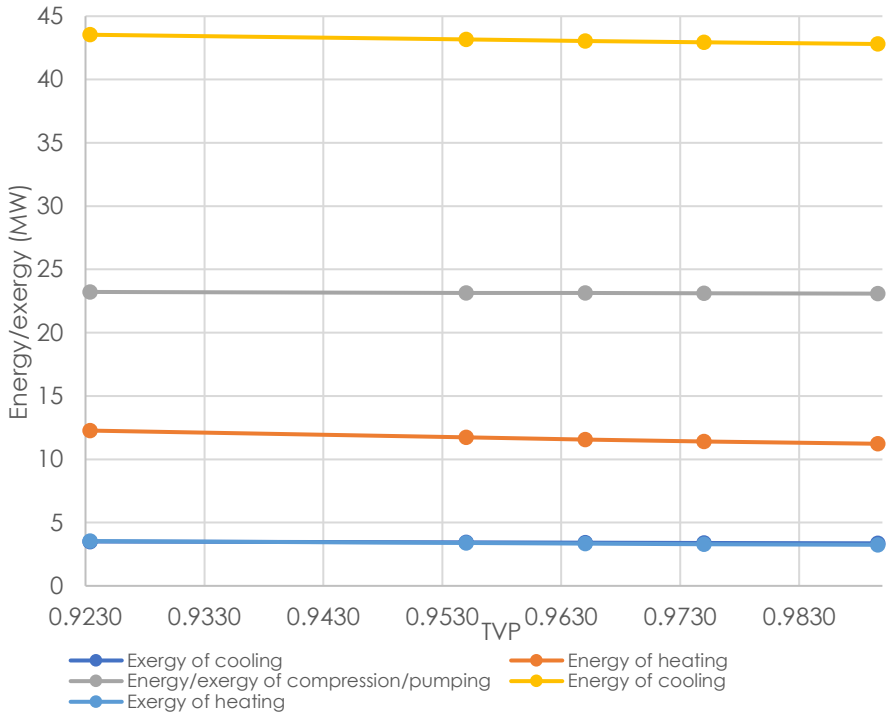

Figure 18 Energy/exergy of heating, compression and pumping of Case 1 for various TVP of the export oil

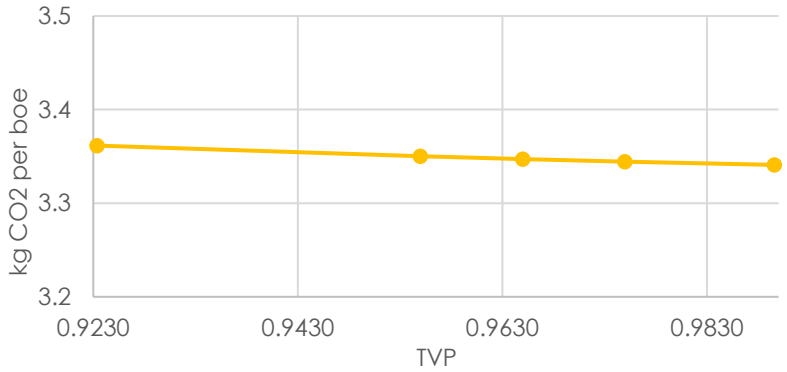

Figure 19 *Specific CO_2 emissions* of Case 1 for various TVP of the export oil

EnU, ExU and *ExD* show a decrease for higher TVP specifications highlighting a better performance of the process for less strict specifications of TVP. This is a result of the decrease in both heat and work demands of the platform, while the oil and gas produced are of practically the same energy/exergy content (< 0.0% deviation) (Figure 18). As it would be expected *Specific power consumption* and *Specific CO_2 emissions* decrease proportionally to the power demands (practically constant LHV of the export gas). It needs to be pointed out that *EnU* indicators show the highest decrease for higher TVP, since heat has a more dominant effect on this indicator compared to the others explained by the difference between the energy and the exergy form of heating.

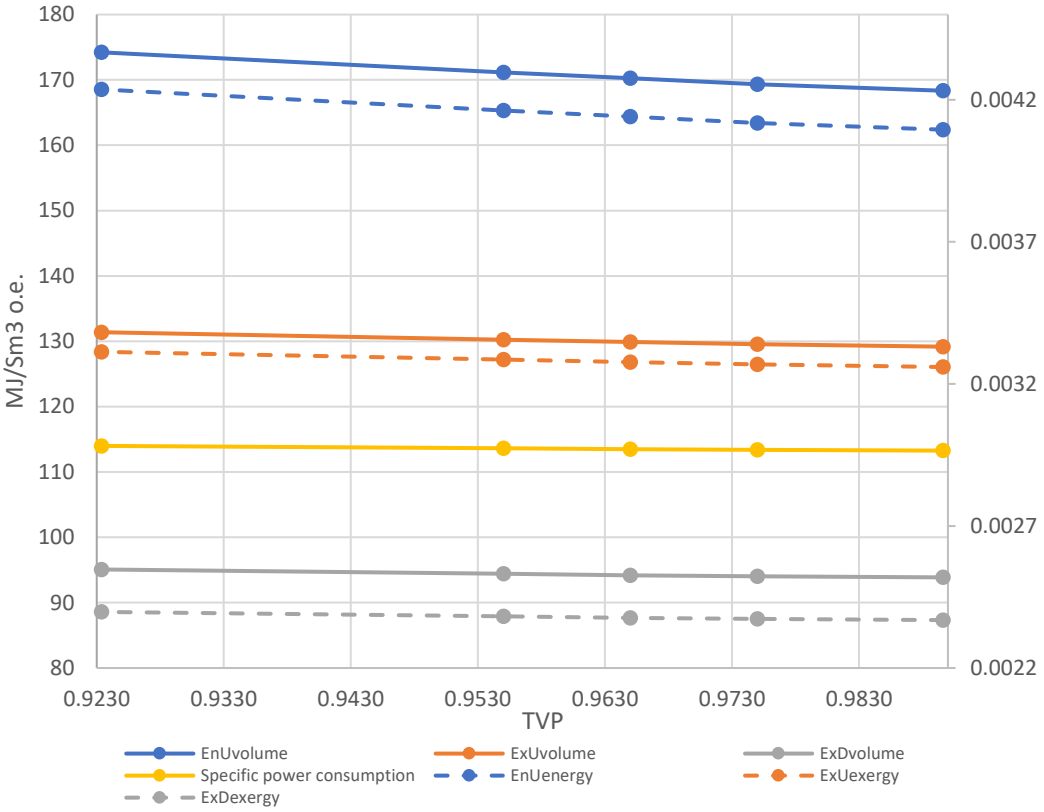

Figure 20 *EnU, ExU, ExD* & *Specific power consumption* of Case 1 for various TVP of the export oil (solid lines are read on the left axis and dashed lines on the right axis)

Total exergy efficiency shows again no difference for various TVP specifications. *Task exergy efficiency* ε_{II-3} is the only indicator that exhibits a decrease of around 1% for higher TVP, while the rest of the *Task exergy* and the *Component-by-Component exergy efficiencies* increase (0.4-1%). The ε_{II-3} drops for higher TVPs, as it is very sensitive to changes in the product and feed exergy. For higher TVPs the flow of the export oil is higher and the flow of the export gas is lower, as explained by the lower GLR for higher TVP (a part of the components that take part in the process are displaced from the gas to the oil product). In this way the exergy of the gas decreases for higher TVP and the exergy of the oil increases. Since the exergy increase is higher than the exergy decrease, there is a slight drop in the product exergy for higher TVP of up to 0.001%. This growth is enough to outweigh the decreases in work and heat duties resulting in higher ε_{II-3} values. This is not the case for the rest of the *Task exergy* and *Component-by-Component exergy efficiencies* where the chemical exergy of the products is not taken into account in the product exergy and thus the values change mainly in respect with the heat and work increases/decreases.

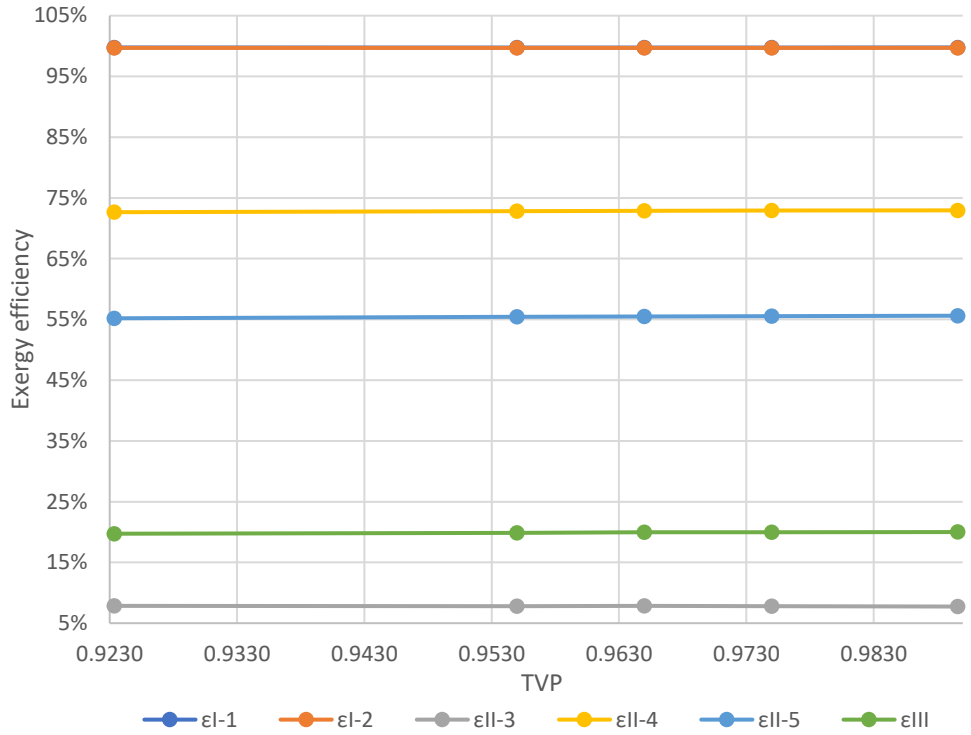

Figure 21 *Total, Task* & *Component-by-Component exergy efficiency* of Case 1 for various TVP of the export oil

Next in order, Figure 22 illustrates the change in the values of the calculated indicators for a 6.7% increase in the CDB and decrease in the TVP specification, so as to get a better view of how indicators react to changes in the product specifications.

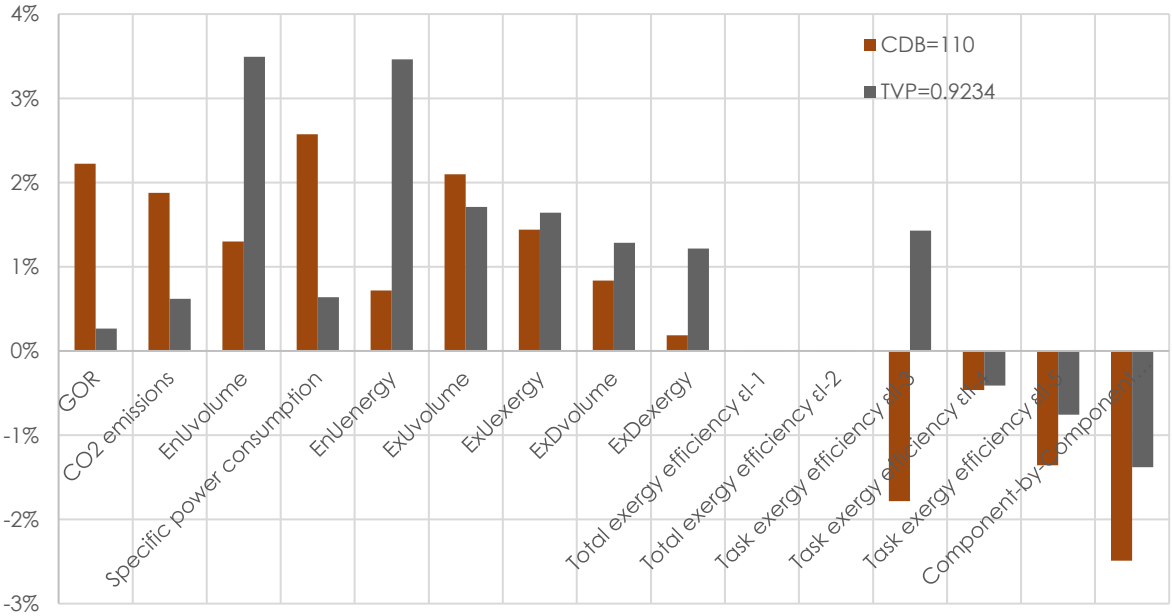

Figure 22 Change (%) in the values of the indicators calculated for the same change (6.7%) of the CDB and the TVP product specifications.

According to Figure 22 the same change of the CDB and TVP specification results in a much higher GLR change for the CDB case (8 times higher). This is why the volume export rate of the product is more affected by the change of CDB (1% vs 0.1%) and thus for similar work increases (1% and 2% for the TVP and the CDB change, respectively) *Specific power consumption* and *CO_2 emissions* react more to the CDB change (4- and 3-times higher change, respectively). As presented above in case of the TVP drop there is a 9% increase in heating duties compared with the 2% heat rise for the same change in CDB. This high increase in the heating duties of the TVP change is reflected in the *EnU* indicators.

ExUvolume highlights the effect of both the work and heat exergy increases and the difference in the volume flow rate of the export product resulting in close variations of the indicators for a 6.7% change in the TVP and CDB. This is also the case for the *ExUexergy*, but for the exergy of the export product. *ExDexergy* on the other hand underlines the higher exergy destruction taking place for the case of the TVP change that results from struggling at higher temperatures in case of higher TVPs. The changes in *Total exergy efficiency* are once more insignificant to be compared.

In all cases except for the *task exergy efficiency* ε_{II-3} the indicators show the same behavior towards the CDB or TVP change. ε_{II-3} gives a different direction for the performance of the platform, because of its high sensitivity to minor changes (e.g. 0.001%) in the product exergy. In this way the effect of the work and heat exergy increases or decreases is difficult to show. For the rest of the *task* and *component-by-component exergy efficiencies* the CDB change shows a higher effect. The increase in heat and work exergy demands is higher for the TVP decrease (1.6% vs 0.6%), as also is the increase in the exergy of the useful products (0.001% vs 0.0001%). This greater rise in the product exergy in case of the TVP seems to be the determining factor explaining the greater drop in case of the CDB. *Task exergy efficiency* ε_{II-5} and *Component-by-Component exergy efficiency* that take into account this physical exergy difference of the displacement of some components from the export gas to the export oil in the fuel exergy term give an even higher difference between the drop in the indicators for the TVP and CDB change.

Al in all, it could be said that the same change in the TVP and CDB specifications of the two products of the process may give different information depending on the indicator used. Even though the overall picture remains the same for the two cases different indicators show relatively different changes. *EnU, ExU, ExD* and *Specific power consumption* and *CO_2 emissions* are not consistent to the efficiency drop for the two cases as they consider both the changes in the power and heat demands and the changes in the volume flow rate and the exergetic content of the product, with each indicator paying different attention to each of these parameters. At the same time *task* and *component-by-component exergy efficiencies* highlight the distribution of the components in the products of the process leading to the same behavior of the indicators for the same CDB and TVP change.

Further calculations of variations in other specifications, such as the CDT of the export gas, or even changes in the CDB and TVP through manipulating a different parameter (e.g., pressure instead of temperature) could also be tested in order to have a more complete view of the effect of the product specifications on the performance indicators.

5.2.3 The effect of the decrease in the pressure of the gas exported on the thermodynamic indicators

The energy and exergy consumption of the platform for the case under discussion is presented in Figure 23.

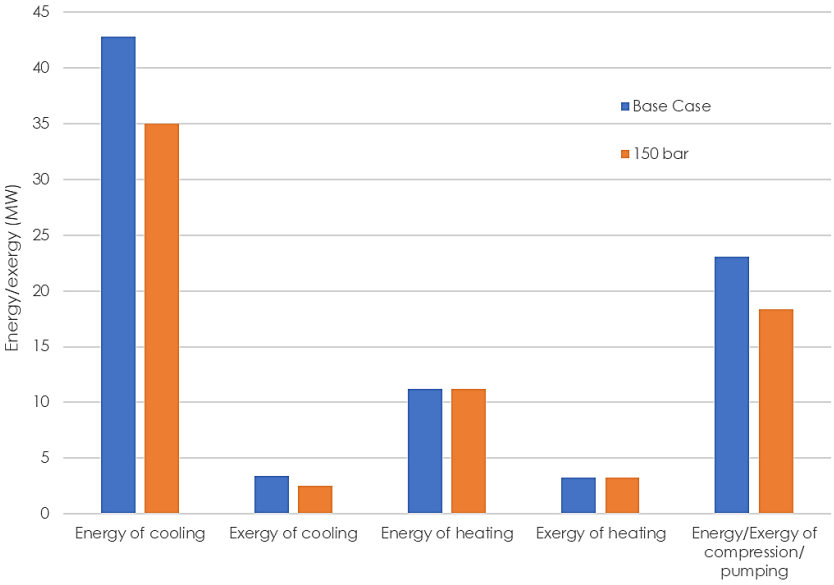

Figure 23 Energy/Exergy consumption in case of decrease in pressure of the export gas compared to the Base Case

According to Figure 23, work duties and cooling duties associated with the compression train show a drop of 20% and 18%, respectively. it should be pointed out that exergy destruction exhibits a drop of 1.2 MW that represents the amount of exergy savings in case of less cooling and compressing in the compression train.

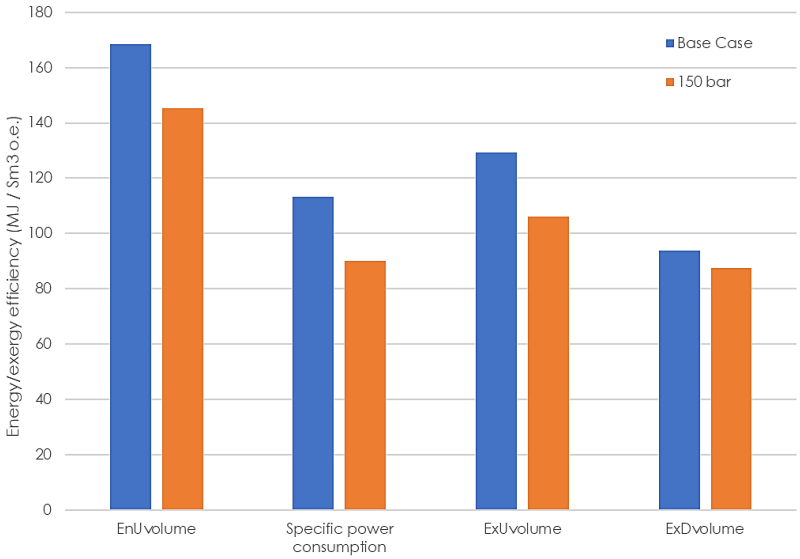

Figure 24 *EnUvolume, ExUvolume, ExDvolume, Specific power consumption* in case of decrease in pressure of the export gas compared to the Base Case

In case of lower export pressure of the gas produced all energy-based indicators show an increase in the platform's efficiency ranging from 14% to 20%, as work demands decrease in order to produce oil and gas with a constant energetic content and flowrate (Figure 24, Figure 25, Figure 26).

ExU and *ExD* indicators give again a higher efficiency of up to 18% (Figure 24, Figure 25). *ExUexergy* and *ExDexergy* show a lower rise of 7% and 8%, respectively, due to a 0.03% drop in the exergetic content of the export products which is a result of the drop in the pressure of the export gas. ε_{I-1} and ε_{I-2} remain constant, which is explained by the lack of sensitivity of the *total exergy efficiency*, as also denoted by the minor change between the values of the indicators presented in previous cases (Figure 27).

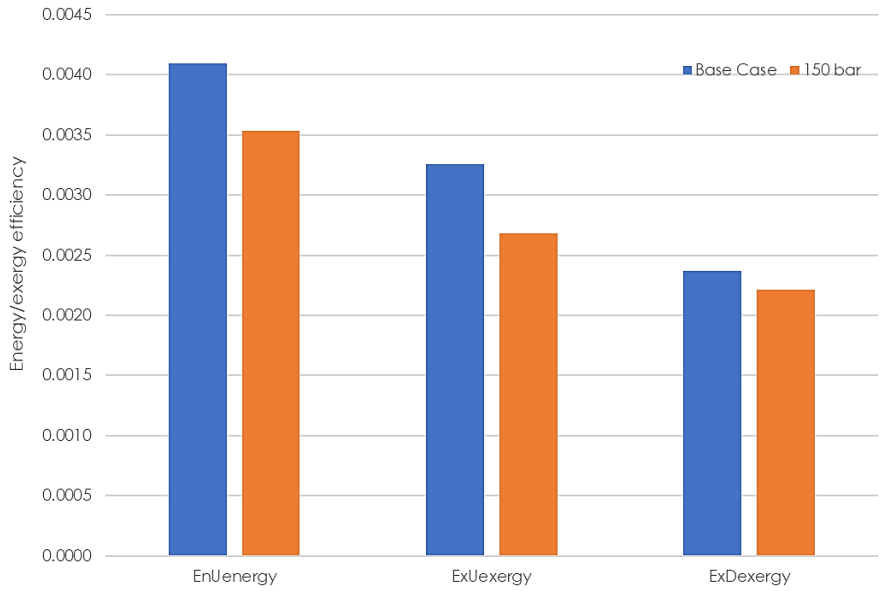

Figure 25 *EnUenergy, ExUexergy, ExDexergy* in case of decrease in pressure of the export gas compared to the Base Case

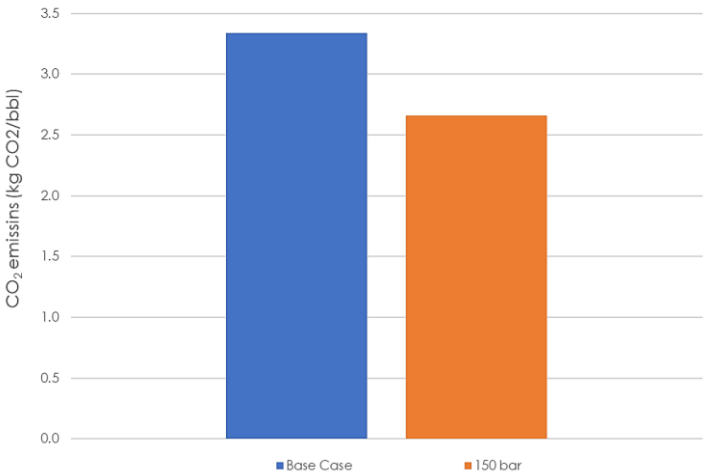

Figure 26 *Specific CO_2 emissions* in case of decrease in pressure of the export gas compared to the Base Case

The ε_{II-3} indicator is of negative value, as the exergy of the feed stream is in this case higher than the exergy of the output streams (Figure 27). This is a result of higher input pressures and temperatures of the input streams in comparison to the pressures and temperatures of the oil and gas streams. In this case, the reductions of physical exergy greatly outweigh the increases of chemical exergy, leading to negative task exergy efficiencies. The negative result of the indicator in this case leads to no possible comparison between the two cases.

According to Figure 27, ε_{II-5} and ε_{III} are the only indicators that give a worse performance of the process in case of lower export pressure of the gas. This shows that the exergy gain in the physical exergy term of the export gas is more important than the same amount of exergy gained by avoiding compression. It could, thus be said that these indicators show the effect of the drop in heat and work duties on the products and that they consider more important the increase in the physical exergy of the products than the same drop in the fuel exergy of the process.

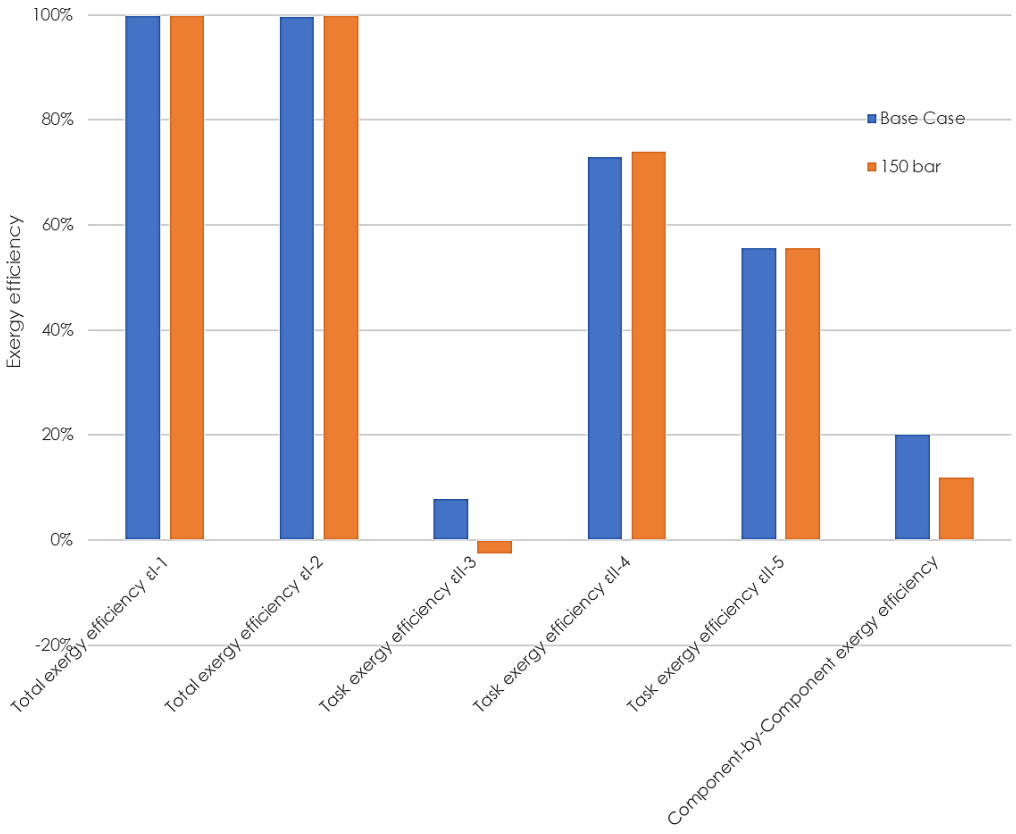

Figure 27 *Total, Task, Component-by-Component exergy efficiency* in case of decrease in pressure of the export gas compared to the Base Case

According to Table 37 exergy loss ratio riser drops for cooling, as lower are the cooling demands of the platform. The *exergy destruction ratio* shows a drop for the gas compression train from 30.1% to 25.0%, which results to a rise in the ratios of the other subsystems. The *efficiency defect* of the gas compression and exportation system drops while the for the rest of the subsystems it remains constant.

Table 37 Exergy loss ratio and exergy destruction ratio in the case of pressure drop of the export gas compared with the Base Case

Energy/Exergy used/destroyed		Base Case 1	Pressure drop of export gas
Exergy loss ratio	cooling	65.2%	58.5%
	gas exhausted	0.1%	0.1%
	wastewater	34.7%	41.4%
Exergy destruction ratio	production manifold	56.8%	60.7%
	separation	11.7%	12.5%
	gas compression and exportation	30.1%	25.0%
	gas recompression	1.1%	1.4%
	oil pumping	0.1%	0.1%
	wastewater treatment	0.3%	0.3%
Efficiency defect	production manifold	1.3E-3	1.3E-3
	separation	2.7E-4	2.7E-4
	gas compression and exportation	7.1E-4	3.2E-5
	gas recompression	3.2E-5	3.2E-5
	oil pumping	1.5E-6	1.5E-6
	wastewater treatment	7.3E-6	7.3E-6

The results of the changes of frame conditions and products specifications tested in this Chapter are grouped in Figure 28. The diagram shows the increase in efficiency for each case examined in this Chapter percentage-wise from the Base Case scenario. It should be noted that for the CDB and TVP cases investigated the greatest change examined is presented in the figure.

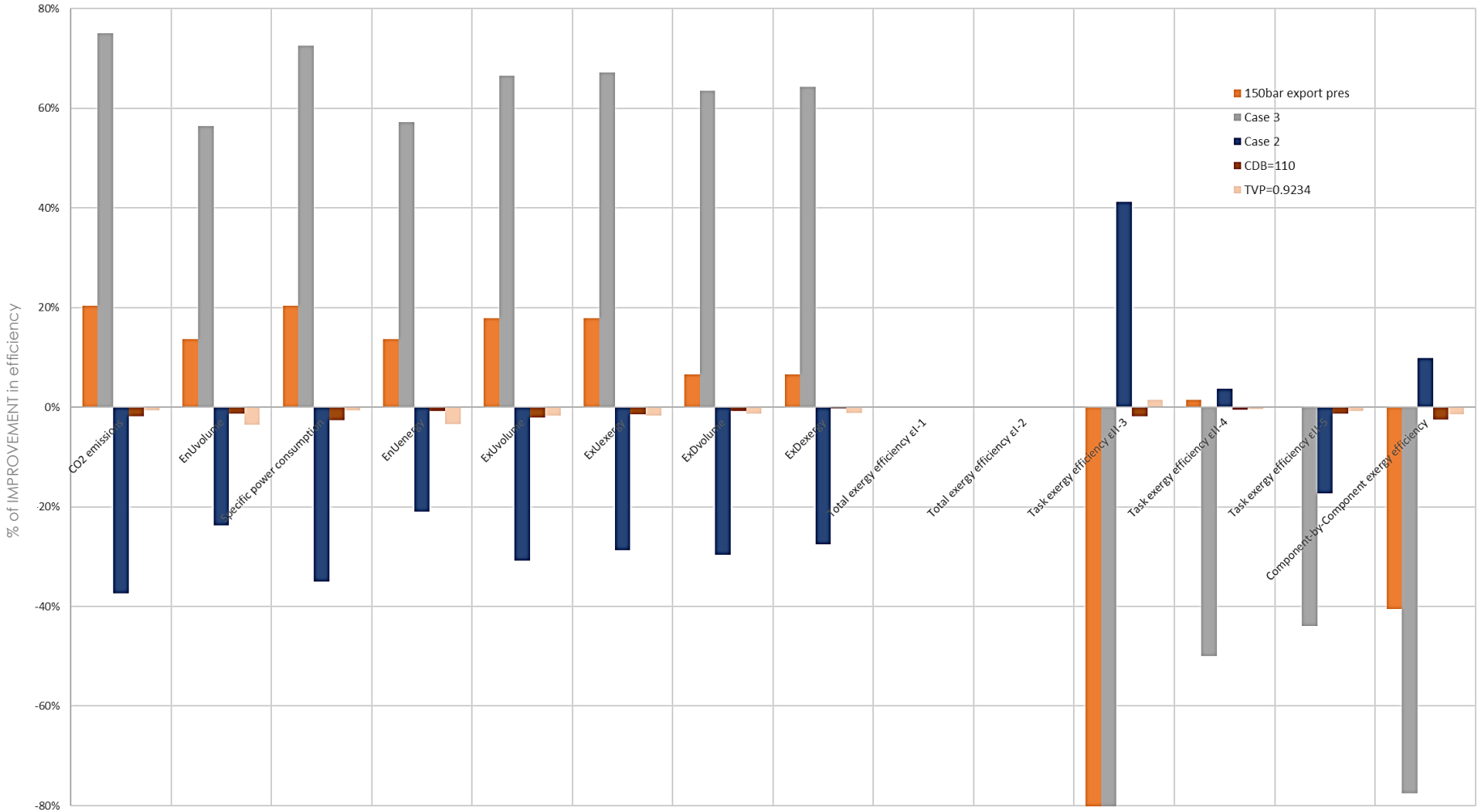

Figure 28 % of improvement in efficiency of the Base Case for the different changes in frame conditions and product specifications (changes over 80% are not visible in this diagram)

6. Case studies over changes in the design parameters

A group of different design choices for the process presented in Chapter 3 is examined in order to evaluate the performance of the indicators towards design changes in the processing plant. The changes investigated in these respects correspond to the three case studies presented below.

6.1 Description of the Case studies

6.1.1 The effect of the adiabatic efficiency increase of the rotating equipment on the thermodynamic indicators

One of the most common ways to improve the efficiency of an oil and gas processing plant is to increase the efficiency of the compressors and pumps taking part in the process. In this work the rise in efficiency is investigated using the indicators presented above for an increase in the adiabatic efficiency of all rotating from 75% to 85%.

For this case a simulation is conducted based on Case 1 and results are presented in paragraph 6.2.1.

6.1.2 The effect of cooling at lower temperatures on the thermodynamic indicators

A method that could be used to increase the efficiency of the platform through limiting the work demands is cooling the fluid entering the compressors at lower temperatures. However, this approach results in higher cooling demands that may even lead to worse performance of the process.

The effect of a temperature drop in cooling is examined in this case based on the Base Case scenario. On that account, the temperatures of the inlet gas of the compressors in the recompression train changes from 33 to 28°C and the temperature of the gas entering the second stage compression stage drops from 32.8 to 25°C. These pressure changes ensure that there is no liquid in the feed of the compressors and that all product specifications are satisfied. It is noteworthy that the stream leaving the export gas cooler in this case is a vapour-liquid mixture of a vapour fraction of 0.9997. The temperature changes conducted are presented in Table 38.

Table 38 Temperature decrease of the gas compressed

Parameter changed	Value of Base Case	New Case
Outlet temperature of the 1st and 2nd stage cooler (°C)	33.0	28.0
Outlet temperature of the 1st export gas cooler (°C)	32.8	25.0

The results of the energy and exergy analysis conducted, as well as the calculation of the indicators is given in paragraph 6.2.2 .

6.1.3 The effect of the pressure and temperature levels of the separation train on the thermodynamic indicators

The pressure and temperature levels of the separation train are two parameters that affect both the energy and exergy demands of a platform and the oil and gas compositions and flowrates. They are thus responsible for simultaneous changes in the heating, cooling and work demands, as well as the GLR, the flowrates and the energy/exergy contents of the products etc. In this Chapter the effect of the change in the separation conditions is tested in order to receive different energy and exergy demands, while the specifications of the products remain practically the same (less than 0.3% change). For that reason, the temperature of the second-stage separation is selected to rise, as well as the pressure of the third-stage separation. It is pointed out that no change in the pressures of the first and second stage of the separation train takes place, while the temperature of the second- and third-stage separation rise, as a result of the temperature change in the oil heater. The pressure and temperature changes conducted in the process are presented in Table 39.

Table 39 Change of the pressure and temperature levels of the separation train

Parameter changed	Value of Base Case	New Case
Outlet temperature of the oil heater (°C)	85	105
Pressure of the 3rd separation stage (bar)	1.5	2.1

For the case presented here a simulation is conducted based on Case 1 and results are presented in paragraph 6.2.3 .

6.2 Results & Discussion

The results of the energy and exergy analysis as well as the calculation of the performance indicators conducted for the cases examined above are presented and discussed in this paragraph.

6.2.1 The effect of the adiabatic efficiency increase of the rotating equipment on the thermodynamic indicators

The energy and exergy consumption of the platform for the case under discussion is presented in Figure 29.

According to Figure 29 the increase in the efficiency of the pumps and compressors examined results in a 12% decrease in work duties, as well as a 6% drop in cooling demands, mainly due to less cooling in the compression train (lower temperature of the streams leaving the compressors and entering the coolers).

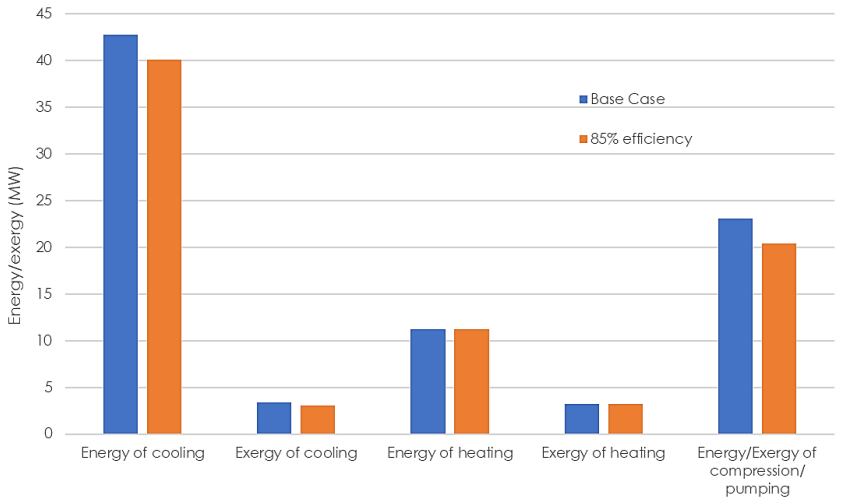

Figure 29 Energy/Exergy consumption in case of adiabatic efficiency increase of pumps and compressors compared to the Base Case

Figure 30, Figure 31 and Figure 32 show *that EnU, ExU, ExD, Specific power consumption and Specific CO_2 emissions* show an increase in efficiency in case of the higher efficiency of the rotating equipment varying from 8% to 12%. Off course, the exergy-based indicators and the *Specific power consumption and Specific CO_2 emissions* show the highest change as work demands contribute more to the inlet energy/exergy term (or the emissions).

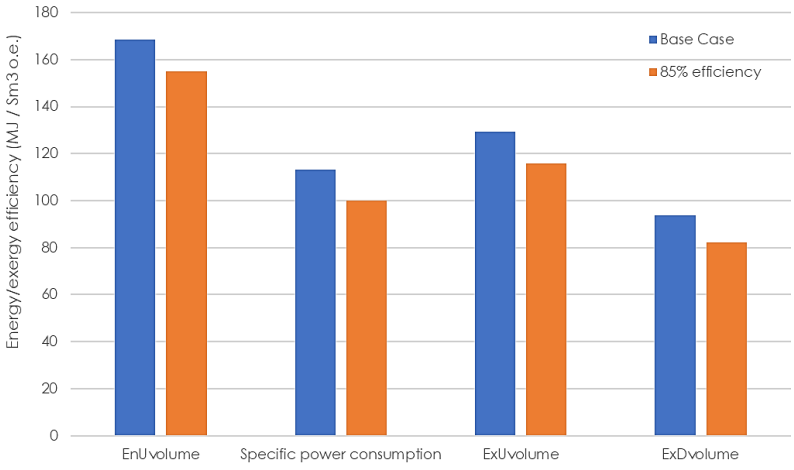

Figure 30 *EnUvolume, ExUvolume, ExDvolume, Specific power consumption* in case of adiabatic efficiency increase of pumps and compressors compared to the Base Case

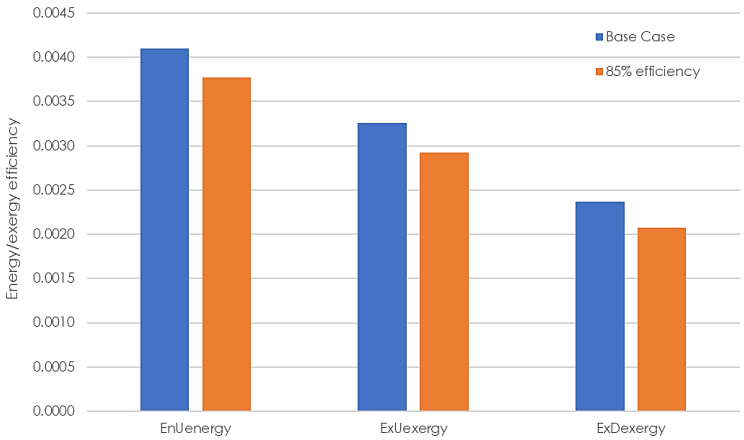

Figure 31 *EnUenergy, ExUexergy, ExDexergy* in case of adiabatic efficiency increase of pumps and compressors compared to the Base Case

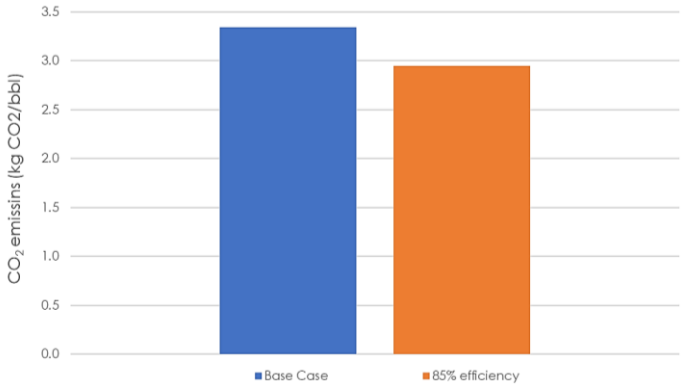

Figure 32 *Specific CO_2 emissions* in case of adiabatic efficiency increase of pumps and compressors compared to the Base Case

According to Figure 33 *Total exergy efficiency* is once more insensitive to changes, while the rest of the indicators show an increase of up to 11%. ε_{II-4} exhibits the smallest increase of 3%. This is because by the way ε_{II-3} and ε_{II-4} are defined, the second indicator will always show a lower change in case of deviations in heat and work for the same exergy of the useful product (and of the feed).

Table 40 shows the results of *Exergy loss ratio, Exergy destruction ratio* and *Efficiency defect* for the case at issue. According to the *Exergy loss ratio* the exergy losses due to cooling decrease, while based on the *Exergy destruction ratio* less exergy is lost in the compression and recompression train, as well as the oil pumping subsystem. *Efficiency defect* indicates only the drop in exergy destruction in the gas compression, as its small values do not allow the detection of changes in the exergy destruction under a certain limit.

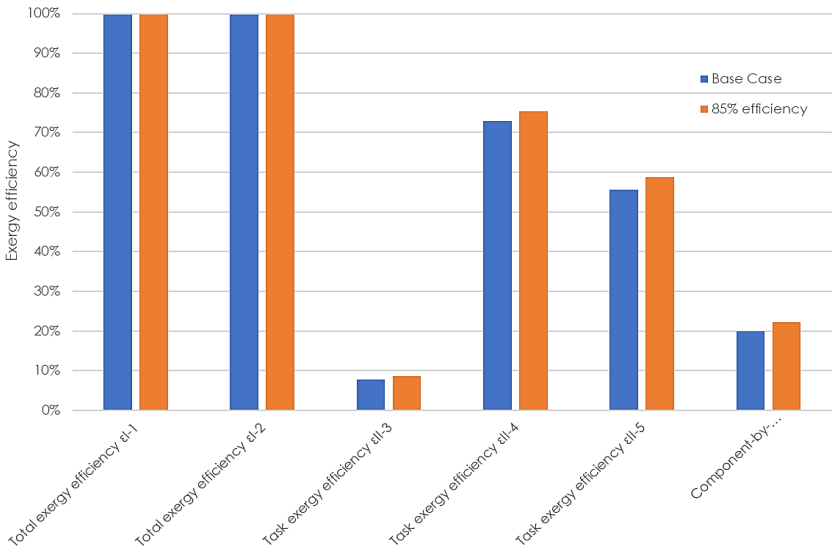

Figure 33 *Total, Task, Component-by-Component exergy efficiency* in case of adiabatic efficiency increase of pumps and compressors compared to the Base Case

Table 40 Exergy loss ratio and exergy destruction ratio in the case of efficiency increase of the rotating equipment compared with the Base Case

Energy/Exergy used/destroyed		Base Case 1	85% efficiency
Exergy loss ratio	cooling	65.2%	62.7%
	gas exhausted	0.1%	0.1%
	wastewater	34.7%	37.3%
Exergy destruction ratio	production manifold	56.8%	64.6%
	separation	11.7%	13.3%
	gas compression and exportation	30.1%	21.6%
	gas recompression	1.1%	0.2%
	oil pumping	0.1%	0.0%
	wastewater treatment	0.3%	0.4%
Efficiency defect	production manifold	1.3E-3	1.3E-3
	separation	2.7E-4	2.7E-4
	gas compression and exportation	7.1E-4	4.5E-4
	gas recompression	3.2E-5	3.4E-5
	oil pumping	1.5E-6	1.6E-6
	wastewater treatment	7.3E-6	7.3E-6

All in all, in case of a 12% increase in the adiabatic efficiency of all pumps and compressors all energy and exergy (except for the *Total exergy efficiency*) show an increase of up to 12% depending on the definition of the indicators. In this case the energy and exergy content, as well as the flowrate of the export products remain practically the same, so the changes in the values of the indicators result from the drop in the energy and exergy demands of the platform.

6.2.2 The effect of cooling at lower temperatures on the thermodynamic indicators

The results of the energy and exergy analysis conducted for the case of cooling at lower temperature are presented in the following Figures.

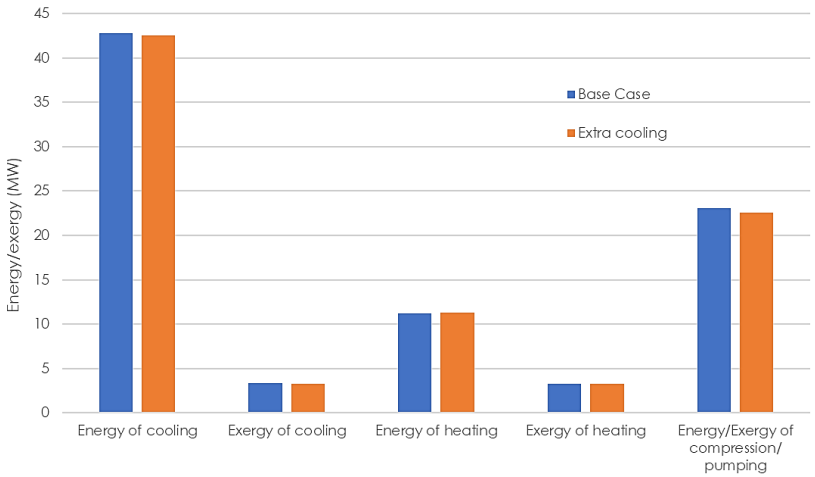

Figure 34 Energy/Exergy consumption in case of cooling at lower temperature compared to the Base Case

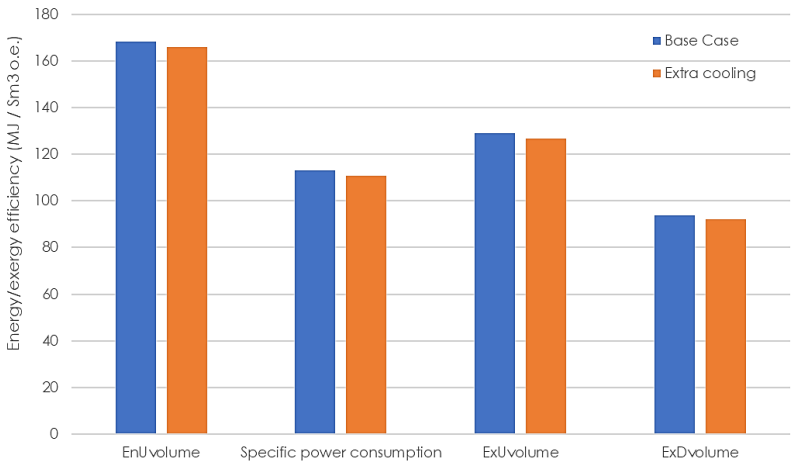

Figure 35 *EnUvolume, ExUvolume, ExDvolume, Specific power consumption* in case of cooling at lower temperature compared to the Base Case

According to Figure 34 cooling demands show overall a slight increase of 1%. This is because the stream entering the last export gas cooler is in this case of lower temperature resulting in lower cooling duties for this specific cooler (33%). For the rest of the coolers there is an increase in energy/exergy due to the lower temperatures of the streams leaving the coolers. Heating demands remain constant, while

energy/exergy for compression and pumping shows a 2% decrease the streams compressed are cooler and heating duties remain the same.

All *EnU, ExU, ExD, Specific power consumption* and *Specific CO_2 emissions* give a better performance of the platform in case of cooling at lower temperatures. More specifically, the indicators show a change between 1% and 2% (Figure 35, Figure 36, Figure 37). It should be noted that the exergy-based indicators, as well as the *Specific power consumption* show the highest change, as they consider heating in terms of exergy, thus changes in work demands are more dominant.

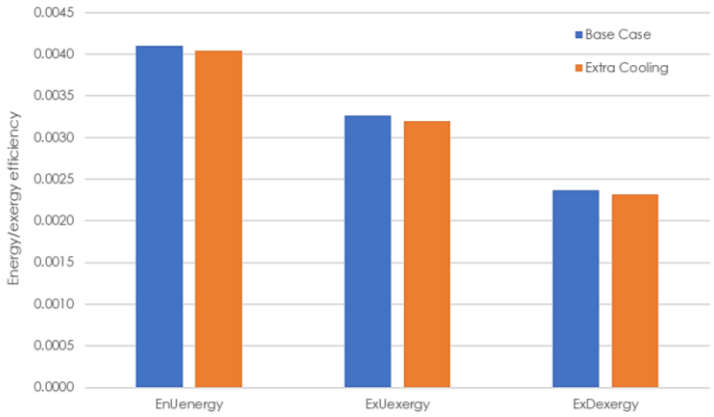

Figure 36 *EnUenergy, ExUexergy, ExDexergy* in case of cooling at lower temperature compared to the Base Case

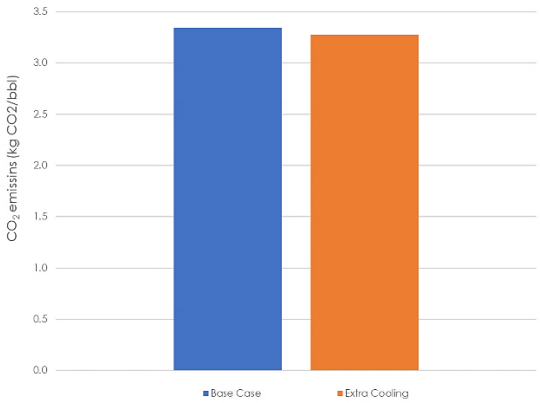

Figure 37 *Specific CO_2 emissions* in case of cooling at lower temperature compared to the Base Case

According to Figure 38 *Total exergy efficiency* remains again constant, while the *Task* and *Component-by-Component exergy efficiency* show a slight change varying from 0% to 2%. ε_{II-3} exhibits the lowest increase of all (0.4%). This is because the cooling at lower temperatures examined here results in a 0.5% decrease in GLR and thus, a 0.0004% decrease in the physical exergy of the products. This slight decrease is enough to almost reach or potentially outweigh the decrease in fuel exergy (exergy of heat and work) (2%). Therefore, it could be said that ε_{II-3} is more sensitive to changes in the physical exergy of the export product than in changes regarding heat and work

duties. This is evident if the high changes of the values of the indicator in case of change in the export pressure of the products as presented above is taken into account.

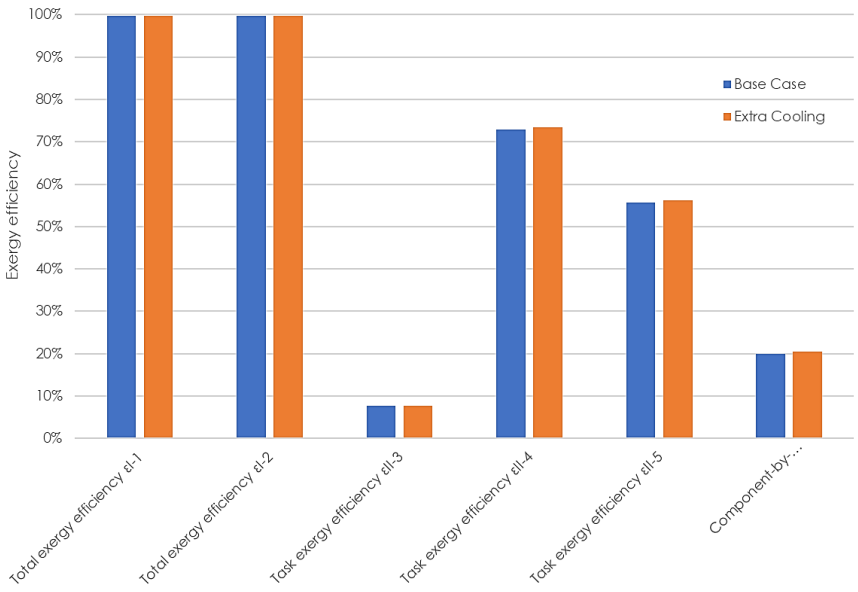

Figure 38 *Total, Task, Component-by-Component exergy efficiency* in case of cooling at lower temperature compared to the Base Case

Table 41 Exergy loss ratio and exergy destruction ratio in the case of cooling at lower temperature compared to the Base Case

Energy/Exergy used/destroyed		Base Case 1	Extra Cooling
Exergy loss ratio	cooling	65.2%	64.6%
	gas exhausted	0.1%	0.1%
	wastewater	34.7%	35.4%
Exergy destruction ratio	production manifold	56.8%	57.8%
	separation	11.7%	12.2%
	gas compression and exportation	30.1%	28.5%
	gas recompression	1.1%	1.1%
	oil pumping	0.1%	0.1%
	wastewater treatment	0.3%	0.3%
Efficiency defect	production manifold	1.3E-3	1.3E-3
	separation	2.7E-4	2.8E-4
	gas compression and exportation	7.1E-4	6.6E-4
	gas recompression	3.2E-5	2.5E-5
	oil pumping	1.5E-6	1.5E-6
	wastewater treatment	7.3E-6	7.3E-6

Table 41 shows the values of *Exergy loss ratio, Exergy destruction ratio* and *Efficiency defect* for the case at issue. According to this table more exergy is lost due to cooling decreases, as also does the exergy destroyed in the gas compression train. This can be explained by lower cooling duties associated with the last cooler of the subsystem. The *Efficiency defect* is insensitive to the small changes in exergy destruction (2%) examined in this case study.

Overall, the decrease in the temperature of cooling results in lower work duties, but not cooling duties as it would be expected. This is why all indicators show an efficiency increase for the case at issue. ε_{II-3} remains practically constant as it focuses more on the changes of the exergy of the export product rather that the fuel exergy.

6.2.3 The effect of the pressure and temperature levels of the separation train on the thermodynamic indicators

The following Figures show the results of the analysis conducted for the case with the higher temperature of the second stage separation and pressure of the last stage separation together with the results of Case 1.

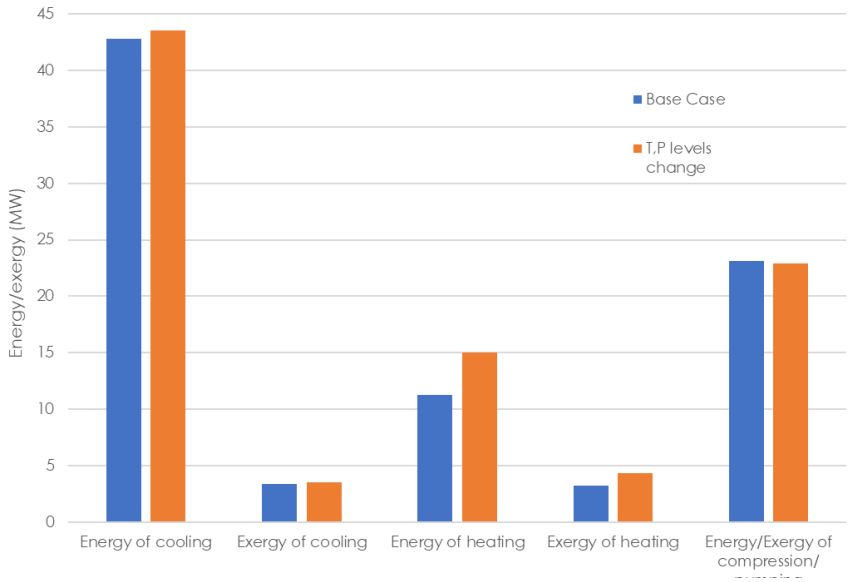

Figure 39 Energy/Exergy consumption in case of different pressure and temperature levels of the separation train compared to the Base Case

Figure 39 shows that in the case study under consideration heating duties show an increase of 34% (3.8 MW) due to the higher outlet temperature of the oil heater. Cooling demands exhibit a 2% rise (3.4 MW) associated again with the higher temperature of the second separation stage that gives higher gas streams leaving this stage of separation and of higher temperature resulting in greater needs for cooling in the second recompression stage. The rest of the compressors and pumps decrease leading to an overall decrease in work of around 1%.

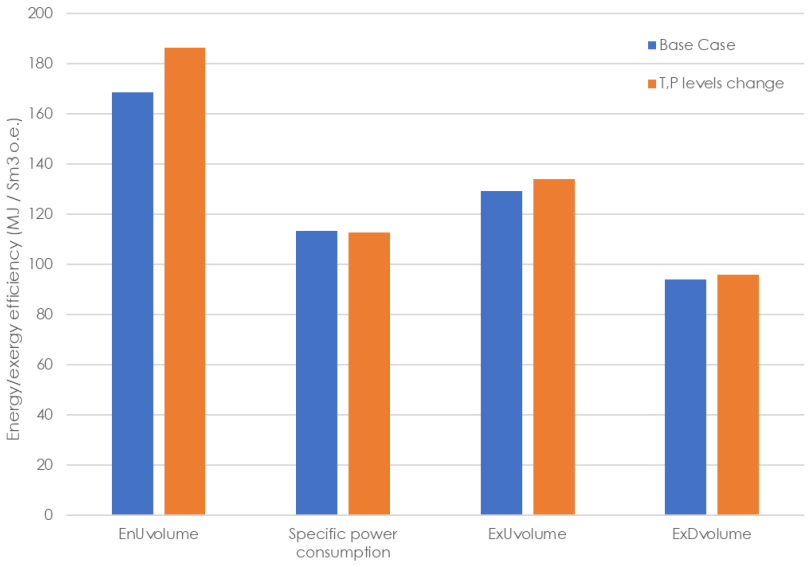

Figure 40 *EnUvolume, ExUvolume, ExDvolume, Specific power consumption* in case of different pressure and temperature levels of the separation train compared to the Base Case

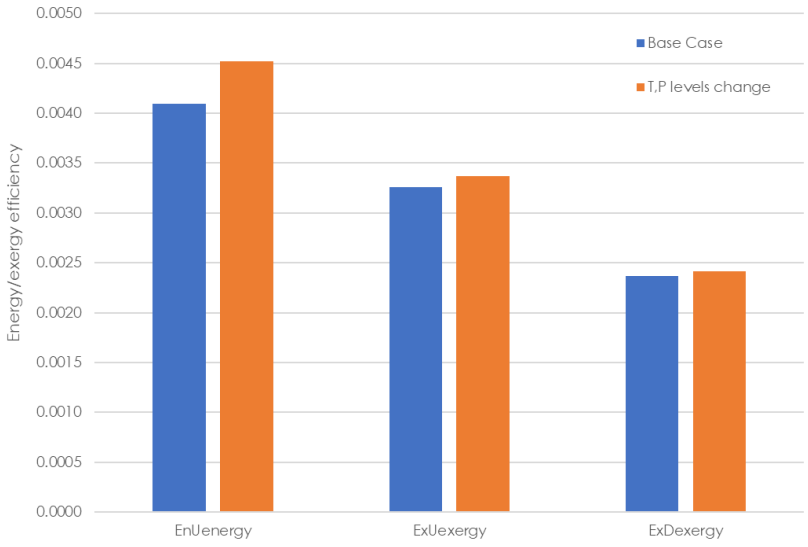

Figure 41 *EnUenergy, ExUexergy, ExDexergy* in case of different pressure and temperature levels of the separation train compared to the Base Case

According to Figure 41 all *EnU, ExU* and *ExD* indicators show a worse efficiency of the platform in case of the temperature and pressure separation levels change investigated. More specifically, the indicators exhibit a rise from 2% to 11%. The highest increase is detected for the energy-based indicators, since the main change in the inlet energy/exergy of the system is that of heating demands. *Specific power consumption* and *Specific CO_2 emissions* (Figure 42), on the other hand indicate a better performance showing a 1% change. This is because in the case study at issue less work is demanded in order to receive a product with the same export rate and energetic content as that of the Base Case.

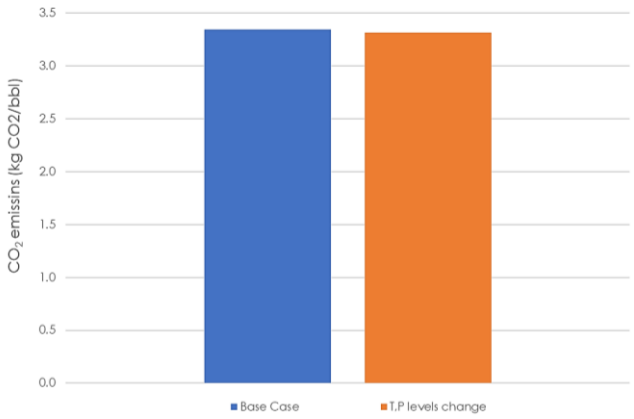

Figure 42 *Specific CO_2 emissions* in case of different pressure and temperature levels of the separation train compared to the Base Case

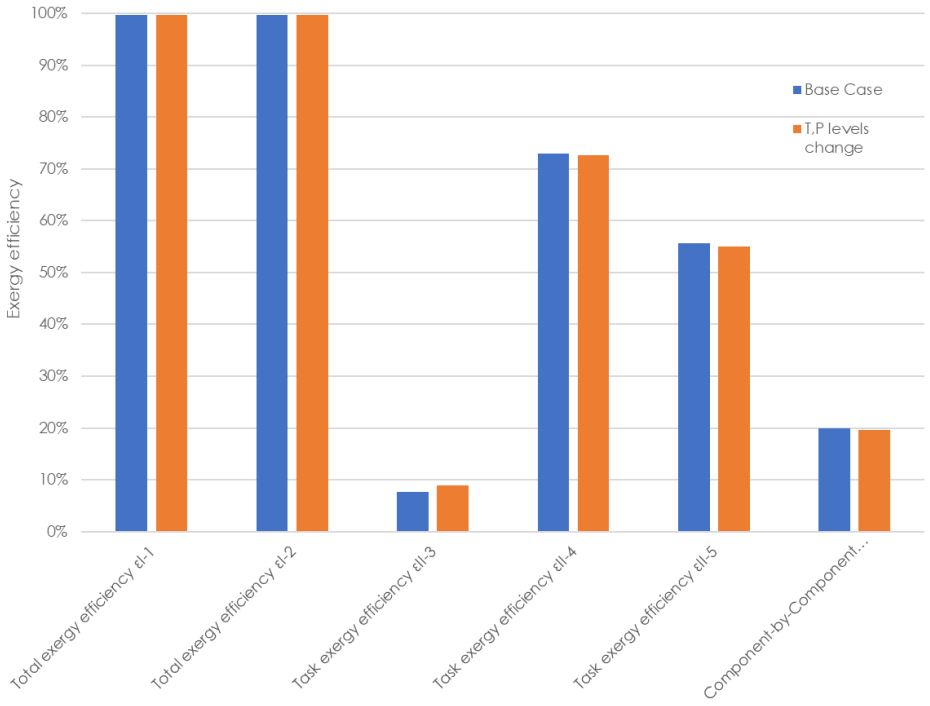

Figure 43 *Total, Task, Component-by-Component exergy efficiency* in case of different pressure and temperature levels of the separation train compared to the Base Case

According to Figure 43 the *Total exergy efficiency* remains once more constant, while ε_{II-5} and ε_{III} show a decrease in efficiency between 1% and 2%. ε_{III} which is sensitive to changes in the chemical exergy increases drops the most, as the fuel exergy increases and the product exergy decreases due to less chemical exergy gains. ε_{II-5} drops because of the higher fuel exergy, while the product exergy remains practically the same given the fact that there is a slight rise in GLR (0.8%) that leads to practically the same physical exergy gains. This indicator is less sensitive to changes in the chemical exergy increases. ε_{II-4} remains more or less constant (0% change), as both the fuel and the product exergy rise. In this case the increase in the product exergy derives from the rise in the physical exergy of the export product. This is mainly a result of higher temperature of the export oil (78 vs 59°C).

Task exergy efficiency ε_{II-3} is the only indicator in Figure 43 that shows a better performance in case of the different separation conditions tested. This is because by the way this indicator is defined the 0.9 MW rise in the fuel exergy have a lower effect than the 0.4 MW increase in the product exergy which is a result of higher physical exergy of the products, as explained above. This indicator, as explained in previous cases is sensitive to the conditions of the export products leading to different results in efficiency compared to the other indicators, or even negative values.

Table 42 Exergy loss ratio and exergy destruction ratio in case of different pressure and temperature levels of the separation train compared to the Base Case

Energy/Exergy used/destroyed		Base Case 1	Different T,P separation levels
Exergy loss ratio	cooling	65.2%	66.2%
	gas exhausted	0.1%	0.0%
	wastewater	34.7%	33.8%
Exergy destruction ratio	production manifold	56.8%	55.5%
	separation	11.7%	13.3%
	gas compression and exportation	30.1%	29.4%
	gas recompression	1.1%	1.5%
	oil pumping	0.1%	0.1%
	wastewater treatment	0.3%	0.3%
Efficiency defect	production manifold	1.3E-3	1.3E-3
	separation	2.7E-4	3.2E-4
	gas compression and exportation	7.1E-4	7.1E-4
	gas recompression	3.2E-5	3.6E-5
	oil pumping	1.5E-6	1.4E-6
	wastewater treatment	7.3E-6	7.3E-6

According to Table 42 the *Exergy loss ratio* shows an increase in the exergy lost due to cooling, while the *Exergy destruction ratio* indicates a rise in the exergy that is destroyed in the separation train and the gas recompression train. The exergy destruction rate in the separation is higher because of the higher exergy of heating in the oil heater, while for the recompression train this is a result of higher cooling demands in the 2nd stage cooler. The *Efficiency defect* is once again insensitive to the small changes in exergy destruction (2%) examined in this case study.

The results of the different design parameters tested in this Chapter are presented in an overall bar chart as a percent of efficiency increase in each case examined compared to the Base Case scenario.

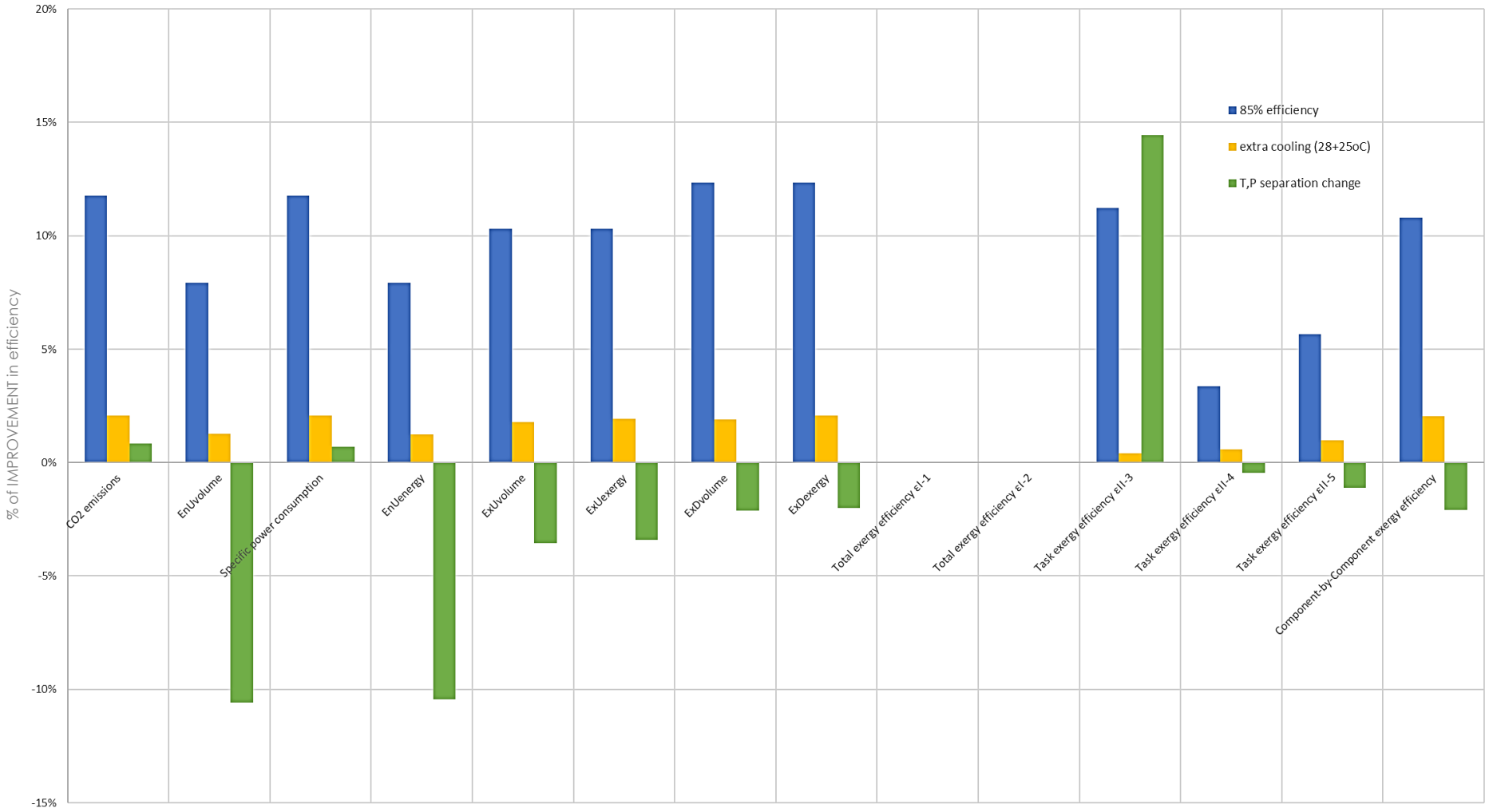

Figure 44 % of improvement in efficiency of the Base Case for the different changes in design parameters

7. The effect of the *oil production lifetime* on the thermodynamic indicators

7.1 Description of the Case

The cases that have been investigated so far do not take into consideration the variations of the conditions and the composition of the well fluid over the production lifetime of the field. However, pressure, temperature, flow, as well as composition changes may have a great impact on the work and heat demands of the platform reflected in the thermodynamic performance indicators calculated. This is why the examination of the effect of the production lifetime on a platform's performance should be investigated through a dynamic simulation that considers changes in the production flows, the well stream compositions and the operating conditions. A more thorough investigation could additionally include the effect of ageing and degradation of the on-site components and processes, which are factors admittedly responsible for the performance decrease of an oil and gas platform. (Ramadan, March 2021), (Voldsund M. , 2014)

Dynamic simulations regarding the time effect on the performance of a platform are based on profiles that show the variation of specific parameters describing the process over time. Production profiles determine the changes in the oil, water and gas flowrates throughout the lifetime of a field and they have usually been generated through reservoir simulations. A typical oil, water and gas production profile for a black-oil is given in Figure 45. According to this profile, the oil flowrate reaches a maximum in a short period of time, it remains steady for a few years and then it starts dropping. Water begins to increase significantly after the first years of the production, until it reaches a maximum and then starts declining. The gas flowrate is usually a function of the GOR and thus it is determined by the oil production. (Guo, Song, Ghalambor, & Lin, 2014)

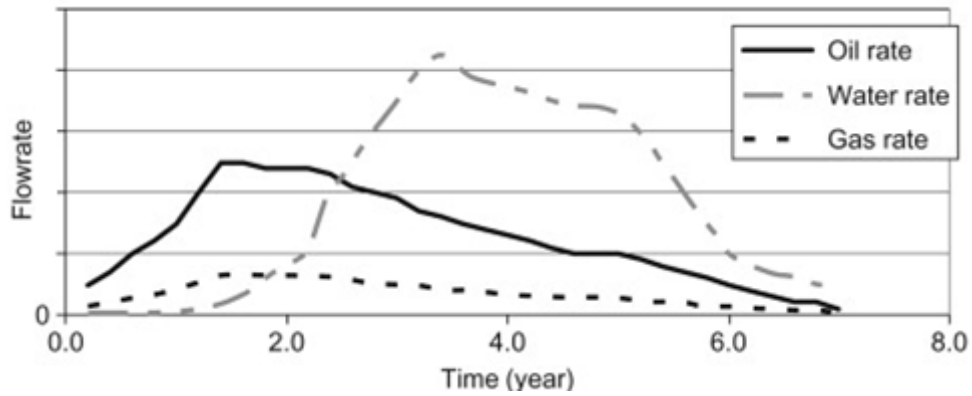

Figure 45 Typical oil, water, and gas production profiles. *(Guo, Song, Ghalambor, & Lin, 2014)*

In this thesis the effect of the pressure and the flow rate change of the inlet well stream over the years is examined under the assumption of constant reservoir fluid inlet temperature and composition. It should, also be noted that the degradation of the equipment is not taken into consideration and the pressure and temperature levels of the process are considered to be kept the same over time. Calculations have been conducted for Case 1 given the production profile of the field of Figure 46 provided by Equinor. The time point of 2021 corresponds to the inlet flowrate of the Base Case for which calculations have already been presented. This is also the case for the pressure profile given in Figure 47. The pressure profile has been created based on the production profile

and the pressures corresponding to 2021 (120 bars) and 2046 (60 bars) assuming that the pressure and the flow rate of the reservoir fluid stream follow the same profile. Energy and exergy analysis has been conducted for 6 different time points for every 5 years of the lifetime of the field (2021-2026-2031-2036-2041-2046) and the results are presented in Paragraph 7.2 .

Figure 46 Production profile of Case 1

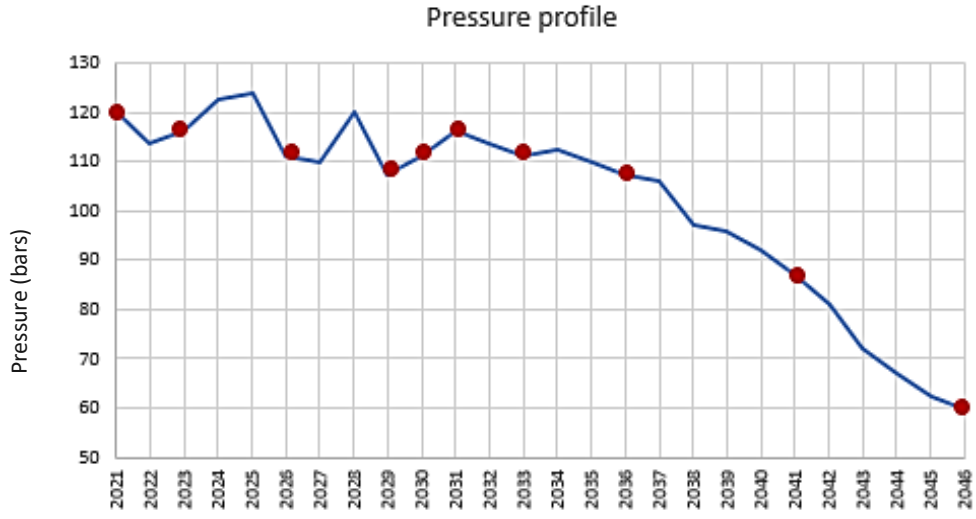

Figure 47 Pressure profile of Case 1

However, the aforementioned approach may give misleading results regarding the performance of the platform over time, due to the simplifications of the process over some parameters important for the calculation of work and heat duties. More specifically, under more realistic conditions the substantial variations of the reservoir properties lead to significant performance losses over the lifetime of the field. This implies the use of control strategies, such as anti-surge recycle and energy-intensive techniques like gas and water injection. The first method is used in order to maintain the volume flow rate of compressors and pumps over a minimum in order to prevent the equipment from surging, while the second method is a way to enhance oil recovery from the reservoir. These techniques lead to greater power consumption and exergy destruction rates and

thus – if included in the process- different conclusions may arise. (Voldsund M. , 2014) So, in order to receive more realistic and representative results anti-surge recycle is included in the process for all years except for 2021 and calculations are carried out for three selected time points (2026, 2031 & 2036).

Anti-surge recycle is based on the flow diagram of Figure 48 and it is applied in all four compressors taking part in the process (recompression train (2), rich gas compression train (2)). According to this diagram a part of the stream leaving the compressor at a high pressure is first throttled at a low pressure, which is the pressure of the stream entering the compressor. This recycle stream is then mixed with the stream entering the separator and cooled at the temperature of the latter, so that the separation conditions remain the same. The flowsheet of the process when anti-surge recycle is used is presented in Figure F62 (Appendix F).

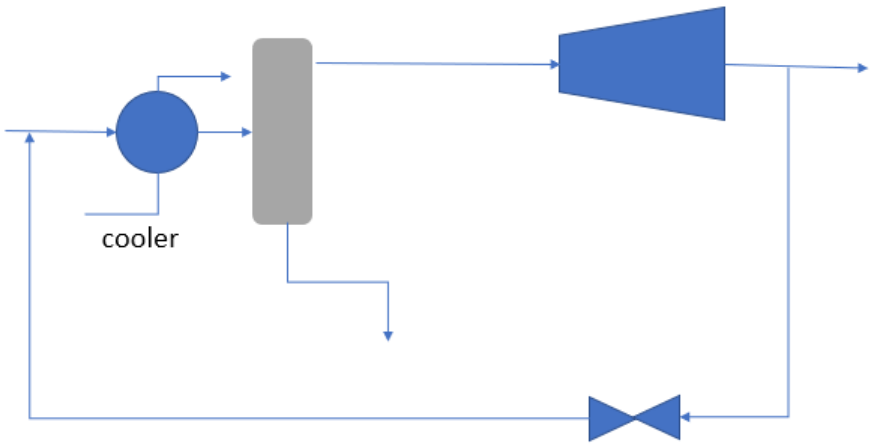

Figure 48 Anti-surge recycle flow diagram

The minimum volume flow rate in order to prevent surging is generally defined by compressor performance curves. However, in this case this value is assumed to be equal to the volume flow rate of the inlet stream in each compressor for Case 1 in 2021. The recycle ratio for each compressor is calculated using the *ADJUST* function in the ASPEN HYSYS ® simulation. Table 43 shows the volume flow rates of the inlet stream and the recycle ratios for each compressor in 2026, 2031 and 2036.

Table 43 Anti-surge recycle data for 2026, 2031 & 2036

Compressor	Volume flow rate of the stream entering the compressor (m^3/h)	Recycle ratio		
		2026	2031	2036
1st stage recompressor	1.078E4	15.38%	7.15%	21.42%
2nd stage recompressor	1340	15.09%	6.87%	21.08%
Export gas compressor 1	738	13.24%	5.65%	18.93%
Export gas compressor 2	3468	13.24%	5.71%	18.82%

The analysis presented above takes into account the need to use a recycle stream in the rotating equipment when the volume flow rate of the reservoir fluid entering the process decreases over the years. It does not, however considers the effect of the pressure drop of the well stream on the design parameters of the processing plant. The reservoir pressure drop over time results in a lower difference between the well and the inlet pressure that leads to a reduced production of hydrocarbons. In order to maintain the production at the desired levels it is necessary to either increase the reservoir pressure, which is commonly done by injection of either gas or water, or to lower the inlet pressure, which requires modifications on the installed process equipment including the separator. (Benavides, 2013) The second method is investigated in this case.

In order to investigate the effect of the change in the pressure conditions over time with the aim to maintain the production between the desirable boundaries the pressure of the first stage separation (outlet of the production manifold) drops from 51.21bars to 35 bars when the pressure of the reservoir fluid goes down 108bars. The first time point for which the pressure of the inlet well stream is below 108 bars is 2036 (107.4 bars). For that point calculations are made when both antisurge recycle and pressure decrease of the first stage separation are taken into account. This time point is representative of the highest impact of the pressure decrease throughout the years, since it corresponds to the highest well stream pressure for which pressure decrease of the separation is applied. For the years after 2036 the pressure difference between the well stream and the separation will be lower.

Calculations for this approach are again made based on the ASPEN HYSYS ® simulation of the Base Case and the results are given in Paragraph 7.2 .

7.2 Results & Discussion

Three different cases have been examined for the effect of production lifetime on the performance of the platform at issue:

1. Change in the inlet volume flow rate and the pressure of the well stream entering the process according to the time profiles (solid lines with dots in the diagrams)
2. Change in the inlet volume flow rate and the pressure of the well stream entering the process according to the time profiles together with the implementation of anti-surge recycle in the compressors of the processing plant (triangle marks in the diagrams)
3. Change in the inlet volume flow rate and the pressure of the well stream entering the process according to the time profiles together with the implementation of anti-surge recycle in the compressors of the processing plant and the application of pressure drop in the 1st stage separation in order to maintain the production at the desired levels (x marks in the diagrams)

The results of the calculation have been gathered in Figure 49,Figure 50 Figure 51 and Figure 52. In these figures more time points that much the profiles of one of the six years investigated can also be found. It should be noted that the indicators focusing on the performance of each sub-system are out of scope for these calculations that aim to investigate the overall performance of the platform.

When no other change has been made in the platform (i) it seems that heat and work demands follow the trend of the profiles presented above showing a general decrease over the years. This can be explained by the fact that the flow of all streams in the process has been reduced, while pressure and temperature levels have remained constant leading to lower compression and pumping duties, less cooling of the streams compressed and less heating for separation. (Figure 49 – solid lines)

Consequently, almost all indicators show a better performance of the platform over the years (Figure 51,Figure 52) (lines with dots). *Specific Power consumption* (as well as CO_2 *emissions*) remains practically constant since the pressure levels of the system do not change over time and thus the work demands are practically proportional to the inlet flow rate. The highest drop-efficiency increase is given by the *ExD* indicators (around 46% efficiency increase). This is because in the case under discussion the pressure decrease over the years results in lower pressure drop in the production manifold and thus less exergy destruction rates.
The same trends can be found in the *Task* and *Component-by-Component exergy* indicators. This is not the case for *Total exergy efficiency* which again does not respond to the changes made in the process. *Task exergy indicators* ε_{II-3} and *Component-by-Component exergy efficiency* ε_{III} show the highest increase over the years (over 140%). This can be explained by the strong effect of the pressure difference between the inlet and the outlet streams on the indicators, as seen in Figure 52.

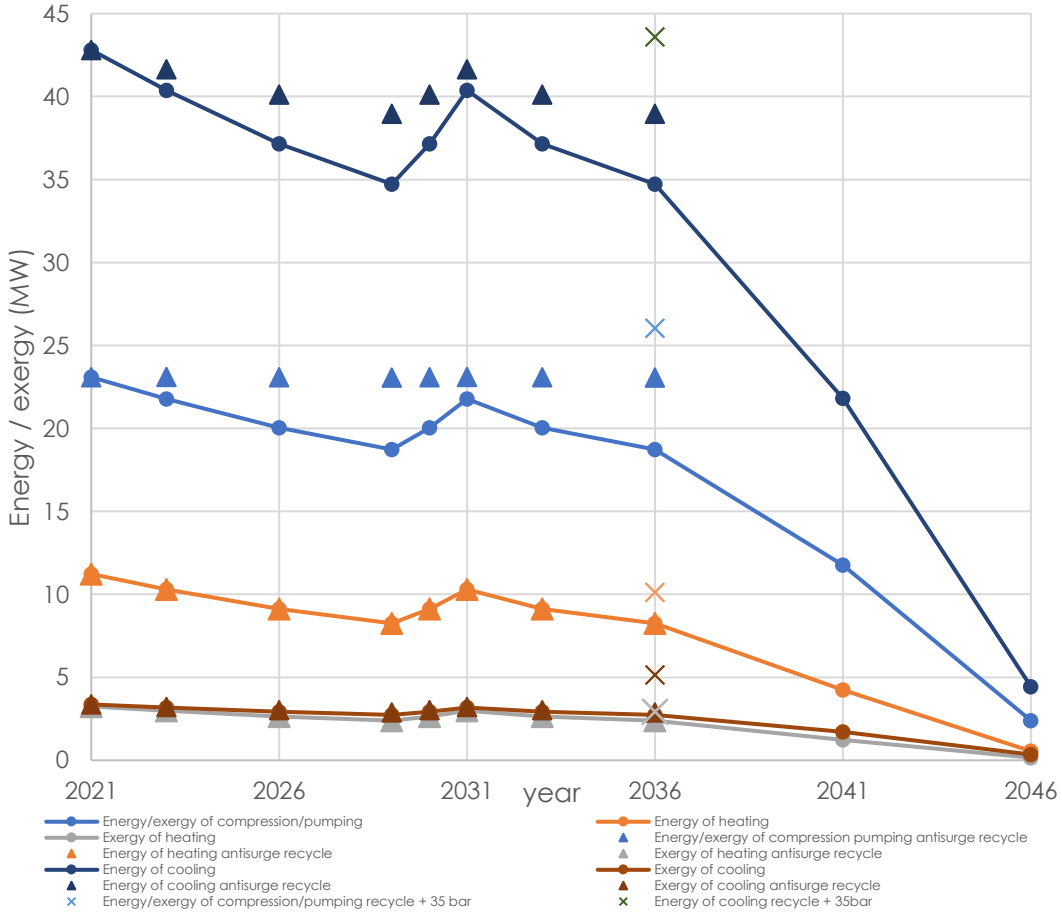

Figure 49 Energy/exergy of heating, compression and pumping of Case 1 over time (solid lines correspond to change i, triangles to change ii and x marks to change iii)

The results of these calculations in case the anti-surge recycle is taken into consideration are presented in Figure 49, Figure 51 and Figure 52 (triangles) together with the results of the previous calculations. According to Figure 49 the work duties of the platform remain practically the same over time, since the flowrate and the pressure difference in all four compressors are constant (slight deviation of 0.1% due to lack of antisurge recycle in the pump of export oil). Heat demands drop over the years following the trend

of the well stream flow rate, as also happens in case no anti-surge recycle is used. Cooling demands decrease over time, too. This is because throttling, which is added in the recycle loop leads to cooling of the streams substituting a great part of cooling duties. *EnU*, *ExU, ExD*, *Specific power consumption* (and *CO_2 emissions* similarly to *Specific power consumption*) (Figure 51) follow again the trend of the inlet pressure and flow rate indicating a general drop in efficiency over the years unlike the results gained by previous calculations that did not take the anti-surge recycle into consideration. *Total* exergy efficiency (Figure 52) shows again no practical change over time. *Task exergy efficiency* ε_{II-3} shows an increase (23%) and *Component-by-Component exergy efficiency* ε_{III} remains practically constant (± 1%) over the years. As explained before, this is a result of the strong effect of the pressure difference between the inlet and the outlet streams. This is not the case for the *Task exergy efficiencies* ε_{II-4} & ε_{II-5} that fluctuate according to the pressure and volume flow rate profile of the well stream showing an overall decrease in efficiency over time reaching a drop of 5% and 6% due to the use of anti-surge recycle.

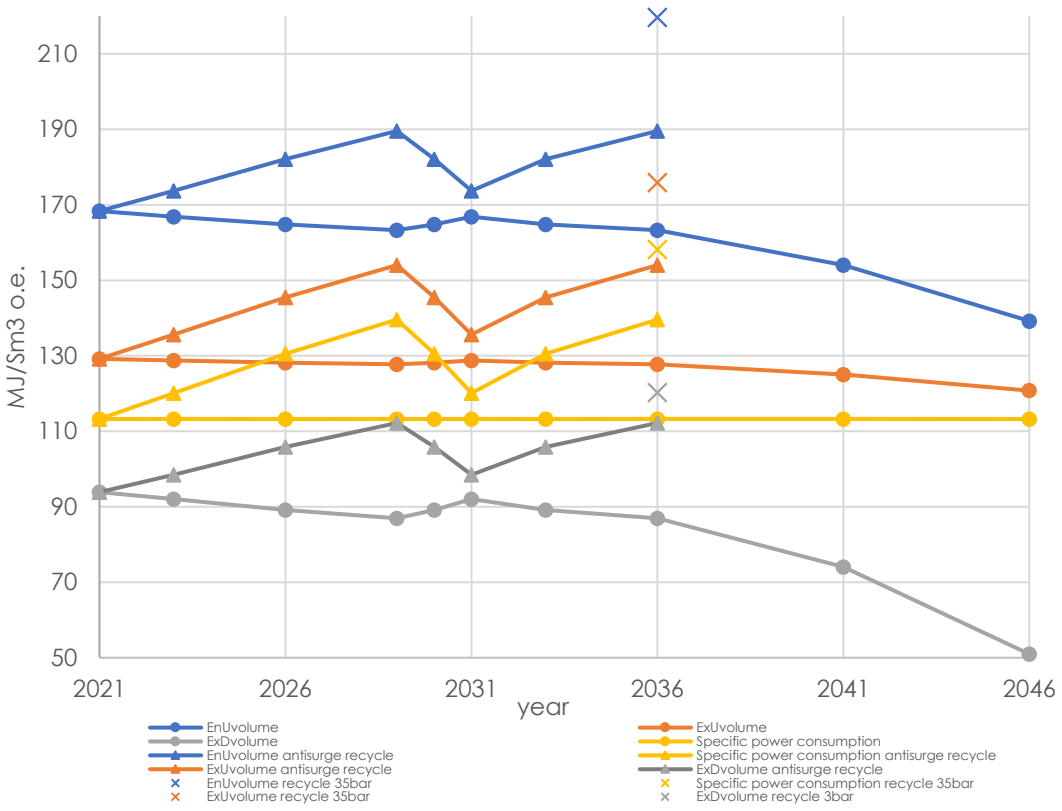

Figure 50 *EnUvolume, ExUvolume, ExDvolume* and *Specific power consumption* of Case 1 over time (solid lines with dots correspond to change i, triangles to change ii and x marks to change iii)

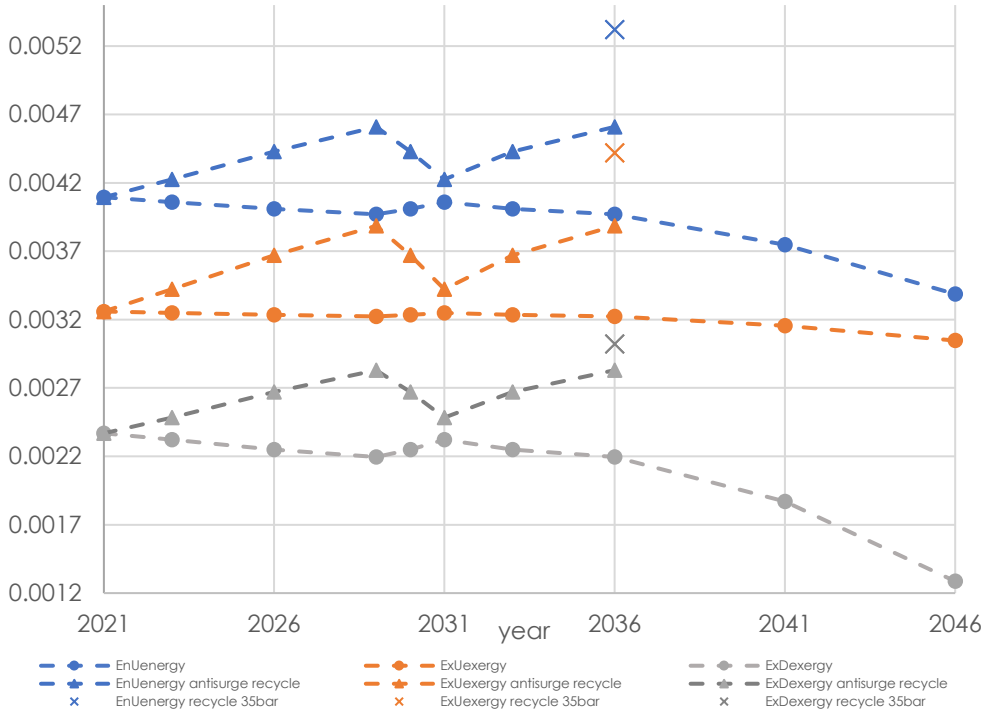

Figure 51 *EnUenergy, ExUexergy* and *ExDexergy* of Case 1 over time (dashed lines with dots correspond to change i, triangles to change ii and x marks to change iii)

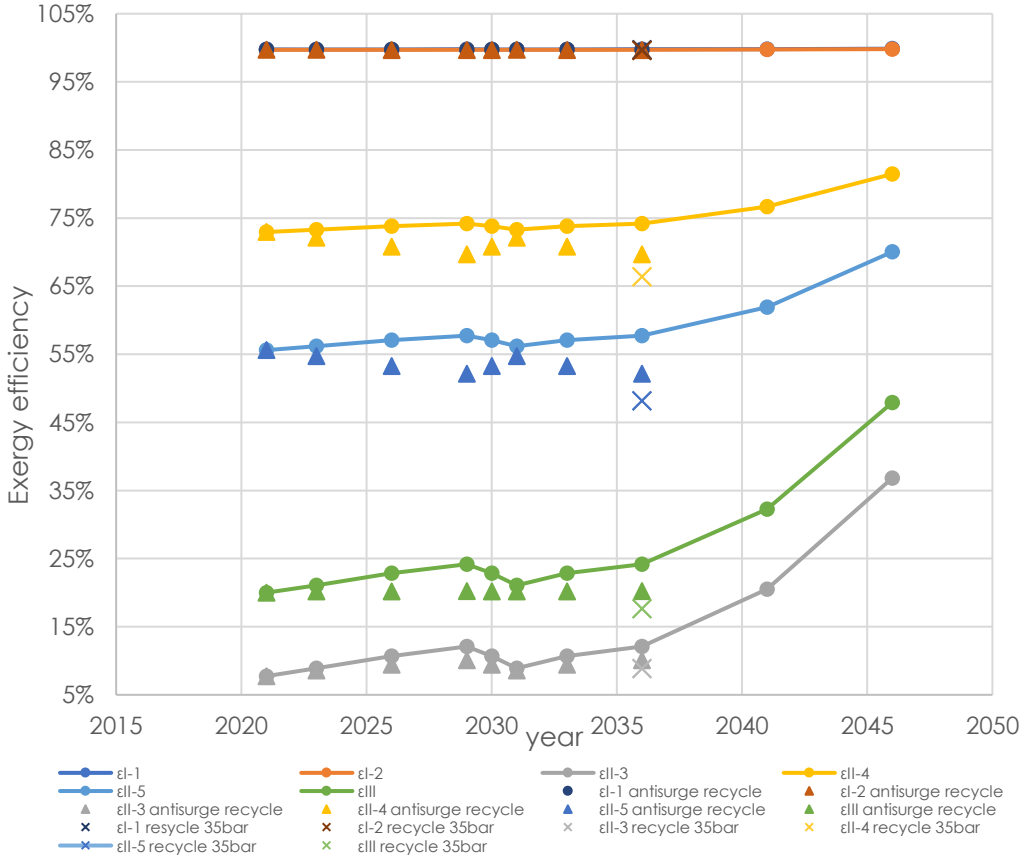

Figure 52 Total, Task & Component-by-Component exergy efficiency of Case 1 over time (solid lines with dots correspond to change i, triangles to change ii and x marks to change iii)

The results of the calculations for applying a pressure drop (from 51.21 to 35 bars)for the time point of 2036 are presented again in Figure 49, Figure 51 and Figure 52 (x marks). According to Figure 49 work demands exhibit an increase of 13% (compared to the case of antisurge recycle but no pressure decrease). This work rise is based on the increase in the volume flowrate of the gas entering the compression train due to the pressure drop of the 1st separation stage (more gas is separated in the 1st stage separation). The 2% increase of the GLR indicates this greater gas production of the case at issue. Because of the higher amounts of gas flowing in the compression train, no antisurge recycle is necessary in that part of the system. On the other hand, recycle increases in the recompression train, since the oil treated in this case is less than before. These recycle ratios are presented in Table 44. Due to the higher amounts of gas processed in this case, cooling demands increase, too (9%).

Table 44 Anti-surge recycle data for 2036 in case of pressure decrease in separation

Compressor	Recycle ratios 2036
1st stage recompressor	24.90%
2nd stage recompressor	53.79%
Export gas compressor 1	0%
Export gas compressor 2	0%

As a result, the *EnU, ExU, ExD, Specific power consumption* indicators (and *Specific CO_2 emissions* which is not presented separately as it follows the trend of *Specific power consumption*) show an increase that varies from 7 to 16% compared to the antisurge recycle analysis with no pressure decrease. *Total exergy efficiency* once more remains unchanged to such deviations. *Task* and *Component-by-Component exergy efficiency* show a drop between 5 and 13%. By the way ε_{II-3} and ε_{II-4} are defined ε_{II-4} will always show a lower change in case of deviations in heat and work for the same exergy of the useful product (and of the feed), as is the case here (12% vs 5% decrease, respectively). ε_{III} shows the highest drop in efficiency (13%), as this indicator takes into account the displacement of some components from the oil to the gas export product. In this way an amount of exergy that was considered to be useful is now part of the fuel exergy.

All in all, the results that occur from the calculations of the efficiency of the platform over time fluctuate according to the flowrate profile showing a general drop in efficiency when anti-surge recycle is included (except for ε_{II-3} and ε_{III}). This drop in efficiency can be even higher when the need for pressure decrease in the first stage separation stage is taken into account (up to 16%). However, it should be mentioned that if the effect of time on the efficiency of an oil and gas process is to be examined more thoroughly the use of compressor curves is necessary in order to calculate the recycle flow required. In that direction the variation of the rest of the conditions of the reservoir fluid stream (temperature, composition etc.), the degradation of the equipment and the use of gas and water injection should also be examined.

8. A new concept for the efficiency increase of an offshore oil and gas processing plant

In this Chapter a new idea regarding the efficiency increase of an offshore oil and gas processing plant - like the one examined in this work - is presented. Energy and exergy analysis is performed for the new processing system and calculations of the thermodynamic indicators are conducted in order to evaluate the level of the rise in efficiency.

8.1 Development of the idea

Defining the problem

The analysis on the thermodynamic performance indicators presented above gives important information regarding the parts of the process where most inefficiencies occur triggering the use of the indicators for a better understanding of the breakdown of energy and exergy in a process and for developing ideas focusing on the efficiency increase.

Calculations of the indicators given above suggest that regardless the heat and power consumption of the oil and gas processing plant, a large proportion of the total exergy destruction rate -if not the largest- takes place in the production manifold. More specifically, in all cases examined more than 22% of the exergy destroyed was detected in the production manifold. This number corresponds to over 8 MW of exergy lost due to internal irreversibilities associated with throttling. According to similar cases investigated in literature, even when flaring and seawater injection is included in the system over 19% of the total exergy destruction rate takes place in the production manifold as given by the values of the *Exergy destruction ratio* (Voldsund M. , 2014).

This high amount of exergy destroyed in the production manifold is a result of choking a high-pressure fluid and thus destroying an amount of high-pressure exergy that could otherwise be recovered in the form of work. So, the question that arises is what changes could be made in the process with the aim to utilize this part of exergy that is until now lost in order to cover a part of the work duties of the platform and increase the efficiency of the processing plant.

Suggesting a solution

An initial approach would be the replacement of the choke valves in the production manifold with liquid turbines that can expand liquid streams in order to produce mechanical work. However, liquid expanders are of limited use in the industry, as they are prone to cavitation and they show certain use limitations (e.g. fully liquid entering and exiting streams) leading towards a different direction for the confrontation of the problem (2004) (Song, Sun, & Wang, 2015).

Liquid expanders may be rarely used in the oil and gas industry, however turbines that can work under multiphase flow are frequently operated in case of gas streams carrying a small amount of liquids. If such a multiphase flow expander is to be implemented an extra separation stage should be included in the process that can meet the separation requirements without adding extra size and weight on the platform. Both these technologies have been developed and in this work a combination is proposed in order to replace most of the choking taking place in the production manifold. The application of a **combined separation-multiphase flow expansion** system is schematically presented in Figure 53, while further details are given below.

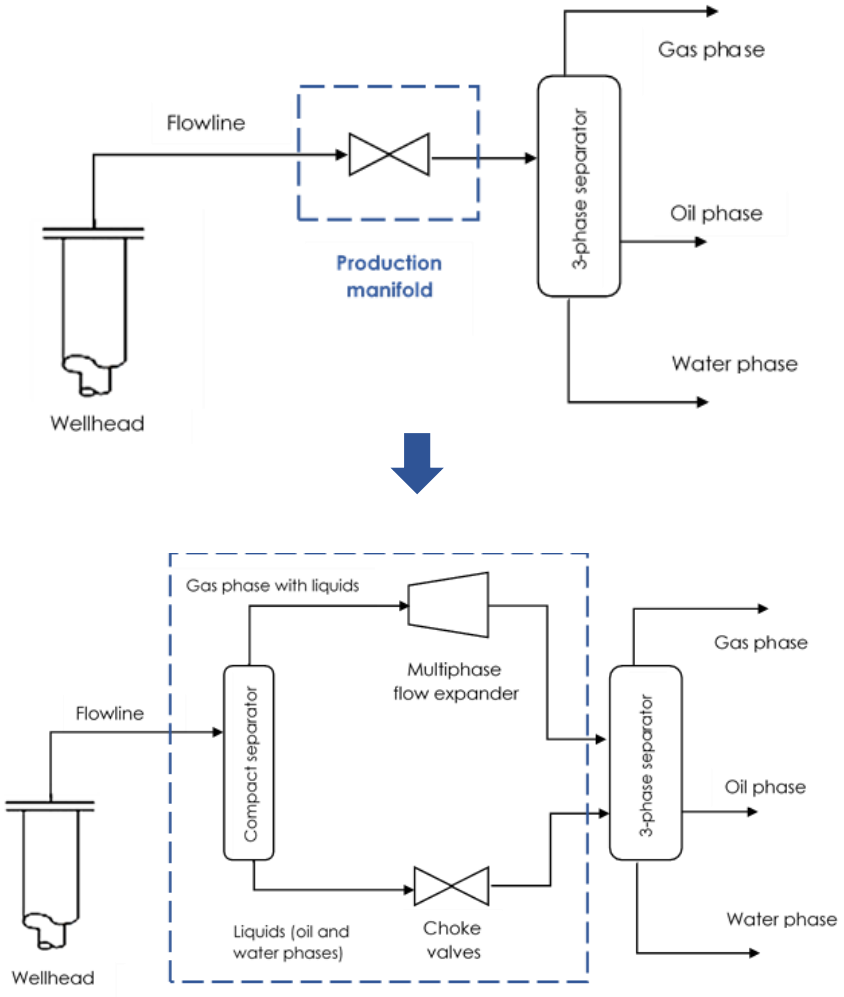

Figure 53 Schematic overview of the substitution of choking in the *production manifold* with a combined separation – multiphase expansion system

As explained above, the application of a combined separation-multiphase expander system requires the use of innovative equipment that can work under multiphase flow conditions with limited size, weight and cost charges. That would include the implementation of **multiphase flow expanders**, which can depressurize a gas with a liquid fraction of up to 0.10. This is a typical number corresponding to a great range of investigations with the focus on the liquid content of the gas processed in a turbine (Charron, Pagnier, Marchetta, & Stihle, 2004). Multiphase flow expanders show a tolerance towards liquids in the processing stream regardless the phase of the liquids, this means that they can process gas with both oil and water contents. As far as the approach presented in this work is concerned, most of the heavier water phase is expected to be separated from the gas steam, while the main part of the liquids in the processing stream consists of oil/condensate. In the case under discussion the liquid tolerant expander is tested for a mass liquid (oil) phase fraction of 5%.

This type of expansion would allow the use of **Compact separation systems** (separators with lower efficiencies of 99-99.9%). The Compact Separation technology can be applied instead of typical separation vessels in order to reach lower equipment size and weight and manufacturing costs. Compact separation shows, on top of that, slug tolerance which is important when treating a well fluid. The main challenge about the existing technology is designing such devices which could process multiphase mixtures (oil, water, gas and sand) on the long term. Inline washing of the equipment treating

multiphase flow streams should also be examined and included in the combined separation-expanding system. (Nguyen, Voldsund, Breuhaus, & Elmegaard, 2016), (Eurostars, 2012), (ETI Offshore, 2020), (Kristiansen, Sørensen, & Nilssen, 2016)

This method that aims to increase the energy and exergy efficiency of an oil and gas processing plant is examined for the Base Case investigated in this work. Simulations and energy and exergy analysis are conducted and the results of the indicators are evaluated.

8.2 Process description and Simulation

For the simulation of the combined separation-multiphase expander case the choke valve of the production manifold is replaced with a two-phase separator with a 5% (w/w) entrainment of the light liquid in the gas stream that works at the pressure of the inlet well stream. The gas stream is then expanded in a multiphase flow expander, while the liquid stream is choked; both to the HP of the separation train. The two streams enter the 3-phase separator in order to receive the gas, oil and water phases of the reservoir fluid stream.

At this point, it is highlighted that when the combined system is applied the temperature of the 3-phase separation is lower than that of the Base Case (approximately 37 vs 64 °C) due to the lower temperature of the expanded gas entering the separation. For that reason, the oil is heated to a higher temperature (95 vs 85°C) in order to achieve the TVP specifications of the oil produced.

8.3 Results

An energy and exergy analysis has been performed for the new system and the results of the analysis are presented against the values corresponding to the Base Case scenario in the following figures.

According to Figure 54 the substitution of throttling with a separation – expansion system results in a 27% reduction of the work demands of the platform, while heating duties remain practically the same. The destroyed exergy shows a drop of 78% followed by an exergy destruction decrease in the production manifold of 8.4 MW. In this case the *exergy destruction ratio* of the production manifold falls from 57% to 19%.

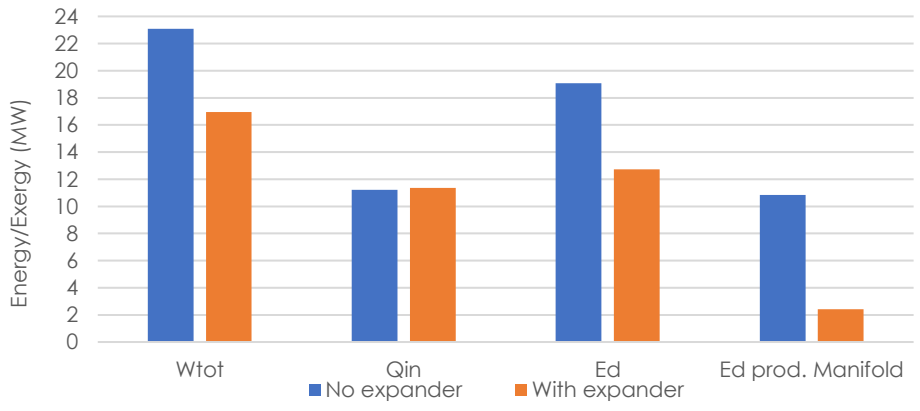

Figure 54 Energy/Exergy consumption/destruction drop for the Base Case when a separation-expansion system is implemented in the production manifold

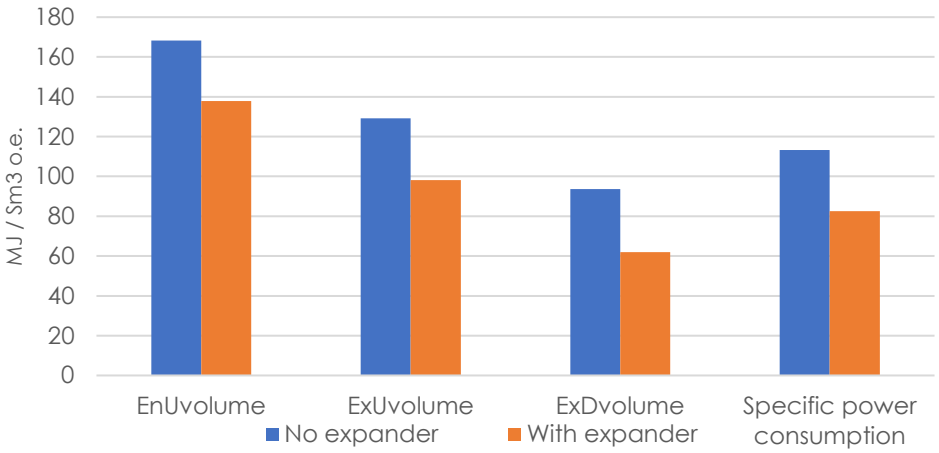

Figure 55 *EnUvolume, ExUvolume, ExDvolume, Specific power consumption* decrease of the Base Case for the implementation of a separation - expansion system in the production manifold

An efficiency increase occurs for all *EnU, ExU, ExD* and *Specific power consumption* indicators exhibiting a decrease that varies from 18% to 34%. As it is evident, the exergy-based indicators show a greater rise in efficiency as they not only take into account the work production in the expander, but also the gain in exergy destruction due to the substitution of the choke valve (Figure 55, Figure 56). The *Specific CO_2 emissions* -which is the most commonly used indicator of all- show a decrease from 3.3 to 2.5 kg CO_2 per bbl (Figure 57). These values could convince of the advantage of installing such a system in the production manifold of an offshore oil and gas processing plant.

At this point it is important to highlight that the 5% w/w liquid phase fraction of the gas stream entering the multiphase expander corresponds to the looser possible standards regarding separation in the production manifold. Expansion less tolerant to inlet liquids shows again an increase in efficiency. More specifically, *Specific CO_2 emissions* in case of no liquid entering the expander is only 2.3% lower than the value presented below which corresponds to a 5% liquid fraction.

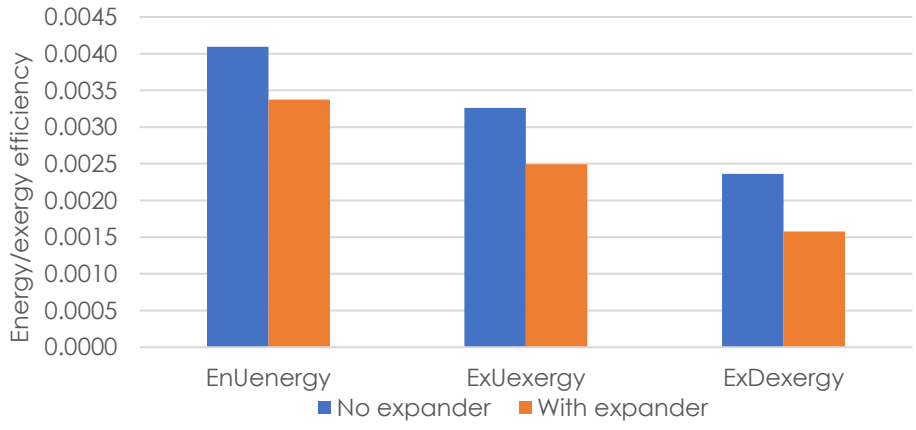

Figure 56 *EnUenergy, ExUexergy, ExDexergy* decrease of the Base Case for the implementation of a separation - expansion system in the production manifold

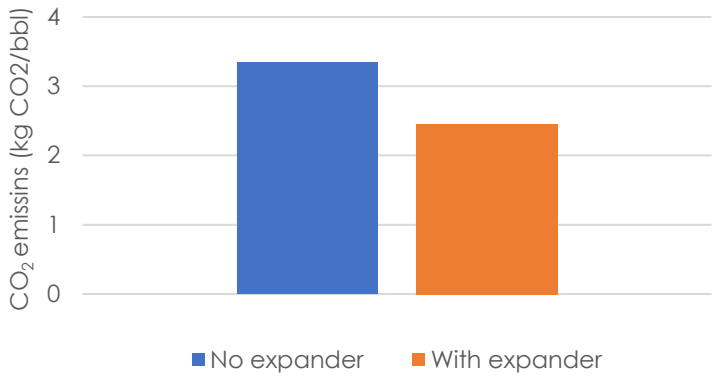

Figure 57 *Specific CO_2 emissions* decrease of the Base Case for the implementation of a separation - expansion system in the production manifold

Total exergy efficiency on the other hand remains practically unchanged to the aforementioned change of the process explained by the lack of sensitivity of the indicator, while *Task* and *Component-by-Component exergy efficiency* exhibit a rise of up to 30%. *Task exergy efficiency* ε_{II-4} shows the lowest increase (8%), because -as is also the case of the ε_{II-3} – it highlights the drop in work and heat demands for practically the same exergy of the export products. This exergy increase has a lower effect on the ε_{II-4} indicator compared with the ε_{II-3} , as in the fuel exergy of ε_{II-4} takes part the exergy of the feed, too. Even though the displacement of some components from the gas to the oil product -as implied by the 2% drop in GLR – results in an increase in the physical exergy decreases (part of fuel exergy) and a decrease in the physical exergy increases (part of product exergy) of the *Component-by-Component exergy efficiency*, this indicator exhibits the highest rise of 30%. This is because the gain in chemical exergy outweighs the drop in the physical exergy increases, as also is the case for the decrease in work and heat demands and the physical exergy decreases. The same displacement of the component is represented by *Task exergy efficiency* ε_{II-5}, but expressed in physical exergy increases and decreases of the streams (not on a component basis) showing an increase of 14%.

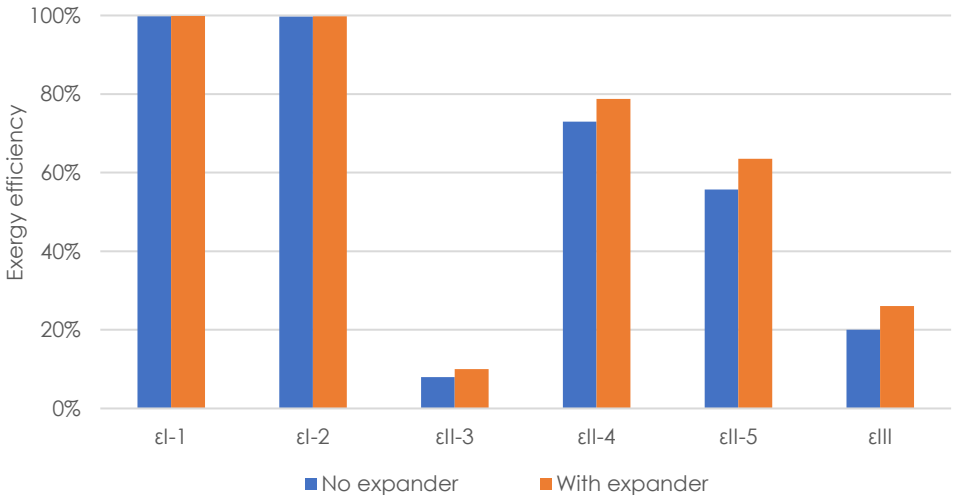

Figure 58 *Total, Task, Component-by-Component exergy efficiency* increase of the Base Case for the implementation of a separation - expansion system in the production manifold

All in all, the substitution of throttling in the production manifold with a combined separation – multiphase expansion system would result in an efficiency increase that varies from 8% to 34%, according to the indicator used for the analysis (*Total exergy efficiency* excluded). This change in the design of the platform shows that most of the indicators exhibit the process upgrades to a lower or a higher extent depending on the way the indicators are defined. Therefore, this idea, especially when evaluated under an exergy background seems extremely promising for the efficiency increase of an offshore oil and gas processing plant.

9. Evaluation of the thermodynamic indicators

9.1 Basic concepts and assumptions for the application of the evaluation method of the thermodynamic indicators

In this Paragraph the method presented in Paragraph 2.5 is applied for the evaluation of the indicators presented above. For that reason, first a further explanation regarding the calculations included, as well as assumptions made is given for the four stages of the process.

Stage One: Establishing Evaluation Criteria

The criteria used for the evaluation of the indicators are the following: *Simplicity, Workload, Clear approach, Sensitivity, Comparability* and *Motivation* as presented in Paragraph 2.4 . It is assumed that these six criteria are independent, so that a weighted average can be used for the calculation of the total score. This may not be the case for some of the criteria that take into account one or more common parameters for their calculation (e.g. both simplicity and workload consider the application of an exergy analysis for the calculation of the indicator as a parameter that decreases the performance of the indicator in terms of simplicity and workload). A statistical hypothesis test (such as a *chi square test*) could be implemented in order to investigate the independency of criteria used for a sample of values calculated based on the scoring process presented below. In case of dependent criteria solutions may vary from a simple combination of the criteria that are not preference independent of each other into a single criterion to more complex models for combining scores across criteria. Here, the assumption of independent criteria is used for a simpler and more transparent decision that can be implemented more quickly and by a wider range of users. (Department for Communities and Local Government UK)

Stage Two: Scoring the Products

As presented above, the way some of the criteria are defined (see *Comparability*, *Sensitivity*) does not allow a general ranking of the indicators. This is why the *relative scaling* method is used. This means that in this case, an indicator that responds in the best way -compared to the other ones- to the criterion at issue receives a score of 1 and an indicator that responds in the worst way -compared to the other ones- to the criterion receives a score of 0. This approach has been selected in order to address the inability to identify the best and the worst response possible for some of the criteria presented. For example, *Sensitivity* suggests that the indicator changes along with the alterations made in the design parameters of the process. However, there is no maximum amount of change defined that can respond to the score of 1. This is why this score is granted to the highest change observed in the set of cases examined in terms of *Sensitivity* and vice versa. This is also the case for the *Comparability* criterion, except for the fact that in that case the highest score is given to the indicator that shows the minimum change of all.

This approach along with the assumption that the indicators would respond to a certain change in the process in the same way (the same relative change) no matter the size of the change (e.g. adiabatic efficiency increase of the compressors from 75% to 85% and increase of the same parameter from 75% to 90%) allows to take into account the change of the indicators for the various test investigated under equal terms (without taking into account the level of the impact of each change in the process). This reasoning is included in the process of scoring for the criteria of *Sensitivity* and *Comparability.* For the rest of the criteria a set of parameters that prevent the indicator from fulfilling the criterion are taken into account and *penalties* are assigned to every each of indicator that meets one or more of these parameters. An extra assumption applied in this scoring process is that of the lack of uncertainty with time, so that the same scores can be used for future evaluations of the indicators, too. The score assignment of the indicators is presented more extensively in Appendix G.

Stage Three: Setting weighting factors for the criteria examined

In this work weighting factors are not assigned to each criterion, but the criteria are presented in detail and scores are calculated for each combination of criterion-indicator so that the process of scoring is set. The aim of this procedure is not to calculate the best indicator, but to prepare a score matrix and a formula that can be used by anyone who wants to evaluate how important the application of one of the indicators calculated would be in an oil and gas processing plant. In that direction, the weighting factors are calculated by the intended user according to the application desired and used in the scoring formula.

Stage Four: Computing the overall score for each indicator

For the calculation of the total scores of the indicators it should be first noted that no categorization in *Mandatory* and *Desirable Criteria* has been applied, while the weighted average method is used under the assumption presented above.

It should be noted that the aforementioned process aims to evaluate the indicators that can be used alone to describe the function of the process. Under this condition the exergy accounting indicators cannot be examined since they cannot give an overview of the process, but they are used to identify where inefficiencies occur in a process. However, these indicators can give a complete inspection of the efficiency of a process when combined with PIs describing the entire process. This is why the three following cases of indicators are included in the scoring process:

1. Single PI that shows the efficiency of the entire process
2. Combination of an exergy-based PI with the *Exergy destruction ratio*
3. Combination of an exergy-based PI with the *Exergy destruction ratio* and the *Exergy loss ratio*

It is highlighted that only exergy-based indicators take part in the combinations, as the main advantage of the energy-based indicators is the lack of exergy analysis of the system (in terms of workload, simplicity etc.), which would be lost in case a combination with *Exergy destruction ratio* and the *Exergy loss ratio* would be selected. At the same time the combination of a single indicator with only the *exergy loss ratio* is not examined, as in that case no inspection of the inefficiencies of the subprocesses would be achieved (unlike the combination of the single indicator with the *exergy destruction ratio*).

These three cases of the indicators investigated can give a complete inspection of the efficiency of a process when combined with PIs describing the entire process.

9.2 Sensitivity & Comparability – Cases examined

In order to score each indicator against the *Sensitivity* and the *Comparability* criteria a set of cases that investigate the effect of changes in the design choices and the frame conditions, respectively is examined, according to the analysis conducted in previous Chapters. The case studies used for the scoring process of these two criteria are briefly presented below.

Sensitivity

In order to measure the sensitivity of each indicator towards the design choices and measures the following design parameters are tested. The corresponding case studies can be found in Chapters 6 and 8.

1. Efficiency increase of the rotating equipment
2. Cooling at lower temperatures
3. Substitution of the production manifold choke valve with a separation – multiphase expander system
4. Changing the Pressure and Temperature levels of the separation train

Comparability

The different frame conditions that follow have been tested in order to measure the comparability of each indicator in case of different reservoir fluids, product specifications etc. and they are based on the case studies presented in Chapter 5.

1. Pressure drop of the gas exported
2. Changing the reservoir fluid treated in the process (Case 3)
3. Increase in the CDB specification of the export gas from 103.1 to 110.0 bars
4. Changing the reservoir fluid treated in the process (Case 2)
5. Decrease in the TVP specification of the export oil from 0.9862 to 0.9234

These parameters have been chosen as a wide sample that represents different changes that can be made in an oil and gas processing plant and that can show a different behavior of the indicators at issue. The effect of these changes in the indicators presented in this work (only the indicators describing the entire process) in terms of efficiency increase compared with the Base Case scenario is given in the bar chart of Figure 59.

For the scoring process of Sensitivity and Comparability these percentage changes are used in absolute terms, as presented in Appendix G.

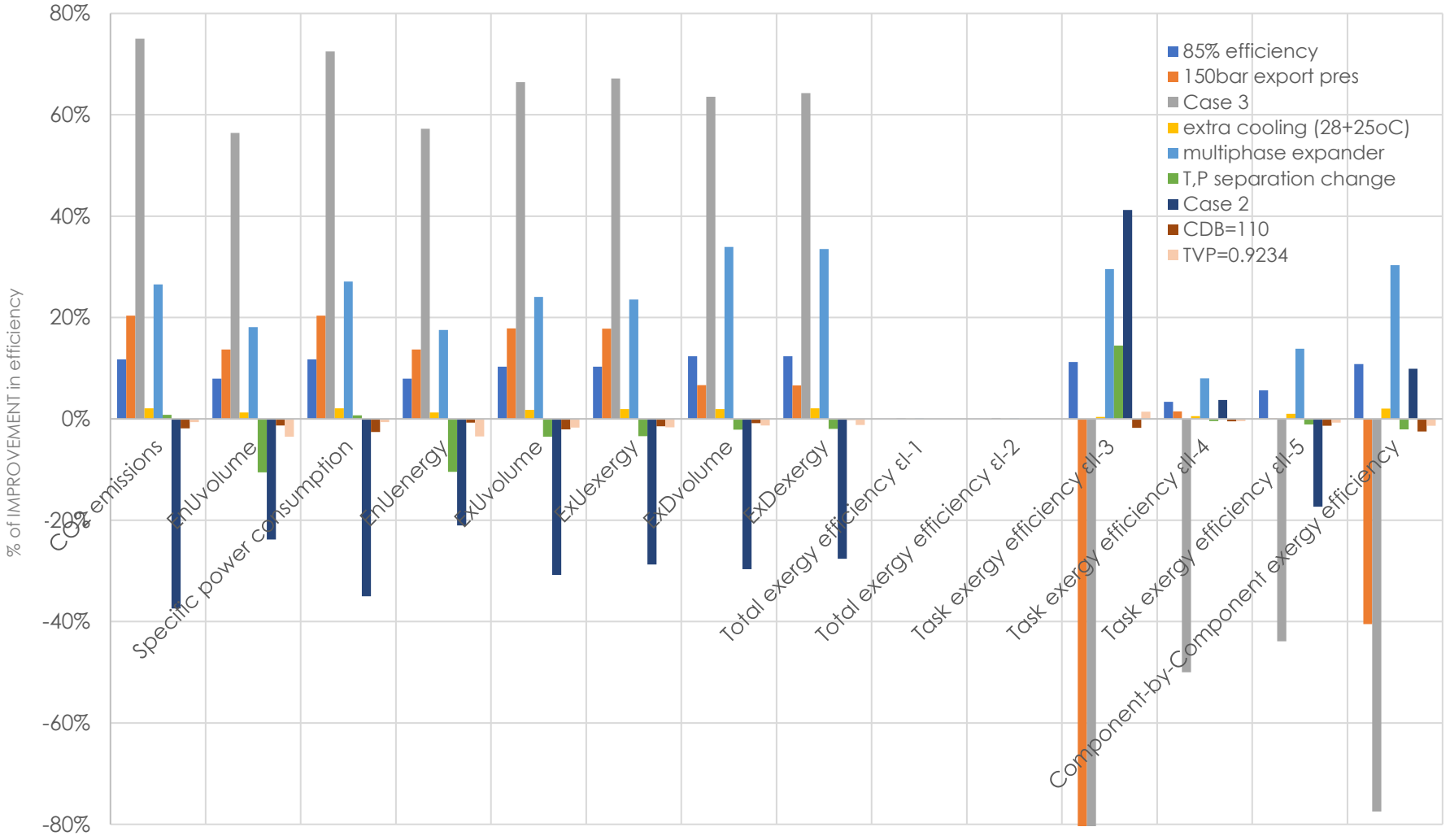

Figure 59 % of efficiency improvement from the Base Case scenario for the different changes in design parameters and frame conditions. (bars may exceed 80% without being presented in the figure)

9.3 Calculations & Results

As described above three different cases of indicators are investigated in this scoring process. These cases include indicators that have been calculated both for the Base Case scenario and for the extra Cases describing changes in the design parameters and the frame conditions of the Base Case. They, also include a combination of some exergy-accounting indicators with exergy-based indicators that describe the entire process. The indicators and the combinations examined are presented in Table 45.

Table 45 Indicators and combination of indicators investigated in the scoring process

Single indicators	Combinations with *Exergy destruction ratio*		Combinations with *Exergy destruction ratio* and *Exergy loss ratio*		
Specific CO2 emissions per unit of produced petroleum					
EnU_{volume}					
EnU_{energy}					
$Specific\ power\ consumption$					
ExU_{volume}	ExU_{volume}	$+ y_d^*$	ExU_{volume}	$+ y_d^*$	$+ y_l^*$
ExU_{exergy}	ExU_{exergy}	$+ y_d^*$	ExU_{exergy}	$+ y_d^*$	$+ y_l^*$
ExD_{volume}	ExD_{volume}	$+ y_d^*$	ExD_{volume}	$+ y_d^*$	$+ y_l^*$
ExD_{exergy}	ExD_{exergy}	$+ y_d^*$	ExD_{exergy}	$+ y_d^*$	$+ y_l^*$
ε_{I-1}	ε_{I-1}	$+ y_d^*$	ε_{I-1}	$+ y_d^*$	$+ y_l^*$
ε_{I-2}	ε_{I-2}	$+ y_d^*$	ε_{I-2}	$+ y_d^*$	$+ y_l^*$
ε_{II-3}	ε_{II-3}	$+ y_d^*$	ε_{II-3}	$+ y_d^*$	$+ y_l^*$
ε_{II-4}	ε_{II-4}	$+ y_d^*$	ε_{II-4}	$+ y_d^*$	$+ y_l^*$
ε_{II-5}	ε_{II-5}	$+ y_d^*$	ε_{II-5}	$+ y_d^*$	$+ y_l^*$
ε_{III}	ε_{III}	$+ y_d^*$	ε_{III}	$+ y_d^*$	$+ y_l^*$

The process of scoring is briefly presented in Paragraphs 2.5 and 9.1 . A more detailed description of the rankings is given in Appendix G.

The scores assigned to each indicator and each combination, as well as the total score of the indicators are presented in Table 46 and Table 47. For the calculation of the overall score of the indicators a set of weighting factors have been given to the criteria examined. As mentioned before, the weights are to be calculated by the user based on one of the methods mentioned in Paragraph 2.5 . In this case, a simple example is presented for the calculation of the total scores that takes into account weighting factors that could correspond to a use of the indicators by a group of engineers working on the efficiency of oil and gas processing plants. Since the indicators are calculated and assessed by a number of experts *Simplicity* seems to be the least important criteria (0.01), followed by the *Workload* (0.04). *Sensitivity* (0.35) and *Clear approach* (0.25) are of the highest interest from the perspective of the scientists, since they focus on both the well-functioning and the theoretical basis of the indicator.

According to the example presented in Table 46 and Table 47 the combination of the *Task exergy efficiency* ε_{II-4} together with the *Exergy destruction ratio* y_d^* is the most appropriate to use with a total score of 0.71 in case of an efficiency evaluation of an oil and gas processing plant by experts of this field. Indicators that score within ~10% of this option should be considered relatively equal in satisfying the criteria (e.g.. the *Task exergy efficiency* ε_{II-4}).

In this case, even though there is not a specific path which should be followed for the elimination of some of the "best-scored indicators" and the selection of a single most appropriate option, one of the following alternatives could be tested:

i. Examine how the ranking of options might change under different scoring (different *penalties*) or weighting systems. These different scoring and weighted systems may correspond to a different interest group or use of the indicator (e.g. except for the use by experts examine also the use of the indicators by the department of management). This process may show that two or three options always come out best, though their order may shift. If the differences between these best options under different weighting systems are small, then accepting a second-best option can be shown to be associated with little loss of overall benefit.
ii. Prioritize the relatively equal options according to the weights of the criteria and based on the scores of the indicator against each criterion. For instance, in the example presented here (Table 46, Table 47) ε_{II-4} and $\varepsilon_{II-4}+ y_d^*$ choices show practically the same total scores (0.71 and 0.70, respectively), while they share the exact same score for the higher weighted criterion (*Sensitivity*). However, when it comes to the second in priority criterion (*Clear approach*) $\varepsilon_{II-4}+ y_d^*$ shows a higher score (1.00 vs 0.90) and thus it could be chosen to be used as more appropriate than ε_{II-4}.

The overall process presented for the evaluation of the indicators investigated in this thesis constitutes a method someone can use in order to decide which indicator is the best to use for the case examined.

Table 46 Score calculation 1/2

Weighting factors	Criteria	*Specific CO_2 emissions per unit of produced petroleum*	EnU_{volume}	*Specific power consumption*	EnU_{energy}	ExU_{volume}	ExU_{exergy}	ExD_{volume}	ExD_{exergy}	ε_{I-1}	ε_{I-2}	ε_{II-3}	ε_{II-4}	ε_{II-5}	ε_{III}
0.35	Sensitivity	0.46	0.42	0.41	0.50	0.41	0.49	0.59	0.67	1.00	1.00	0.00	0.86	0.68	0.47
0.25	Clear approach	0.00	0.70	0.70	0.20	0.70	0.50	0.70	0.50	0.50	0.50	0.50	1.00	0.90	0.80
0.04	Workload	0.85	1.00	1.00	0.95	0.45	0.15	0.45	0.15	0.15	0.15	0.15	0.45	0.45	0.35
0.15	Motivation	0.20	0.20	0.20	0.20	0.20	0.20	0.45	0.45	0.50	0.75	0.00	0.50	0.50	0.50
0.20	Comparability	0.90	0.81	0.90	0.80	0.85	0.86	0.98	1.00	0.00	0.00	0.95	0.26	0.45	0.93
0.01	Simplicity	0.90	1.00	0.90	1.00	0.55	0.55	0.50	0.50	0.40	0.40	0.35	0.20	0.20	0.10
1	Total	**0.43**	**0.58**	**0.59**	**0.48**	**0.55**	**0.51**	**0.67**	**0.64**	**0.56**	**0.59**	**0.33**	**0.70**	**0.65**	**0.64**

Table 47 Score calculation 2/2

Weighting factors	Criteria	$ExU_{volume} + y_d^*$	$ExU_{exergy} + y_d^*$	$ExD_{volume} + y_d^*$	$ExD_{exergy} + y_d^*$	$\varepsilon_{I-1} + y_d^*$	$\varepsilon_{I-2} + y_d^*$	$\varepsilon_{II-3} + y_d^*$	$\varepsilon_{II-4} + y_d^*$	$\varepsilon_{II-5} + y_d^*$	$\varepsilon_{III} + y_d^*$	$ExU_{volume} + y_d^* + y_l^*$	$ExU_{exergy} + y_d^* + y_l^*$	$ExD_{volume} + y_d^* + y_l^*$	$ExD_{exergy} + y_d^* + y_l^*$	$\varepsilon_{I-1} + y_d^* + y_l^*$	$\varepsilon_{I-2} + y_d^* + y_l^*$	$\varepsilon_{II-3} + y_d^* + y_l^*$	$\varepsilon_{II-4} + y_d^* + y_l^*$	$\varepsilon_{II-5} + y_d^* + y_l^*$	$\varepsilon_{III} + y_d^* + y_l^*$
0.35	Sensitivity	0.41	0.49	0.59	0.67	1.00	1.00	0.00	0.86	0.68	0.47	0.41	0.49	0.59	0.67	1.00	1.00	0.00	0.86	0.68	0.47
0.25	Clear approach	0.60	0.40	0.60	0.40	0.40	0.40	0.40	0.90	0.80	0.70	0.05	0.35	0.05	0.35	0.35	0.35	0.35	0.35	0.25	0.15
0.04	Workload	0.41	0.11	0.41	0.11	0.11	0.11	0.11	0.41	0.41	0.31	0.10	0.10	0.10	0.10	0.10	0.10	0.10	0.10	0.10	0.00
0.15	Motivation	0.45	0.45	0.45	0.45	0.75	0.75	0.25	0.75	0.75	0.75	0.70	0.70	0.70	0.70	1.00	1.00	0.50	1.00	1.00	1.00
0.20	Comparability	0.85	0.86	0.98	1.00	0.00	0.00	0.95	0.26	0.45	0.93	0.85	0.86	0.98	1.00	0.00	0.00	0.95	0.26	0.45	0.93
0.01	Simplicity	0.50	0.50	0.45	0.45	0.35	0.35	0.30	0.15	0.15	0.05	0.45	0.45	0.40	0.40	0.30	0.30	0.25	0.10	0.10	0.00
1	Total	**0.55**	**0.52**	**0.64**	**0.61**	**0.57**	**0.57**	**0.34**	**0.71**	**0.66**	**0.65**	**0.44**	**0.55**	**0.53**	**0.64**	**0.59**	**0.59**	**0.36**	**0.60**	**0.55**	**0.54**

10. Discussion

In this Chapter the results of the energy and exergy analysis, as well as of the calculation of the thermodynamic indicators presented for the different case studies examined are discussed, while the method of selecting the most appropriate indicator is commented based on the cases analyzed.

According to the case studies presented in previous paragraphs the energy-based indicators, as well as *ExU* and *ExD* change according to the variations in heat and work consumption of the platform in case of a certain process treating a given well fluid (of a specific flowrate) and small deviations in the GLR (up to 2%). *ExUexergy* and *ExDexergy* can at the same time highlight the effect of the different export conditions, but again following the trend of the power and heat demands. The exergy-based indicators reflect mainly the changes in work duties, as the exergy of work has a higher contribution to these indicators compared to the energy-based ones. On the other hand, *Specific power consumption* and *CO_2 intensity* may remain the same in case of an increase or decrease in heating demands in the platform for the production of the same oil and gas (in terms of volume rate and LHV).

In case the lifetime of the field is examined and if anti-surge recycle is used for the rotating equipment, the energy-based and the *ExU* and *ExD* indicators show the effect of the flowrate of the inlet reservoir fluid stream expressed in the term of the LHV, the exergy and the volume flow rate of the products. If pressure drop in the first separation stage is applied the indicators once more show the effect of the changes in power and heat demands together with the exergy destruction due to pressure drop in case exergy-based indicators are considered.

When a certain platform is investigated for different reservoir fluids treated then the performance of the platform expressed by the indicators presented above is not determined by the heat and power consumption of the platform, but by the well fluid processed. For example, even in case of a 300% increase in the work demands of Case 3, *EnUvolume* would still indicate that this case corresponds to the most efficient platform. So, the energy-based indicators, as well as the *ExU* and *ExD* indicators show that the heavier the reservoir fluid of a platform (lower GLR) the lower the energy/exergy consumed per unit of products, thus the higher the efficiency of the platform.

Task and *Component-by-Component exergy efficiency*, on the other hand show that even if a platform consumes less exergy per unit of product it may not optimally utilizes the exergy resources available. The aim of these indicators is to present how much of the available exergy is utilized for the oil and gas production and what part of the exergy available is destroyed or lost. In this case *Task* and *Component-by-Component exergy efficiency* show that the heavier the reservoir fluid the least efficiently the available exergy is used leading to worse performances.

More specifically for the three different *Task exergy efficiencies* presented in this work:

Task exergy efficiency ε_{II-3} is heavily influenced by changes in the conditions of the inlet well stream and the export products even leading to negative results, that off course do not allow a fair comparison between different cases of oil and gas facilities or a deep understanding of the efficiency calculated. Only in case of minor changes in the exergy of the products (<=0.001% deviation) ε_{II-3} shows the effect of changes in the heat and power consumption of the platform.

Task exergy efficiency ε_{II-4} considers both the changes in heat and power demands and the changes in the exergy of the export products in case of variations in the outlet conditions of the platform or in the allocation of the components in the two product streams. However, by the way ε_{II-3} and ε_{II-4} are defined ε_{II-4} always shows a lower change in case of deviations in heat and work for the same exergy of the useful product and feed, while ε_{II-3} may focus on the increase or decrease in the exergy of the export products disregarding the deviations in heat and power demands.

Task exergy efficiency ε_{II-5}, as well as *Component-by-Component exergy efficiency* ε_{III} take into account the allocation of the components in the two product streams, but the latter is expressed on a component basis. ε_{III} shows a higher sensitivity to the inlet and outlet conditions of the platform which is highlighted in case the lifetime of the field is investigated, as well as to the chemical exergy increases term the deviation of which may outweigh any other change in the exergies of the process.

The *Total exergy efficiency* on the other hand is always high and insensitive to any type of changes in the process, due to the high exergy of the hydrocarbons passing through the system.

As far the *Exergy destruction ratio* and the *Efficiency defect* are concerned, both show the distribution of exergy in the subsystems of the process. However, the changes in the exergy destroyed in the process are usually not reflected in the *Efficiency defect* due to the small values of this indicator. At the same time *Exergy destruction ratio* gives the same results even when the component chemical exergy is not used, which is not the case for the *Efficiency defect.*

The Exergy loss ratio highlights where in the process exergy is mainly lost. In all cases in this work, cooling is the main reason for exergy losses, while if the utility system were considered within the bounds of the process then different results would be expected for the various cases examined.

All in all, exergy-based indicators can compare the changes in a platform on equal terms taking into account the resources available and the products in terms of exergy. This is the case of the concept proposed for the implementation of the combined separation-multiphase flow expander system in the production manifold. The exergy-based indicators consider not only the work production in the expander as exergy gain, but also the exergy destruction savings due to the substitution of the choke valve highlighting the importance of exergy analysis and how it can be applied in order to propose and investigate possible improvements in an oil and gas processing plant.

When it comes to the method proposed for the evaluation of the thermodynamic indicators investigated in this thesis a simplified Multicriteria analysis approach is performed. Trough this method a number of criteria is set and the scores linking each indicator (or combination of indicators) to each criterion is calculated. The weighting factors determining the importance of each criterion for the scoring process is defined according to the intended use of the indicators. The example presented in the previous Chapter shows that if a group of experts is going to use the indicators for evaluating the performance of an oil and gas platform the best solution is the combination of the *Task exergy efficiency* ε_{II-4} and the *Exergy destruction ratio.*

In fact, if the case study with the different reservoir fluids is examined ε_{II-4} shows that the higher the GLR the higher the efficiency of the process, as lower is the exergy of heating, compression/pumping and cooling in order to produce oil and gas with the highest physical exergy. The ε_{II-4} indicates that for the case with the highest GLR less exergy resources are demanded, probably because the separation process is easier (for

the given separation conditions), as separation takes place mainly in the first stages and less oil is treated in the last ones. Here comes the *Exergy destruction ratio* which confirms this view showing that for the heaviest reservoir fluids more exergy is destroyed in the separation train and not in the production manifold as usual.

The combination of the indicators selected gives indeed an overview of the processing plant at issue highlighting the parts of it where inefficiencies occur and can be used for the comparison of different cases, as well as for the optimization of the process.

11. Conclusions and recommendations for further work

11.1 Conclusions

The objective of this thesis is the energy and exergy analysis of a typical offshore oil and gas processing plant with the aim to calculate a set of thermodynamic performance indicators found in literature, evaluate the results and identify improvement potentials suggesting a new idea for the reduction of CO_2 emissions of an oil and gas platform.

On that account a typical North Sea offshore oil and gas process is considered and simulated in ASPEN HYSYS® (Base Case – Case 1). The data required is provided by the oil and gas company Equinor, Norway. The system investigated in this work includes the oil and gas processing plant, without considering the utility system, while the seawater or gas injection and the gas purification are also excluded from the analysis.

The performance indicators presented in this thesis are grouped in four different categories regarding the energy or exergy basis that they use and the system under investigation. So, they are divided to energy- or exergy-based indicators and indicators that focus on the performance of the entire system or those that are funded on energy/exergy accounting.

According to the analysis conducted for the processing plant of the Base Case the power consumption of the platform is around 23.1 MW and it is mainly used for the compression of the produced gas (20.5 MW) in the gas compression and exportation subsystem. The energy provided for heating is significantly lower, at 11.2 MW, while the thermal energy of cooling that leaves the system ranges around 42.8 MW and it is mainly consumed in the gas compression train (24.3 MW). Exergy losses due to cooling account for 65% of the losses in the platform. The total exergy destruction within the boundaries of the system is around 19.1 MW and it is mostly related to throttling in the Production manifold (contribution of 57%).

In order to evaluate the energy and exergy performance of the plant the set of indicators presented in this work is calculated and assessed for different case studies focusing on some of the design parameters and frame conditions of the process. An investigation over the effect of the component chemical exergy calculations and the effect of the time profile of the field is also conducted.

Testing the indicators over the contribution of the component chemical exergy shows that only the ExU_{volume}, ExD_{volume}, ε_{II-4}, ε_{II-5}, ε_{III} and y_d^* exergy-based indicators give the same results in case the component chemical exergy is excluded from calculations. This

adds to the practicality of these indicators, as it gives the possibility of lower computational complexity.

The changes in the product specifications and frame conditions investigated in Chapter 5 focus on the reservoir fluid treated, the export pressure of the gas produced and the CDB and TVP specifications of the gas and oil product, respectively. Results are controversial regarding variations in the well stream fluid, as energy-based and *ExU*, *ExD* indicators give a lower efficiency for higher GLR, while *Task* and *Component-by-Component exergy efficiency* show the opposite behavior. This is because the former take into account the energy/exergy consumed per unit of product whereas the latter consider the optimal utilization of the exergy resources. In case of specification testing the indicators show overall a decrease in efficiency for higher CDBs, as well as for lower TVPs. Last, when a lower pressure is demanded for the export gas most of the indicators give a higher efficiency for the platform under discussion.

The design parameters examined in this work are the efficiency of the rotating equipment, the temperature of cooling and the temperature and pressure levels of the separation, as found in Chapter 6. The rise in pumps' and compressors' efficiency, as well as the decrease in the temperature of cooling shows an overall increase in efficiency. When a higher temperature of oil heating and a higher pressure in the last stage separation are applied efficiency drops. However, there are some indicators that show a different direction.

The efficiency of an oil and gas processing plant changes during the lifetime of the field, as the volume flow rate, the pressure, the temperature, the composition etc. of the well stream treated are not constant over time. In this work the efficiency of the platform over time is examined in case of deviations in the flowrate and inlet pressure of the reservoir fluid. According to the analysis presented in Chapter 7 if the anti-surge recycle for compression is not taken into account false results that show an increasing efficiency over the years can occur. However, when anti-surge recycle is applied work demands are practically steady over time and the efficiency follows the trend of the profiles showing a general drop throughout the years. This drop is even higher when pressure drop in the first stage separation should be applied in order to maintain the oil and gas production at the desired levels.

The analysis conducted for all the different cases examined in this work gives an overall view of the performance of the indicators.

In general, energy-based indicators are easier and quicker to use. They change according to the variations in heat and power demands when a specific platform with small deviations in the products (eg. small changes in GLR) is examined. However, some of them may not reflect important changes in heating duties (*Specific power consumption*, *CO_2 intensity*) giving incomplete information regarding the performance of the process. In case of different platforms examined they focus on the reservoir fluid treated in the process and they not promote the most efficient utilization of the resources. *ExU* and *ExD* indicators seem to perform similarly, but when they are expressed per product exergy (*ExUexergy*, *ExDexergy*) they show not only the effect of heat and power demands, but also the effect of the different export conditions.

Total exergy efficiency, on the other hand is insensitive to any type of changes in the process, due to the high exergy of the hydrocarbons passing through the system producing misleading results and conclusions over the performance of the platform. This

is not the case for the *Task* and *Component-by-Component exergy efficiency*. These indicators focus on the optimal utilization of the exergy resources of a processing plant and not the type of field examined. *Task exergy efficiency* ε_{II-3} is heavily influenced by changes in the conditions of the inlet well stream and the export products even leading to negative results that prevent the user from understanding and evaluating the changes made in a process. It may, thus focus on the increase or decrease in the exergy of the export products disregarding the deviations in heat and power demands. *Task exergy efficiency* ε_{II-4}, on the other hand considers both the changes in heat and power demands and the changes in the exergy of the export product for variations in the outlet conditions of the platform or in the allocation of the components in the two product streams. What is more, *Task exergy efficiency* ε_{II-5}, as well as *Component-by-Component exergy efficiency* ε_{III} take into account the distribution of the components in the two product streams, but the latter shows a higher sensitivity to the inlet and outlet conditions of the platform, as well as the chemical exergy increase of the process.

The *Exergy destruction ratio* and the *Efficiency defect* give inspection of the distribution of exergy in the subsystems of the process. However, the former is easier to use and assess, as it can be calculated without the component chemical exergy term and it better shows the changes in exergy destruction allocation even in case of small deviations. Furthermore, the *Exergy loss ratio* can show where in the process exergy is mainly lost to the environment indicating and it is more useful when the utility system is also included in the analysis.

The exergy analysis performed for the Base Case of this work gives important information regarding the efficiency of the plant pinpointing where in the process inefficiencies occur showing that throttling in the production manifold is responsible for a great part of high-pressure energy/exergy destruction that could otherwise be utilized. On this reasoning, a new idea is developed in order to increase the efficiency of the platform promoting a more effective energy/exergy utilization. This approach is funded on the combination of compact separation of the well stream entering the processing plant together with multiphase flow expansion of the wet gas stream produced for the substitution of throttling in the Production manifold. The implementation of such a system promotes not only the exergy destruction savings, but also the conversion of a part of the destroyed exergy into work. More specifically, the substitution of throttling in the production manifold with a combined separation – multiphase expansion system results in rise in efficiency of up to 34%. Therefore, this idea, especially when evaluated under an exergy background seems extremely promising for the efficiency increase or more practically the CO_2 emissions drop of an offshore oil and gas processing plant. What should be further examined for the application of this combined system is the design of devices that could process multiphase mixtures on the long term, as well as the inline washing of the equipment treating multiphase flow streams.

As seen from the case studies analyses, as well as the proposal of the new idea for the efficiency increase of an oil and gas processing plant, different indicators respond differently to changes taking place in the platform. Even though exergy analysis shows the benefit of evaluating these changes under equal terms and identifying possibilities for improvement, selecting the most appropriate indicator to use for the examination of an oil and gas platform is not a straightforward process. In this work an evaluation procedure is proposed that is based on the *Multicriteria analysis* that aims to reveal the most appropriate indicator or combination of indicators according to the desired use through a scoring process. For that reason, a set of six criteria is established that aim to cover all the characteristics an indicator is desired to attain and scores are assigned to each indicator against each criterion. The weighting factors defined from the user derive from the expected application and determine the priority of the criteria when calculating

the overall score of the indicators. According to an example presented in this work in which more attention is paid to the clear definition and the sensitivity of the indicator, rather than the simplicity of calculations and interpretation the combination of the *Task exergy efficiency* ε_{II-4} and the *Exergy destruction ratio* are considered to be the most appropriate for the investigation of an oil and gas processing. This methodology can be used by different users for the scores assigned in this work or it can be a basis for a completely new evaluation analysis according to the process at issue.

All in all, the thermodynamic indicators calculated give a variety of information regarding the efficiency of the process and the characteristics of it. More specifically, the energy-based indicators can give a quick inspection of the efficiency of a process, without any complex calculations. On the other hand, exergy analysis can give more details for the process at issue, as in this way the parts of the process where exergy destruction takes place can be detected and suggestions for improving their performance can be made. This is, also the case for the new idea proposed in this thesis aiming to the upgrade of an offshore oil and gas processing plant. Under this scope, the valuableness of the exergy analysis is recognized laying the groundwork for regular use for the evaluation of and oil and gas process.

11.2 Further work

The energy and exergy analysis and the thermodynamic performance calculations presented in this work open for possible further work on this topic.

More specifically, the selection of the thermodynamic indicators studied could be extended including all the indicators presented in this thesis, as well as focusing on more complex exergy approaches such as the Exergoeconomic, Exergoenvironmental and Advanced exergy-based analysis in order to gain a further insight into the real improvement potential of the processes.

To that direction, more design elements of the real offshore processing plants could be included in this analysis, such as seawater or gas injection, utility system, gas sweetening, dehydration etc. and the approach could be additionally applied to onshore gas treatment units. At the same time, a connection to real data through setting up a live process could take place, in order to examine the response of the indicators to variations taking place in a real process.

A new idea for the improvement of the performance of the offshore oil and gas processes is proposed in this work that sets the foundation for further work on the implementation of a combined separation-multiphase flow expansion system for the substitution of choking in the production manifold. On this basis, more investigation could be performed over the appropriate technical choices regarding the necessary equipment, the inline washing, as well as the flow properties and restrictions related to the multiphase flow expansion.

This approach shows that the indicators presented in this work could be used for the optimization of oil and gas platforms in order to propose methods for the most efficient performance of a process resulting to the minimum possible energy consumption and/or exergy destruction.

Finally, exergy analysis sets the framework of a fair comparison between the energy passing through a system that could be generally applied to various systems that may or may not include chemical reactions. The thermodynamic indicators presented in this work could be applied with some alterations to various processes in order to investigate their general performance.

References

Abdollahi-Demneh, F., Moosavian, M., Omidkhah, M., & Bahmanyar, H. (2011). Calculating exergy in flowsheeting simulators: A HYSYS implementation. *Elsevier, 36*(8), 5320-327.

Baehr, H. (1950). *Energie und Exergie – Die Anwendung des Exergiebegriffs in der Energietechnik.* Dusseldorf, Germany: VDI-Verlag.

Bejan, A., Tsatsaronis, G., & Moran, M. (1996). *Thermal Design and Optimization.* New York, USA: John Wiley & Sons.

Benavides, S. O. (2013). *SEPARATION TECHNOLOGIES IN OIL AND GAS PRODUCTION.* Norwegian University of Science and Technology (NTNU).

BP. (2013). BP Statistical Review of World Energy June 2013. London, England, United Kingdom: BP.

BP. (2019). *BP Statistical Review of World Energy 68th edition.* BP.

Brodyansky, V., Sorin, M., & Le Goff, P. (1994). *The Efficiency of Industrial Processes: Exergy Analysis and Optimization.* Amsterdam, The Netherlands: Elsevier.

Brown, S. (May 2007). *Standardized Technology Evaluation Process (STEP): User's Guide and Methodology for Evaluation Teams.* MITRE.

Butler, J., Morrice, D., & Mullarkey, P. (2001). A Multiple Attribute Utility Theory Approach to Ranking and Selection. In *Management Science* (pp. 800-816). INFORMS.

Charron, Y., Pagnier, P., Marchetta, E., & Stihle, S. (2004). Multiphase Flow Helixo-Axial Turbine: Applications and Performance. *11th Abu Dhabi international Petroleum Exhibition and Conference.* Abu Dhabi: Society of Petroleum Engineers Inc.

Cornelissen, R. (1997). *Thermodynamics and sustainable development (PhD thesis).* University of Twente.

Cornelissen, R., & Hirs, G. (2002). The value of the exergetic life cycle assessment. *Energy conversion and management, 43*, 1417-1424.

de Oliveira Jr., S., & van Hombeeck, M. (1997). Exergy analysis of petroleum separation processes in offshore platforms. . In *Energy Conversion and Management* (pp. 38(15-17):1577-1584).

Department for Communities and Local Government UK. (n.d.). *Multi-criteria analysis: a manual.*

Edmunds, T. (2001). *Multiattribute Utility Analysis (MAU) to Support Decisions.* Systems and Decision Sciences Technology, Lawrence Livermore National Laboratory.

Edwards, W. (1994). SMART and SMARTER: Improved Simple Methods for Multiattribute Utility Measurement. In *Organizational Behavior and Human Decision Processes* (pp. 306-325). Elsevier.

ETI Offshore. (2020). *http://www.eti-offshore.com/*. Retrieved June 1, 2021, from http://www.eti-offshore.com/what-we-do

European Comission . (n.d.). Retrieved from Official website of the European Union: https://ec.europa.eu/clima/policies/international/negotiations/paris_en

European Comission. (n.d.). *Official website of the European Union*. Retrieved 12 21, 2020, from https://ec.europa.eu/clima/policies/strategies/2050_en

Eurostars. (2012). *https://www.era-learn.eu/*. Retrieved June 1, 2021, from https://www.era-learn.eu/network-information/networks/eurostars/cut-off-05-03-2015/production-of-electricity-at-surface-and-subsea-with-innovative-unique-choke-turbine

Forman, E., & Gass, S. (2001). The Analytic Hierarchy Process—An Exposition. In *Operations Research* (pp. 49/4:469-486). INFORMS.

Fratzscher, W., Brodjanskij, V., & Michalek, K. (1986). *Exergie: Theorie und Anwendung.* Leipzig, Germany: Deutscher Verlag f¨ur Grundstoffindustrie.

Geneletti, D. (2014, July). *Multi Criteria Analysis (MCA)*. Retrieved from www.aboutvalues.net : http://aboutvalues.net/data/method_navigator/values_method_profile_multi_criteria_analysis_en.pdf

Goedkoop, M., & Spriensma, R. (2001). The Eco-Indicator 99: A Damage Oriented Method for Life Cycle Impact Assessment. In *Methodology Report.* Amersfoort, Netherlands,.

Grassmann, V. (1950). Zur allgemeinen Definition des Wirkungsgrades. *Chemie, 4*(1), 77-80.

Guo, B., Song, S., Ghalambor, A., & Lin, T. (2014). Chapter 2 - General Design Information. In *Offshore Pipelines (Second Edition)* (pp. 13-20). Gulf Professional Publishing.

https://www.ucalgary.ca/. (n.d.). (University of Calgary) Retrieved June 4, 2021, from http://people.ucalgary.ca/~design/engg251/First%20Year%20Files/eval_matrices.pdf

IEA. (2019, December 19). *World Energy Outlook 2018.* Retrieved from https://www.iea.org/: https://www.iea.org/reports/world-energy-outlook-2018/themes#abstract

Internantional Energy Agency. (2012). *Energy Technology Perspectives 2012 - Pathways to a Clean Energy System.* Paris: IEA.

Jøssang, K. (2013). *Evaluation of a North Sea oil platform using exergy analysis.* Trondheim: Norwegian University of Science and Technology.

Kelly, S., & Morozyuk, T. (2009). Advanced exergetic analysis: Approaches for splitting the exergy destruction into endogenous and exogenous parts. *Energy, 34*, 384-391.

Kotas, T. (1980). Exergy concepts for thermal plant: First of two papers on exergy techniques in thermal plant analysis. *International Journal of Heat and Fluid Flow, 2*(3), 105-114.

Kotas, T. (1980). Exergy Criteria of Performance for Thermal Plant: Second of two papers on exergy techniques in thermal plant analysis. *International Journal of Heat and Fluid Flow, 2*(4), 147-163.

Kotas, T. (1985). *The Exergy Method of Thermal Plant Analysis.* Great Britain: Anchor Brendon Ltd. Tiptree, Essex.

Kotas, T. (1995). *The Exergy Method of Thermal Plant Analysis.* Malabar, USA: Krieger Publishing.

Kristiansen, O., Sørensen, Ø., & Nilssen, O. (2016). CompactSep™ - Compact Subsea Gas-Liquid Separator for High-Pressure Wellstream Boosting. *Offshore Technology Conference.* Texas, USA.

Lazzaretto, A., & Tsatsaronis, G. (1999). On the calculation of efficiencies and costs in thermal systems. In *Proceedings of the ASME Advanced Energy Systems Division, volume 39* (pp. 421-430). New York, USA: In S. M. Aceves, S. Garimella, and R. B. Peterson,editors.

Lazzaretto, A., & Tsatsaronis, G. (2006). SPECO: A systematic and general methodology for calculating efficiencies and costs in thermal systems. *Energy, 31*, 1257-1289.

Lior, N., & Zhang, N. (2007). Energy, exergy, and Second Law performance criteria. *Energy, 32*(4), 281-296.

Mahmudi, M., & Sadeghi, M. (2014). A novel three pseudo-component approach (ThPCA) for thermodynamic description of hydrocarbon-water systems. *Journal of Petroleum Exploration and Production Technology, 4*, 281-289.

Manning, F., & Thompson, R. (1991). *Oilfield processing of petroleum: Natural Gas, volume 1.* Tulsa, USA: PennWell Books,.

Margarone, M., Magi, S., Gorla, G., Biffi, S., Siboni, P., Valenti, G., . . . Macchi, E. (March 2011). Revamping, Energy Efficiency, and Exergy Analysis of an Existing Upstream Gas Treatment Facility. *J. Energy Resour. Technol., 133*(1).

Martínez, D., Ebenhack, B., & Wagner, T. (2019). Chapter 2 - Dealing with energy units, measures, and statistics. In *Energy Efficiency* (pp. 35-66). Elsevier.

Maxwell, J. (1950). *Data book on hydrocarbons: application to process engineering.* California: University of California.

Meyer, L., Tsatsaronis, G., Buchgeister, J., & Schebek, L. (2009). Exergo environmental analysis for evaluation of the environmental impact of energy conversion system. *Energy, 34*(1), 75-89.

Modelling and Decision Support Tools. (2007). (Institute for Manufacturing, University of Cambridge.) Retrieved June 4, 2021, from http://www.ifm.eng.cam.ac.uk/dstools/#3

Mokhatab, S., Poe, W., & Mak, J. (2015). *Handbook of Natural Gas Transmission and Processing.* Gulf Professional Publishing.

Moran, M., Shapiro, H., Boettner, D., & Bailey, M. (2019). *Principles of Engineering Thermodynamics 8th Edition in SI Units (Voutsas E.).* Thessaloniki: Tziolas Publications.

Morozyuk, & Tatiana. (2012). Understanding and improving energy conversion systems with the aid of exergy-based methods. *Int. J. of Exergy, 11*, 518-542.

Morozyuk, T. (2008). *A General Exergy-Based Method for Combining a Cost Analysis With an Environmental Impact Analysis: Part I — Theoretical Development.*

Morozyuk, T. (2009). Advanced Exergy Analysis for Chemically Reacting Systems – Application to a Simple Open Gas-Turbine System. *International Journal of Thermodynamics, 12*.

Morris, D., & Szargut, J. (1986). Standard chemical exergy of some elements and compounds on the planet earth. *Enery, 11*(8), 733-755.

Munson, Young, & Okiishi. (2002). *Fundamentals of Fluid Mechanics.* New York: Wiley.

NeqSim. (2021, June 16). Retrieved from https://folk.ntnu.no/solbraa/neqsim/NeqSim.htm

Nesselmann, K. (1952). ¨Uber den thermodynamischen Begriff der Arbeitsf¨ahigkeit. *Allgemeine W¨armetechnik, 3*(5-6), 97-104.

Nguayen, T.-V., Voldsund, M., Elmegaard, B., Ertesvåg, I., & Kjelstrup, S. (2014). On the definition of exergy efficiencies for petroleum systems: Application to offshore oil and gas processing. *Energy, 73*, 264-281.

Nguyen, T.-V., Pierobon, L., Elmegaard, B., Haglind, F., Breuhaus, P., & Voldsund, M. (2013). Exergetic assessment of energy systems on North Sea oil and gas platforms. *Energy, 62*, 23-36.

Nguyen, T.-V., Voldsund, M., Breuhaus, P., & Elmegaard, B. (2016). Energy efficiency measures for offshore oil and gas platforms. *Energy, 117*(2), 325-340.

Norwegian Petroleum. (n.d.). Retrieved 11 30, 2020, from https://www.norskpetroleum.no/en/calculator/about-energy-calculator/

Norwegian Petroleum. (2020, 10 7). *norskpetroleum*. Retrieved 12 21, 2020, from https://www.norskpetroleum.no/en/environment-and-technology/emissions-to-air/

NTUA. (2019). *Lecture presentation on solid fuels in the course of "Technology of Energy"*. Retrieved 12 28, 2020, from file:///C:/Users/HP/Downloads/Solid%20Fuels%20new%20print.pdf

Qualls, W. R., Eaton, A. P., ConocoPhillips Company, Meher-Homji, C. B., & Bechtel Corporation, Turbomachinery Group. (2004). Liquid expanders in the Phillips optimized cascade LNG process. *14th, International conference on liquified natural gas.* Illinois: Gas Technology Institute.

Ramadan, A. (March 2021). *Energy optimization of offshore gas; Master's thesis in Natural Gas Technology.* NTNU.

Rian, A., & Ertesv˚ag, I. (2012). Exergy Evaluation of the Arctic Snøhvit Liquefied Natural Gas Processing Plant in Northern Norway – Significance of Ambient Temperature. *Energy & Fuels, 26*, 1259-1267.

Riboldi, L., & O. Nord, L. (2017). Concepts for lifetime efficient supply of power and heat to off-shore installations in the North Sea. *Energy Conversion and Management, Volume 148*, 860-875.

Ritchie, H., & Roser, M. (2020). Energy. *Our World in Data*, Retrieved from: 'https://ourworldindata.org/energy'.

Rivero, R., Rendon, C., & Monroy, L. (1999). The Exergy of Crude Oil Mixtures and Petroleum Fractions: Calculation and Application. *International Journal of Thermodynamics, 2*, 115-123.

Rystad Energy. (2021, January 12). *https://www.rystadenergy.com/.* Retrieved May 31, 2021, from https://www.rystadenergy.com/newsevents/news/press-releases/an-analysis-of-the-upstream-industrys-dirty-laundry-whose-production-has-the-lowest-co2-intensity/

Saaty, T. (1983). Priority Setting in Complex Problems. *EEE Transactions on Engineering Management, 30*(3), 140-15.

Sato, N. (2004). *Chemical Energy and Exergy: An Introduction to Chemical Thermodynamics for Engineers.* Amsterdam, The Netherlands: Elsevier,.

Smith, R. (2005). *Chemical Process Design and Integration.* Chichester: John Wiley and Sons.

Solbraa, E. (n.d.). *Oil stabilization process example using NeqSim*. Retrieved 12 30, 2020, from https://colab.research.google.com/github/equinor/neqsimprocess/blob/master/example/oilstabilizationprocess.ipynb#scrollTo=ZcXDwRhhhuYL

Song, P., Sun, J., & Wang, K. (2015). Swirling and cavitating flow suppression in a cryogenic liquid turbine expander through geometric optimization. *SAGE Journals*, 628-646.

Sorin, M., Paris, J., & Brodjanskij, V. (1994). Thermodynamic evaluation of a distillation. In *In Thermodynamics and the Design, Analysis, and Improvement of Energy Systems, volume 33* (pp. 125-134). New York, USA: ASME.

Stewart, M. (2019). *Surface Production Operations Pumps and Compressors. 4th Volume.* Cambridge: Gulf Professional Publishing.

Svalheim, S., & King, D. (2003). Life of Field Energy Performance. Society of Petroleum Engineers.

Svalheim, S., & King, D. (2-5 September 2003). Life of Field Energy Performance. *SPE Offshore Europe Oil and Gas Exhibition and Conference.* 2-5 September.

Szargut, J. (1980). International progress in second law analysis. *Energy, 5*, 709-718.

Szargut, J. (1989). Chemical exergies of the elements. *Chemical exergies of the elements,, 32*(4), 269-286.

Szargut, J. (1998). Exergy in the thermal systems analysis. In A. Bejan and E. Mamut, editors, Proceedings of the NATO Advanced Study Institute on Thermodynamic Optimization of Complex Energy Systems. In *volume 69 of NATO Science Series* (pp. 137-10). Neptun, Romania: Academic Publishers.

Szargut, J., Morris, D., & Steward, F. (1988). *Exergy Analysis of Thermal, Chemical and Metallurgical Processes.*

Tsatsaronis, G. (1993). Thermoeconomic analysis and optimization of energy systems. *Progress in Energy and Combustion Science, 19*, 227-257.

Tsatsaronis, G. (2007). Definitions and nomenclature in exergy analysis and exergoeconomics. *Energy, 32*, 249-253.

Tsatsaronis, G., & Cziesla, F. (2002). volume 16, chapter Thermoeconomics. In *Encyclopedia of Physical Science and Technology,* (pp. 659-680). Academic Press.

Tsatsaronis, G., & Park, M.-H. (2002). On avoidable and unavoidable exergy destructions and investment costs in thermal systems. *Energy Conversion and Management, 43*, 1259-1270.

Ulvila, J., & et al. (2001). *A Framework for Information Assurance Attributes and Metrics.* Technical Report 01-1. Decision Sciences Associates.

Voldsund, I., Ertesv˚ag, I., He, W., & Kjelstrup, S. (2013). Exergy analysis of the oil and gas processing a real production day on a North Sea oil platform. *Energy, 55*, 716-727.

Voldsund, M. (2014). Exergy analysis of offshore oil and gas processing (Phd Thesis).

Voldsund, M., Ertesv˚ag, I., Røsjorde, A., He, W., & Kjelstrup, S. (2010). Exergy analysis of the oil and gas separation processes on a North Sea oil platform. In D. Favrat, editor. *Proceedings of ECOS 2010: 23rd International Conference on Efficiency, Cost, Optimization, Simulation, and Environmental Impact of Energy Systems.* Lausanne, Switzerland.

Voldsund, M., He, W., Røsjorde, A., Ertesv˚ag, I., & Kjelstrup, S. (2012). Evaluation of the oil and gas processing at a real production day on a north sea oil platform using exergy analysis. In U. Desideri, G. Manfrida, and E. Sciubba, editors. *Proceedings of ECOS 2012: 25th International Conference on Efficiency, Cost, Optimization, Simulation, and Environmental Impact of Energy Systems.* Perugia, Italy.

Voldsund, M., Nguyen, T.-V., Elmegaard, B., Ertesvåg, I., & Kjelstrup, S. (2014, 12). Thermodynamic Performance Indicators for Offshore Oil and Gas Processing: Application to Four North Sea Facilities. Society of Petroleum Engineers.

Appendices

Appendix A – User variables

Ambient Pressure

```
Sub VariableChanged()
        On Error GoTo ErrorHandler
    Dim MS As Streams
    Dim ST As ProcessStream
    Dim X As InternalVariableWrapper
    Dim P0 As Double
    P0=ActiveVariableWrapper.Variable.GetValue()
Set MS=ActiveObject.Flowsheet.MaterialStreams
For Each ST In MS
    Set X=ST.GetUserVariable("AmbPres")
    X.Variable.SetValue(P0)
    Next ST
ErrorHandler:
End Sub
```

Ambient Temperature

```
Sub VariableChanged()
        On Error GoTo ErrorHandler
    Dim MS As Streams
    Dim ST As ProcessStream
    Dim X As InternalVariableWrapper
    Dim T0 As Double
    T0=ActiveVariableWrapper.Variable.GetValue()
Set MS=ActiveObject.Flowsheet.MaterialStreams
For Each ST In MS
    Set X=ST.GetUserVariable("AmbTemp")
    X.Variable.SetValue(T0)
    Next ST
ErrorHandler:
End Sub
```

Physical exergy

```
Sub PostExecute()
    On Error GoTo ErrorHandler
    Dim Stream As Fluid
    Set Stream=ActiveObject.DuplicateFluid
    Dim Exergy As RealVariable
    Set Exergy=ActiveVariableWrapper.Variable
    Dim T0,P0,H,S,H0,S0 As Double
    Dim X As InternalVariableWrapper
    Set X=activeobject.GetUserVariable("AmbTemp")
    T0=X.Variable.GetValue()
    Set X=activeobject.GetUserVariable("AmbPres")
    P0=X.Variable.GetValue()
    If(Stream.VapourFraction.IsKnown And Stream.Pressure.IsKnown And Stream.MolarFlow.IsKnown
And T0<>-32767 And Stream.MolarFractions.IsKnown(0)) Then
        H=Stream.MolarEnthalpy.GetValue("kJ/kgmole")
        S=Stream.MolarEntropy.GetValue("kJ/kgmole-C")
        Stream.Temperature.SetValue(T0,"C")
        Stream.Pressure.SetValue(P0,"kPa")
        Stream.TPFlash()
        H0=Stream.MolarEnthalpy.GetValue("kJ/kgmole")
        S0=Stream.MolarEntropy.GetValue("kJ/kgmole-C")
        Exergy.SetValue((H-H0-(T0+273.15)*(S-S0))*Stream.MolarFlow.GetValue("kgmole/h"),"kJ/h")
        Else
            Exergy.Erase()
    End If
    ErrorHandler:
End Sub
```

Chemical exergy of mixing

```
Sub PostExecute()
   On Error GoTo ErrorHandler
   Dim Stream,StreamPure As Fluid
   Set Stream=ActiveObject.DuplicateFluid
   Dim Exergy As RealVariable
   Set Exergy=ActiveVariableWrapper.Variable
   Dim T0,P0,H0,S0,HPureSum,SPureSum,HPure,SPure As Double
   Dim X As InternalVariableWrapper
   Set X=activeobject.GetUserVariable("AmbTemp")
   T0=X.Variable.GetValue()
   Set X=activeobject.GetUserVariable("AmbPres")
   P0=X.Variable.GetValue()

   Dim Comps As HYSYS.Components
   Dim Comp As HYSYS.Component
   Dim var,var2 As Integer
   Dim MolFrac, MolFracPure As Variant


   If(Stream.VapourFraction.IsKnown And Stream.Pressure.IsKnown And Stream.MolarFlow.IsKnown
And T0<>-32767 And Stream.MolarFractions.IsKnown(0)) Then

      Stream.Temperature.SetValue(T0,"C")
      Stream.Pressure.SetValue(P0,"kPa")
      Stream.TPFlash()
      H0=Stream.MolarEnthalpy.GetValue("kJ/kgmole")
      S0=Stream.MolarEntropy.GetValue("kJ/kgmole-C")

      HPureSum = 0
      SPureSum = 0
      Set StreamPure = ActiveObject.DuplicateFluid
      StreamPure.Temperature.SetValue(T0,"C")
      StreamPure.Pressure.SetValue(P0,"kPa")
      MolFrac = StreamPure.MolarFractionsValue
      MolFracPure = StreamPure.MolarFractionsValue

      Set Comps = Stream.Components
      For var2 = 0 To Comps.Count-1
         MolFracPure(var2) = 0
      Next var2

      For var = 0 To Comps.Count-1
         Set Comp = Comps.Item(var)
         MolFracPure(var) = 1
         StreamPure.MolarFractions.SetValues(MolFracPure)
         StreamPure.Temperature.SetValue(T0,"C")
         StreamPure.Pressure.SetValue(P0,"kPa")
         StreamPure.TPFlash()
         HPure = StreamPure.MolarEnthalpy.GetValue("kJ/kgmole")
         SPure = StreamPure.MolarEntropy.GetValue("kJ/kgmole-K")
         HPureSum = HPureSum + MolFrac(var)*HPure
         SPureSum = SPureSum + MolFrac(var)*SPure
         MolFracPure(var) = 0
      Next var

      Exergy.SetValue(H0-HPureSum-(T0+273.15)*(S0-SPureSum))*Stream.MolarFlow.GetValue


   Else
         Exergy.Erase()
   End If
   ErrorHandler:
End Sub
```

Component chemical exergy

```
Sub PostExecute()
On Error GoTo ErrorHandler
Dim Stream As Fluid
Set Stream=ActiveObject.DuplicateFluid
Dim chemc As RealVariable
Set chemc=ActiveVariableWrapper.Variable
Dim h,MS As Double
Dim m As Variant
'Dim c(24) As Integer
Dim c(24) As Double
'std chemical exergy [kJ/kg]
c(0)=25.7020
c(1)=457.6233
c(2)=173.1863
c(3)=47178.4591
c(4)=46842.7383
c(5)=46552.9970
c(6)=46568.6641
c(7)=46486.8833
c(8)=46352.5701
c(9)=46199.6598
c(10)=46051.5020
c(11)=45988.5533
c(12)=45893.9324
c(13)=45954.4985
c(14)=45915.8539
c(15)=45797.8818
c(16)=45470.3941
c(17)=52151.4963
c(18)=50028.5999
c(19)=49051.9274
c(20)=48501.8926
c(21)=48501.8926
c(22)=48171.7256
c(23)=48171.7256
c(24)=47929.5660

MS=Stream.MassFlow.GetValue("kg/h")
m=Stream.MassFractionsValue
Dim var As Integer
CCSum=0

Dim Comps As HYSYS.Components
Set Comps=Stream.Components
For var=0 To Comps.Count-1
CCSum=CCSum+(c(var)*m(var))
Next var

'hour=3600sec
h=3600
'chemical exergy [kW]
chemc.SetValue(MS*CCSum/h)


ErrorHandler:
End Sub
```

Pressure of reservoir fluid

```
Sub VariableChanged()
        On Error GoTo ErrorHandler
    Dim MS As Streams
    Dim ST As ProcessStream
    Dim X As InternalVariableWrapper
    Dim Pin As Double
    Pin=ActiveVariableWrapper.Variable.GetValue()
Set MS=ActiveObject.Flowsheet.MaterialStreams
For Each ST In MS
    Set X=ST.GetUserVariable("Pin")
    X.Variable.SetValue(Pin)
    Next ST
ErrorHandler:
End Sub
```

Temperature of reservoir fluid

```
Sub VariableChanged()
        On Error GoTo ErrorHandler
    Dim MS As Streams
    Dim ST As ProcessStream
    Dim X As InternalVariableWrapper
    Dim Tin As Double
    Tin=ActiveVariableWrapper.Variable.GetValue()
Set MS=ActiveObject.Flowsheet.MaterialStreams
For Each ST In MS
    Set X=ST.GetUserVariable("Tin")
    X.Variable.SetValue(Tin)
    Next ST
ErrorHandler:
End Sub
```

Physical exergy of a part of a stream in the feed

```
Sub PostExecute()
    On Error GoTo ErrorHandler
    Dim Stream,StreamPure As Fluid
    Set Stream=ActiveObject.DuplicateFluid
    Dim Exergy As RealVariable
    Set Exergy=ActiveVariableWrapper.Variable
    Dim T0,P0,T,P,Hi0,Si0,Hij,Sij,eij As Double
    Dim X As InternalVariableWrapper
    Set X=activeobject.GetUserVariable("AmbTemp")
    T0=X.Variable.GetValue()
    Set X=activeobject.GetUserVariable("AmbPres")
    P0=X.Variable.GetValue()
    Set X=activeobject.GetUserVariable("Tin")
    T=X.Variable.GetValue()
    Set X=activeobject.GetUserVariable("Pin")
    P=X.Variable.GetValue()

    Dim Comps As HYSYS.Components
    Dim Comp As HYSYS.Component
    Dim var,var2 As Integer
    Dim MolFrac, MolFracPure As Variant

    eij=0

        Set StreamPure = ActiveObject.DuplicateFluid
        StreamPure.Temperature.SetValue(T0,"C")
        StreamPure.Pressure.SetValue(P0,"kPa")
        MolFrac = StreamPure.MolarFractionsValue
        MolFracPure = StreamPure.MolarFractionsValue
```

```
        Set Comps = Stream.Components
        For var2 = 0 To Comps.Count-1
           MolFracPure(var2) = 0
        Next var2

        For var = 0 To Comps.Count-1
           Set Comp = Comps.Item(var)
           MolFracPure(var) = 1
           StreamPure.MolarFractions.SetValues(MolFracPure)
           StreamPure.Temperature.SetValue(T0,"C")
           StreamPure.Pressure.SetValue(P0,"kPa")
           StreamPure.TPFlash()
           Hi0 = StreamPure.MolarEnthalpy.GetValue("kJ/kgmole")
           Si0 = StreamPure.MolarEntropy.GetValue("kJ/kgmole-K")
           eij = eij - MolFrac(var)*(Hi0-((T0+273.15)*Si0))
           MolFracPure(var) = 0
        Next var

Set StreamPure = ActiveObject.DuplicateFluid
        StreamPure.Temperature.SetValue(T,"C")
        StreamPure.Pressure.SetValue(P,"kPa")
        MolFrac = StreamPure.MolarFractionsValue
        MolFracPure = StreamPure.MolarFractionsValue

        Set Comps = Stream.Components
        For var2 = 0 To Comps.Count-1
           MolFracPure(var2) = 0
        Next var2

        For var = 0 To Comps.Count-1
           Set Comp = Comps.Item(var)
           MolFracPure(var) = 1
           StreamPure.MolarFractions.SetValues(MolFracPure)
           StreamPure.Temperature.SetValue(T,"C")
           StreamPure.Pressure.SetValue(P,"kPa")
           StreamPure.TPFlash()
           Hi0 = StreamPure.MolarEnthalpy.GetValue("kJ/kgmole")
           Si0 = StreamPure.MolarEntropy.GetValue("kJ/kgmole-K")
           eij = eij + MolFrac(var)*(Hi0-((T0+273.15)*Si0))
           MolFracPure(var) = 0
        Next var

Exergy.SetValue(eij*Stream.MolarFlow.GetValue)

   ErrorHandler:
End Sub
```

Physical exergy of a part of a stream in each product

```
Sub PostExecute()
   On Error GoTo ErrorHandler
   Dim Stream,StreamPure As Fluid
   Set Stream=ActiveObject.DuplicateFluid
   Dim Exergy As RealVariable
   Set Exergy=ActiveVariableWrapper.Variable
   Dim T0,P0,T,P,Hi0,Si0,Hij,Sij,eij As Double
   Dim X As InternalVariableWrapper
   Set X=activeobject.GetUserVariable("AmbTemp")
   T0=X.Variable.GetValue()
   Set X=activeobject.GetUserVariable("AmbPres")
   P0=X.Variable.GetValue()
   T=Stream.Temperature.GetValue("C")
   P=Stream.Pressure.GetValue("kPa")

   Dim Comps As HYSYS.Components
   Dim Comp As HYSYS.Component
```

```
    Dim var,var2 As Integer
    Dim MolFrac, MolFracPure As Variant

    eij=0

        Set StreamPure = ActiveObject.DuplicateFluid
        StreamPure.Temperature.SetValue(T0,"C")
        StreamPure.Pressure.SetValue(P0,"kPa")
        MolFrac = StreamPure.MolarFractionsValue
        MolFracPure = StreamPure.MolarFractionsValue

        Set Comps = Stream.Components
        For var2 = 0 To Comps.Count-1
            MolFracPure(var2) = 0
        Next var2

        For var = 0 To Comps.Count-1
            Set Comp = Comps.Item(var)
            MolFracPure(var) = 1
            StreamPure.MolarFractions.SetValues(MolFracPure)
            StreamPure.Temperature.SetValue(T0,"C")
            StreamPure.Pressure.SetValue(P0,"kPa")
            StreamPure.TPFlash()
            Hi0 = StreamPure.MolarEnthalpy.GetValue("kJ/kgmole")
            Si0 = StreamPure.MolarEntropy.GetValue("kJ/kgmole-K")
            eij = eij - MolFrac(var)*(Hi0-((T0+273.15)*Si0))
            MolFracPure(var) = 0
        Next var

Set StreamPure = ActiveObject.DuplicateFluid
        StreamPure.Temperature.SetValue(T,"C")
        StreamPure.Pressure.SetValue(P,"kPa")
        MolFrac = StreamPure.MolarFractionsValue
        MolFracPure = StreamPure.MolarFractionsValue

        Set Comps = Stream.Components
        For var2 = 0 To Comps.Count-1
            MolFracPure(var2) = 0
        Next var2

        For var = 0 To Comps.Count-1
            Set Comp = Comps.Item(var)
            MolFracPure(var) = 1
            StreamPure.MolarFractions.SetValues(MolFracPure)
            StreamPure.Temperature.SetValue(T,"C")
            StreamPure.Pressure.SetValue(P,"kPa")
            StreamPure.TPFlash()
            Hi0 = StreamPure.MolarEnthalpy.GetValue("kJ/kgmole")
            Si0 = StreamPure.MolarEntropy.GetValue("kJ/kgmole-K")
            eij = eij + MolFrac(var)*(Hi0-((T0+273.15)*Si0))
            MolFracPure(var) = 0
        Next var

Exergy.SetValue(eij*Stream.MolarFlow.GetValue)

    ErrorHandler:
End Sub
```

Appendix B – Component-by-Component physical exergy decoupling Example

The separation of Figure B60 is carried out, in which the components of the inlet stream (j=1) are separated into two outlet streams: one of the gaseous phase (k=1) and one of the liquid phase (k=2). The components taking part in the separation are the following: methane (i=1), ethane (i=2), propane (i=3). The flow of each component in each of the three streams (j=1, k=1, k=2) is noted in the figure.

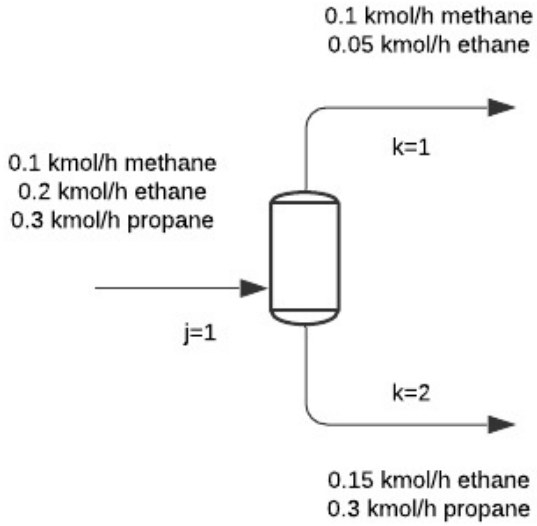

Figure B60 Separation example for the component-by-component analysis

The physical exergy of each part at the outlet $E^{\dot{ph}}_{j,k,out}$ and at the inlet $E^{\dot{ph}}_{j,k,in}$ is expressed as:

$$E^{\dot{ph}}_{1,1,in} = \sum_{i=1:3} n^{\cdot}_{i,1,1}\, e^{\widehat{ph}}_{i,1} = 0.1 e^{\widehat{ph}}_{1,1} + 0.05 e^{\widehat{ph}}_{2,1}, \quad e^{\widehat{ph}}_{i,1}\ in\ the\ inlet\ conditions\ of\ the\ stream\ j = 1$$

$$E^{\dot{ph}}_{1,1,out} = \sum_{i=1:3} n^{\cdot}_{i,1,1}\, e^{\widehat{ph}}_{i,1} = 0.1 e^{\widehat{ph}}_{1,1} + 0.05 e^{\widehat{ph}}_{2,1} \quad e^{\widehat{ph}}_{i,1}\ in\ the\ outlet\ conditions\ of\ the\ stream\ k = 1$$

$$E^{\dot{ph}}_{1,2,in} = \sum_{i=1:3} n^{\cdot}_{i,1,1}\, e^{\widehat{ph}}_{i,1} = 0.15 e^{\widehat{ph}}_{2,1} + 0.3 e^{\widehat{ph}}_{3,1}, \quad e^{\widehat{ph}}_{i,1}\ in\ the\ inlet\ conditions\ of\ the\ stream\ j = 1$$

$$E^{\dot{ph}}_{1,2,out} = \sum_{i=1:3} n^{\cdot}_{i,1,1}\, e^{\widehat{ph}}_{i,1} = 0.15 e^{\widehat{ph}}_{2,1} + 0.3 e^{\widehat{ph}}_{3,1}, \quad e^{\widehat{ph}}_{i,1}\ in\ the\ outlet\ conditions\ of\ the\ stream\ k = 2$$

Appendix C – Calculation of the exergy of heating/cooling

According to the exergy balance of Equation 2 the exergy destroyed due to heating/cooling is:

Using heat exchangers: $\dot{Q}_k = 0$

$$\begin{aligned} \dot{Ed} &= 0 - 0 + \sum \dot{m_{in}} e_{in} - \sum \dot{m_{out}} e_{out} \\ &= -\Delta(\dot{m}_{heated-cooled\ stream}\ e_{heated-cooled\ stream}) \\ &\quad - \Delta(\dot{m}_{heating-cooling\ medium}\ e_{heating-cooling\ medium}) \end{aligned} \tag{C55}$$

Using heaters/coolers: $\dot{Q}_k \neq 0$

$$\begin{aligned} \dot{Ed} &= \sum_k \left(1 - \frac{To}{Tk}\right) \dot{Q}_k - 0 + \sum \dot{m_{in}} e_{in} - \sum \dot{m_{out}} e_{out} \\ &= \sum_k \left(1 - \frac{To}{Tk}\right) \dot{Q}_k - \Delta(\dot{m}_{heated-cooled\ stream}\ e_{heated-cooled\ stream}) \end{aligned} \tag{C56}$$

Equations 47,48 and give:

$$\sum_k \left(1 - \frac{To}{Tk}\right) \dot{Q}_k = -\Delta(\dot{m}_{heating-cooling\ medium}\ e_{heating-cooling\ medium}) \tag{C57}$$

Appendix D - Selection of pressure ratio and number of stages in Gas Compression Stage

In the process under consideration the rich gas produced in the gas recompression stage is further compressed from 51.21 bar to the export pressure of 200 bar. At this point a very significant design parameter- the pressure ratio of each compression stage – needs to be examined in order to define the number of stages to be used for the rich gas compression, as well as the discharge pressure and temperature of each compression stage.

The compression ratio per stage is given by Equation D58.

$$R = \left(\frac{P_2}{P_1}\right)^{\frac{1}{n}} \tag{D58}$$

where R is the compression ratio per stage, P_2 is the discharge pressure (psia), P_1 is the suction pressure (psia) and n is the number of stages. (Stewart, 2019)

The minimum work is obtained when the pressure ratios in all stages of a multistage compression unit are the same. (Smith, 2005)

High compression ratios correspond to lower compression efficiencies, due to the higher actual volume of the gas compressed, and can possibly lead to severe mechanical stress and high temperature problems. When multistage compression with intercooling is used the total work required for the gas compression is lower, due to the decrease of the actual volume of the gas compressed. However, the higher the number of stages is, the greater the amount of cooling medium required, as well as the capital cost regarding heat exchangers and compressors are. The minimum cost (both fixed and variable) of the compression – heat exchanging system could give the optimum number of stages of the rich gas compression in terms of cost. In the case under examination, no economic evaluation is used for the selection of the compression ratio, but the number of stages is selected to be the minimum number of compression stages that results in a discharge temperature lower than the upper limit corresponding to the type of compressor used.

In order to define the number of stages used for the rich gas compression, first the type of compressors is selected. The type of compressors results from the required discharged pressure of the rich gas (200 bars = 2886 psig ≈ $2.9*10^3$ psig), as well as the volume flow of the rich gas entering the compressor (actual volume flow: 7385m^3/h = 260798.8 c.f./h = 4346.6 c.f./m ≈ $4*10^3$ c.f./m). The type of compressors used in the case under consideration is the centrifugal compressor. The discharge temperature of centrifugal compressors is set to the typical range of 250-300 °F (121-149 °C). Considering a conservative discharge temperature of 130° the minimum number of compression stages is calculated.

For a single-stage compression from 51.21 bars to 200 bars, the outlet temperature of the compressed rich gas is 146.4°C (>130°C). When a two-stage compression with intercooling included (rich gas entering the second compressor as saturated vapour) is used the temperatures of the rich gas leaving the two compressors are 84.03°C for the first and 88.95°C for the second compressor. The two discharge temperatures are within the acceptable limits (<130°C). The compression ratio in this case is 1.406 (typical compression ratios: 1.2-5.0) and is calculated for equal pressure ratios of 1.976 for a two-stage compression system. This is how a two-stage compression with equal pressure ratios of 1.976 is selected for the export gas compression of the case under examination.

Appendix E – Property Table

Table E48 Reservoir fluid composition (mass fractions) of Cases 1, 2 & 3

Case 1 – Base Case		Case 2 – Gas-condensate field		Case 3 – Oil field	
Nitrogen	0.0044	Nitrogen	0.0073	Nitrogen	0.0015
CO_2	0.0435	CO_2	0.0437	CO_2	0.0062
H_2O	0.0540	H_2O	0.0721	H_2O	0.0082
C7*	0.0364	C6 star*	0.0113	C6 pseudo*	0.0034
C8*	0.0415	C7 star*	0.0162	C7-C8 pseudo*	0.0064
C9*	0.0278	C8 star*	0.0160	C9-C12 pseudo*	0.0603
C10*	0.0249	C9 star*	0.0112	C13-C18 pseudo*	0.1867
C11*	0.0189	C10-11star*	0.0180	C19-C29 pseudo*	0.2906
C12*	0.0162	C12 star*	0.0070	C30+ pseudo*	0.3520
C13*	0.0225	C13-C14 star*	0.0127	Methane	0.0218
C14*	0.0135	C15-C16 star*	0.0102	Ethane	0.0117
C15*	0.0183	C17-C18 star*	0.0078	Propane	0.0112
C16*	0.0110	C19-C22 star*	0.0103	i-Butane	0.0077
C17*	0.0148	C23-C29 star*	0.0103	n-Butane	0.0114
C18*	0.0114	C30-C40 star*	0.0109	i-Pentane	0.0095
C19*	0.0121	C41-C80 star*	0.0100	n-Pentane	0.0113
C20*	0.0697	Methane	0.5257		
Methane	0.3507	Ethane	0.0801		
Ethane	0.0692	Propane	0.0633		
Propane	0.0542	i-Butane	0.0123		
i-Butane	0.0122	n-Butane	0.0246		
n-Butane	0.0247	i-Pentane	0.0087		
i-Pentane	0.0117	n-Pentane	0.0104		
n-Pentane	0.0145				
n-Hexane	0.0219				

Table E49 Properties of pseudocomponents – Case 3

	Normal boling point [C]	MW (g/mol)	Liq Density [kg/m3]	Tc [C]	Pc [bar]	Vc [m3/kmole]	Acentricity
C6 pseudo*	68.12	86.18	661.50	234.25	30.12	0.37	0.30
C7-C8 pseudo*	104.40	99.07	750.40	289.45	31.02	0.40	0.28
C9-C12 pseudo*	169.78	138.64	800.50	367.05	25.24	0.53	0.39
C13-C18 pseudo*	263.77	213.76	850.20	457.75	19.66	0.74	0.55
C19-C29 pseudo*	386.28	333.84	895.50	520.65	17.97	0.86	0.65
C30+ pseudo*	541.29	525.00	939.80	624.95	13.30	1.19	0.94

Table E50 Properties of pseudocomponents – Case 1

Pseudo component	MW (g/mol)	Relative density
C7*	91.3	0.746
C8*	104.1	0.768
C9*	118.8	0.790
C10*	136.0	0.787
C11*	150.0	0.793
C12*	164.0	0.804
C13*	179.0	0.817
C14*	188.0	0.830
C15*	204.0	0.835
C16*	216.0	0.843
C17*	236.0	0.837
C18*	253.0	0.840
C19*	270.0	0.850
C20*	291.0	0.877

Table E51 Properties of pseudocomponents – Case 2

	Normal boling point [C]	MW (g/mol)	Liq Density [kg/m3]	Tc [C]	Pc [kPa]	Vc [m3/kmole]	Acentricity
C6 star*	68.75	84.70	667.60	234.25	29.69	0.37	0.30
C7 star*	91.95	91.00	738.90	265.23	34.36	0.45	0.45
C8 star*	116.75	104.80	762.00	290.20	30.03	0.48	0.49
C9 star*	142.25	121.00	768.20	314.97	25.52	0.54	0.54
C10-11star*	175.50	139.57	786.92	341.45	22.59	0.61	0.59
C12 star*	208.35	161.00	804.00	368.33	20.18	0.68	0.65
C13-C14 star*	236.37	181.82	820.19	392.67	18.61	0.76	0.71
C15-C16 star*	273.40	212.81	839.09	425.27	16.93	0.89	0.79
C17-C18 star*	306.25	243.70	853.46	454.79	15.73	1.02	0.86
C19-C22 star*	341.70	279.11	867.52	486.54	14.79	1.18	0.94
C23-C29 star*	404.30	343.08	890.81	539.12	13.88	1.49	1.07
C30-C40 star*	485.03	463.93	925.43	584.51	12.47	2.12	1.26
C41-C80 star*	586.85	687.19	1008.30	727.63	13.46	3.43	1.31

Appendix F – Process Flowsheets

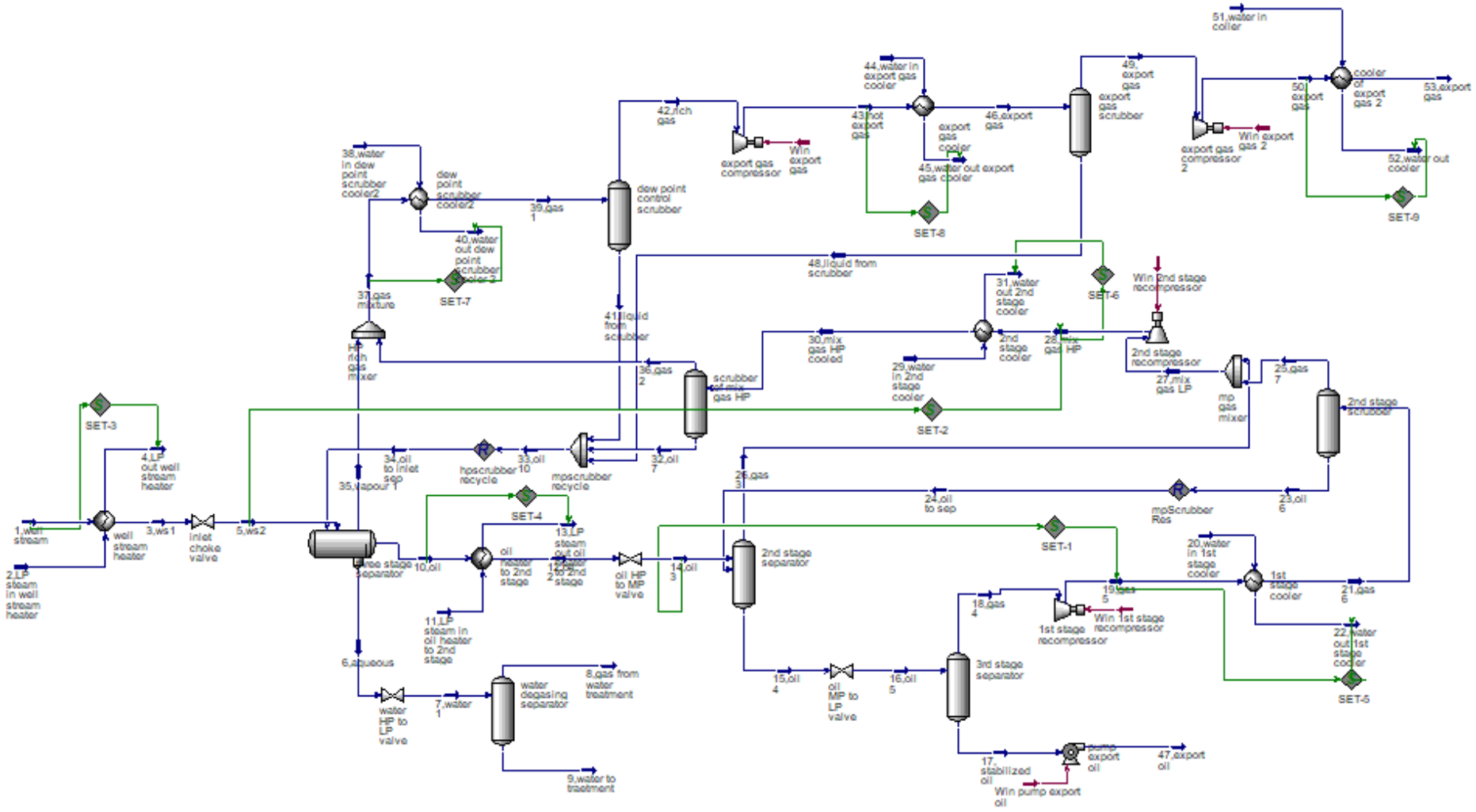

Figure F61 Flowsheet of Case 1

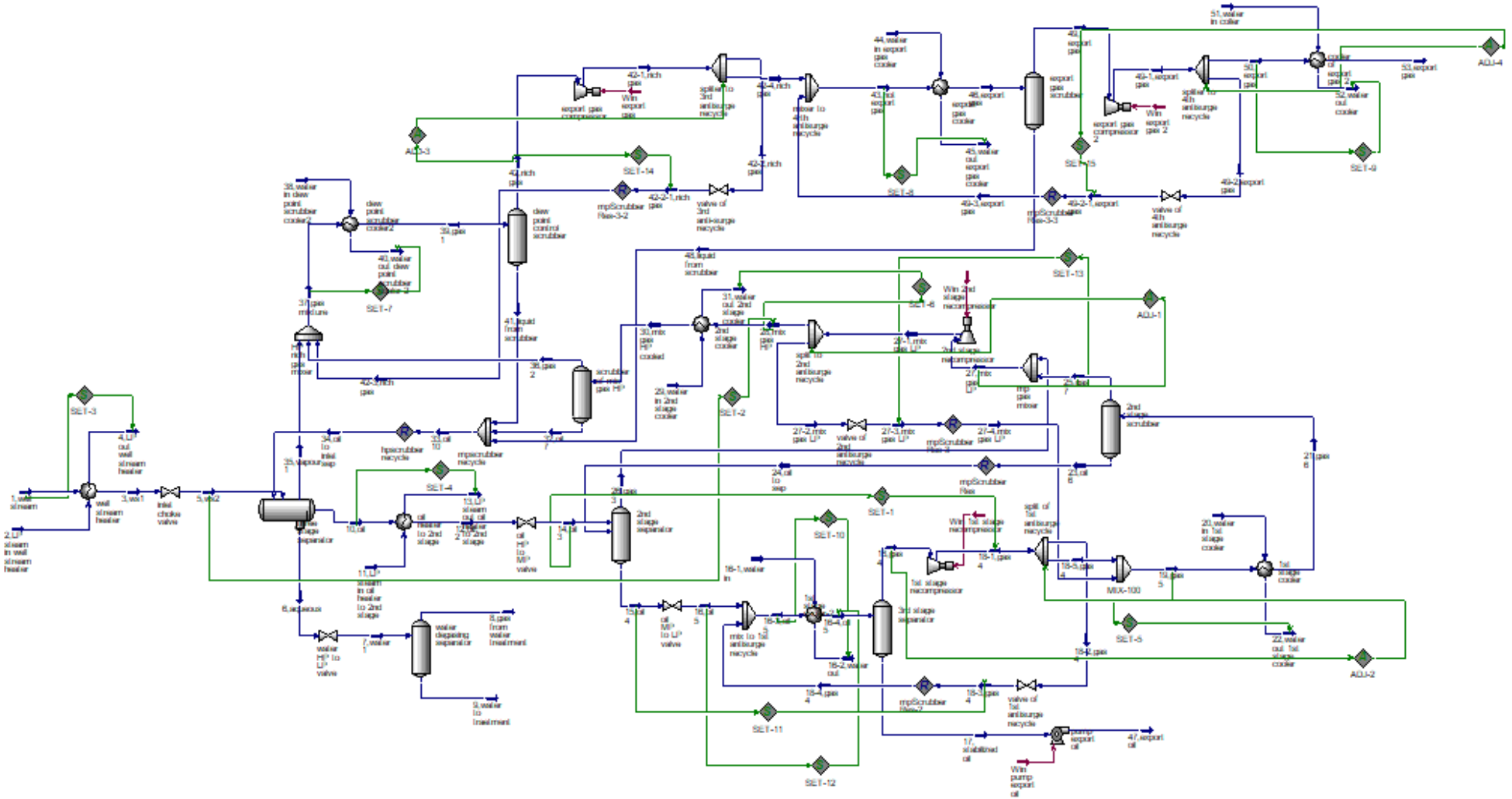

Figure F62 Flowsheet of Case 1 using antisurge recycle

Appendix G – Method of scoring the indicators against the evaluation criteria

First the scoring process of the indicators and their combinations against the criteria of *Sensitivity* and *Comparability* is presented. The ranking in case of these two criteria differs from that of the rest of the criteria, as *Sensitivity* and *Comparability* can be based on numerical data obtained from the tests on the process parameters and the frame conditions of the Base Case. *Workload*, *Simplicity*, *Motivation* and *Clear approach* are on the other hand, founded on qualitative parameters the importance of which is subjectively assessed.

Sensitivity

In order to assign a score to each indicator first all the changes in the design parameters are examined separately. As described above, for a specific case examined the bar charts of Figure G65 represent the absolute percentage change of the indicators from the values of the Base Case scenario. For every case examined the indicator with the lowest percentage change receives the score of 0 and the indicator with the highest bar receives the score of 1, as presented in Figure G63 for the case of the adiabatic efficiency increase of the compressors and the pumps. The rest of the indicators are scored proportionally.

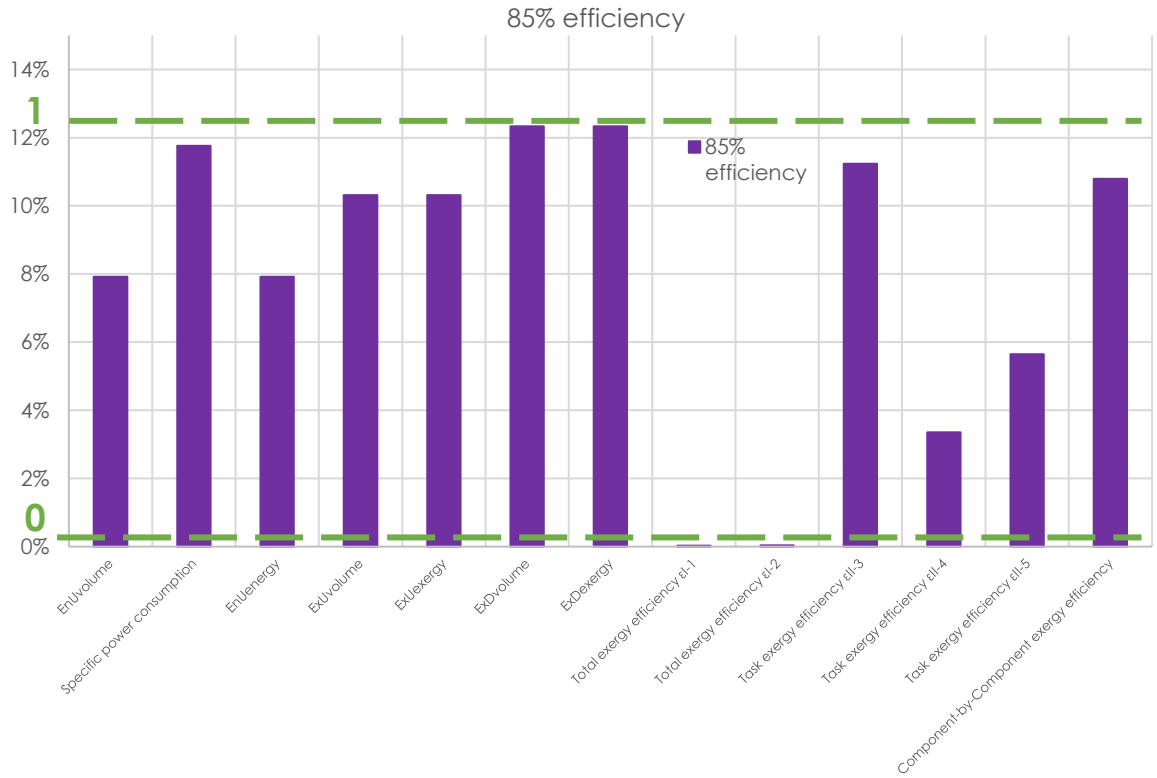

Figure G63 Absolute percentage change of the indicators for an increase of the efficiency of the compressors and pumps from 75% to 85% (design parameter) and scoring method

This process is applied to every case examined for the *Sensitivity* and the values are presented in a table (Table G52). The next step is to calculate the average score for each indicator from the different scores of the same indicator for every case examined and normalize the scores calculated, so that the indicator that changes less than the others receives the score of 0 and the indicator that exhibits the highest average change receives the score of 1. The results of these calculations are presented in Table G52.

Table G52 Scoring table of *Sensitivity*

Case	*Specific CO_2 emissions per unit of produced petroleum*	EnU_{volume}	EnU_{energy}	*Specific power consumption*	ExU_{volume}	ExU_{exergy}	ExD_{volume}	ExD_{exergy}	ε_{I-1}	ε_{I-2}	ε_{II-3}	ε_{II-4}	ε_{II-5}	ε_{III}
85% efficiency	0.95	0.64	0.95	0.64	0.84	0.84	1.00	1.00	0.00	0.00	0.91	0.27	0.46	0.87
Extra cooling	1.00	0.61	1.00	0.60	0.85	0.93	0.92	0.99	0.00	0.00	0.19	0.27	0.47	0.98
Multiphase expander	0.78	0.53	0.80	0.52	0.71	0.69	1.00	0.99	0.00	0.00	0.87	0.23	0.41	0.89
T, P levels change	0.06	0.73	0.05	0.72	0.24	0.24	0.15	0.14	0.00	0.00	1.00	0.03	0.08	0.14
Sensitivity Scores	**0.90**	**0.81**	**0.90**	**0.80**	**0.85**	**0.86**	**0.98**	**1.00**	**0.00**	**0.00**	**0.95**	**0.26**	**0.45**	**0.93**

This method of scoring is based on the fact that the sample of cases examined is representative of the changes in the process design parameters that are usually detected in an offshore oil and gas processing plant. At the same time a relative scoring is used under the assumption of the same relative behavior of the indicators towards different levels of the same parameter change, so that the gravity of each change is not taken into account (e.g. same scoring for the change in adiabatic efficiency in case of increase from 75% to 85% and from 75% to 90% efficiency).

It should be noted that *Sensitivity* scores are calculated only for the case of the single indicator examined, as only indicators that describe the efficiency of the process as a whole respond to the requirements of the *Sensitivity* criterion. The *Sensitivity* score of the combinations is defined by the single indicator describing the entire process that takes part in the combination.

Comparability

Scoring an indicator against the *Comparability* criterion follows the exact same method as for the *Sensitivity* ranking. The only difference is that for the *Comparability* different cases are examined and that the highest change in the indicators is assigned with the score of 0 and the lowest change is assigned with the score of 1. This is because, according to this criterion the indicator should be insensitive to changes in the frame conditions of the process. The scoring method based on the bar chart of changes is given in Figure G64.

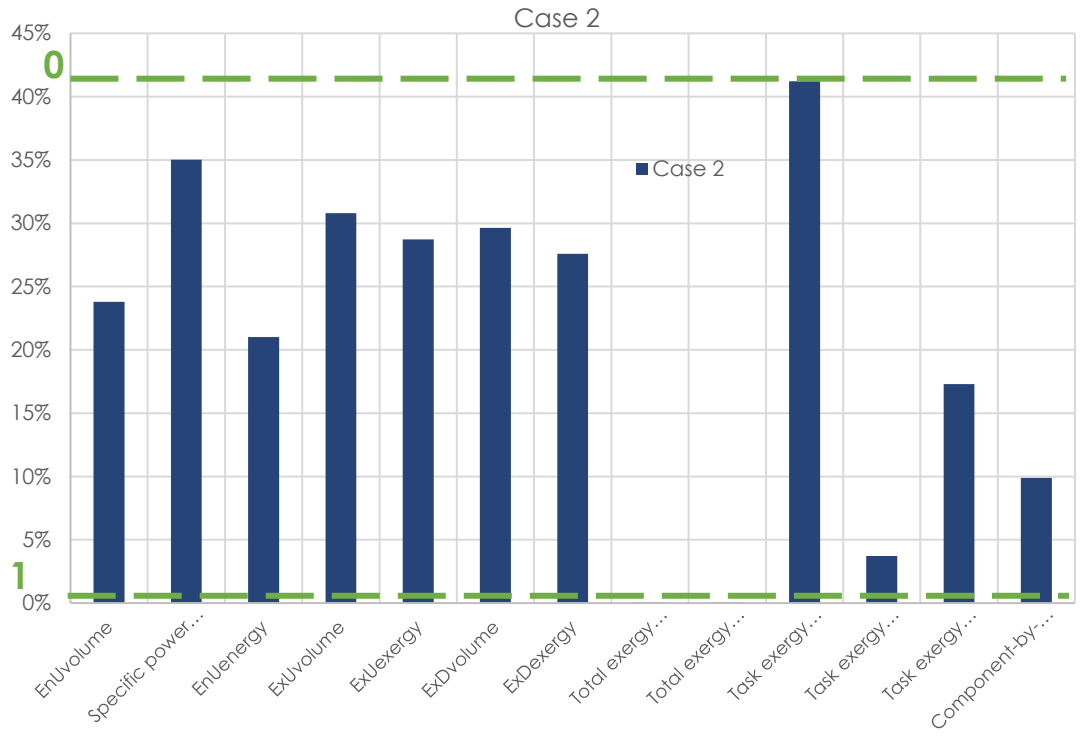

Figure G64 Absolute percentage change of the indicators for a change in the composition of the reservoir fluid (frame conditions) and scoring method

Again, the *Comparability* scores are calculated only for the single indicators examined. Ranking for the *Comparability* criterion is given in Table G53.

Table G53 Scoring table of *Comparability*

Case	*Specific CO_2 emissions per unit of produced petroleum*	EnU_{volume}	EnU_{energy}	*Specific power consumption*	ExU_{volume}	ExU_{exergy}	ExD_{volume}	ExD_{exergy}	ε_{I-1}	ε_{I-2}	ε_{II-3}	ε_{II-4}	ε_{II-5}	ε_{III}
P decrease of the export gas	0.85	0.90	0.85	0.90	0.87	0.87	0.95	0.95	1.00	1.00	0.00	0.99	1.00	0.70
Case 3	0.75	0.81	0.76	0.81	0.78	0.78	0.79	0.79	1.00	1.00	0.00	0.84	0.86	0.75
CDB increase	0.27	0.50	0.00	0.72	0.19	0.44	0.68	0.93	1.00	1.00	0.31	0.82	0.47	0.03
Case 2	0.09	0.42	0.15	0.49	0.25	0.30	0.28	0.33	1.00	1.00	0.00	0.91	0.58	0.76
TVP decrease	0.82	0.00	0.82	0.01	0.51	0.53	0.63	0.65	1.00	1.00	0.59	0.88	0.78	0.61
Sensitivity Scores	**0.46**	**0.42**	**0.41**	**0.50**	**0.41**	**0.49**	**0.59**	**0.67**	**1.00**	**1.00**	**0.00**	**0.86**	**0.68**	**0.47**

The bar chart of the absolute percentage change of the indicators in each change of parameters examined for the scoring process of Sensitivity and Comparability is presented below.

At this point it is highlighted that the direction in which indicators change is not taken into account for the two criteria presented above. These two criteria focus on the sensitivity of the indicators toward changes in the design parameters and the process configurations and not on the increase or decrease in efficiency which an indicator exhibits when the change in parameters is tested. However, the rise or drop in efficiency an indicator may show cannot be overlooked, especially in cases where an indicator shows a direction in the efficiency opposite than the rest of the indicators (e.g. all indicators show an increase in efficiency except for ε_{II-3}). This behavior of an indicator may confuse the user and sometimes lead to incorrect conclusions. This is why this parameter is investigated in the criterion of *Simplicity* rather that those of *Sensitivity* and *Comparability*, as presented below.

For the rest of the criteria a set of parameters that prevent the indicator from fulfilling the criterion investigated each time is set. Each parameter corresponds to a *penalty* in the scoring procedure. These *penalties* are a quantitative approach of the difficulty every parameter sets for the indicator in the scope of satisfying the criterion at issue, so that the indicator with the most *penalties* gets a score of 0 and the indicator with the minimum sum of *penalties* reaches the score of 1 (score for a certain criterion). In this way the score of each indicator towards each of the *Workload*, *Simplicity*, *Motivation* and *Clear approach* is calculated as:

$$\begin{aligned} &Score\ of\ the\ indicator\ m\ for\ the\ criterion\ l \\ &= 1 - \sum_{j} penalty\ j\ of\ the\ criterion\ l\ that\ responds\ to\ the\ indicator\ m \end{aligned} \tag{G59}$$

It should be pointed out that unlike *Sensitivity* and *Comparability*, the score of the indicators for the *Workload*, *Simplicity*, *Motivation* and *Clear approach* is calculated separately for the single indicators and their combinations.

More specifically, for the rest of the indicators the scoring process is presented below.

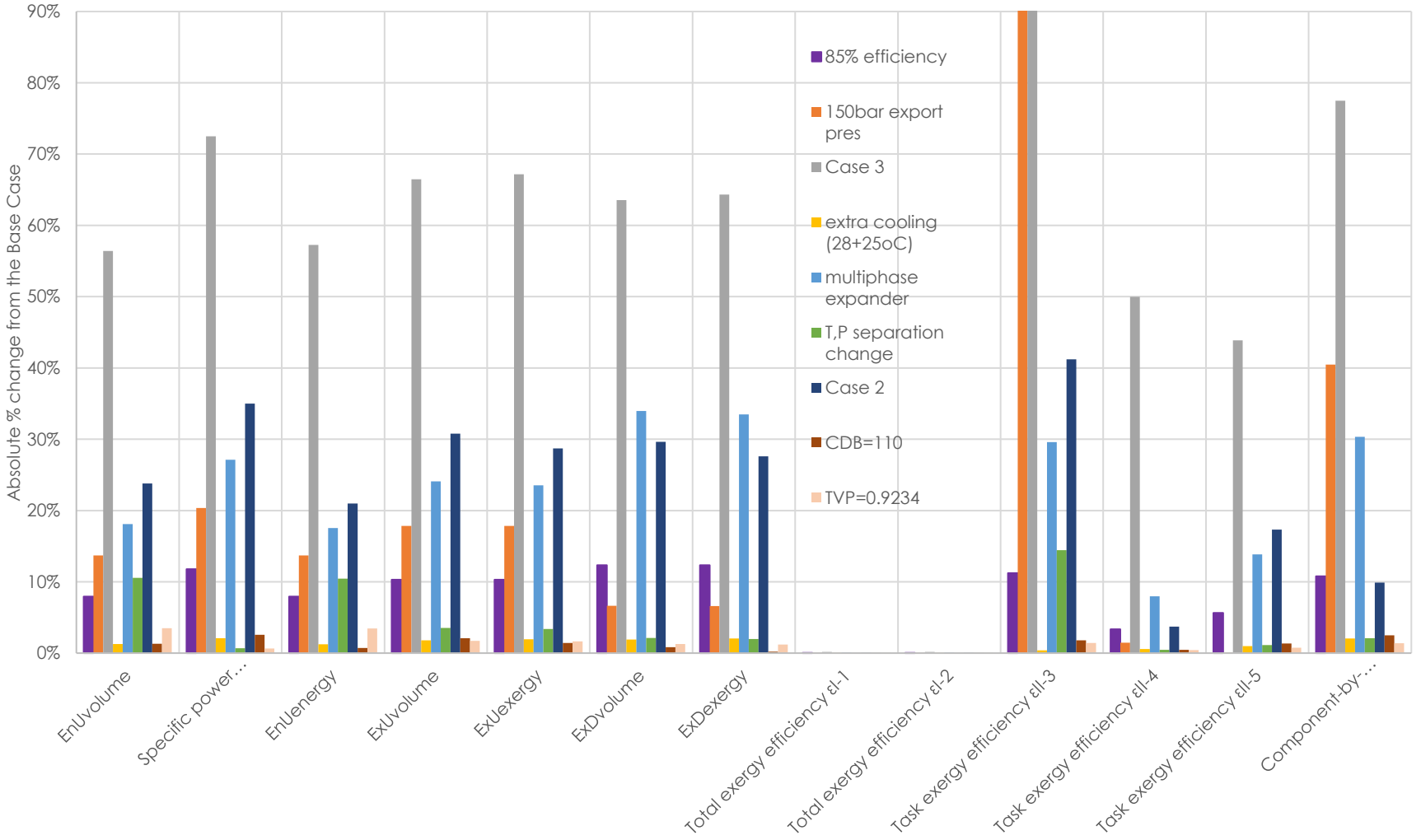

Figure G65 Absolute percentage change from the Base Case scenario for the different changes in design parameters and frame conditions. (ε_{II-3} changes (grey and orange bars) may exceed 90% without being presented in the figure)

Workload

The parameters that increase the amount of time necessary for the calculations or the complexity of the calculations focus on the complications of setting up a method or an algorithm for conducting the calculations and not on the computational time required. This is because the computational time is almost the same in all cases and depends on the convergence time of the simulation. So, the parameters investigated are the following.

1. Setting up a method for the calculation of the Lower Heating Values. The method can be based on Dulong's formula or other formulas presented in literature or developed internally and the calculations can be performed inside the simulation or separately for example in a spreadsheet.

2. Investigating and defining the method of producing heat and power consumed in the processing plant, as well as calculating or estimating the factor converting the fuel consumption to kg of CO_2 emitted.

3. Conducting an exergy analysis in the process under consideration. This includes studying the method of exergy analysis and calculating exergy terms for all the streams of the process.

4. Including the *Component chemical exergy* in the analysis. This requires the calculation of the standard chemical exergies of all the chemical compounds taking part in the process, as well as the pseudocomponents used. This procedure includes searching in tables in literature for the standard chemical exergies of the components, calculate the standard chemical exergies of the pseudocomponents based on empirical equations and add extra coding in the UVs for the calculation of the *component chemical exergy*.

5. Adding in UVs extra coding for the calculation of the component-based exergy differences for the calculation of the *Component-by-Component exergy efficiency (C-b-C)*.

6. Investigating the sub-systems of the process where inefficiencies occur and conducting calculations of the *exergy destruction ratio* for the sub-systems investigated in case an exergy analysis has already been done for the process at issue.

7. Conducting extra calculations of the *exergy lost ratio* after having identified the parts of the process where exergy is lost to the environment in case an exergy analysis and calculations of the *exergy destruction ratio* have been conducted.

The following table (Table G54) shows the breakdown of the penalties for the different indicators and their combinations for the *Workload*. The scores of all indicators for the criterion of *Workload* are presented in this table. The different colors in Table G54 represent the penalties that correspond to each of the three cases (single indicator, combination with the *Exergy destruction ratio*, combination with the *Exergy destruction ratio* and the *Exergy loss ratio*).

Some details should be given regarding the assignment of the *penalties* to the indicators of the three cases. First, the calculation of the standard chemical exergies is considered to be necessary only in case the indicator does not provide the same results when the component chemical exergy is calculated or not, as presented in Chapter 4. It should, also be noted that the values of the penalties allocated derive from the experience of setting up and making calculations for the processing plant examined. In

case previous calculations for the same process have already been made – that may include for example calculations of the LHV or the Fuel consumption method - the corresponding parameters could receive a lower *penalty*.

Table G54 Scoring table of *Workload*

Workload	1.LHV	2.Fuel consumption	3.Exergy analysis	4.Standard chemical exergies	5.Extra coding for C-b-C 6.Extra investigation/ calculation for *exergy destruction ratio* 7.Extra investigation/ calculation for *exergy loss ratio*	Single indicator	*+Exergy destruction ratio*	*+Exergy destruction ratio +Exergy loss ratio*
Penalties	0.05	0.10	0.55	0.30	0.10 0.04 0.01			
Specific CO_2 emissions per unit of produced petroleum	x	x				0.85		
EnU_{volume}						**1.00**		
$Specific\ power\ consumption$						**1.00**		
EnU_{energy}	x					0.95		
ExU_{volume}			x	x	x x	0.45	0.41	0.10
ExU_{exergy}			x	x	x x	0.15	0.11	0.10
ExD_{volume}			x	x	x x	0.45	0.41	0.10
ExD_{exergy}			x	x	x x	0.15	0.11	0.10
ε_{I-1}			x	x	x x	0.15	0.11	0.10
ε_{I-2}			x	x	x x	0.15	0.11	0.10
ε_{II-3}			x	x	x x	0.15	0.11	0.10
ε_{II-4}			x	x	x x	0.45	0.41	0.10
ε_{II-5}			x	x	x x	0.45	0.41	0.10
ε_{III}			x	x	x x x	0.35	0.31	**0.00**

Simplicity

The parameters examined in case of the *Simplicity* criterion for which penalties are assigned to the indicators focus on the difficulty of understanding the terms of the indicators and communicating the indicator in terms of definition and results among a great variety of people (engineers, management etc.). These parameters are the following.

1. Including the concept of exergy. The theory of exergy is not widely known as is that of energy. This means that every exergy-based indicator in order to be communicated requires a presentation of the idea of exergy.

2. Including the concept of exergy destruction without demanding an exergetic analysis of the system and the presentation of the exergy balance.

3. Introducing the concept of product and fuel exergy that requires a thorough presentation of the exergy balance in the scope of the exergy analysis.

4. Including differences of the exergy terms for the definition of the product and fuel exergy within the framework of the exergy analysis.

5. Incorporating the term of the chemical exergy increases (ΔEch) that is included in the product exergy.

6. Displaying results of different direction (eg. increase vs decrease in efficiency) than the rest of the indicators for a certain change in the design parameters or the frame conditions of the process that may lead to confusing results.

7. Including specific exergies or exergies on a component level that result in more complicated calculations and thus product and fuel exergetic terms.

8. Presentation of an extra indicator in case of the combination of two or three different indicators for the description of the efficiency of a process.

The penalties assigned to each indicator and combination of indicators based on the above-mentioned parameters are presented in the Scoring table that follows (Table G55).

It should be noted that the only parameters that change when a combination of indicators is examined is the extra complication of presenting more than one indicators for the evaluation of the process (parameters 8 and 9 of Table G55).

Table G55 Scoring table of *Simplicity*

Workload	1.Exergy concept	2.Exergy destruction	3.Product & Fuel exergy	4.Exergy differences	5.ΔEch	6.Confusing results	7.Specific exergies & component exergies	8.Extra indicator presented	9.Extra indicator presented	Single indicator	*+Exergy destruction ratio*	*destruction ratio*	*+Exergy loss ratio*
Penalties	0.45	0.05	0.15	0.05	0.05	0.10	0.10	0.05	0.05				
Specific CO_2 emissions per unit of produced petroleum						x				0.90			
EnU_{volume}										**1.00**			
Specific powe consumption						x				0.90			
EnU_{energy}										**1.00**			
ExU_{volume}	x							x	x	0.55	0.50	0.45	
ExU_{exergy}	x							x	x	0.55	0.50	0.45	
ExD_{volume}	x	x						x	x	0.50	0.45	0.40	
ExD_{exergy}	x	x						x	x	0.50	0.45	0.40	
ε_{I-1}	x		x					x	x	0.40	0.35	0.30	
ε_{I-2}	x		x					x	x	0.40	0.35	0.30	
ε_{II-3}	x		x	x				x	x	0.35	0.30	0.25	
ε_{II-4}	x		x	x	x	x		x	x	0.20	0.15	0.10	
ε_{II-5}	x		x	x	x		x	x	x	0.20	0.15	0.10	
ε_{III}	x		x	x	x	x	x	x	x	0.10	0.05	**0.00**	

Clear approach

The criterion of *Clear approach* focuses on the parameters that can be interpreted in different ways when investigating the indicators presented. These parameters may represent the lack of clarity in the definition of some indicators or the possible variations in the methods selected for the calculation of certain terms of the indicators. So, the measures of *Clear approach* can be considered as a guide for consistent calculations of the indicators, so that the results can be comparable. The parameters to be considered are the following.

1. Defining the method of calculating the Lower Heating Value of the product streams, as presented above.

2. Determining the method of calculating the heat and power production, as given in previous criterion.

3. Defining (or calculating) the factor converting the fuel consumption to kg of CO_2 emitted, as presented above.

4. Using specific exergy tables and empirical equations for the calculation of the specific exergy of the pseudocomponents for consistent results. At the same time, the empirical equations are not funded on a solid theoretical basis, while they include terms that can be calculated using various methods, such as the APIs of the pseudocomponents.

5. Assuming that the partial molar physical exergy of each component in a stream is equal to the molar exergy of the same component when it is pure at the temperature and pressure of the stream-mixture. This assumption made in case of the *Component-by-Component exergy efficiency* shows that this indicator is open to different interpretations and simplifications.

6. Defining the mass or molar basis used for the calculations, due to different results occurring in these two cases.

7. Defining the method of converting the Sm^3 to Sm^3 o.e. The conversion factor may be based on an approximation found in literature or other data basis used or it can be calculated especially for the case under examination incorporating the heating values of the oil and gas produced on the platform.

8. Setting the boundaries of the sub-systems investigated so that the results of the indicators can be compared under the same conditions.

9. Determining which are the waste products of the process at issue again for a fair comparison between the results of the indicators.

The scoring table of the *Clear approach* criterion (Table G56) highlights in which cases each penalty applies and presents the scores assigned to each indicator and the combinations.

Table G56 Scoring table of *Clear approach*

Workload	1.LHV	2.Work and power production	3.CO_2 conversion factor	4.Standard chemical exergies	5.Assumption of partial molar physical exergy	6.Mass basis	7.Sm^3 o.e.	8.Sub-systems boundaries	9.Waste product definition	Single indicator	*+Exergy destruction ratio*	*+Exergy destruction ratio +Exergy loss ratio*
Penalties	0.80	0.10	0.10	0.50	0.20	0.10	0.30	0.10	0.05			
Specific CO_2 emissions per unit of produced petroleum	x	x	x							**0.00**		
EnU_{volume}							x			0.70		
$Specific\ power\ consumption$							x			0.70		
EnU_{energy}	x									0.20		
ExU_{volume}				x			x	x	x	0.70	0.60	0.05
ExU_{exergy}				x				x	x	0.50	0.40	0.35
ExD_{volume}				x			x	x	x	0.70	0.60	0.05
ExD_{exergy}				x				x	x	0.50	0.40	0.35
ε_{I-1}				x				x	x	0.50	0.40	0.35
ε_{I-2}				x				x	x	0.50	0.40	0.35
ε_{II-3}				x				x	x	0.50	0.40	0.35
ε_{II-4}				x				x	x	**1.00**	0.90	0.35
ε_{II-5}				x		x		x	x	0.90	0.80	0.25
ε_{III}				x	x			x	x	0.80	0.70	0.15

Motivation

Motivation focuses on the possibility of providing the distance of the efficiency of the process from an achievable target (practically or thermodynamically), as well as providing information regarding the part of the process where the highest potential to enhance inefficiency exists. The parameters examined –as given below- aim to highlight to what extent these two targets are achieved.

1. Negative results that can occur from the calculations of an indicator. These results neither are comparable nor show the distance from the minimum efficiency possible.

2. No expected maximum of the indicators that corresponds to the minimum possible efficiency, even though a minimum value of zero represents the best case scenario for the efficiency of the process.

3. No possibility to indicate where in the system examined exergy is destroyed.

4. No possibility to indicate where in the system exergy is lost to the environment.

The penalties assigned to each indicator and combination of indicators based on the given parameters are presented in the Scoring table below (Table G57, Table G55).

It should be highlighted that in case of the combination with the *Exergy destruction ratio* parameter 3 is no longer applied, while in case of the combination with both *Exergy destruction ratio* and *Exergy loss ratio* parameters 3 and 4 stop being valid (Table G57, Table G55).

Table G57 Scoring table of *Motivation*

Workload	1.Negative results	2.No expected maximum	3.No possibility to pinpoint the destroyed exergy	4.No possibility to pinpoint the lost exergy	Single indicator	*+Exergy destruction ratio*	*+Exergy destruction ratio +Exergy loss ratio*
Penalties	0.50	0.30	0.25	0.25			
Specific CO_2 emissions per unit of produced petroleum		x	x	x	0.20		
EnU_{volume}		x	x	x	0.20		
$Specific\ power\ consumption$		x	x	x	0.20		
EnU_{energy}		x	x	x	0.20		
ExU_{volume}		x	x	x	0.20	0.45	0.70
ExU_{exergy}		x	x	x	0.20	0.45	0.70
ExD_{volume}		x		x	0.45	0.45	0.70
ExD_{exergy}		x		x	0.45	0.45	0.70
ε_{I-1}			x	x	0.50	0.75	**1.00**
ε_{I-2}			x	x	0.75	0.75	**1.00**
ε_{II-3}	x		x	x	**0.00**	0.25	0.50
ε_{II-4}			x	x	0.50	0.75	**1.00**
ε_{II-5}			x	x	0.50	0.75	**1.00**
ε_{III}			x	x	0.50	0.75	**1.00**

The scores calculated and presented in Table G52, Table G53, Table G54, Table G55, Table G56 and Table G57 are incorporated in the overall scoring table presented in Chapter 9 together with the weighting factors of the criteria (Table 46, Table 47). The total scores of the indicators result from the individual scores of the indicators towards the different criteria based on Equation 51.

Chrysanthi Papadimitriou

Thermodynamic performance indicators in offshore oil and gas processes

NTNU
Norwegian University of
Science and Technology